

AN ABSTRACT OF THE THESIS OF

Da-Ren Dung for the degree of Master of Science in Civil Engineering and Forest Products presented on September 8, 1999. Title: A Practical Method to Analyze the System Effects of a Metal-Plate-Connected Wood Truss Assembly.

Signature redacted for privacy.

Abstract approved: _____

Thomas H. Miller

Signature redacted for privacy.

Rakesh Gupta

This study presents a practical method to model an actual Metal-Plate-Connected (MPC) roof truss assembly using a commercial program, SAP2000, to investigate its system performance. Truss assembly modeling was examined because the conventional single truss design method ignores system effects, such as variability of modulus of elasticity (MOE), interaction of sub-assemblies, realistic boundary conditions, etc.

Two types of semi-rigid MPC joint models, linear spring (LS) joint model and a truss plate manufacturer's (TPM's) joint model, were used for the truss and truss assembly models. To verify the truss models using the LS joint model, the predicted deflections of individual trusses and the load sharing of nine-truss roof assembly models were compared with experimental results from the literature. Fourteen individual trusses (the components of the actual roof truss assembly) using TPM's joint models were also verified by comparing the Combined Stress Index (CSI) values with the CSI values provided by the TPM. Both design and one set of random material properties were used in the analysis of the actual roof truss assembly model.

The predictions for truss models using the LS joint model for truss deflections and load sharing effect agree with the experimental results. The CSI values for individual trusses with the TPM's joint model matched the CSI values provided by the TPM.

The load distribution in an actual roof truss assembly is strongly influenced by the interaction of sub-assemblies and by the boundary conditions. In the truss assembly, the prediction of location and value of maximum CSI are different from those for the single truss. The truss with the maximum CSI value of 0.91 among fourteen individual truss types decreased to 0.52 and 0.51 when this truss is in the assembly with design and random material properties, respectively. Moreover, the truss with a maximum CSI of 1.03 in the assembly (with design properties) had a CSI value of only 0.95 as an individual truss. Although the CSI of one truss type increased over 1.0 in the assembly, the CSI of most other trusses decreased (by as much as 43%). So, the behavior of a single truss is different when the truss is in the assembly. The benefits of using an assembly model compared to the conventional truss design method are in providing increased safety through improved analysis and in a potential reduction in construction cost.

© Copyright by Da-Ren Dung

September 8, 1999

All Rights Reserved

**A Practical Method to Analyze the System
Effects of a Metal-Plate-Connected Wood Truss Assembly**

by

Da-Ren Dung

A THESIS

Submitted to

Oregon State University

**In partial fulfillment of
the requirements for the
degree of**

Master of Science

Presented September 8, 1999

Commencement June, 2000

Master of Science thesis of Da-Ren Dung presented on September 8, 1999

APPROVED:

Signature redacted for privacy..

Co-Major Professor, representing Civil Engineering

Signature redacted for privacy.

Co-Major Professor, representing Forest Products

Signature redacted for privacy.

Head of Department of Civil, Construction, and Environmental Engineering

Signature redacted for privacy.

Head of Department of Forest Products

Signature redacted for privacy.

Dean of Graduate School

I understand that my thesis will become part of the permanent collection of Oregon State University libraries. My signature below authorizes release of my thesis to any reader upon request.

Signature redacted for privacy.

Da-Ren Dung, Author

ACKNOWLEDGMENT

I would like to express my sincere thanks to my major professors, Dr. Thomas H. Miller of the department of Civil, Construction and Environmental Engineering and Dr. Rakesh Gupta of the Department of Forest Products, for their insightful discussions and constant guidance on this project.

I would also like to give special thanks to my friends, Dr. Wen-Chyi Su and Zhong Li, for their advice and help throughout this project.

Financial support for this research was provided by the Department of Forest Products, Oregon State University.

TABLE OF CONTENTS

	<u>Page</u>
1. INTRODUCTION	1
1.1 Objectives	3
1.2 Scope	3
2. LITERATURE REVIEW	5
2.1 MPC Joint	5
2.2 Truss and Truss Assembly Models	6
2.3 Actual Truss and Truss Assembly Tests	9
3. TRUSS AND TRUSS ASSEMBLY MODELS	12
3.1 MPC Joint Model	12
3.1.1 LS Joint Model	12
3.1.2 TPM's Joint Model	14
3.2 Frame Elements	19
3.2.1 Truss Members	19
3.2.2 Plywood Sheathing Beam Elements	21
3.3 Boundary Conditions for Actual Roof Truss Assembly Model	26
3.4 Material Properties for Actual Roof Truss Assembly Model	27
3.5 CSI Equations	28
3.6 Truss and Truss Assembly Models	33
3.6.1 Single Truss Using LS Joint Model	33
3.6.2 Single Truss Using TPM's Joint Model	34
3.6.3 Nine-Truss Assembly Using LS Joint Model	43
3.6.4 An Actual Roof Truss Assembly Model	43

TABLE OF CONTENTS (Continued)

	<u>Page</u>
4. RESULTS AND DISCUSSION	52
4.1 Verifications of Single Truss Using LS Joint Models	52
4.2 Verifications of CSI Values for Single Trusses Using TPM's Joint Model	55
4.3 Verification of Nine-Truss Assembly Using LS Joint Model	57
4.4 Actual Roof Truss Assembly Model	63
4.4.1 MOE	66
4.4.2 Interaction of Sub-Assemblies	71
4.4.3 Boundary Conditions	77
4.4.4 Modeling Methods	79
5. CONCLUSIONS AND RECOMMENDATIONS	82
BIBLIOGRAPHY	85
APPENDICES	89

LIST OF FIGURES

<u>Figure</u>	<u>Page</u>
3.1 Bottom Chord Tension Splice Joint Detail in 3:12 Slope, 28-Foot-Span, Semi- Rigid Truss Model with 3"x7" Metal Plate Using Linear Spring Elements	15
3.2 Heel Joint Detail in 3:12 Slope, 28-Foot-Span, Semi-Rigid Truss Model with 3"x10" Metal Plate Using Linear Spring Elements	16
3.3 Truss Plate Manufacturer's Semi-Rigid Joint Model for Peak Joints	17
3.4 Truss Plate Manufacturer's Semi-Rigid Joint Model for Heel Joints	18
3.5 Assigned Material and Geometric Properties for the Frame Element	20
3.6 Section Properties Calculated by SAP2000 for the Frame Element	20
3.7 Detail of a Sheathing Beam	21
3.8 Assigned Material and Geometric Properties for the Sheathing Beam Element	22
3.9 Section Properties Calculated by SAP2000 for the Sheathing Beam Element	22
3.10 Sheathing Beam Tributary Areas and Continuity in Truss System Modeled by SAP2000	24
3.11 Actual Roof Truss Assembly with Sheathing Beam Elements	25
3.12 Boundary Condition for The Actual Roof Truss Assembly Model	26
3.13 MOE Lognormal Distribution for Mean Value 1.6E+06 psi	29
3.14 MOE Lognormal Distribution for Mean Value 1.4E+06 psi	30
3.15 Dimensions for Wood Members	32

LIST OF FIGURES (Continued)

<u>Figure</u>	<u>Page</u>
3.16 3:12 Slope, 28-Foot-Span Metal-Plate-Connected Fink Truss Tested at the FPL (Wolfe et al. 1986)	35
3.17 6:12 Slope, 28-Foot-Span Metal-Plate-Connected Fink Truss Tested at the FPL (Wolfe et al. 1986)	36
3.18 Semi-Rigid Joint Model Using SAP2000 Nlink (LS) Elements for 3:12 slope, 28-Foot-Span Fink Truss	37
3.19 Semi-Rigid Joint Model Using SAP2000 Nlink (LS) Elements for 6:12 slope, 28-Foot-Span Fink Truss	38
3.20 Truss Design Loads for Girder Trusses BGR, JGR and ASGR	40
3.21 MPC Truss Type A from a Truss Plate Manufacturer	41
3.22 The TPM's Model for Truss Type A with Semi-Rigid Joints Using SAP2000	42
3.23 Placement of Plywood Sheathing on 28-Foot-Span Nine-Truss Roof Assembly	44
3.24 Nine-Truss Assembly Modeled by SAP2000	45
3.25 The Actual Roof Truss Assembly	46
3.26 Roof Truss Assembly (Plan View)	48
3.27 Elevation View of Roof Truss Assembly	49
3.28 Close-Up of Truss Types J1, J2 and J3	50
4.1 CSI Values for Truss Type A Using SAP2000 and TPM Models	56
4.2 Three Sub-Assemblies in The Actual Roof Truss Assembly (Plan View)	72
4.3 The Connection between Truss Type A1 and Truss Type BGR-1	73

LIST OF FIGURES (Continued)

<u>Figure</u>	<u>Page</u>
4.4 Roof Truss Sub-Assembly (Plan View)	75
4.5 The Reaction Comparison for Truss Types A1-4, A-3 and A-2	76
4.6 Close-Up of Truss Type J Series and Trusses ASGR, AS1, AS2, and AS3	80

LIST OF TABLES

<u>Tables</u>	<u>Page</u>
3.1 The Number of Each Truss Type in The Actual Roof Truss Assembly	47
3.2 Truss Span Differences between Design Drawing and Truss Analog for Truss Types J1, J2 and J3	51
4.1 Deflection Comparisons for 3:12 Slope Fink	53
4.2 Deflection Comparisons for 6:12 Slope Fink	54
4.3 Load-Sharing Comparison for 3:12 Slope Truss Assembly with High Stiffness Variability	58
4.4 Load-Sharing Comparison for 6:12 Slope Truss Assembly with High Stiffness Variability	59
4.5 Load-Sharing Comparison for 3:12 Slope Conventional Truss Assembly	60
4.6 Load-Sharing Comparison for 6:12 Slope Conventional Truss Assembly	61
4.7 CSI Comparison for Maximum CSI Values from Individual Trusses and Truss Assembly	65
4.8 The Effect of MOE on Load Distribution (Reactions) for the Truss Type A1 Series with Design and Random Material Properties	68
4.9 The Effect of MOE on Load Distribution (Reactions) for the Truss Type A2 Series with Design and Random Material Properties	69
4.10 The Maximum CSI Values from Truss Types A2 Series and B Series	78
4.11 The Maximum CSI Values from the Truss Type J Series	81

LIST OF APPENDICES

	<u>Page</u>
Appendix A Comparison Between SAP2000 and ETABS	90
Appendix B Stiffness Derivation for NLLINK Elements for Semi-Rigid Truss Model	91
Appendix C Conversion Factors for Strength	101
Appendix D CSI Values Calculation	104
Appendix E Truss Design Drawings from the TPM	109
Appendix F The TPM's Models (Analog) for Individual Trusses with Semi-Rigid Joints	125
Appendix G SAP2000 Input and Output Files	141
Appendix H CSI Values for Individual Trusses Using SAP2000 Truss Model and TPM Model	152
Appendix I Comparison Between Two Types of Semi-Rigid Joints	166
Appendix J Joint Reactions for Truss Type A1 Series in the Assembly	183
Appendix K CSI Comparison for Individual Trusses with Different Boundary Conditions	187

LIST OF APPENDIX FIGURES

<u>Figure</u>	<u>Page</u>
B.1 Plate-Wood Contact Area for Heel Joint at Top Chord	93
B.2 Heel Joint Detail in Truss Type A, A1, and A2	95
B.3 Bottom-Chord-Tension-Splice Joint Detail for Truss Type ASGR	96
E.1 MPC Truss Type A1 from a Truss Plate Manufacturer	110
E.2 MPC Truss Type A2 from a Truss Plate Manufacturer	111
E.3 MPC Truss Type AS1 from a Truss Plate Manufacturer	112
E.4 MPC Truss Type AS2 from a Truss Plate Manufacturer	113
E.5 MPC Truss Type AS3 from a Truss Plate Manufacturer	114
E.6 MPC Truss Type ASGR from a Truss Plate Manufacturer	115
E.7 MPC Truss Type B from a Truss Plate Manufacturer	116
E.8 MPC Truss Type BGR from a Truss Plate Manufacturer	117
E.9 MPC Truss Type J from a Truss Plate Manufacturer	118
E.10 MPC Truss Type J1 from a Truss Plate Manufacturer	119
E.11 MPC Truss Type J2 from a Truss Plate Manufacturer	120
E.12 MPC Truss Type J3 from a Truss Plate Manufacturer	121
E.13 MPC Truss Type JGR from a Truss Plate Manufacturer	122
E.14 MPC Truss Type BGB from a Truss Plate Manufacturer	123

LIST OF APPENDIX FIGURES (Continued)

<u>Figure</u>	<u>Page</u>
E.15 MPC Truss Type AGB from a Truss Plate Manufacturer	124
F.1 The TPM's Model for Truss Type A1 with Semi-Rigid Joints Using SAP2000	126
F.2 The TPM's Model for Truss Type A2 with Semi-Rigid Joints Using SAP2000	127
F.3 The TPM's Model for Truss Type AS1 with Semi-Rigid Joints Using SAP2000	128
F.4 The TPM's Model for Truss Type AS2 with Semi-Rigid Joints Using SAP2000	129
F.5 The TPM's Model for Truss Type AS3 with Semi-Rigid Joints Using SAP2000	130
F.6 The TPM's Model for Truss Type ASGR with Semi-Rigid Joints Using SAP2000	131
F.7 The TPM's Model for Truss Type B with Semi-Rigid Joints Using SAP2000	132
F.8 The TPM's Model for Truss Type BGR with Semi-Rigid Joints Using SAP2000	133
F.9 The TPM's Model for Truss Type J with Semi-Rigid Joints Using SAP2000	134
F.10 The TPM's Model for Truss Type J1 with Semi-Rigid Joints Using SAP2000	135
F.11 The TPM's Model for Truss Type J2 with Semi-Rigid Joints Using SAP2000	136

LIST OF APPENDIX FIGURES (Continued)

<u>Figure</u>	<u>Page</u>
F.12 The TPM's Model for Truss Type J3 with Semi-Rigid Joints Using SAP2000	137
F.13 The TPM's Model for Truss Type JGR with Semi-Rigid Joints Using SAP2000	138
F.14 The TPM's Model for Truss Type BGB with Semi-Rigid Joints Using SAP2000	139
F.15 The TPM's Model for Truss Type AGB with Semi-Rigid Joints Using SAP2000	140
G.1 MPC Truss Type A1	142
G.2 TPM's Joint Model for Truss Type A1 Using SAP2000	143
H.1 CSI Values for Truss Type A1 Using SAP2000 Model and TPM's Output	153
H.2 CSI Values for Truss Type A2 Using SAP2000 Model and TPM's Output	154
H.3 CSI Values for Truss Type AS1 Using SAP2000 Model and TPM's Output	155
H.4 CSI Values for Truss Type AS2 Using SAP2000 Model and TPM's Output	156
H.5 CSI Values for Truss Type AS3 Using SAP2000 Model and TPM's Output	157
H.6 CSI Values for Truss Type ASGR Using SAP2000 Model and TPM's Output	158
H.7 CSI Values for Truss Type B Using SAP2000 Model and TPM's Output	159

LIST OF APPENDIX FIGURES (Continued)

<u>Figure</u>	<u>Page</u>
H.8 CSI Values for Truss Type BGR Using SAP2000 Model and TPM's Output	160
H.9 CSI Values for Truss Type J Using SAP2000 Model and TPM's Output	161
H.10 CSI Values for Truss Type J1 Using SAP2000 Model and TPM's Output	162
H.11 CSI Values for Truss Type J2 Using SAP2000 Model and TPM's Output	163
H.12 CSI Values for Truss Type J3 Using SAP2000 Model and TPM's Output	164
H.13 CSI Values for Truss Type JGR Using SAP2000 Model and TPM's Output	165
I.1 CSI Values for Two Types of Semi-Rigid Joint Models for Truss Type A	168
I.2 CSI Values for Two Types of Semi-Rigid Joint Models for Truss Type A1	169
I.3 CSI Values for Two Types of Semi-Rigid Joint Models for Truss Type A2	170
I.4 CSI Values for Two Types of Semi-Rigid Joint Models for Truss Type AS1	171
I.5 CSI Values for Two Types of Semi-Rigid Joint Models for Truss Type AS2	172
I.6 CSI Values for Two Types of Semi-Rigid Joint Models for Truss Type AS3	173

LIST OF APPENDIX FIGURES (Continued)

<u>Figure</u>	<u>Page</u>
I.7 CSI Values for Two Types of Semi-Rigid Joint Models for Truss Type ASGR	174
I.8 CSI Values for Two Types of Semi-Rigid Joint Models for Truss Type B	175
I.9 CSI Values for Two Types of Semi-Rigid Joint Models for Truss Type BGR	176
I.10 CSI Values for Two Types of Semi-Rigid Joint Models for Truss Type J	177
I.11 CSI Values for Two Types of Semi-Rigid Joint Models for Truss Type J1	178
I.12 CSI Values for Two Types of Semi-Rigid Joint Models for Truss Type J2	179
I.13 CSI Values for Two Types of Semi-Rigid Joint Models for Truss Type J3	180
I.14 CSI Values for Two Types of Semi-Rigid Joint Models for Truss Type JGR	181
I.15 Moment Diagrams of Truss Member 4 of Truss Type A with Different Peak Joint	182
J.1 Joint A in Truss Type A1-4	183
J.2 Free Body Diagram of Joint A	184
J.3 Joint A in Truss Type A1-4 with Different Boundary Condition	185

LIST OF APPENDIX FIGURES (Continued)

<u>Figure</u>	<u>Page</u>
K.1 CSI Comparison for Truss Type A with Different Boundary Conditions, Hinge-Roller and Hinge-Hinge	188
K.2 CSI Comparison for Truss Type A1 with Different Boundary Conditions, Hinge-Roller and Hinge-Hinge	189
K.3 CSI Comparison for Truss Type A2 with Different Boundary Conditions, Hinge-Roller and Hinge-Hinge	190
K.4 CSI Comparison for Truss Type AS1 with Different Boundary Conditions, Hinge-Roller and Hinge-Hinge	191
K.5 CSI Comparison for Truss Type AS2 with Different Boundary Conditions, Hinge-Roller and Hinge-Hinge	192
K.6 CSI Comparison for Truss Type AS3 with Different Boundary Conditions, Hinge-Roller and Hinge-Hinge	193
K.7 CSI Comparison for Truss Type ASGR with Different Boundary Conditions, Hinge-Roller and Hinge-Hinge	194
K.8 CSI Comparison for Truss Type B with Different Boundary Conditions, Hinge-Roller and Hinge-Hinge	195
K.9 CSI Comparison for Truss Type BGR with Different Boundary Conditions, Hinge-Roller and Hinge-Hinge	196
K.10 CSI Comparison for Truss Type J with Different Boundary Hinge-Roller and Hinge-Hinge	197
K.11 CSI Comparison for Truss Type J1 with Different Boundary Conditions, Hinge-Roller and Hinge-Hinge	198
K.12 CSI Comparison for Truss Type J2 with Different Boundary Conditions, Hinge-Roller and Hinge-Hinge	199

LIST OF APPENDIX FIGURES (Continued)

<u>Figure</u>	<u>Page</u>
K.13 CSI Comparison for Truss Type J3 with Different Boundary Conditions, Hinge-Roller and Hinge-Hinge	200
K.14 CSI Comparison for Truss Type JGR with Different Boundary Conditions, Hinge-Roller and Hinge-Hinge	201
K.15 Simplified TPM's Truss Model	202

LIST OF APPENDIX TABLES

<u>Tables</u>	<u>Page</u>
B.1 Joint Stiffness Values for The Truss Models	100
J.1 Axial Forces and Shear Forces for Five Members	184
J.2 Axial Forces and Shear Forces for Five Members (check)	186

A PRACTICAL METHOD TO ANALYZE THE SYSTEM EFFECTS OF A METAL-PLATE-CONNECTED WOOD TRUSS ASSEMBLY

1. INTRODUCTION

Metal-Plate-Connected (MPC) trusses are used in over 90% of all residential, commercial and agricultural buildings in the United States. The conventional design method for an MPC wood truss assembly is based on single truss design. For a truss assembly, this procedure may cause over-design because of ignoring system effects. From Wolfe and LaBissoniere's results (1991), the strength of a truss assembly was larger than that predicted based on single truss design, because of the system effects. The current National Design Specification (NDS, 1997) does consider system effects in its repetitive member factor ($C_r=1.15$), but this is applied only for bending and not for tension and compression.

A practical method will be presented here to analyze an actual wood roof truss assembly, to investigate its system performance, and to examine the benefits of modeling the entire truss assembly over the conventional single truss design method. For an actual roof truss assembly, the Combined Stress Index (CSI) values for truss members in the entire assembly will be calculated and they will be compared with the CSI values for the same type of isolated individual truss to examine the system effects. In this study, the analytical models will be developed for the entire truss assembly, so the system effects will be considered directly and the results will be a more complete description of behavior than those extended

from individual truss models. Variability of modulus of elasticity (MOE), interaction of sub-assemblies, boundary conditions and modeling methods will be considered in the modeling of the actual roof truss assembly.

Since MPC wood trusses are extensively used in roof truss assemblies (Showalter and Grundahl, 1991), a design method that considers the system effects may lead to significant savings in wood use. Mtenga (1998) suggested that the truss designer can obtain the following benefits by considering the system effects: (1) the system can carry more load, (2) the cross-sectional areas of members can be reduced, (3) the truss spacing and the sheathing span can be increased, and (4) lower lumber grades may be used.

Conventionally, MPC joints are analyzed as either pinned or rigid connections. In this study, there are also two different types of semi-rigid joints used for the truss models. One type of semi-rigid joint uses linear spring (LS) elements, and the other type uses joint models from a truss plate manufacturer (TPM). Both types of the semi-rigid joints will be explained later in more detail in Chapter 3.

In this study, a widely used structural analysis program, SAP2000 (1997), was used to model the MPC trusses and truss assemblies. This commercial software offers a linear spring element to model the semi-rigid connections and a powerful graphical interface for users.

1.1 Objectives

The objective of this study is to develop an efficient and practical method using a commercially-available computer program, SAP2000, to analyze MPC wood trusses and roof truss assemblies. This approach may be an improvement over the conventional single truss design methods, by more accurately modeling the entire truss assembly, including the system effects, and potentially providing benefits of improved safety and reduced construction cost over the conventional design method.

1.2 Scope

There are three major aspects to this study:

1. The use of LS elements for the semi-rigid joints to model individual trusses and nine-truss roof assemblies from the literature, and the use of a TPM's semi-rigid joint models to model individual trusses using the computer program SAP2000 (1997);
2. The truss models using LS joints were verified by comparison with experimental results from the literature. The individual truss models using TPM's joints were verified by comparison with output results from a TPM;
3. The actual roof truss assembly with the TPM's joint models was analyzed and CSI values for each truss member determined. From a

comparison of CSI values for truss members in an assembly and in individual trusses, the system effects were investigated.

By using the computer program, SAP2000 (1997), a practical method is presented to analyze an actual roof truss assembly that includes plywood sheathing and fourteen different types of trusses. There are fifty-six trusses in this roof assembly. The study will compare the CSI values for individual trusses with the CSI values for the same trusses that are assembled together in a roof assembly to show the system effects and examine potential benefits of modeling the entire truss assembly system.

2. LITERATURE REVIEW

2.1 MPC Joint

The most common models for the connections at metal-plate-connected (MPC) truss joints are either pinned or rigid, but these do not accurately represent the real semi-rigid behavior of MPC joints. The stiffness of a semi-rigid joint is somewhere between that of pinned and rigid connection (Suddarth 1963). From Gupta's (1990) research results, the maximum deflection of a 28-foot-span MPC Fink truss with semi-rigid joints was 34% less than for a model with all pinned joints.

To analyze truss-plate connections, Gupta (1990 and 1994), Foschi (1977b), McCarthy and Wolfe (1987), Gebremedhin et al. (1992), Gupta and Gebremedhin (1992), and Stahl et al. (1994) developed joint connection models to examine the performance and mechanics of the joints. Gebremedhin et al. (1992) observed the nonlinear characteristics of the load-deformation relationship. The results also showed that a 2-parameter nonlinear model predicted the load-deformation curve quite well. In Vatovec's (1996) and Mtenga's (1991) joint models, the nonlinear load-deformation relationship was also considered. The models were accurate in predicting connection behavior, but may be too complex for practical design usage. For ease of application, linear load-deformation behavior and simplified joint models are used in this study. Experimental results were only available for the

behavior of heel joints and bottom- chord tension splice joints, so only these joints were modeled as semi-rigid in the MPC trusses in this study.

2.2 Truss and Truss Assembly Models

In Maraghechi and Itani's (1982) study, light-frame trusses were modeled using two types of elements: beam elements and joint elements. The joint element was composed of three linear springs without physical dimensions, providing moment, shear, and axial resistance. Their results indicated that rotational stiffness was proportional to the connection contact area.

In Li's (1997) single truss models, two types of elements were used, linear spring elements for joints and beam elements for truss members. The stiffness of a spring element was calculated from the plate-wood contact area following the approach of Foschi (1977b). Truss members were modeled by beam elements. The connections between beam elements were pinned, rigid, or semi-rigid joints. This truss model (Li, 1997) will be modified for use with SAP2000 (1997) in this study.

Varoglu and Barrett (1984) and Varoglu (1985) used Forintek's structural analysis computer program, SATD (Structural Analysis for Trusses and Diaphragms), as a base line and developed a new program, SAT (Structural Analysis for Trusses), for simulation studies. SAT's theoretical background was discussed by Foschi (1977a). In Varoglu's (1985) study, the computer programs were improved and tested using different input conditions. In the strength and

stiffness analyses, the predicted results using SAT showed that the load-deflection responses agreed with the experimental values (Wolfe et al., 1986).

Cramer and Wolfe (1989) developed a three-dimensional frame analysis program, ROOFSYS, based on the matrix stiffness-method and Wang's (1983) and Vanderbilt's (1974) work. The semi-rigid connections and nonlinear behavior of a truss system were simplified to a linear model with simple hinged connections. The partially composite T-beam effect was also included using Kuenzi and Wilkinson's (1971) approach. This model could predict the load distribution quite well when extreme variations in truss stiffness occur.

In LaFave (1990) and LaFave and Itani (1992), experimental results and analytical studies were compared to estimate the load sharing effect and predict the load distribution in a wood truss roof system. Roof assembly sheathing was three ply, APA rated, white fir plywood panels. In this roof truss system model, a three-dimensional frame element with six degrees of freedom at each end was used. The semi-rigid behavior of truss joints was modeled using the stiffness matrix (Wang 1986). There is very limited model verification performed in this study, so its application to a wide range of truss configurations and plate connectors is questionable.

The NARSYS program (Nonlinear Analysis of Roof SYStem) by Mtenga (1991), and Cramer et al. (1993), was presented as a method for determining the strength of roof assemblies. This program included linear elastic, three-dimensional frame elements to represent the wood truss members, nonlinear springs and rigid

links to represent the joint connections, and deep beams to represent the roof sheathing. The sheathing beams were pin-connected to the trusses. Warner and Wheat (1986) developed the algorithm for NARSYS. The metal-plate load-slip properties followed Foschi's (1977b) definitions. This study's (Cramer et al. 1993) results showed that the conventional design of repetitive use members in a roof assembly was conservative. The study also indicated that roof slope and other truss characteristics could cause significant changes in the system effects.

In Li's (1997) assembly model, a nine-truss roof assembly was modeled using ETABS (1995). The Fink roof truss assembly studied had a 28-foot-span and 15/32" plywood sheathing. Two types of elements, beam elements and spring elements, were used to model the truss assembly. Beam elements were used for truss members and plywood sheathing and spring elements were used for the semi-rigid connections. Experimental results of King and Wheat (1987), Wolfe and McCarthy (1989), and Wolfe and LaBissoniere (1991) were used to verify this model, and the predictions of truss performance using this model were very good. Li's (1997) roof truss assembly model will be modified for this study.

Li (1997) modeled MPC trusses using the computer program, ETABS (1995), but a different computer program, SAP2000 (1997), is used for this study. For a truss system analysis, SAP2000 has several advantages over ETABS. A discussion of these two computer programs is included in Appendix A.

2.3 Actual Truss and Truss Assembly Tests

Wolfe et al. (1986) tested two 28-foot-span Fink truss configurations, with slopes of 3:12 and 6:12, using Southern Pine No. 2 lumber, to failure. Linear load-deformation behavior was observed for the trusses up to twice their design load. In King and Wheat's (1987) study, nine parallel-chord, MPC trusses were uniformly loaded up to the full design load. In the load-deflection responses and load versus axial force curves, all of the trusses exhibited linear behavior. The deflections, axial forces and bending moments from their test results will be used to verify the MPC truss model used in this study. Wolfe and McCarthy (1989) and Wolfe and LaBissoniere (1991) presented two reports describing the performance of a full-scale roof assembly. Report I (Wolfe and McCarthy, 1989) emphasized high truss stiffness variability in truss assemblies. Report II (Wolfe and LaBissoniere, 1991) examined the development and verification of conventional roof assembly models. In both reports, the Fink type trusses were fabricated using Southern Pine 2"x4" No. 2 lumber with slopes of 3:12 and 6:12. They were designed for a 2' truss spacing and a 28' span. 15/32-in.-thick CD exterior grade sheathing was used and the lumber MOE values were divided into three categories. In Report II (Wolfe and LaBissoniere, 1991), there was a gable end for each roof, and it was one of the previously failed trusses sheathed with plywood as a partition wall.

In Report I (Wolfe and McCarthy, 1989), the actual truss assemblies used a combination of 16-gauge and 20-gauge connector plates. 16-gauge metal-connector-plates (MCPs) were used on critical joints to cause failure in the wood

members, while other joints used 20-gauge MCPs. In Report II (Wolfe and LaBissoniere, 1991), all the MCPs were 20-gauge connector plates. The results demonstrated the following important points for Report I (Wolfe and McCarthy, 1989):

1. Stiffer trusses carry a greater share of the load in the assembly.
2. The load-deflection behavior in the assembly was approximately linear.
3. In the range of design load, the average truss deflection within the assembly is 50 percentage lower than that of an individual truss outside the assembly. The average failure loads increased 20 percent inside the assembly compared to individual trusses outside the assembly.

In Report II (Wolfe and LaBissoniere, 1991), the results of this study show that the interactions within the assembly control the deflections of members, because repetitive member roof assemblies behave like parallel systems. The most significant conclusions are the following:

1. When the top chord of an individual truss was loaded to the design load, the loaded truss in the assembly only carries 30 to 60 percent of the applied load and distributes 70 to 40 percent of the load to the adjacent unloaded trusses through the plywood sheathing.
2. By increasing the effective moment of inertia of the top chord, the effective stiffness will increase because of the composite action between the sheathing and the top chord. In the Fink truss roof assembly, there was a 24 percent stiffness increase from composite action.

The experimental results from these two reports will be used to verify the MPC truss models in this study.

3. TRUSS AND TRUSS ASSEMBLY MODELS

3.1 MPC Joint Model

In addition to traditional pinned and rigid joint models, the following two joint models were used to represent the semi-rigid behavior of MPC joints.

3.1.1 Linear Spring Joint Model

In the modeling using linear spring (LS) elements for the semi-rigid joints, both Frame elements and Nlink elements are used by SAP2000 (1997).

From the Analysis Reference Volume 1 of SAP2000 (1997), Nlink elements have no physical dimensions (zero-length). The Nlink elements are linear spring elements used for modeling the semi-rigid connections in this study. Each Nlink element is assumed to be composed of six separate springs. The force-deformation relationships for these springs may be coupled or independent of each other. These springs can be used for nonlinear or linear analysis. Every Nlink element has six deformational degrees of freedom, three axial stiffnesses (K_x , K_y , and K_z) and three rotational stiffnesses (K_{xx} , K_{yy} , and K_{zz}). There are six types of Nlink elements in SAP2000 (1997) and these types are viscoelastic damping, gap, hook, uniaxial plasticity, biaxial-plasticity base isolator, and friction-pendulum base isolator. The differences among these six types involve the various properties of the nonlinear springs, but all of the Nlink elements are the same for linear

analyses. In this study, these springs are all linear for simplification, although the actual load-displacement relationships for the MPC joints are nonlinear. The spring force-deformation relationships can be expressed in the following matrix form:

$$\begin{Bmatrix} f_{u1} \\ f_{u2} \\ f_{u3} \\ f_{r1} \\ f_{r2} \\ f_{r3} \end{Bmatrix} = \begin{bmatrix} K_x & 0 & 0 & 0 & 0 & 0 \\ 0 & K_y & 0 & 0 & 0 & 0 \\ 0 & 0 & K_z & 0 & 0 & 0 \\ 0 & 0 & 0 & K_{xx} & 0 & 0 \\ 0 & 0 & 0 & 0 & K_{yy} & 0 \\ 0 & 0 & 0 & 0 & 0 & K_{zz} \end{bmatrix} \begin{Bmatrix} d_{u1} \\ d_{u2} \\ d_{u3} \\ d_{r1} \\ d_{r2} \\ d_{r3} \end{Bmatrix} \quad (3.1)$$

where

f_{u1} =axial force	d_{u1} =displacement in axial direction
f_{u2} =shear force in the x-y plane	d_{u2} =displacement in f_{u2} shear direction
f_{u3} =shear force in the x-z plane	d_{u3} =displacement in f_{u3} shear direction
f_{r1} =torsion	d_{r1} =torsional angle due to f_{r1}
f_{r2} =bending moment in the x-z plane	d_{r2} =rotational angle due to f_{r2} in the x-z plane
f_{r3} =bending moment in the x-y plane	d_{r3} =rotational angle due to f_{r3} in the x-y plane

K_x , K_y , and K_z are the three axial stiffnesses and K_{xx} , K_{yy} , and K_{zz} are the three rotational stiffnesses of the internal springs. Example calculations for the stiffnesses of Nllink elements used as MPC joints are shown in Appendix B.

Two Nllink elements are used for each semi-rigid joint and they are connected by a *rigid link* modeled by a Frame element. The ‘rigid link’ has the same dimensions, i.e. 1.5 in. x 3.5 in., as the two connected truss members and its

MOE value is the same as that of steel (Li, 1997). The length of the rigid link is the distance between the two Nlink elements. In Figure 3.1, this metal plate is assumed to be divided evenly by the ends of the two truss bottom chords. The distance between A and B is the length of the rigid link. A and B are the centers of gravity for each separate plate contact area. In Figure 3.2, the metal plate is assumed to be divided evenly by the intersection line between the truss top chord and truss bottom chord. Point C is where the two centerlines of the top chord and bottom chord of truss intersect. Z1 and Z2 axes go through the centers of gravity of the plate-wood contact areas at the top chord and bottom chord, respectively. Points D and E are the intersection points at which the centerline of truss bottom chord and the two axes, Z1 and Z2, intersect. The distance between C and E is the length of the rigid link.

The modeling method using LS elements for the semi-rigid connections is the same as Li's (1997). The stiffnesses of the metal plates can be represented using the stiffnesses of the LS elements.

3.1.2 TPM's Joint Model

Truss Plate Manufacturer's (TPM's) joint models for peak and heel joints are shown in Figures 3.3 and 3.4, respectively. The TPM's joint model was also used for truss type A2 at the bottom chord panel joints and for truss types AS1, AS2, AS3 and ASGR at the top chord panel joints. The joint model uses a combination of rigidly connected elements as shown in Figures 3.3 and 3.4. Material properties

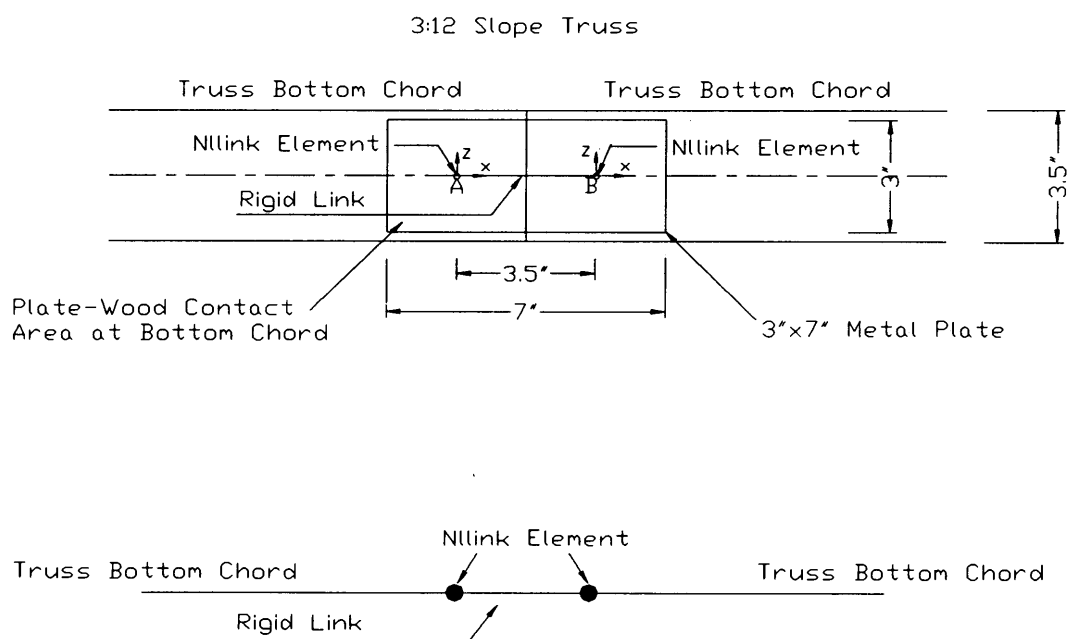


Figure 3.1 Bottom Chord Tension Splice Joint Detail in 3:12 Slope, 28-Foot-Span, Semi-Rigid Truss Model with 3" x 7" Metal Plate Using Linear Spring Elements

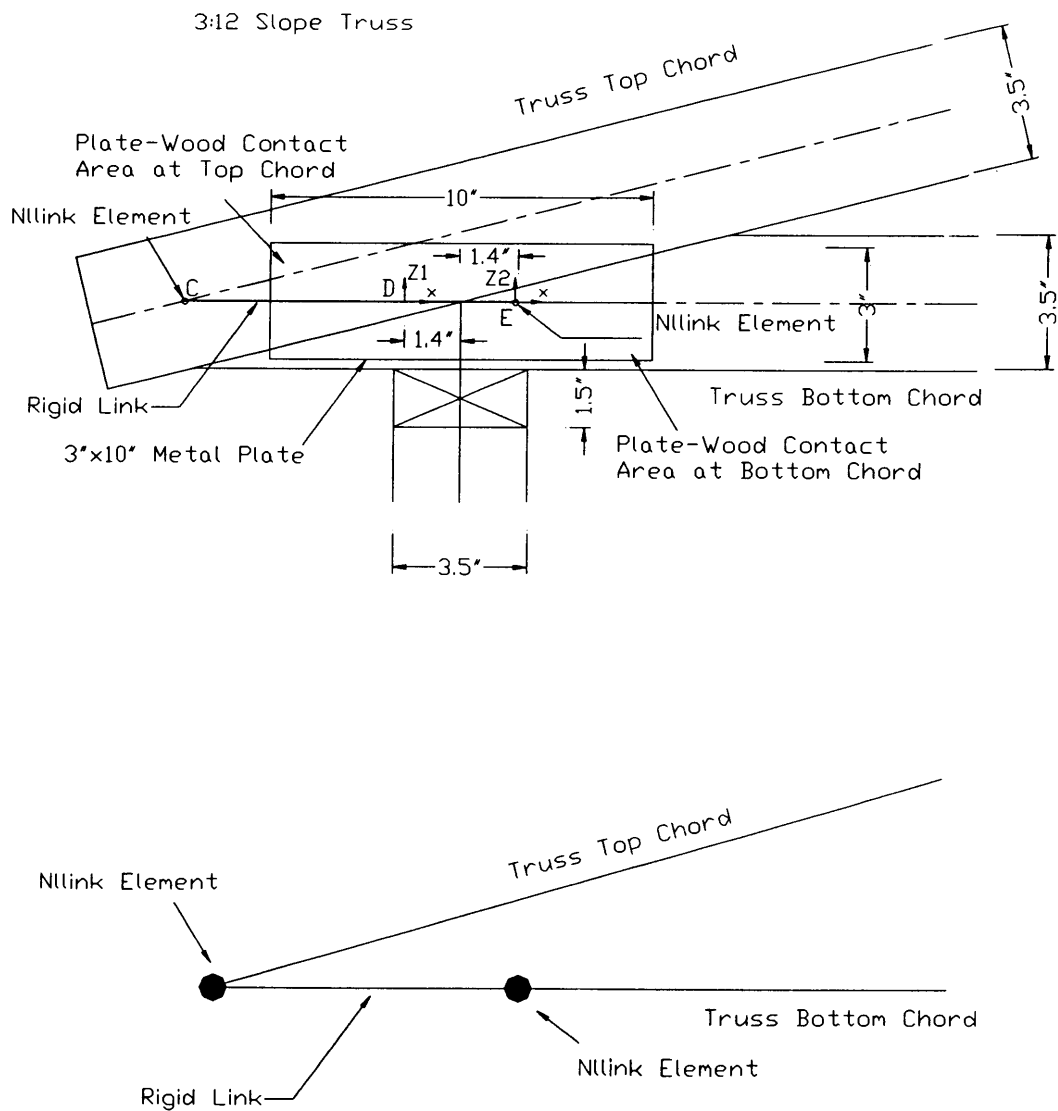


Figure 3.2 Heel Joint Detail in 3:12 Slope, 28-Foot-Span, Semi-Rigid Truss Model with 3" x 10" Metal Plate Using Linear Spring Elements

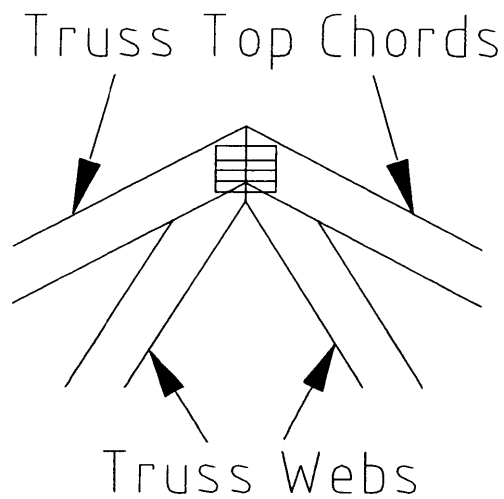
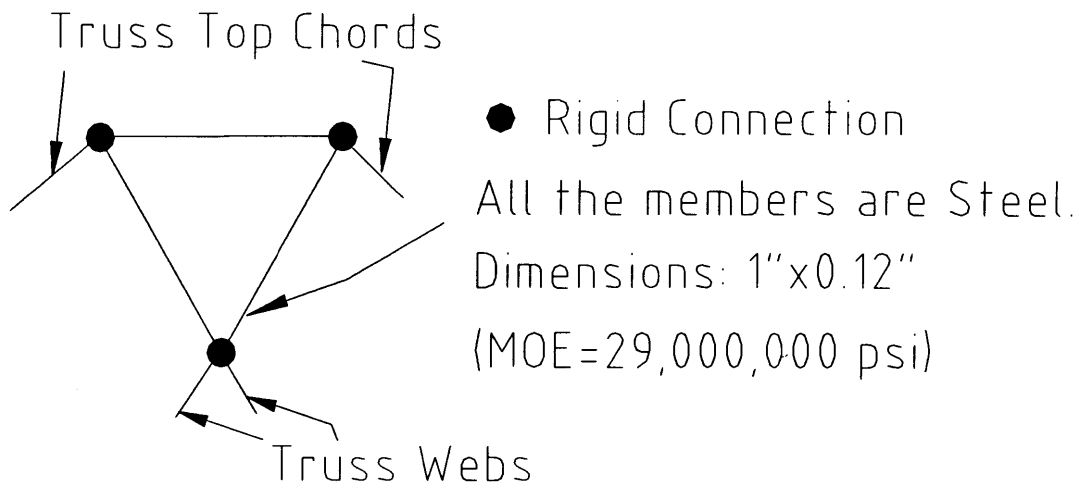


Figure 3.3 Truss Plate Manufacturer's Semi-Rigid Joint Model for Peak Joints

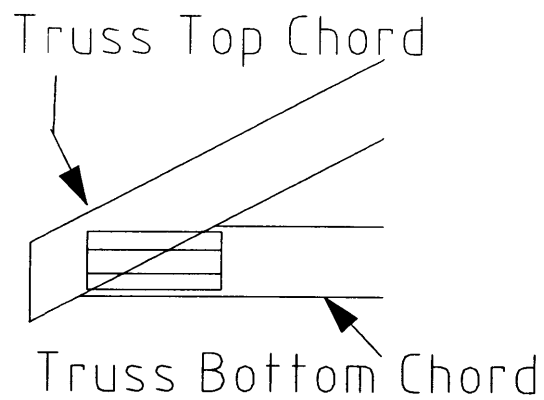
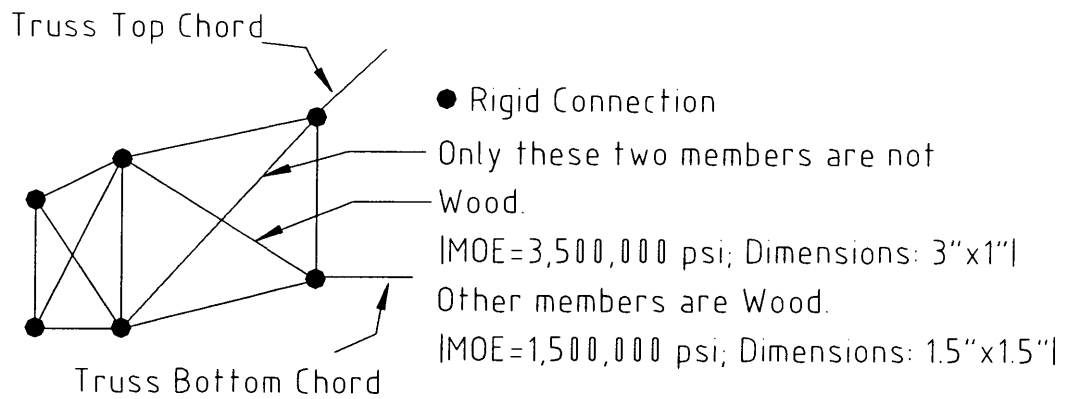


Figure 3.4 The Truss Plate Manufacturer's Semi-Rigid Joint Model for Heel Joints

for all the members in joint models were obtained from the TPM. Since the joint model is proprietary, no other information is available.

3.2 Frame Elements

3.2.1 Truss Members

Frame elements are used to model wood truss members, including top chords, bottom chords, and webs. In SAP2000 (1997), the Frame element uses a general, three-dimensional, beam-column formulation including the effects of biaxial bending, torsion, axial deformation, and biaxial shear deformations. The Frame element is modeled as a straight line between two joints, and it has six degrees of freedom at each end. Using the function “Frame Section”, the material and geometric properties can be defined for the Frame elements. Figure 3.5 shows an example of the assigned material and geometric properties for a frame element in SAP2000 and Figure 3.6 shows the section properties calculated by SAP2000. For this frame element, the user only assigns MOE, Poisson’s ratio and the dimensions for the rectangular section, then SAP2000 automatically calculates the other section properties for the element.

To model the truss members in this study, frame elements are placed along the actual members’ centerlines with constant, rectangular cross sections. The frame elements are joined with pinned, rigid, and semi-rigid connections. Their design material properties are assigned from the NDS (1991).

Dimensions	
Depth (t3)	3.5
Width (t2)	1.5

Analysis Property Data	
Mass per unit Volume	0.
Weight per unit Volume	0.
Modulus of elasticity	1600000
Poisson's ratio	0.2
Coeff of thermal expansion	0.

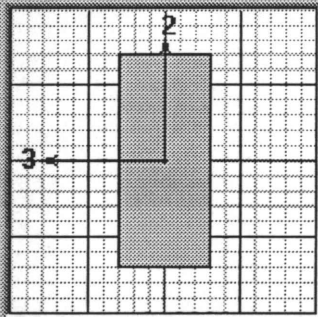


Figure 3.5 Assigned Material and Geometric Properties for the Frame Element

Section Name		TC1	
Properties			
Cross-section (axial) area	5.25	Section modulus about 3 axis	3.0632
Torsional constant	2.8774	Section modulus about 2 axis	1.3126
Moment of Inertia about 3 axis	5.3594	Plastic modulus about 3 axis	4.5948
Moment of Inertia about 2 axis	0.9844	Plastic modulus about 2 axis	1.969
Shear area in 2 direction	4.375	Radius of Gyration about 3 axis	1.0105
Shear area in 3 direction	4.375	Radius of Gyration about 2 axis	0.433

Figure 3.6 Section Properties Calculated by SAP2000 for the Frame Element

3.2.2 Plywood Sheathing Beam Elements

The sheathing beam elements are also modeled using Frame elements. The sheathing can be assigned the same thickness, width, and MOE as the actual plywood. Plywood material for the roof truss assembly in this study is American Plywood Association (APA) rated sheathing, 15/32", 3-ply Southern Pine (MOE: 1.4×10^6 psi) with a span rating of 32/16. As shown in Figure 3.7, the minor axis of a sheathing beam is aligned with the truss top chord, and its major axis is perpendicular to the slope of the truss top chords.

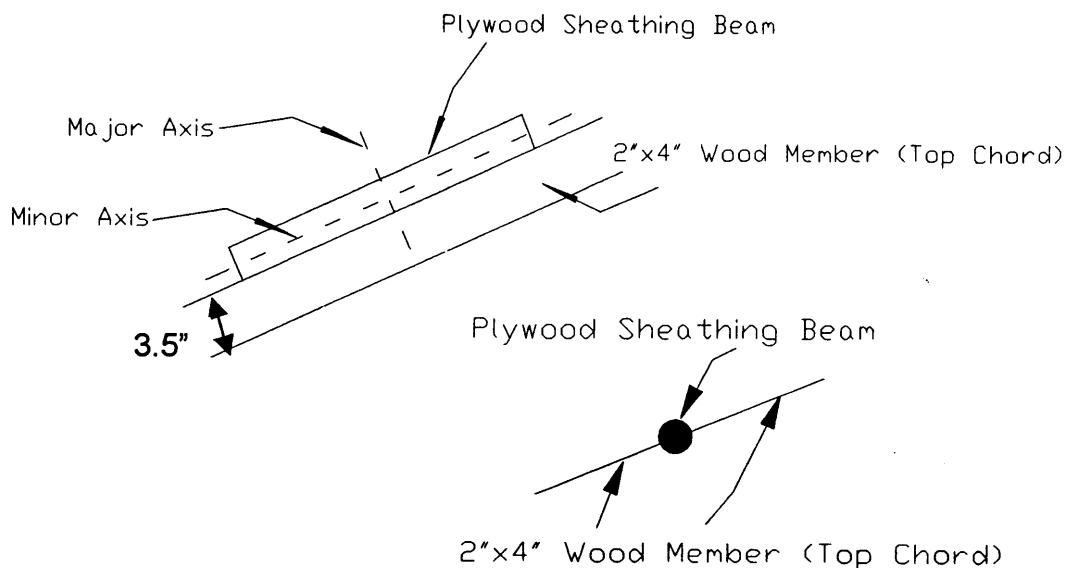


Figure 3.7 Detail of a Sheathing Beam

Figure 3.8 shows an example of the assigned material and geometric properties for a sheathing beam and Figure 3.9 shows the section properties calculated by SAP2000. For this sheathing beam element, the user only assigns

Dimensions	
Depth (t3)	0.4688
Width (t2)	33.34

Analysis Property Data	
Mass per unit Volume	0.
Weight per unit Volume	0.
Modulus of elasticity	1400000
Poisson's ratio	0.2
Coeff of thermal expansion	0.

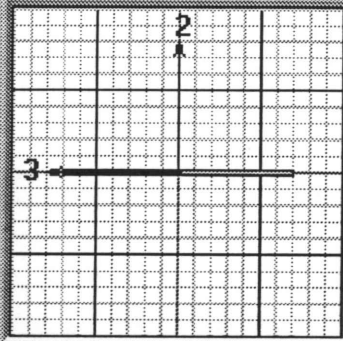


Figure 3.8 Assigned Material and Geometric Properties for the Sheathing Beam Element

Section Name		SHEATHIN	
Properties			
Cross-section (axial) area	15.6298	Section modulus about 3 axis	1.2212
Torsional constant	1.1349	Section modulus about 2 axis	86.8495
Moment of Inertia about 3 axis	0.2863	Plastic modulus about 3 axis	1.8318
Moment of Inertia about 2 axis	1447.782	Plastic modulus about 2 axis	130.2743
Shear area in 2 direction	13.0248	Radius of Gyration about 3 axis	0.1353
Shear area in 3 direction	13.0248	Radius of Gyration about 2 axis	9.6244

Figure 3.9 Section Properties Calculated by SAP2000 for the Sheathing Beam Element

MOE, Poisson's ratio the dimensions for the rectangular section, then SAP2000 automatically calculates the other section properties for the sheathing beam element.

Discontinuities (or gaps) between the sheathing are modeled by pinned connections as shown in Figure 3.10 for the nine-truss assembly. The sheathing beam elements are rigidly connected to the top chords of trusses. The sheathing beam element has a thickness of $15/32''$. In the figure, the tributary area for each sheathing beam is shown using the shaded and unshaded areas. For the actual roof truss assembly model, the sheathing beam element also has a thickness of $15/32''$. Because the configurations of the component trusses are different, the plywood sheathing areas are different. In the actual roof truss assembly model, all of the sheathing beams are rigidly connected to the truss top chords, and there is no sheathing discontinuity modeled because no specific information for placement of plywood sheathing was provided by the TPM. Moreover, this simplified the model of the complex assembly and helped to limit the number of variables for the analysis of system effects. Finally, the modeling of the gaps in the sheathing beams still needs more development. For the above reasons, the plywood sheathing is modeled without gaps for the actual roof truss assembly. Figure 3.11 shows the actual roof truss assembly model with sheathing beam elements.

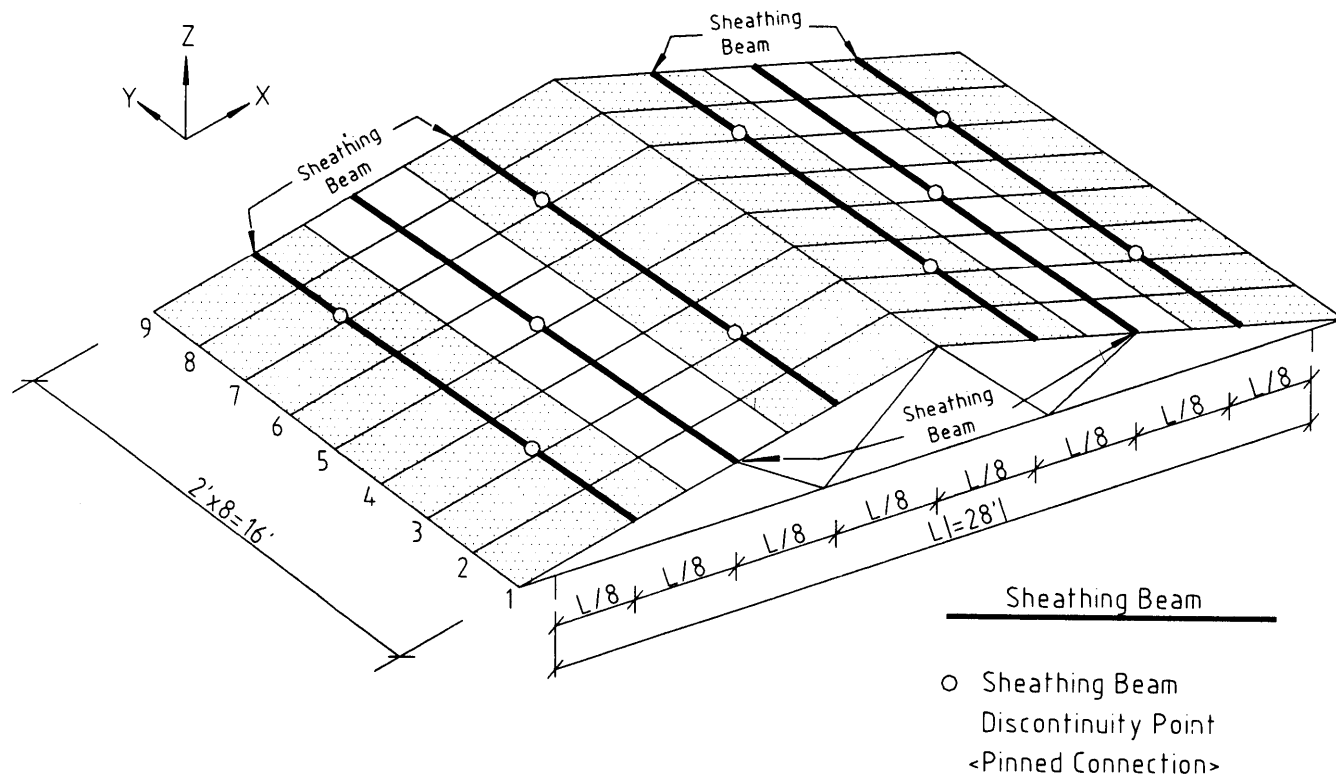


Figure 3.10 Sheathing Beam Tributary Areas and Continuity in Truss System Modeled by SAP2000

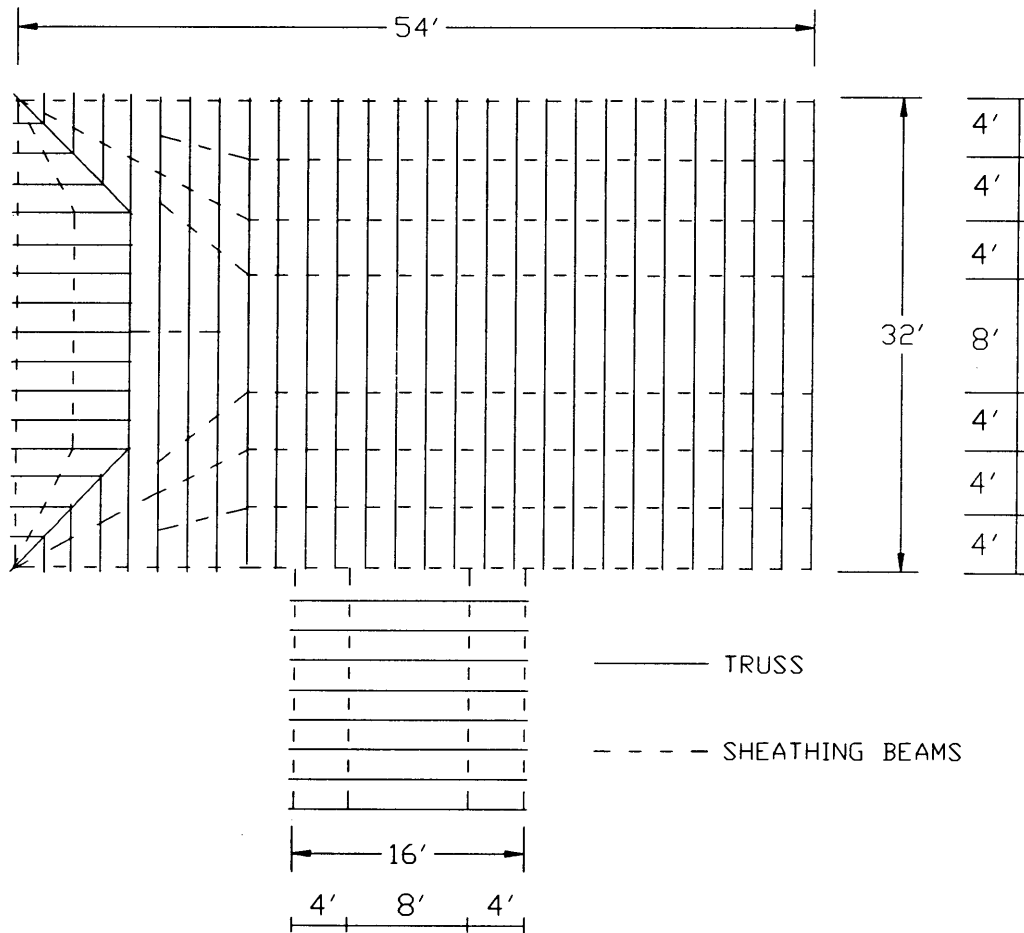


Figure 3.11 Actual Roof Truss Assembly with Sheathing Beam Elements

3.3 Boundary Conditions for Actual Roof Truss Assembly Model

The boundary conditions for the model of the actual roof truss assembly should simulate the connections between the walls and trusses. This study assumed that the trusses are connected to the walls using pinned connections. However, the walls are not rigid bodies and their stiffnesses depend on their geometry and material properties. Because the stiffnesses of the walls are unknown, the entire boundary of the roof system was modeled using hinged joints for the actual roof truss assembly model in this study, both for simplicity and for symmetry as in the real situation. In the conventional design method, the support conditions for a single truss are a hinged support on one end and a roller support on the other end (more detail is discussed in section 4.4.3.). Figure 3.12 shows the boundary conditions for the model of the actual roof truss assembly.

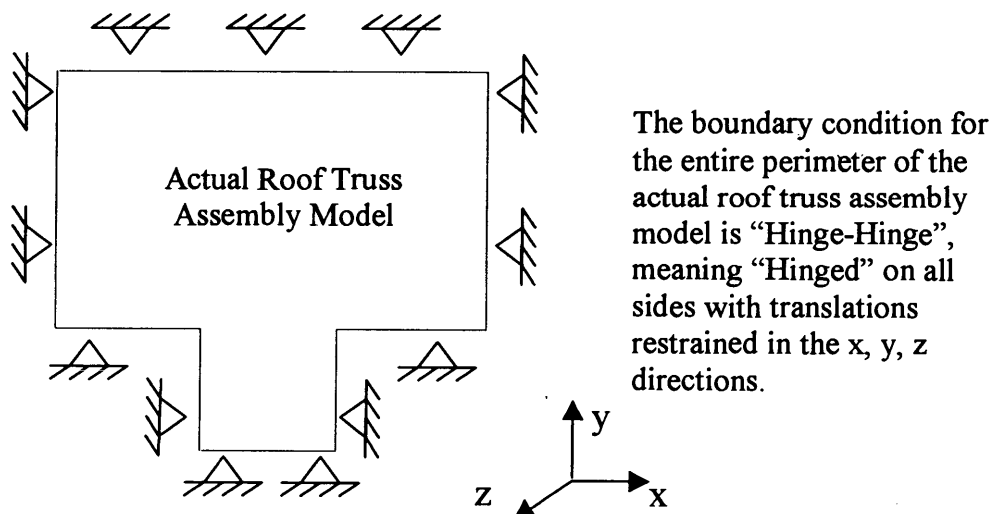


Figure 3.12 Boundary Condition for The Actual Roof Truss Assembly Model

3.4 Material Properties for Actual Roof Truss Assembly Model

There are two kinds of material properties used in the analyses of the actual roof truss assembly, design and random material properties. Design material properties are obtained from the NDS (1991) and random material properties are obtained as explained below.

Wood is a natural material and its mechanical properties vary within the same species. For this reason, the MOE (modulus of elasticity) values for different truss members vary within a truss. The conventional design method uses a single value (the design value) for MOE from the NDS (1991) for all members. An individual member in a truss can have a higher or lower MOE value than the design value. The main focus of the study was to use design material properties to study the system effects in roof truss assemblies. Realistically, random material properties should be used with Monte-Carlo simulation to study the system effects in roof truss assembly. Since this was not the focus of the study, only one set of random material properties was used to evaluate the system effects, and whose results could be used as starting point for future studies.

The MOE data are best characterized by a lognormal distribution (Gupta 1990). The coefficient of variation (COV) for the modulus of elasticity of visually graded lumber is 25% (NDS 1997). From the input files for the actual roof truss assembly from the TPM, there are forty pieces of lumber with an MOE design value of 1.6×10^6 psi and one hundred and eighty-five pieces of lumber with an MOE design value of 1.4×10^6 psi. A FORTRAN program was used to generate

random MOE values following a lognormal distribution. The original lognormal distributions and generated random MOE values are shown in Figures 3.13 and 3.14.

Wood tensile (TS), compressive (CS), and bending strengths (BS), are used in the CSI values calculations. Random values for these mechanical properties can be calculated by Gerhards' (1983) test results (for Southern Pine) based on the random MOE values:

$$\text{Tension Strength (TS)} = -717 + 0.002823 * \text{MOE}(\text{pounds/in.}^2)$$

$$\text{Compressive Strength (CS)} = 1245 + 0.001949 * \text{MOE}(\text{pounds/in.}^2)$$

$$\text{Bending Strength (BS)} = 90 + 0.004276 * \text{MOE}(\text{pounds/in.}^2)$$

TS, CS, and BS values from these formulas are the ultimate strengths. They were converted to design values using a procedure shown in Appendix C.

3.5 CSI Equations

In this study, the Combined-Stress-Index (CSI) calculations for wood members follow the NDS (1997) and ANSI/TPI (1-1995) equations.

Bending and Axial Tension:

$$CSI = \frac{f_t}{F'_t} + \frac{f_b}{F_b * } \leq 1.0 \quad (3.2)$$

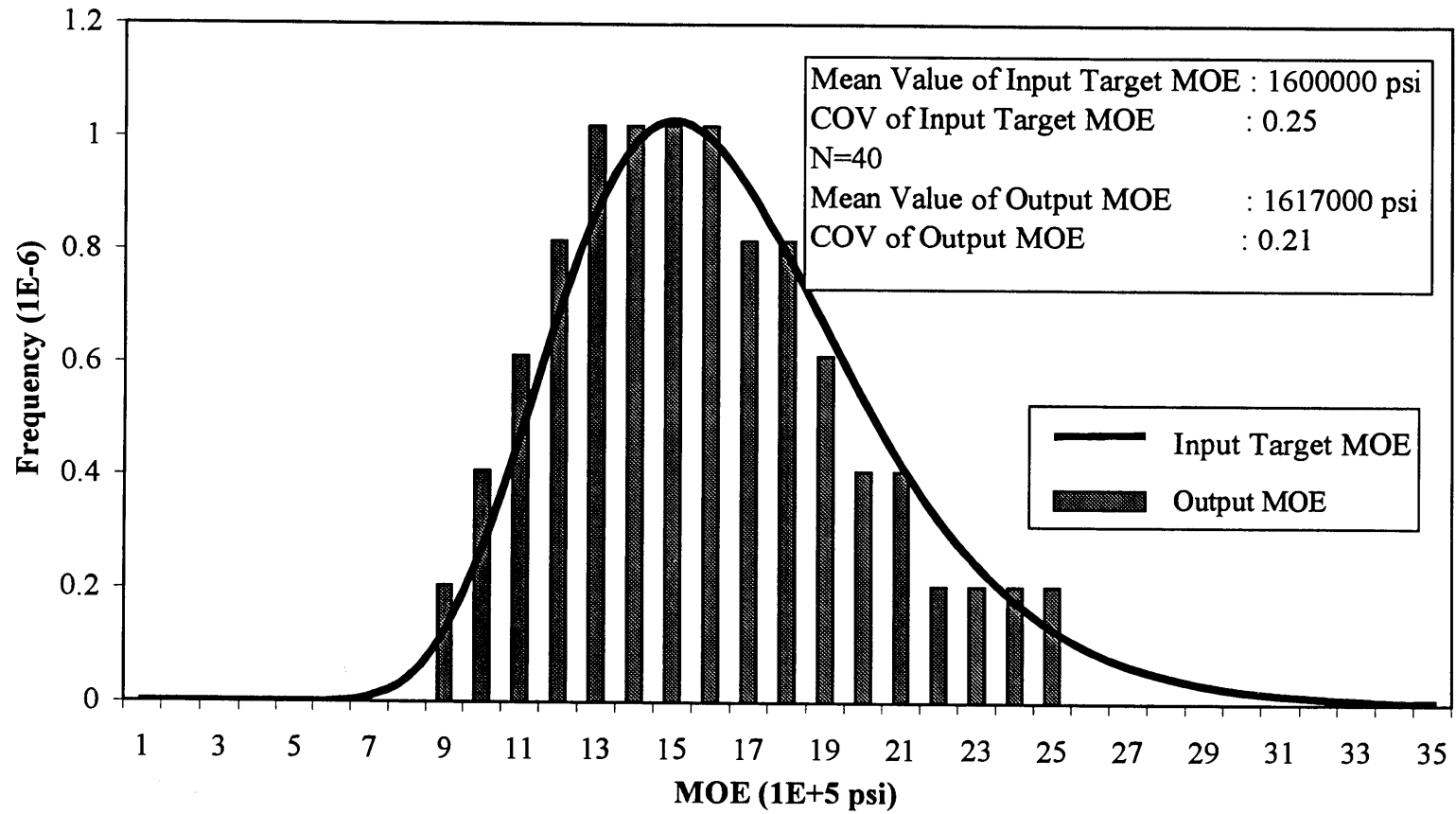


Figure 3.13 MOE Lognormal Distribution for Mean Value 1.6E+06 psi

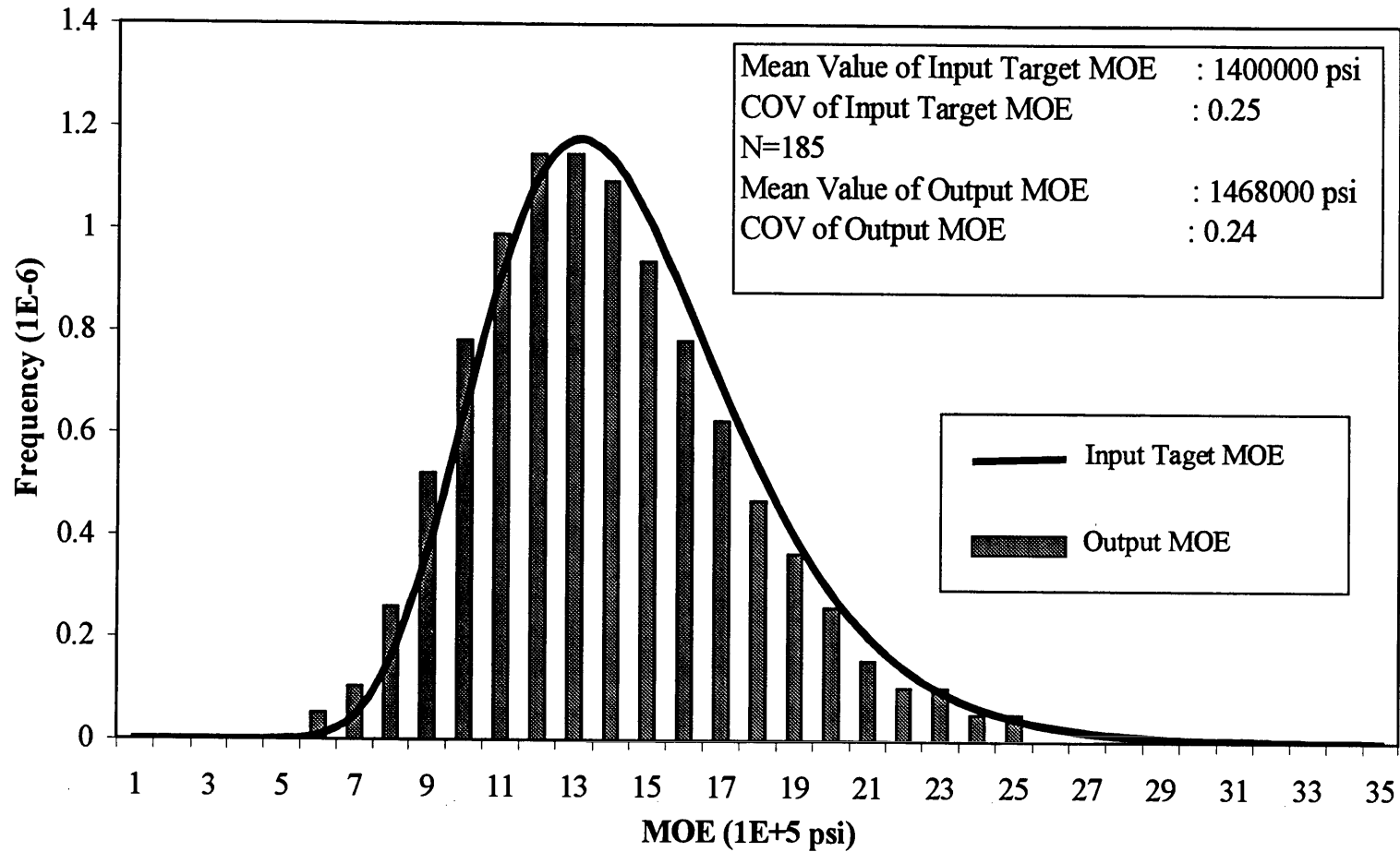


Figure 3.14 MOE Lognormal Distribution for Mean Value 1.4E+6 psi

Bending and Axial Compression:

$$CSI = \left(\frac{f_c}{F'_c} \right)^2 + \left(\frac{f_{bx}}{F'_b \left(1 - \frac{f_c}{F_{cEx}} \right)} \right)^2 + \left(\frac{f_{by}}{F'_{by} \left(1 - \frac{f_c}{F_{cEy}} - \left(\frac{f_{bx}}{F_{bEx}} \right)^2 \right)} \right)^2 \leq 1.0 \quad (3.3)$$

Where

f_t = Axial Tension Stress

f_b = Bending Stress

f_c = Axial Compression Stress

F'_t = Tabulated Tension Design Value Multiplied by Applicable Adjustment Factors (C_D),

C_D = Load Duration Factor

F'_b = Tabulated Bending Design Value Multiplied by Applicable Adjustment Factors (C_r and C_D)

C_r = Repetitive Member Factor, for truss chords or similar members with spacing not more than 24" on centers and not less than three in number and are jointed by floor, roof or other load distributing elements adequate to support the design load. (C_r was used to modify F_b for both assemblies and individual trusses in this study.)

F'_c = Tabulated Compression Design Value Multiplied by Applicable Adjustment Factors (C_D)

F_b^* = Tabulated Bending Design Value Multiplied by All Applicable Adjustment Factors except C_L

f_{bx} = Actual Edgewise Bending Stress (Bending Load Applied to Narrow Face of Member

f_{by} = Actual Flatwise Bending Stress (Bending Load Applied to Wide Face of Member

$E' = E(C_T)(C_M)$, $C_T = 1 + 2300L_e / (0.59E)$, L_e = the effective buckling length,

E = MOE

$$F_{cEx} = \frac{(0.3)E'}{\left(\frac{L_e}{d1}\right)^2}, \text{ d1= wide face dimension (see Figure 3.15)}$$

$$F_{cEy} = \frac{(0.3)E'}{\left(\frac{L_e}{d2}\right)^2}, \text{ d2= narrow face dimension (see Figure 3.15)}$$

$$F_{bE} = \frac{(0.561)E'}{\left(\frac{L_e d}{b^2}\right)^2}, \text{ b=width; d=depth}$$

F'_{by} = allowable flatwise bending design value

Appendix D shows an example of how to calculate these CSI values.

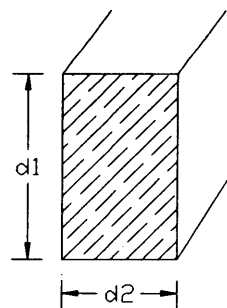


Figure 3.15 Dimensions for Wood Members

The Combined Stress Index (CSI) will be employed in the analysis. A CSI value for combined stresses from bending and axial load is determined from an interaction equation (Breyer et al. 1998). For example, for combined tension stresses, “the interaction equation is a straight –line expression made up of two terms known as stress ratios (equation 3.2). The first term measures the effect of axial tension, and the second term evaluates the effect of bending. In each case the actual stress is divided by the corresponding allowable stress. It may be convenient to think of the stress ratios as percentages or fractions of total member capacity used to resist axial tension and bending. The sum of these fractions must be less than the total member capacity, 1.0, in design. Here, the CSI is used as a measure of how close the member is to failure. For combined compression stresses, a modified non-linear equation is used, and where the moment amplification effect due to axial compression is included (see equation 3.3).

3.6 Truss and Truss Assembly Models

3.6.1 Single Truss Model Using LS Joint Model

In the single truss models using LS joint models, only heel joints and bottom-chord-tension-splice joints are modeled as semi-rigid, because test data from the literature are available only for those joints. Other connections are modeled as pinned or rigid joints.

Figures 3.16 and 3.17 show trusses with 3:12 and 6:12 top chord slopes, respectively, for the 28-foot-span Fink truss configuration tested at the FPL by Wolfe et al. (1986). Figures 3.18 and 3.19 show the corresponding SAP2000 models. Truss design loads were 55 lb/ft for the 3:12 trusses and 66 lb/ft for the 6:12 trusses (applied only to the top chord). The 3:12 sloped truss had a design live load of 17.5 lb/ft² and the 6:12 sloped truss had a design live load of 23 lb/ft². The dead load was 10 lb/ft² in each case. The truss design loads were applied on the horizontal projection. Truss spacing is 2' from center to center. These individual truss models were verified by comparison with experimental results (Wolfe et al., 1986) as discussed in Chapter 4.

3.6.2 Single Truss Model Using TPM's Joint Model

For the single truss models using the TPM's semi-rigid joint models, there are fourteen individual trusses examined. The TPM provided input and output files from the analysis of the trusses. The input files include dimensions, grades, coordinates of nodes, and pinned or rigid connections of truss members. The output files include the CSI values, axial forces, bending moments, and shear forces along the lengths of the truss members. The modeling of the fourteen trusses follows the TPM's design, so the single truss models using SAP2000 (1997) have the same geometry, load case, dimensions, and properties as the truss models from the TPM. The load case specifies the applied loads on the top chords and bottom chords. Live load and dead load for the top chords are 20 psf and 10 psf, respectively. Dead load

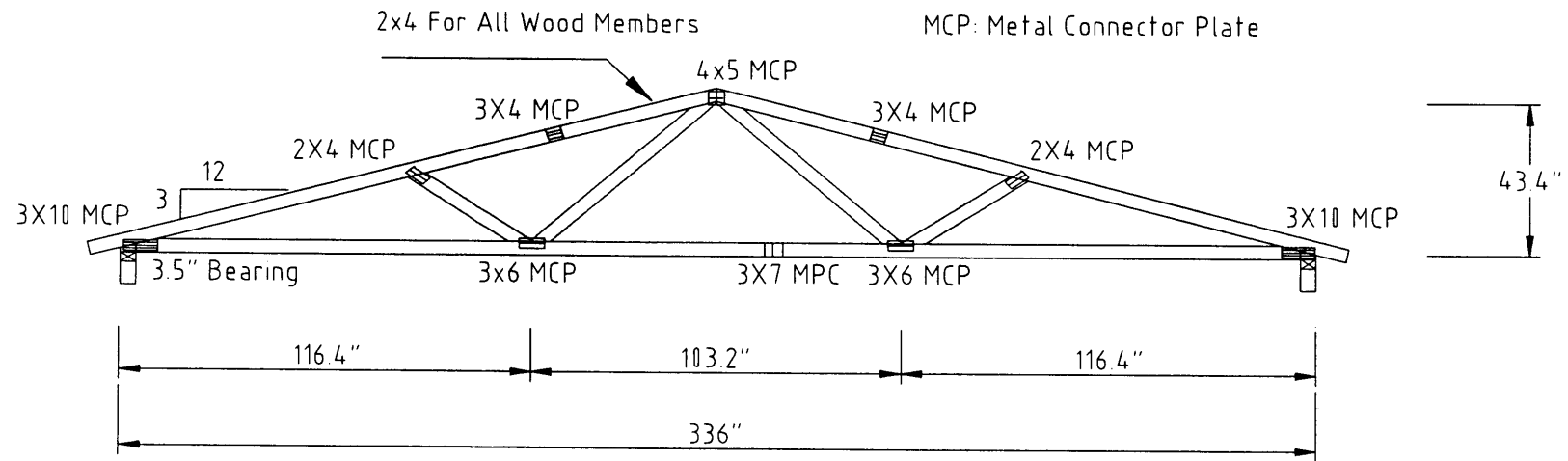


Figure 3.16 3:12 Slope, 28-Foot-Span Metal-Plate-Connected Fink Truss Tested at the FPL (Wolfe et al. 1986)

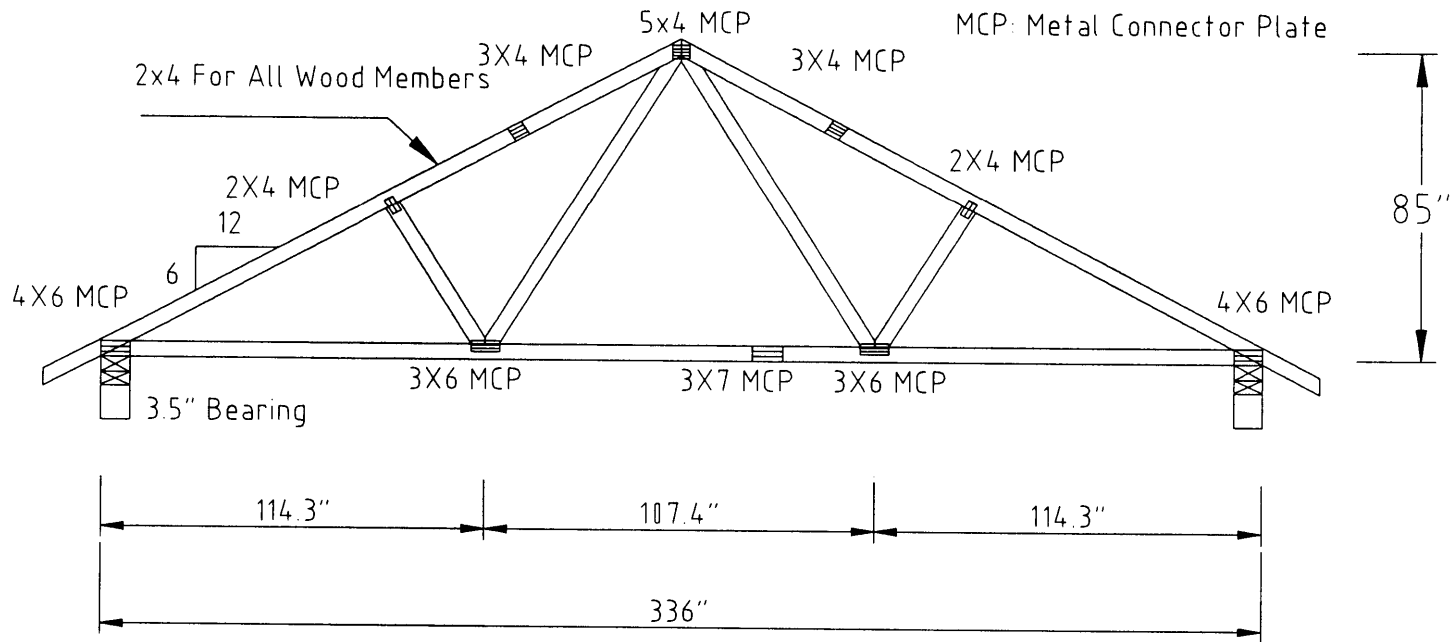


Figure 3.17 6:12 Slope, 28-Foot-Span Metal-Plate-Connected Fink Truss Tested at the FPL (Wolfe et al. 1986)

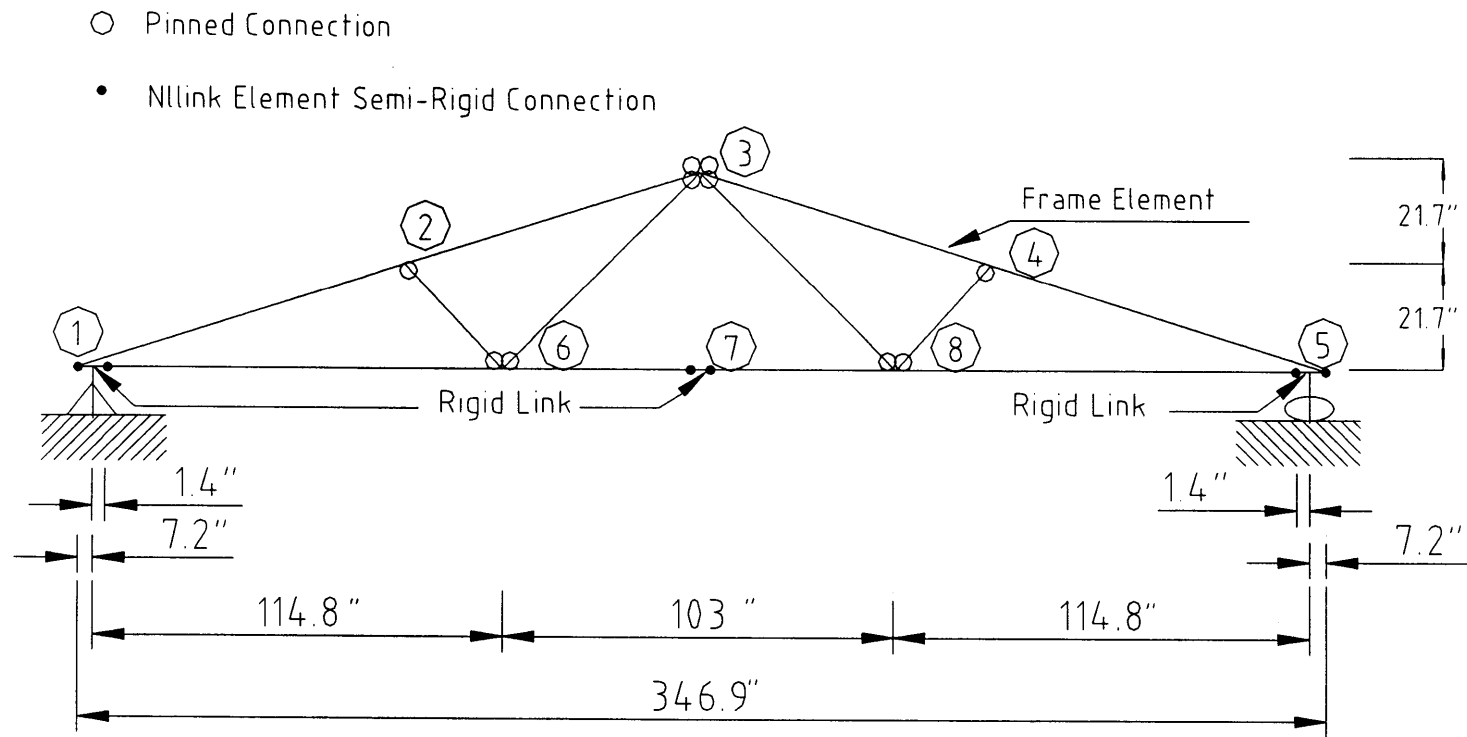


Figure 3.18 Semi-Rigid Joint Model Using SAP2000 Nlink (LS) Elements for 3:12 Slope, 28-Foot-Span Fink Truss

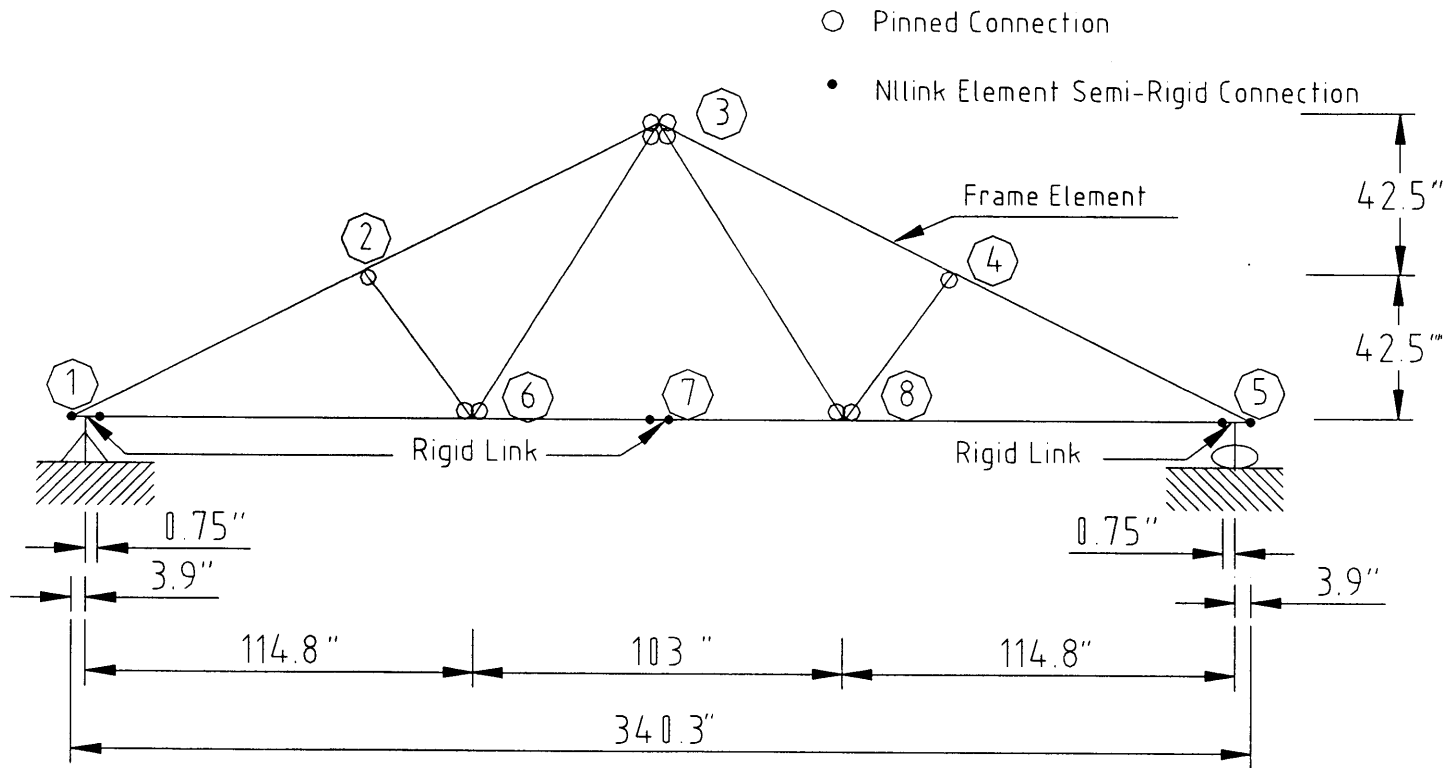
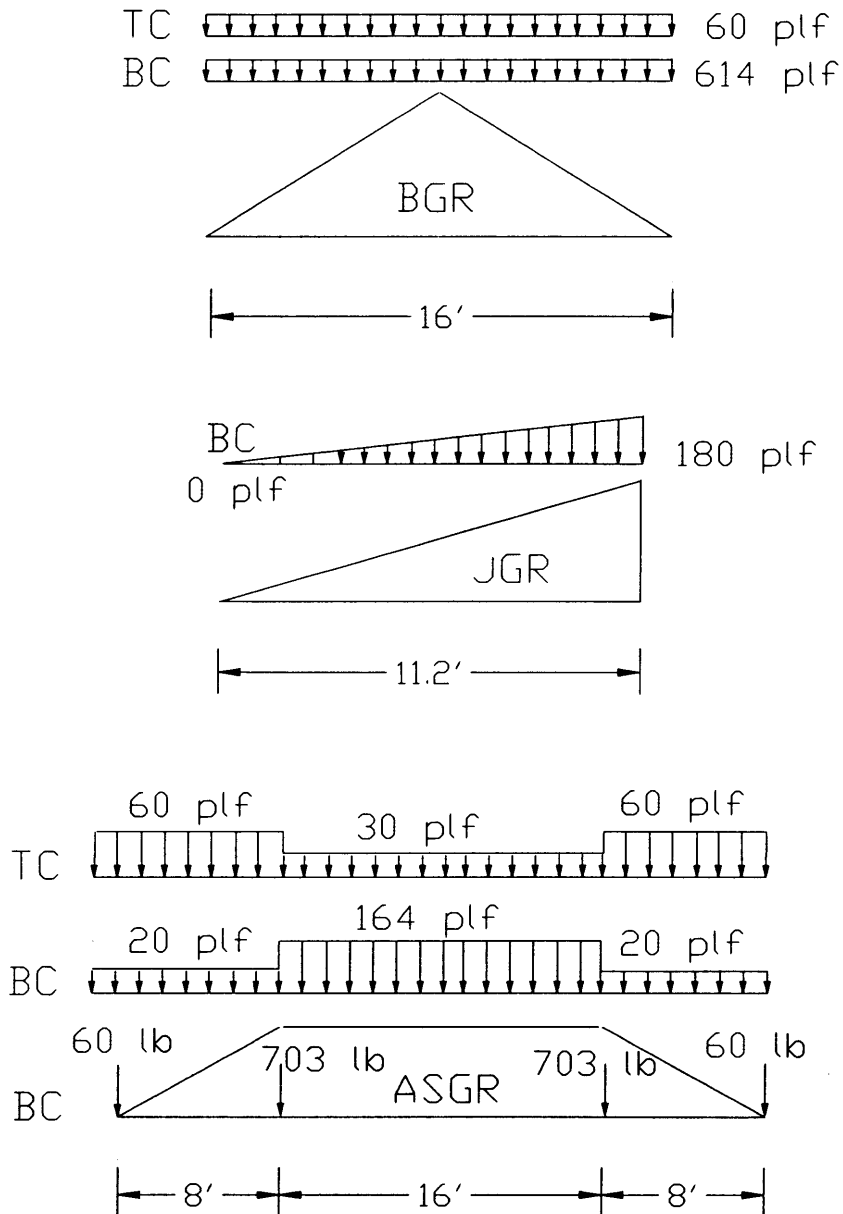


Figure 3.19 Semi-Rigid Joint Model Using SAP2000 Nlink (LS) Elements for 6:12 Slope, 28-Foot-Span Fink Truss

for the bottom chords is 10 psf. The truss design loads are applied on the horizontal projection and truss spacing is 2' from center to center. The transferred loads from other trusses were considered for the girder truss types ASGR, BGR and JGR. The girder truss types BGR and JGR are used to support one end of the intersecting trusses and the trusses are carried on the bottom chord of the girder trusses by hangers. The girder truss type ASGR is used to support perpendicular framing in hip roofs and the hip framing is carried on both the top and bottom chords of the girder truss by nailing or by hangers. For the girder trusses, truss design loads are different from other trusses. Figure 3.20 shows the design loads for the girder trusses. The fourteen truss models using SAP2000 (1997) were verified by comparison of the CSI values with those from the output data from the TPM. The trusses are fabricated using Southern Pine and Spruce-Pine-Fir. In the entire roof truss assembly model, there are also two gable end trusses included. The gable end trusses are connected to the walls, so they have no design loads. One of the fourteen types of the TPM's trusses is shown in Figure 3.21 and the others and two gable end trusses are shown in Appendix E. Figure 3.22 shows the corresponding SAP2000 model and the other models are shown in Appendix F. The complete SAP2000 input and output files for a single truss model using the TPM's joint model are included in Appendix G. The semi-rigid joints of the TPM's single truss models are used mainly for heel joints and peak joints, and sometimes for panel joints (e.g. truss types A2, AS1, AS2, AS3 and ASGR). The other joints of the TPM's models are modeled using rigid or pinned connections.



NOTE: TC: TOP CHORD; BC: BOTTOM CHORD

Figure 3.20 Truss Design Loads for Girder Trusses BGR, JGR and ASGR

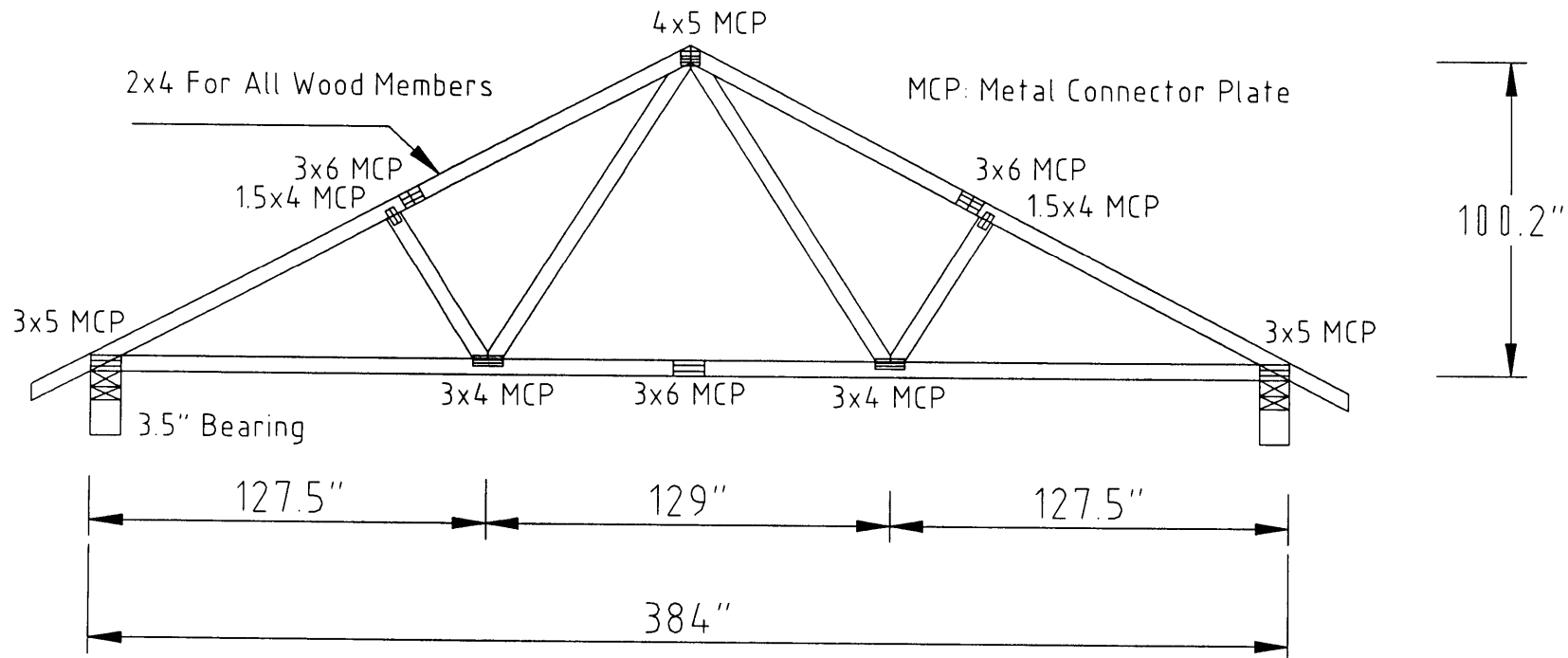


Figure 3.21 MPC Truss Type A from a Truss Plate Manufacturer

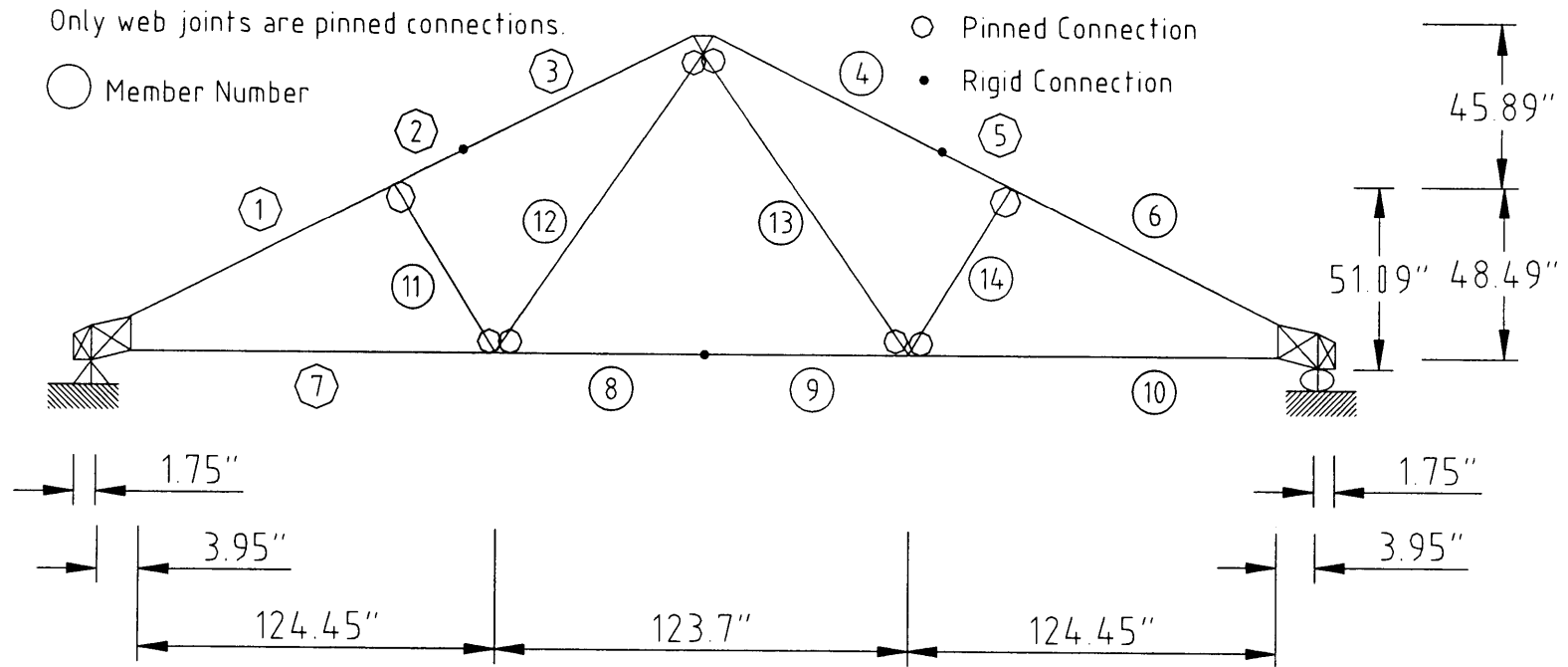


Figure 3.22 The TPM's Model for Truss Type A with Semi-Rigid Joints Using SAP2000

3.6.3 Nine-Truss Assembly Model Using LS Joint Model

Figure 3.23 shows a nine-truss roof assembly containing 28-foot-span Fink trusses with 15/32" plywood sheathing and Figure 3.24 shows the corresponding nine-truss roof assembly model. The nine-truss assembly models have two different slopes, 3:12 and 6:12. In the truss assembly model analysis, the sheathing beams play a very important role. They connect the individual trusses together in three-dimensions as a system, and they function as bridges that transfer loads among the trusses to cause the load sharing effect. In the nine-truss assembly model, the material property data are obtained from the literature (Wolfe and McCarthy 1989, Wolf and LaBissoniere 1991) and the boundary condition is "Hinge-Roller". Truss design loads were 55 lb/ft for the slope of 3:12 and 66 lb/ft for the slope of 6:12 (applied only on the top chord). Truss design loads were applied on the horizontal projection and each truss was loaded one at a time. Truss spacing is 2' from center to center.

3.6.4 An Actual Roof Truss Assembly Model

The actual roof truss assembly model used in this study has fourteen different types of trusses. The TPM's semi-rigid joint models are used for the actual roof truss assembly model. The designs for the individual trusses of an actual roof truss assembly were provided by the truss plate manufacturer. The actual roof truss assembly is shown in Figure 3.25. The numbers of each type of truss are listed in Table 3.1.

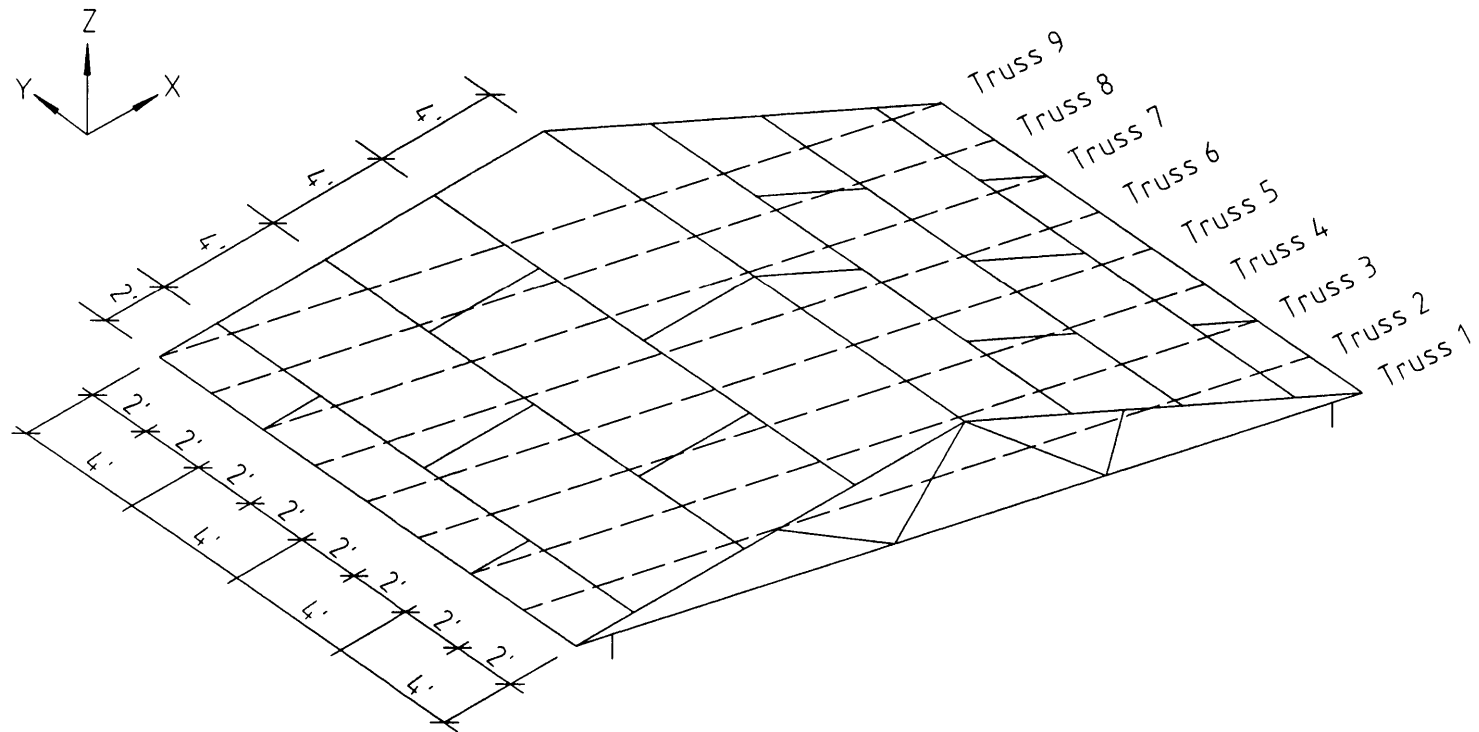


Figure 3.23 Placement of Plywood Sheathing on 3:12 Slope, 28-Foot-Span Nine-Truss Roof Assembly

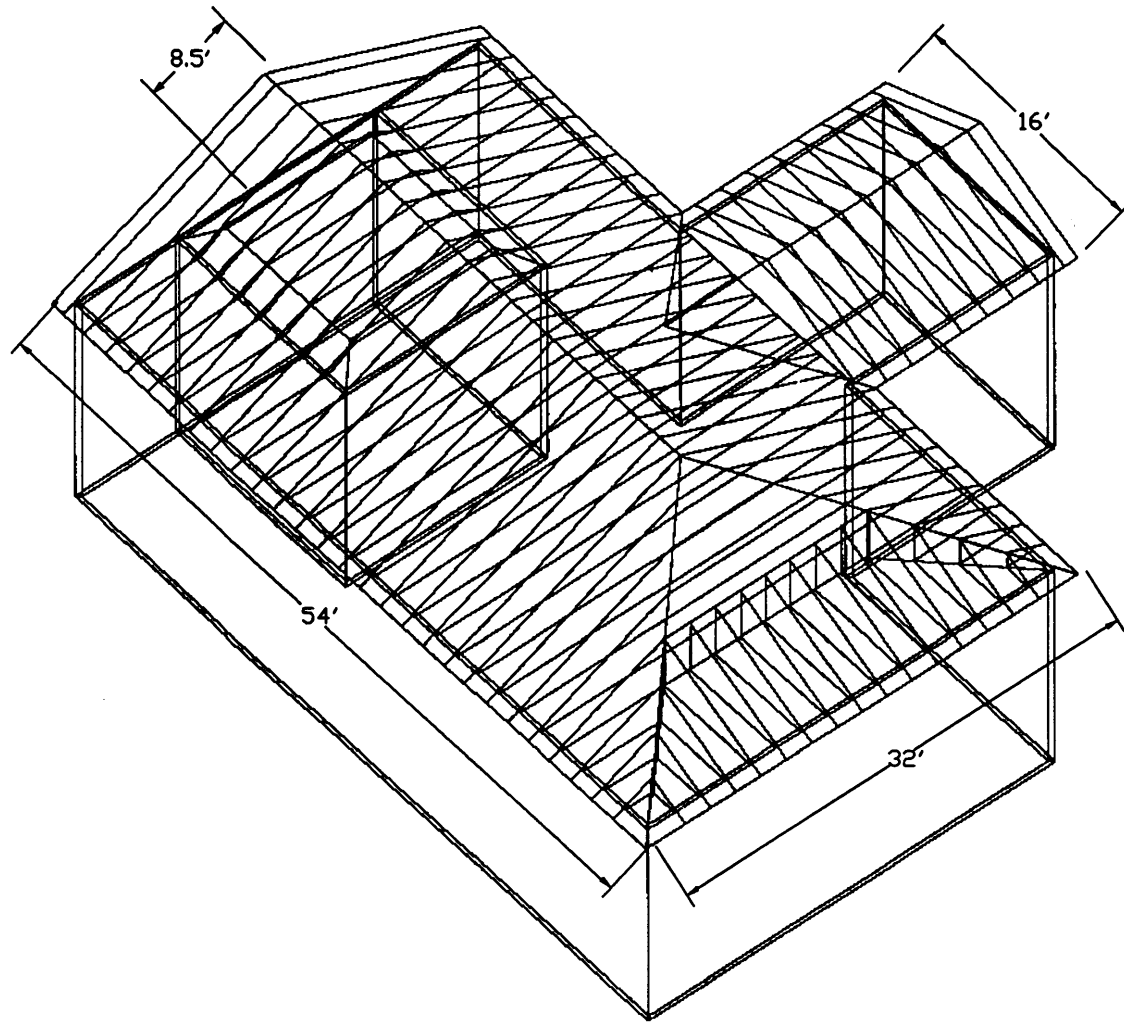


Figure 3.25 The Actual Roof Truss Assembly

The truss assembly model is shown in Figures 3.26~3.27. Some truss types, A, A1, A2, etc, have more than one truss in the truss assembly model, so these trusses are labeled to show their locations. For example, truss “A1-7” means the seventh truss in the truss type A1 series.

Truss Type	A	A1	A2	AS1	AS2	AS3	ASGR
Number	4	8	7	1	1	1	1
Truss Type	B	BGR	J	JGR	J1	J2	J3
Number	7	1	9	2	4	4	4

Table 3.1 The Number of Each Truss Type in The Actual Roof Truss Assembly

Both design and random material properties are used in the analysis and comparison. The boundary condition for the entire perimeter of the actual roof truss assembly model is “Hinge-Hinge”. The sub-assemblies described in section 4.4.2 were also modeled similar to the full assembly. The same truss design loads as used for the fourteen individual truss types are applied in the actual roof truss assembly except for the girder trusses. For the girder trusses ASGR and BGR, truss design loads were 60 lb/ft on the top chords and 20 lb/ft on the bottom chords (based on a 2' tributary width). For the girder truss JGR, there was no design load applied to it. Figure 3.28 shows a close-up view of truss types J1, J2 and J3. In the figure, there are offsets of 3.71” on the boundary of these trusses because of the difference between the truss spans from the truss design drawings and from the truss analogs.

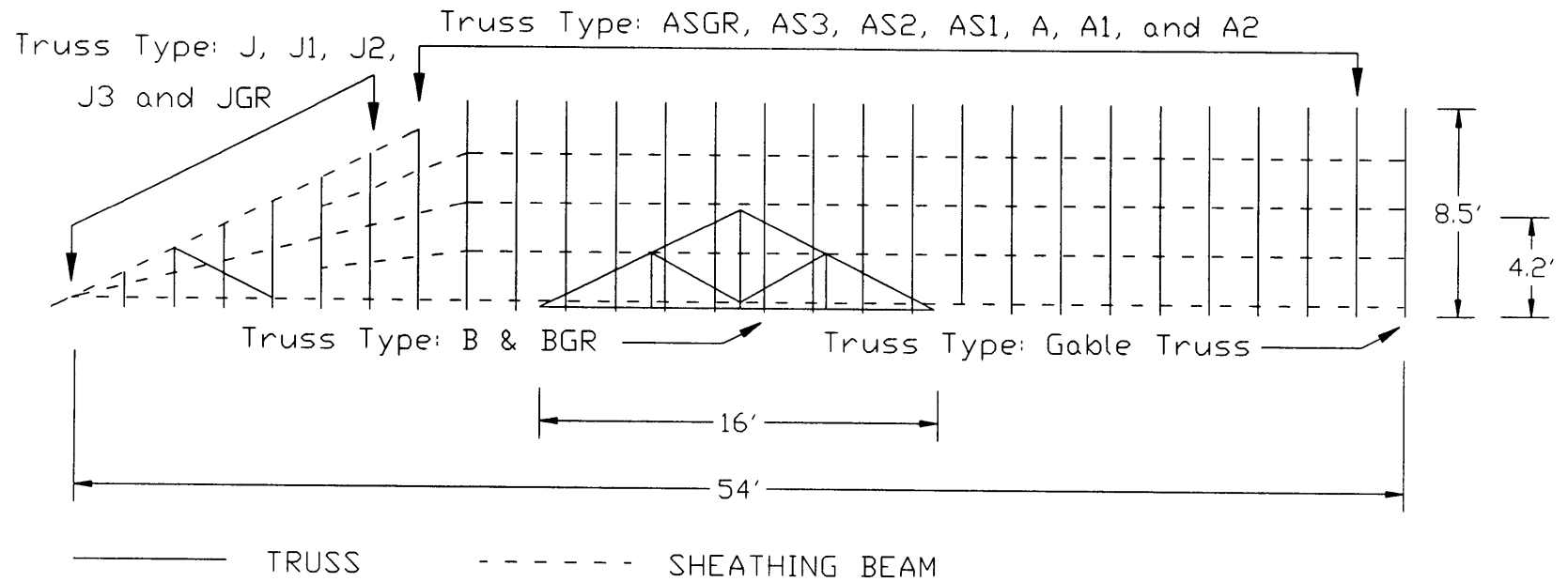


Figure 3.27 Elevation View of Roof Truss Assembly

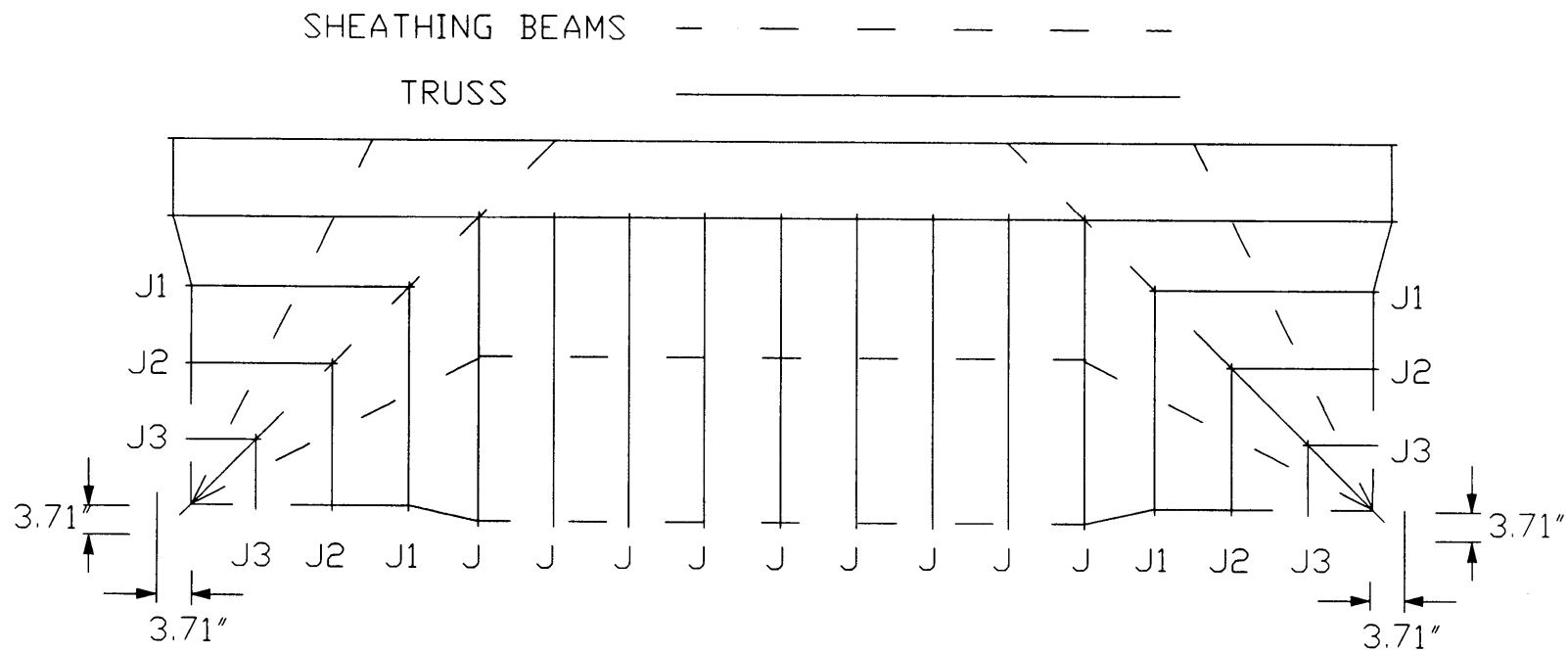


Figure 3.28 Close-Up of Truss Types J1, J2 and J3

The truss span is defined as the horizontal measurement between the outside faces of the two bearings or supports. Table 3.2 shows the differences for truss types J1, J2 and J3. The design drawings and truss analogs for these trusses are shown in Appendix E and Appendix F, respectively.

Truss Type	Truss Span/Design Drawing (in.)	Truss Span/Analog (in.)	Difference (in.)
J1	71.90	68.19	3.71
J2	47.90	44.19	3.71
J3	23.90	20.19	3.71

**Table 3.2 Truss Span Differences between Design Drawing and Truss Analog
for Truss Types J1, J2 and J3.**

4. RESULTS AND DISCUSSION

4.1 Verifications of Single Trusses Using LS Joint Models

Tables 4.1 and 4.2 show displacement results from Wolfe et al. (1986), Li (1997) and the current study for 3:12 and 6:12 trusses, respectively. The displacements in the tables are the average of displacements at five joints in a truss: peak joint, two top chord joints and two bottom chord joints. Average displacements were determined at the same load level that was used in tests by Wolfe et al. (1986). Li (1997) used ETABS (1995) as an analytical tool to predict deflections of the same trusses. The MOE values of the truss members in the SAP2000 model (this study) and in ETABS are the same as used by Wolfe et al. (1986) in the experiments. In Tables 4.1 and 4.2, the average MOE for the truss is the sum of the MOE value of each truss member divided by the number of truss members in each truss. “Percent Difference” in the table shows the difference between the predicted (by SAP2000 1997) and experimental displacements.

From Tables 4.1 and 4.2, the comparisons show that the average percent difference between experimental and predicted (by SAP2000) displacements is less than 9%. (The average percent difference is calculated using the absolute values of percent differences.) However, the percent difference for some individual trusses is quite high (e.g., 24% for 6H6, 17% for 6M7, etc.) for the following reason:

The average displacements of the trusses depend on the modulus of elasticity (MOE) of the wood members. In general, a higher average MOE for a

Truss Identification	Average MOE of Truss (10^6 psi)	Average Experimental Displacement (in.) (Wolfe et al. 1986) (E)	Displacement Predicted by Model: ETABS (in.) Li (1997)	Displacement Predicted by Model: SAP2000 (in.) Current Study (S)	Percent Difference (S-E)x100/E (%)
3L2	1.24	0.452	0.459	0.460	1.8%
3L3	1.24	0.487	0.487	0.489	2.2%
3L5	1.20	0.467	0.467	0.468	0.2%
3L7	1.25	0.440	0.45	0.451	2.5%
Average		0.459	0.465	0.467	1.7%
3M1	1.75	0.324	0.334	0.335	3.4%
3M3	1.67	0.343	0.334	0.335	-2.4%
3M5	1.73	0.293	0.328	0.329	12.4%
3M7	1.76	0.330	0.325	0.326	-1.1%
Average		0.323	0.330	0.331	4.8%
3H1	2.36	0.266	0.248	0.249	-6.6%
3H4	2.28	0.247	0.264	0.265	7.1%
3H6	2.13	0.287	0.280	0.281	-2.2%
3H7	2.18	0.274	0.272	0.272	-0.8%
Average		0.269	0.266	0.266	4.2%

Table 4.1 Deflection Comparisons for 3:12 Slope Fink Trusses
Test: Wolfe et al. (1986)/ ETABS: Li (1997)/ SAP2000: this study

Truss Identification	Average MOE of Truss (10^6 psi)	Average Experimental Displacement (in.) (Wolfe et al. 1986) (E)	Displacement Predicted by Model: ETABS (in.) Li (1997)	Displacement Predicted by Model: SAP2000 (in.) Current Study (S)	Percent Difference (S-E)x100/E (%)
6L2	1.21	0.172	0.179	0.183	6.3%
6L3	1.23	0.180	0.186	0.189	5.1%
6L5	1.24	0.194	0.176	0.180	-7.2%
6L7	1.26	0.198	0.175	0.179	-9.4%
Average		0.186	0.179	0.183	7.0%
6M1	1.76	0.123	0.121	0.124	0.6%
6M2	1.74	0.136	0.129	0.132	-3.1%
6M4	1.73	0.121	0.127	0.131	8.5%
6M7	1.63	0.117	0.133	0.137	17.4%
Average		0.124	0.128	0.131	7.4%
6H1	2.33	0.107	0.099	0.100	-6.8%
6H2	2.33	0.107	0.101	0.104	-3.3%
6H6	2.23	0.086	0.104	0.107	24.2%
6H7	2.24	0.107	0.104	0.106	-0.6%
Average		0.102	0.102	0.104	8.7%

Table 4.2 Deflection Comparisons for 6:12 Slope Fink Trusses
Test: Wolfe et al. (1986)/ ETABS: Li (1997)/ SAP2000: this study

truss should cause a lower displacement. However, for example, for truss 6H6, the average experimental displacement is much lower compared to the displacements of the other three trusses (6H1, 6H2 and 6H7), even though the MOE of 6H6 is close to that of the other three trusses. It is possible that there is some experimental error in the average displacement (0.086") of truss 6H6. A similar, consistent displacement (0.104", 0.107") of the truss is predicted by both the models (ETABS and SAP2000). The predicted displacements from the truss models using SAP2000 always show the same correlation between the average MOE values and the displacements, that the trusses with higher average MOE values have lower displacements.

Of the twenty-four single trusses, there are only five trusses (3M5, 6L7, 6M4, 6M7 and 6H6) that have percent differences higher than 7.2%. The MOE of the wood varies, and moisture content, slope of grain, density, etc., and any experimental errors would also affect the results, so the trusses with a high percent difference may be the result of experimental errors. Otherwise, the predicted displacements from SAP2000 (1997) and ETABS (Li 1997) were quite good.

4.2 Verifications of CSI Values for Single Trusses Using TPM's Joint Model

The CSI values, determined from a SAP2000 model (using the TPM's joint model), for truss type A are shown in Figure 4.1. The CSI values for the same truss were also provided by the TPM, determined using their own in-house software. As shown in Figure 4.1, the CSI values using SAP2000 are identical to the CSI values

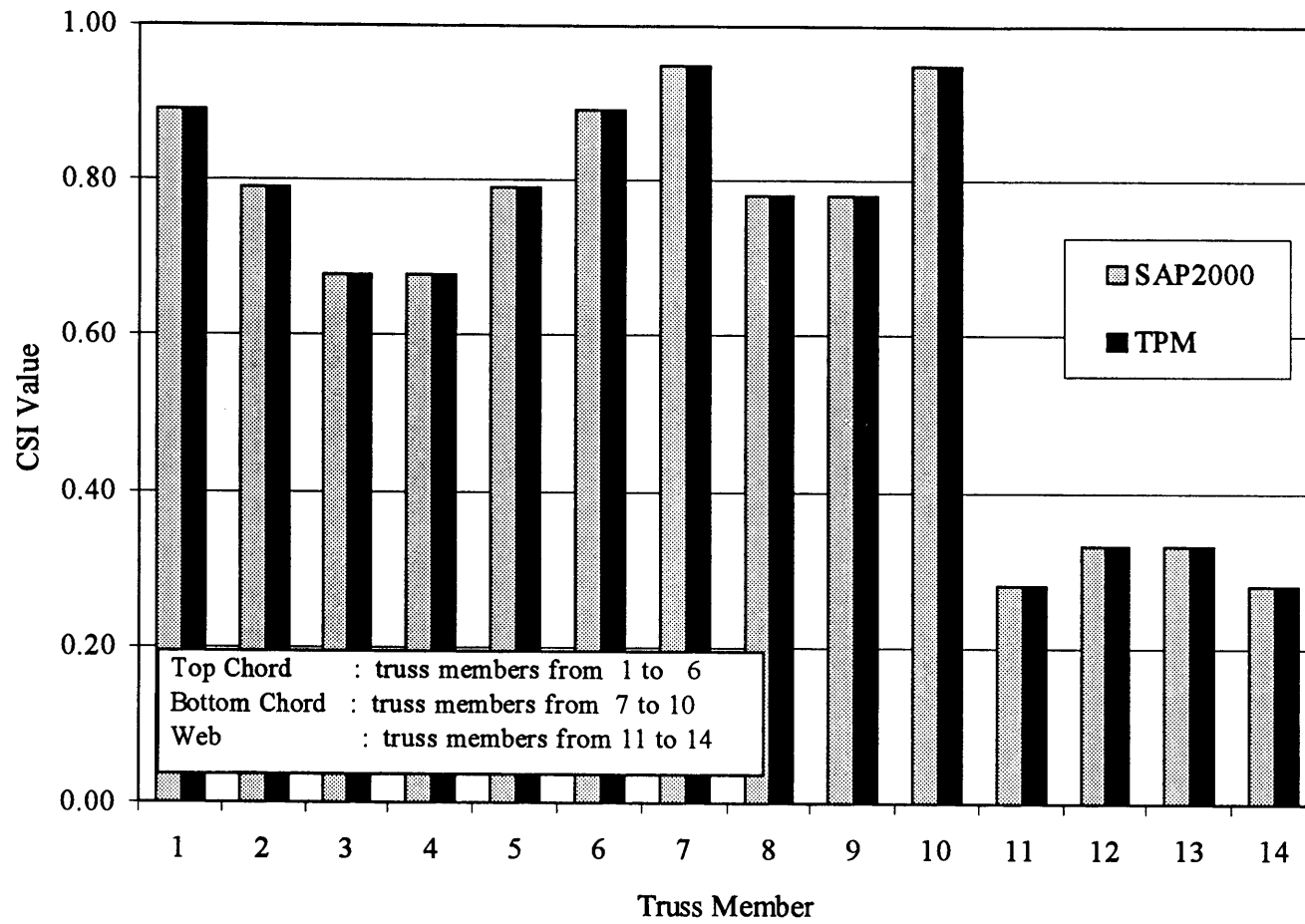


Figure 4.1 CSI Values for Truss Type A Using SAP2000 and TPM Models

provided by the TPM. The ratios of CSI values from SAP2000 model/CSI values from the TPM vary from 0.98 to 1.04. The minor differences may be due to small differences in the truss input data for the analogs and the different finite element software used by the TPM. Comparisons for all of the other truss types are given in Appendix H.

4.3 Verification for Nine-Truss Assembly Using LS Joint Model

Tables 4.3 to 4.6 show the load sharing results from full-scale tests of a nine-truss roof assembly obtained from the literature (Wolfe and McCarthy 1989, Wolfe and LaBissoniere 1991) and as predicted by the SAP2000 model (shown in Figure 3.6) for the same nine-truss assembly. The numbers in the tables are percent load shared by each truss while loading one truss at a time. The load shared by each truss in percent is defined as the sum of the vertical reactions for the truss divided by the total applied load on the assembly. The MOE value for each truss member in the model is the same value as in the tests. The negative numbers in the tables show uplift at the truss. In Tables 4.3 to 4.6, “Truss Loaded” shows which truss type was loaded in the assembly, and “Source” shows the load distributions provided from the experimental test and this study (SAP2000). “Difference” in the tables shows the difference (using absolute value) of load distribution (%) between test and this study. The first row in the tables shows the load distribution among the different trusses (from “Truss 1” to “Truss 9”). For example, from the first row to the forth row in Table 4.3, “Truss 9” was loaded in the nine-truss assembly, and 63% and

Truss Loaded	Source	Truss 1	Truss 2	Truss 3	Truss 4	Truss 5	Truss 6	Truss 7	Truss 8	Truss 9
Truss 9	Test	-4	-4	-1	0	4	6	10	26	63
	SAP2000	-4	-4	-1	1	3	4	6	24	71
	Difference	0	0	0	1	1	2	4	2	8
Truss 8	Test	-2	-2	1	3	6	6	16	48	24
	SAP2000	-2	-2	-1	3	6	10	16	36	34
	Difference	0	0	2	0	0	4	0	12	10
Truss 7	Test	-1	1	3	5	9	12	39	19	13
	SAP2000	-1	-1	0	6	10	17	37	20	12
	Difference	0	2	3	1	1	5	2	1	1
Truss 6	Test	0	3	5	8	17	37	13	9	7
	SAP2000	0	4	5	12	12	29	18	14	6
	Difference	0	1	0	4	5	8	5	5	1
Truss 5	Test	1	5	7	18	45	11	6	6	3
	SAP2000	1	9	10	19	26	14	10	8	3
	Difference	0	4	3	1	19	3	4	2	0
Truss 4	Test	5	10	12	44	16	5	4	3	0
	SAP2000	2	17	17	34	12	9	5	3	1
	Difference	3	7	5	10	4	4	1	0	1
Truss 3	Test	10	20	38	20	7	3	2	1	-1
	SAP2000	5	26	36	22	9	5	0	-1	-2
	Difference	5	6	2	2	2	2	2	2	1
Truss 2	Test	20	49	16	11	6	2	0	-1	-3
	SAP2000	26	45	15	12	6	2	0	-2	-4
	Difference	6	4	1	1	0	0	0	1	1
Truss 1	Test	57	29	12	10	3	0	-1	-2	-6
	SAP2000	61	38	4	3	3	0	-1	-2	-6
	Difference	4	9	8	7	0	0	0	0	0

Table 4.3 Load-Sharing Comparison for 3:12 Slope Truss Assembly with High Stiffness Variability
 Test: Wolfe and McCarthy (1989)
 SAP2000: this study
 Difference: difference (absolute value) between Test and SAP2000

Truss Loaded	Source	Truss 1	Truss 2	Truss 3	Truss 4	Truss 5	Truss 6	Truss 7	Truss 8	Truss 9
Truss 9	Test	-5	-4	-1	1	4	6	7	27	65
	SAP2000	-3	-3	-1	0	2	2	4	25	74
	Difference	2	1	0	1	2	4	3	2	9
Truss 8	Test	-3	-2	1	4	6	6	17	41	29
	SAP2000	-2	-3	-2	2	9	10	15	38	33
	Difference	1	1	3	2	3	4	2	3	4
Truss 7	Test	0	2	3	6	6	10	41	16	16
	SAP2000	-1	-2	-2	4	16	17	40	20	8
	Difference	1	4	5	2	10	7	1	4	8
Truss 6	Test	1	3	5	7	16	34	13	10	10
	SAP2000	0	2	3	10	21	32	15	13	4
	Difference	1	1	2	3	5	2	2	3	6
Truss 5	Test	3	7	7	16	39	11	7	7	5
	SAP2000	1	8	8	16	38	12	9	6	2
	Difference	2	1	1	0	1	1	2	1	3
Truss 4	Test	8	10	13	41	15	4	5	4	2
	SAP2000	2	15	16	35	20	7	3	2	0
	Difference	6	5	3	6	5	3	2	2	2
Truss 3	Test	11	21	39	18	7	3	2	1	-2
	SAP2000	5	24	37	21	15	3	-2	-2	-1
	Difference	6	3	2	3	8	0	4	3	1
Truss 2	Test	25	44	15	13	7	2	1	-1	-6
	SAP2000	27	45	13	12	8	1	-1	-2	-3
	Difference	2	1	2	1	1	1	2	1	3
Truss 1	Test	58	25	12	12	5	1	-1	-2	-4
	SAP2000	67	34	3	2	1	0	-1	-2	-4
	Difference	9	9	9	10	4	1	0	0	0

Table 4.4 Load-Sharing Comparison for 6:12 Slope Truss Assembly with High Stiffness Variability
 Test: Wolfe and McCarthy (1989)
 SAP2000: this study
 Difference: difference (absolute value) between Test and SAP2000

Truss Loaded	Source	Truss 1	Truss 2	Truss 3	Truss 4	Truss 5	Truss 6	Truss 7	Truss 8	Truss 9
Truss 8	Test	-1	-1	1	2	4	7	14	39	34
	SAP2000	-1	-1	0	2	4	8	17	27	44
	Difference	0	0	1	0	0	1	3	12	10
Truss 7	Test	1	1	2	5	6	13	41	14	18
	SAP2000	0	1	1	4	8	14	40	15	17
	Difference	1	0	1	1	2	1	1	1	1
Truss 6	Test	1	4	4	7	12	40	15	7	9
	SAP2000	2	4	5	9	13	27	20	10	10
	Difference	1	0	1	2	1	13	5	3	1
Truss 5	Test	3	6	8	13	37	16	11	4	3
	SAP2000	3	7	12	15	29	13	11	5	5
	Difference	0	1	4	2	8	3	0	1	2
Truss 4	Test	7	10	15	37	15	7	5	3	0
	SAP2000	4	13	21	31	14	8	5	2	2
	Difference	3	3	6	6	1	1	0	1	2
Truss 3	Test	11	21	40	17	7	5	1	0	-2
	SAP2000	8	20	42	19	10	4	0	0	-3
	Difference	3	1	2	2	3	1	1	0	1
Truss 2	Test	20	52	15	10	6	3	1	-3	-5
	SAP2000	29	38	19	12	6	3	0	-1	-6
	Difference	9	14	4	2	0	0	1	2	1
Truss 1	Test	58	28	12	8	3	0	-1	-2	-5
	SAP2000	66	29	7	4	2	1	1	-1	-9
	Difference	8	1	5	4	1	1	2	1	4

Table 4.5 Load-Sharing Comparison for 3:12 Slope Conventional Truss Assembly
 Test: Wolfe and LaBissoniere (1991)
 SAP2000: this study
 Difference: difference (absolute value) between Test and SAP2000

Truss Loaded	Source	Truss 1	Truss 2	Truss 3	Truss 4	Truss 5	Truss 6	Truss 7	Truss 8	Truss 9
Truss 8	Test	-2	-2	1	2	6	11	15	42	27
	SAP2000	-2	-2	-2	2	7	10	17	34	36
	Difference	0	0	3	0	1	1	2	8	9
Truss 7	Test	1	1	3	4	7	17	38	16	15
	SAP2000	-1	-1	-2	4	12	18	43	17	10
	Difference	2	2	5	0	5	1	5	1	5
Truss 6	Test	2	4	6	5	14	42	13	9	7
	SAP2000	0	2	4	10	17	31	20	11	5
	Difference	2	2	2	5	3	9	7	2	2
Truss 5	Test	2	6	8	13	38	17	7	5	3
	SAP2000	0	6	12	15	35	13	11	6	2
	Difference	2	0	4	2	3	4	4	1	1
Truss 4	Test	7	10	17	33	18	9	5	3	1
	SAP2000	2	13	21	34	16	8	4	2	0
	Difference	5	3	4	1	2	1	1	1	1
Truss 3	Test	13	18	40	14	8	7	3	1	-2
	SAP2000	5	20	45	20	11	4	-2	-1	-2
	Difference	8	2	5	6	3	3	5	2	0
Truss 2	Test	22	44	18	9	7	5	0	-2	-4
	SAP2000	26	43	18	11	6	2	-1	-2	-3
	Difference	4	1	0	2	1	3	1	0	1
Truss 1	Test	56	28	16	9	4	1	-2	-5	-8
	SAP2000	66	33	5	3	1	0	-1	-2	-5
	Difference	10	5	11	6	3	1	1	3	3

Table 4.6 Load-Sharing Comparison for 6:12 Slope Conventional Truss Assembly
 Test: Wolfe and LaBissoniere (1991)
 SAP2000: this study
 Difference: difference (absolute value) between Test and SAP2000

71% of the total applied load were carried by “Truss 9” for “Test” and “SAP2000”, respectively. “Difference” between test and SAP2000 is 8 (%). Other portions of the total load were carried by “Truss 1” to “Truss 8”.

In Tables 4.3 and 4.4, the predicted load sharing for truss assembly systems with high stiffness variability for different slopes: 3:12 and 6:12, were compared to the test results from Wolfe and McCarthy (1989). In Tables 4.5 and 4.6, the predicted load sharing for conventional truss assembly systems with low stiffness variability for different slopes: 3:12 and 6:12, were compared to Wolfe and LaBissoniere’s (1991) tests. In the nine-truss assembly with low stiffness variability, “Truss 9” was a previously failed truss connected to the other trusses and “Truss 9” was not loaded in the tests.

In the load sharing verification, the comparison between test and predicted results will focus on the loaded trusses, because we are interested in how large a portion of the total load the loaded truss will carry. From the comparisons in Tables 4.3 and 4.4, the maximum “Difference” for the loaded trusses are 19% and 9% for the 3:12 and 6:12 slope trusses, respectively. The averaged “Difference” for the nine loaded trusses are 7.7% and 3.8% for the 3:12 and 6:12 slope trusses, respectively. Li (1997) compared the same test results with his ETABS model using the same nine-truss assembly, and he found the averaged “Difference” for the nine loaded trusses as 7.4% and 5.6% for the 3:12 and 6:12 slope trusses, respectively. From the comparisons in Tables 4.5 and 4.6, the maximum “Difference” for the loaded trusses are 14% and 10% for the 3:12 and 6:12 slopes,

respectively. The averaged “Difference” for the eight loaded trusses are 8.0% and 5.3% for the 3:12 and 6:12 slope trusses, respectively. In Li’s (1997) study, he found the averaged “Difference” for the eight loaded trusses as 8.9% and 6.3% for the 3:12 and 6:12 slope trusses, respectively.

A summary for the load sharing comparison results follows: 1). All the predicted load distribution percentages have the same trend as the test results in that the load distribution percentage for unloaded trusses decreases away from the loaded truss. 2). In general, the predicted load sharing results in this study are slightly better than the results from Li’s (1997) study comparing averaged “Difference” for the loaded trusses.

It has been shown in the last three sections that the SAP2000 model developed in this study can estimate displacements of single trusses, can estimate load sharing in a nine-truss assembly and predict CSI values for single trusses using the TPM’s joint model.

4.4 Actual Roof Truss Assembly Model

In this section, the results are presented for an actual roof truss assembly, which was analyzed using SAP2000 (1997). Only the TPM’s joint models are used for the actual roof truss assembly for the reasons explained in Appendix I. The actual roof truss assembly is shown in Figures 3.26 and 3.27. There are fourteen different types of individual trusses in this actual roof truss assembly model. The CSI values for the trusses within the assembly were compared with the CSI values

for the fourteen individual, isolated trusses. When these CSI values from the assembly are compared with the CSI values from the fourteen individual trusses, the fourteen individual trusses only used design value material properties. However, in the analysis of the roof truss assembly, both design and random values for material properties were used to calculate CSI values. All of the design values came from the NDS (1991) and depended on the species of the truss members. Random values for MOE were generated following a lognormal distribution with mean value and coefficient of variation from NDS (1991). Other random values for mechanical properties were calculated by Gerhards' (1983) formulas.

The maximum CSI values from the individual trusses, and truss assemblies with design material properties and random material properties are shown in Table 4.7. From Table 4.7, it is observed that only the maximum CSI value of truss type A in the assembly exceeded 1.0 using design or random material properties. The conventional truss design method is unable to predict which truss type will have a CSI value over 1.0 in the assembly. In Table 4.7, from the conventional design method, truss type ASGR has the highest maximum CSI value (0.99) among the fourteen truss types, but the maximum CSI value for truss type ASGR with design material properties actually decreases from 0.99 (individual) to 0.62 in the assembly. However, the CSI value for truss type A increased from 0.95 to 1.03 in the assembly. This phenomenon shows that the behavior of an individual truss will be different when it is within the assembly because of system effects. The truss assembly model can consider the system effects directly, so this modeling approach

Truss Type	Number of Trusses	Maximum CSI value from Individual Truss (Conventional Truss Design) (C)	Maximum CSI Value in Assembly (Using Design Properties) (D)	Percent Different (C-D)×100/C Decreased (%)	Maximum CSI Value in Assembly(Using Random Properties)
A	4	0.95	1.03	-	1.14
A1	8	0.98	0.82	16%	0.97
A2	7	0.93	0.82	12%	0.97
AS1	1	0.86	0.85	1%	0.81
AS2	1	0.91	0.52	43%	0.51
AS3	1	0.81	0.51	37%	0.52
ASGR	1	0.99	0.62	37%	0.50
B	7	0.65	0.59	9%	0.77
BGR	1	0.90	0.58	36%	0.51
J	9	0.82	0.81	1%	0.78
J1	4	0.44	0.62	-	0.62
J2	4	0.18	0.19	-	0.30
J3	4	0.04	0.16	-	0.16
JGR	2	0.52	0.43	17%	0.48

Table 4.7 CSI Comparison for Maximum CSI Values from Individual Trusses and Truss Assembly

can provide a fuller description of the behavior of trusses in the assembly compared to the conventional design method based on a single truss. In general, the maximum CSI value of a truss in an assembly (compared to the individual truss case) is decreased due to the system effects. The decreased maximum CSI values from the truss assembly model also indicate that the conventional design method may over-design most of the trusses. The initial failure of the truss assembly can also not be predicted precisely from the conventional design method, so the truss assembly model may provide increased safety through improved analysis over the conventional design method. The decreased maximum CSI values show that smaller members or lower grade lumber may be used to save on construction cost.

System effects involve the distribution of load among the trusses in the assembly due to the following factors: 1) Variability of modulus of elasticity (MOE), 2) interaction of sub-assemblies, 3) boundary conditions, and 4) modeling methods for the entire assembly. The following sections will focus on discussions of the truss assembly with design material properties. The analysis results for the truss assembly model with random material properties will be used as a case study, because one set of random properties can not provide for general conclusions.

4.4.1 MOE

It is well known in structural engineering that stiffness attracts load. The effect of variability of modulus of elasticity (MOE) on load distribution in an assembly is discussed here. The truss types A1 and A2 series in the actual roof

truss assembly are chosen to illustrate this effect, because these two truss types are the main components in the assembly. In Table 4.7, truss types A1 and A2 have eight and seven trusses, respectively, and also have high maximum CSI values (from conventional truss design). All other truss types either have very few trusses or have substantially lower maximum CSI values (from conventional truss design).

The weighted average MOE (WAM) of the truss was used as a measure of its stiffness. The WAM was weighted based on the lengths of the members, because the lengths of the truss members will affect the contributions to the average stiffness of the truss. Webs are less contributive to the truss stiffness than chord members and chord members always dominate truss failure, so only the MOE values for top and bottom chords are used for WAM calculations. The WAM values are calculated by the following formula:

WAM=

$$\frac{\sum(\text{length of each truss chord member} \times \text{MOE of the truss member})}{\sum(\text{length of each truss chord member in this truss})}$$

The MOE values and load distribution (reactions) for truss type A1 and A2 series are shown in Tables 4.8 and 4.9, respectively. In the tables, the reactions are shown for both supports and we consider the total reaction (L+R) as the load distribution. In general, a truss with higher MOE should attract more load in the assembly, but there are in fact no systematic trends here to show that higher WAM values attracted more load. For the trusses with design material properties, the WAM values are constant (1.459×10^6 psi for trusses A1-1 ~ A1-8 and 1.456×10^6 psi for

DESIGN MATERIAL PROPERTIES

Truss Type	Reactions (lb)			Ave. MOE (10^6 psi) (Design Material)
	L	R	L+R	
A1-1	1364	1535	2899	1.459
A1-2	1374	499	1873	1.459
A1-3	1373	782	2155	1.459
A1-4	1371	758	2129	1.459
A1-5	1373	760	2133	1.459
A1-6	1379	789	2168	1.459
A1-7	1388	502	1890	1.459
A1-8	1396	1576	2972	1.459

RANDOM MATERIAL PROPERTIES

Truss Type	Reactions (lb)			Ave. MOE (10^6 psi) (Random Material)
	L	R	L+R	
A1-1	1396	1441	2837	1.365
A1-2	1411	529	1940	1.639
A1-3	1386	732	2118	1.519
A1-4	1326	666	1992	1.415
A1-5	1389	647	2036	1.365
A1-6	1241	750	1991	1.649
A1-7	1413	442	1855	1.542
A1-8	1456	1594	3050	1.474

Table 4.8 The Effect of MOE on Load Distribution (Reactions) for the Truss Type A1 Series with Design and Random Material Properties
L: Left; R: Right

DESIGN MATERIAL PROPERTIES

Truss Type	Reactions (lb)			Ave. MOE (10^6 psi) (Design Material)
	L	R	L+R	
A2-1	1159	1085	2244	1.456
A2-2	1272	1212	2484	1.456
A2-3	1257	1223	2480	1.456
A2-4	1267	1275	2542	1.456
A2-5	1284	1357	2641	1.456
A2-6	1289	1466	2755	1.456
A2-7	1262	1594	2856	1.456

RANDOM MATERIAL PROPERTIES

Truss Type	Reactions (lb)			Ave. MOE (10^6 psi) (Random Material)
	L	R	L+R	
A2-1	1172	1079	2251	1.608
A2-2	1356	1236	2592	1.556
A2-3	1056	1252	2308	1.446
A2-4	1382	1202	2584	1.452
A2-5	1263	1476	2739	1.396
A2-6	1215	1353	2568	1.452
A2-7	1287	1514	2801	1.553

Table 4.9 The Effect of MOE on Load Distribution (Reactions) for the Truss Type A2 Series with Design and Random Material Properties
L: Left; R: Right

trusses A2-1~ A2~7). Their corresponding reactions are expected to be more or less the same; however, they varied substantially. The trusses with random material properties from Tables 4.8 and 4.9 also did not show that trusses with higher WAM values attract more load. It does not mean there is no such effect in a truss assembly, however, it was not apparent in Tables 4.8 and 4.9. This may be due to the following: 1) other effects, such as the interaction of sub-assemblies and boundary conditions; and/or 2) the variability of WAM values is not high enough to show an effect on load distribution. Thus, the trusses with constant MOE values showed different reactions because of the other effects (discussed later) which dominate the load distribution. The coefficients of variation (COV) for WAM values are 2.5% and 11.9% for trusses with design and random material properties in the actual roof assembly model, respectively. (Sample number: 54; there are fifty-four individual trusses in the entire roof truss assembly.) The COV in MOE from visually graded sawn lumber is 25% (NDS 1997). The COV values calculated for both design and random material properties are less than 12%, so the variability of the WAM values is not very high. Thus, the variability of MOE values is only one source of system effects in an actual roof truss assembly, and here the other effects dominate the load distribution behavior.

4.4.2 Interaction of Sub-Assemblies

There are three sub-assemblies (SB) in the actual roof truss assembly in Figure 4.2, namely SB-A, SB-B and SB-J. SB-A includes truss types, A, A1, A2, AS1, AS2, AS3, and ASGR. SB-B includes truss types B and BGR. SB-J includes truss types J, J1, J2, J3 and JGR. This section on the interaction of sub-assemblies will focus on SB-A and SB-B, because the maximum CSI value is predicted for truss type A, and this is due to the interaction between two sub-assemblies, SB-A and SB-B. The maximum CSI values in SB-J are under 0.82 (shown in Table 4.7), so there is no safety concern. The truss types connecting the two sub-assemblies, SB-A and SB-B, are the truss type A1 series and BGR-1.

At the connections of the two sub-assemblies, SB-A and SB-B, one end of truss type A1 is supported by the bottom chord of the truss type BGR-1. The other end is a hinged support. A connection similar to that between truss type A1 and the bottom chord of truss type BGR-1 is shown in Figure 4.3. The truss A1 support at truss BGR-1 is more flexible than support provided by an end wall. This flexibility is never modeled in conventional design where single trusses are designed one at a time. And, because truss type A1 become less stiff compared to others in the assembly due to one support being more flexible, nearby trusses (truss type A series) attract more load. This is indicated by an increase in CSI values of truss type A and decrease in CSI values of truss type A1 in the assembly. Again, this phenomenon is impossible to observe in conventional design practice.

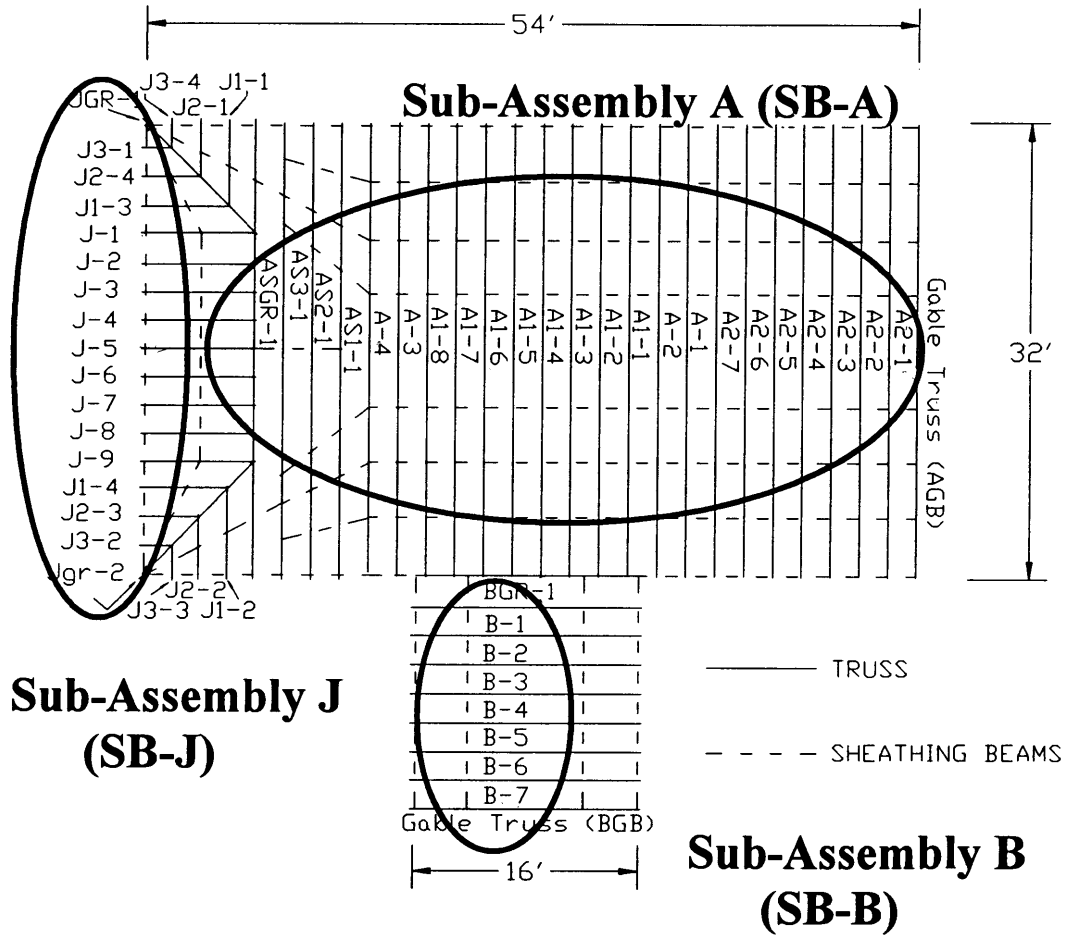


Figure 4.2 Three Sub-Assemblies in The Actual Roof Truss Assembly (Plan View)

The total of the reactions for each truss is used to demonstrate the effect of sub-assembly interaction on truss stiffnesses and ultimately load distribution to each truss. Figure 4.4 shows sub-assembly SB-A (and SB-J). In this sub-assembly, the type A1 series trusses are modeled as being supported by hinge supports at both ends. But when the same trusses are in the entire assembly, the truss type A1 series is supported by a hinge at one end and a flexible “spring” at the other end (the one supported by truss BGR-1). Truss A1-4 from the truss type A1 series and the two adjacent trusses from the truss type A series, A-2 and A-3, were chosen for the reaction comparison. Figure 4.5 shows the reaction forces at the two ends of truss types A1-4, A-2, and A-3. The boundary conditions in the sub-assemblies are “Hinge-Hinge” for all the truss types. The boundary conditions in the assembly for truss types A-3 and A-2 are “Hinge-Hinge” and for truss type A1-4 is “Hinge-Spring”. The “Spring” represents the connection between truss types A1-4 and BGR-1. The reaction at the joint connected to the bottom chord of truss type BGR-1 can be calculated using joint equilibrium as shown in Appendix J.

This reaction comparison shows that the reactions for truss types A1-4, A-3 and A-2 are all very close in the sub-assemblies. The reaction at BGR-1 for truss type A1-4 decreases significantly and the reactions at BGR-1 for truss types A-2 and A-3 increase in the assembly, because truss type A1-4 is more flexible and thus carries less load while truss types A-2 and A-3 carry more of the redistributed load in the assembly. The maximum CSI value is predicted for truss type A because of the interaction of sub-assemblies decreased here, and this in fact raises the CSI

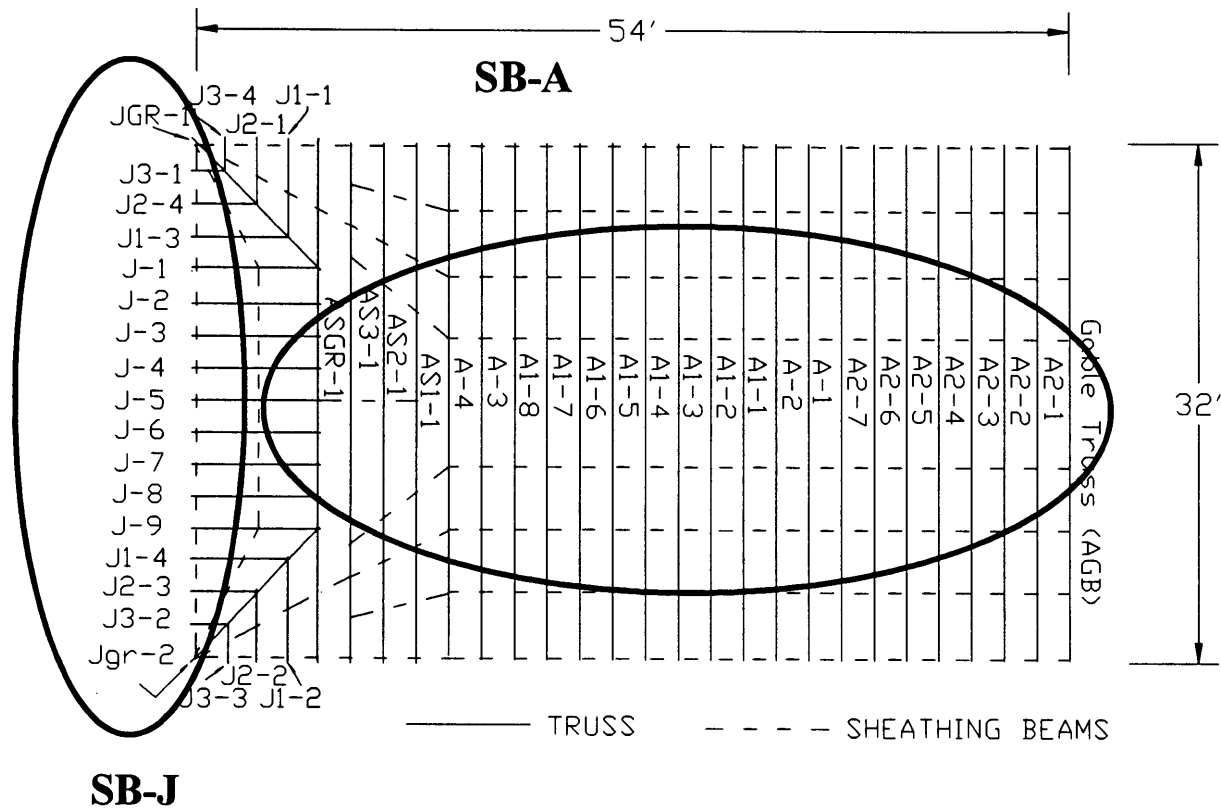


Figure 4.4 Roof Truss Sub-Assembly (Plan View)

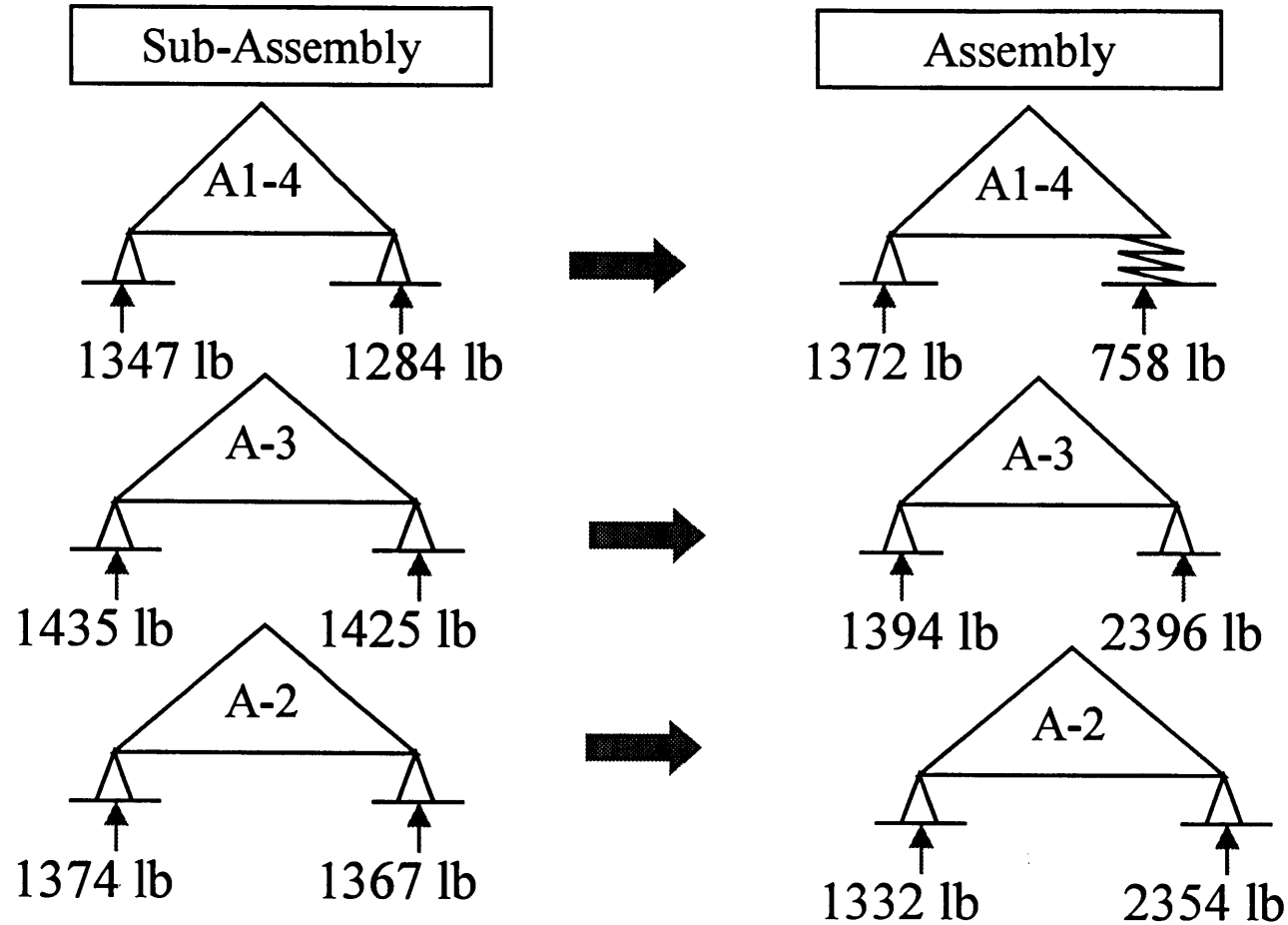


Figure 4.5 The Reaction Comparison for Truss Types A1-4, A-3 and A-2

value over 1.0. Larger members or higher grade lumber should be used for truss type A for adequate safety based on this analysis of the assembly.

4.4.3 Boundary Conditions

Boundary conditions (e.g. supports) in single trusses and truss assemblies can have a significant effect on the load distribution in trusses/assemblies. The boundary condition “Hinge-Roller” is used in the conventional truss design method, but a boundary condition of “Hinge-Hinge” is used for the actual roof truss assembly model in this study. The reason for using the boundary condition “Hinge-Hinge” for the actual roof truss assembly was presented in Chapter 3. To better understand the behavior of a single truss with different boundary conditions, “Hinge-Hinge” and “Hinge-Roller” conditions are compared using CSI values as shown in Appendix K.

In Figure 4.2, there are two truss type A2 and B series connected to the gable end trusses. The maximum CSI values for the truss type A2 and B series in the actual roof truss assembly are listed in Table 4.10. In the table, the maximum CSI values decrease significantly for truss types A2-1 and B-7 in the assembly, because they are close to the gable end trusses. The trusses are near the ends of the roof, and the load sharing effect is significantly influenced by the gable end truss (LaFave and Itani, 1992), so the CSI values of the trusses near the gable end truss will be affected also. Maximum CSI values among truss type A2 and B series drop

by 12% and 9%, respectively, in the assembly as compared to the individual trusses.

In Table 4.10, the stiff gable truss tends to attract load from adjacent trusses to alter the load distribution significantly. The bottom chord of the gable end truss is fully connected to the stiff bearing wall, and the wall will transfer the load from the truss members directly to the foundation.

Truss Type:	A2	A2-1	A2-2	A2-3	A2-4	A2-5	A2-6	A2-7
	Individ.	Trusses in Assembly (Design Material Properties)						
Max. CSI Value	0.93	0.51	0.67	0.72	0.77	0.80	0.82	0.76

Truss Type:	B	B-1	B-2	B-3	B-4	B-5	B-6	B-7
	Individ.	Trusses in Assembly (Design Material Properties)						
Max. CSI Value	0.65	0.44	0.55	0.57	0.58	0.59	0.57	0.41

Table 4.10 The Maximum CSI Values from Truss Types A2 Series and B Series

In the truss type A2 series, truss A2-1 has the minimum CSI value due to its proximity to the gable end truss. For trusses A2-1 to A2-6, the CSI values gradually increase because they are further away from the gable end truss. The CSI value for truss type A2-7 then decreases, as it connects to truss type A. In the truss type B series, truss B-7 has the minimum CSI value for the same reason as truss A2-1. For trusses B-7 to B-1, the CSI value increases at first and then decreases. The CSI value increases initially because the trusses are further away from the stiff gable end truss. The CSI value then decreases as B-1 connects to the other truss type BGR-1. From the previous section discussing the effects of interactions of the sub-

assemblies, truss type BGR-1's connection to SB-A and the interaction of sub-assemblies might also be a reason for trusses B-1, B-2, B-3 and B-4 to have lower CSI values.

4.4.4 Modeling Methods

The behavior of a truss assembly model can be affected by the placement of sheathing beam elements, because sheathing beam elements transfer load among the trusses. In this section, an example will be used to show how modeling methods and the locations of sheathing beams can influence the maximum CSI values for the truss type J series.

Figure 4.6 shows a close-up of the truss type J series and trusses ASGR, AS1, AS2, and AS3. Table 4.11 shows the maximum CSI values for the truss type J series in the actual roof truss assembly model with design material properties. From Figure 4.6, the sheathing beam element only connects truss J-5 from the truss type J series with truss types ASGR, AS1, AS2, and AS3. Truss J-5 has a short span (8 ft) compared with the long spans (32 ft) for truss types ASGR, AS1, AS2 and AS3, so truss J-5 tends to be stiffer. Thus, truss J-5 receives load from these other truss types. From Table 4.11, the maximum CSI value for the truss type J series is for truss J-5, because the sheathing beam only connects truss J-5 to truss types ASGR, AS1, AS2, and AS3. For this reason, truss J-5 becomes the main receiver for the transferred load from truss types ASGR, AS1, AS2, and AS3, and truss J-5 transfers the received load to the adjacent trusses to cause a symmetric distribution

of maximum CSI values in the truss type J series. If there were other sheathing beams from the truss type J series connecting to the trusses in SB-A, the load distribution would be different because of the different locations of the sheathing beams in the analytical model for the assembly.

In this study, we found how several system effects influence the behavior of an actual roof truss assembly. The behavior of the actual, complex assembly can not be predicted precisely using results from a simple nine-truss assembly or the conventional individual truss design method. It is important to model and to consider the system effects directly, and gain a more complete understanding of the behavior of the entire assembly.

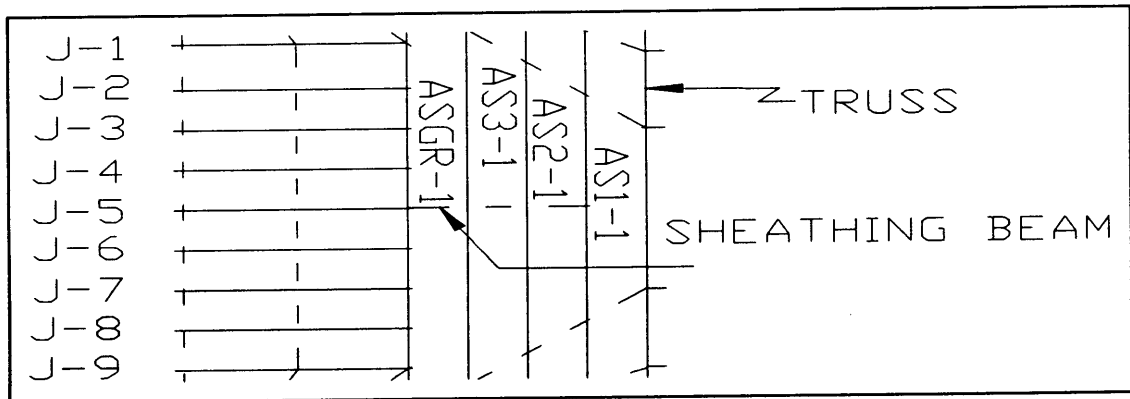


Figure 4.6 Close-Up of The Truss Type J Series and Trusses ASGR, AS1, AS2, and AS3

Truss Type:	J	J-1	J-2	J-3	J-4	J-5	J-6	J-7	J-8	J-9
	Individ.	Trusses in Assembly with Design Material Property								
Maximum CSI Value	0.82	0.63	0.73	0.79	0.80	0.81	0.80	0.79	0.73	0.63

Table 4.11 The Maximum CSI Values from the Truss Type J series

5. CONCLUSIONS AND RECOMMENDATIONS

The objective of this study was to develop an efficient and practical method to analyze wood roof truss assemblies by more accurately modeling the entire truss assembly, including the system effects, and providing benefits of improved safety and reduced construction cost over the conventional single truss design method. In this study, a widely used structural program, SAP2000, was employed as an analysis tool and as a practical approach to model Metal-Plate-Connected (MPC) trusses and truss assemblies.

SAP2000 (1997) can model the semi-rigid behavior of truss connections using linear springs (Nlink elements) or using a truss plate manufacturer's (TPM's) joint model.

The verifications of the truss models included the following: (1) In verifying predictions of average deflection for single trusses using a linear spring (LS) joint model, twenty-four Fink configuration, 28-foot-span, roof trusses with 3:12 and 6:12 slopes tested at the FPL by Wolfe et al. (1986) were used. Predicted displacements for the individual truss models were within 9% of the test values (average % difference) shown in Tables 4.1 and 4.2. (2) In the load sharing verification for a nine-truss assembly using an LS joint model, the average differences for the predicted load sharing values of the truss assembly with high stiffness variability compared with test values (Wolfe and McCarthy, 1989) were 7.7% and 3.8% for the 3:12 and 6:12 slope trusses, respectively. In the load sharing

verification of the conventional nine-truss assembly with low stiffness variability tested by Wolfe and LaBissioniere (1991), the average differences of the predicted load sharing values compared with test values were 8.0% and 5.3% for the 3:12 and 6:12 slope trusses, respectively. (3) In the TPM's model verification for single trusses, the differences between the CSI values from the SAP2000 models and the CSI values from the output data from the TPM were between 4% and -2%. The percent differences are shown in Appendix H.

The SAP2000 model for the actual roof truss assembly was analyzed using both design and random material property values to calculate CSI values to show the system effects and examine the benefits of truss assembly modeling over the conventional design method.

Based on the results of this study, the following conclusions can be drawn:

1. The computer program SAP2000 can be employed as an analysis tool in a practical approach to model MPC trusses and truss assemblies.
2. Behavior (load distribution) of an actual roof truss assembly is influenced strongly by the interaction of sub-assemblies and boundary conditions.
3. The primary benefit of using an assembly model compared to the individual truss design method is in providing increased safety through improved analysis. Because system effects are directly considered in the assembly model, a more complete description of performance (e.g. the location of maximum CSI values) is obtained.

4. The secondary benefit of the assembly model compared to the individual truss design method is the cost consideration. In general, the maximum CSI value of a truss in an assembly (compared to the individual truss case) is decreased due to the system effects. For example, the maximum CSI value of 0.91 for an isolated single truss is decreased to 0.52 (percent difference: 43%) when the truss is in the assembly. For construction cost reduction, smaller members or lower grades may be used for members which have decreased CSI values.

For improved roof truss assembly modeling, recommendations for future research are the following:

1. Consider composite action in the roof truss assembly modeling. Composite action is the interaction of the truss top chords and plywood sheathing that increases the effective section properties of the top chords.
2. Develop the modeling approach for the sheathing gaps. The plywood sheathing plays a very import role in the load sharing effect. In this study, the sheathing gaps are modeled simply as pinned connections. Improved modeling for the sheathing gaps may lead to better predictions of the load sharing effect.
3. In this study, the roof truss assembly model is analyzed using only one set of random material property values. The results from the analysis are thus only those of a case study and many more sets of random material property values are needed for general results.

BIBLIOGRAPHY

- Breyer, D. E., Fridley, K. J. and Cobeen, K. E. 1998. Design of Wood Structures. McGraw-Hill, New York, New York.
- Cramer, S.M., and Wolfe, R.W 1989. Load-distribution model for light-frame wood roof assemblies. *J. of Str. Eng.*, 115(10): 2602-2617.
- Cramer, S.M., Shrestha, D. and Mtenga, P.V. 1993. Computation of member forces in metal plate connected wood trusses. *Str. Eng. Rev.*, 5(3): 209-218.
- ETABS, 1995. Computers and Structures, Inc. Berkeley, California, 94704, USA
- Foschi, R.O. 1977a. Analysis of wood diaphragms and trusses. Part I: Diaphragms. *Can. J. of Civil Eng.*, 4:345-352.
- Foschi, R.O. 1977b. Analysis of wood diaphragms and trusses. Part II: Truss-plate connections. *Can. J. of Civil Eng.*, 4: 353-362.
- Gebremedhin, K.G., Jorgensen, M.C. and Woelfel, C.B. 1992. Load-slip characteristic of metal plate connected wood joints tested in tension and shear. *Wood and Fiber Sci.*, 24(2):118-132.
- Gerhards, C.C. 1983. Characterization of physical and mechanical properties of 2 by 4 truss lumber. Res. Paper, FPL-431, USDA, Forest Products Laboratory, Madison, Wisconsin.
- Gupta, R. 1990. Reliability analysis of semirigidly connected metal plate residential wood trusses. Ph.D Thesis, Cornell University, Ithaca, New York.
- Gupta, R. and Gebremedhin, KG. 1992. Resistance distributions of a metal-plate-connected wood truss. *Forest Prod. J.* 42(7/8): 11-16.
- Gupta, R. 1994. Metal-Plate Connected Tension Joints under Different Loading Conditions. *Wood and Fiber Sci.*, 26(2):212-222.
- King, C.G. and Wheat, D.L. 1987. Deflection and member behavior of metal-plate connected parallel-chord wood trusses. Res. Report, University of Texas, Austin, Texas.

- Kuenzi, E.W and Wilkinson, T.L. 1971. Composite beams - effect of adhesive or fastener rigidity. Res. Paper, FPL-152, USDA, Forest Products Laboratory, Madison, Wisconsin.
- LaFave, K.D. 1990. Experimental and Analytical Study of Load Sharing in Wood Truss Roof System. M.S. Thesis, Washington State University, Pullman, WA.
- LaFave, K. and Itani, R. 1992. Comprehensive load distribution model for wood truss assemblies. *Wood and Fiber Sci.*, 24(1): 79-88.
- Li, Z. 1997. A Practical Approach to Model the Behavior of a Metal-Plate-Connected Wood Truss System. M.S. Thesis, Oregon State University, Corvallis, Oregon.
- Maraghechi, K. and Itani, R. Y. 1982. Influence of truss plate connectors on the analysis of light frame structures. *Wood and Fiber Sci.*, 16(3): 307-322.
- McCarthy, M. and Wolfe, R.W. 1987. Assessment of truss plate performance model applied to Southern Pine truss joints. Res. Paper, FPL-RP-483, USDA, Forest Products Laboratory, Madison, Wisconsin.
- Mtenga, P.V. 1991. Reliability of light-frame wood roof systems. Ph.D Thesis, University of Wisconsin- Madison, Madison, Wisconsin.
- Mtenga, P.V., Cramer, S.M. and Wolfe, R.W. 1995. System factors for light-frame wood truss assemblies. *J. of Str. Eng.*, 121(2): 290-300.
- Mtenga, P. V. 1998. Impact of using a system factor in the design of light-frame roof assemblies. *Forest Product J.*, 48(5): 27-34.
- National Design Specification for Wood Construction, 1991. American Forest & Paper Association, Washington, D.C.
- National Design Specification for Wood Construction, 1997. American Forest & Paper Association, Washington, D.C.
- SAP2000, 1997. Computers and Structures, Inc. Berkeley, California, USA
- Showalter, J.H. Jr. and Grundahl, K.H. 1991. Metal Plate Connected Wood Truss Design by LRFD. ASAE Paper NO. 914539, St. Joseph, MI.

- Skaggs, T.D., Woeste, F.E., Dolan, J.D., and Loferski, J.R. 1994. Safety Factors for Metal-Plate-Connected Wood Trusses: Theoretical Design versus Test Specifications. *Forest Prod. J.* 44(9): 11-18.
- Stahl, D.C., Wolfe, R.W., Cramer, S.M., and McDonald, D. 1994. Strength and Stiffness of Large-Gap Metal-Plate Wood Connections. Res. Paper, FPL-RP-535, USDA, Forest Products Laboratory, Madison, Wisconsin.
- Suddarth, S.K. 1963. A detailed study of a W truss with metal gusset plates. Agricultural Experiment Station, Purdue University, West Lafayette, Indiana. Research Progress Report 50.
- TPI. 1995. National design standard for metal-plate-connected wood truss construction. ANSI/ TPI 1-1995. Truss Plate Institute, Madison, Wisconsin.
- Vanderbilt, M.D. 1974. Matrix Structural Analysis. Quantum Publishers, New York, N.Y.
- Varoglu, E. and Barrett, J.D. 1984. Structural analysis of trusses and truss systems. Res. Report, Forintek Canada Corporation, Vancouver, B.C., Canada.
- Varoglu, E. 1985. Structural analysis of trusses and truss systems. Res. Report, Forintek Canada Corporation, Vancouver, B.C., Canada.
- Vatovec, M. 1996. Analytical and experimental investigation of the behavior of metal- plate-connected wood truss joints. Ph.D Thesis, Oregon State University, Corvallis, Oregon.
- Wang, C.K. 1983. Intermediate Structural Analysis. McGraw-Hill, Inc., New York, N.Y.
- Wang, C.K. 1986. Structural Analysis on Microcomputers. Macmillan, New York, N.Y.
- Warner, J.H. and Wheat, D.L. 1986. Analysis of structures containing layered beam-columns with interlayer slip. Res. Report, University of Texas, Austin, Texas.
- Wolfe, R.W. and Percival D.H. and Moody, R.C. 1986. Strength and stiffness of light-frame sloped trusses. Res. Paper, FPL 471, Forest Products Laboratory, Madison, Wisconsin.

Wolfe, R.W. and McCarthy, M. 1989. Structural performance of light-frame roof assemblies - I. Truss assemblies designed for high variability and wood failure. Res. Paper, FPL-RP-492, USDA, Forest Products Laboratory, Madison, Wisconsin.

Wolfe, R.W. and LaBissoniere, T. 1991. Structural performance of light-frame roof assemblies - II. Conventional truss assemblies. Res. Paper, FPL-RP-499, USDA, Forest Products Laboratory, Madison, Wisconsin.

APPENDICES

APPENDIX A Comparison Between SAP2000 and ETABS

Li (1997) modeled MPC trusses using the computer program, ETABS (1995), but a different computer program, SAP2000 (1997), is used for this study.

For a truss analysis, SAP2000 has the following advantages over ETABS:

1. Ease of data input for the complex truss roof system geometry. The SAP2000 working environment features a powerful graphics interface, that is easy to use, makes data input simplified, and saves time. The “Replicate” function key is especially convenient for building the truss assembly system.
2. Convenience of structural analysis. After completing the input files, the program analysis takes place in the same window. It is not necessary to go back and forth between the input and analysis windows.
3. Capability to handle beam element rotation and calculation of axial force for sloped members. The ETABS program only allows horizontal beams to be oriented in either a horizontal or vertical direction, but there is no such limitation in the SAP2000 program.

APPENDIX B Stiffness Derivation for Nlink Elements for Semi-Rigid Truss Model

In this appendix, the stiffnesses for the nlink elements at heel joints and bottom-chord-tension-splice joints for the semi-rigid truss models are calculated according to the following formulae by Li (1997) and based on Foschi's (1977b) study. The initial stiffnesses (k), including k_{AA} , k_{AE} , k_{EE} and k_{EA} , were obtained from Wolfe and McCarthy (1989). No. 2 Southern Pine 2"x4" lumber and a combination of 16-gauge and 20-gauge metal plates were used in their tests. In their test report, the initial stiffnesses (lb/in.) for joints with 60 teeth are 1598000, 212000, 271000 and 660000 for k_{AA} , k_{AE} , k_{EE} and k_{EA} , respectively. The single tooth value k for each initial stiffness is calculated for this study.

$$k_{AA}=1598000/60=26630\text{b/in.} \quad k_{EA}=660000/60=11000\text{ lb/in.} \quad \beta_1=4.5\text{ teeth/in}^2$$

$$k_{AE}=212000/60=3533\text{lb/in.} \quad k_{EE}=271000/60=4517\text{b/in.} \quad \beta_2=8\text{ teeth/in}^2$$

$$K_x = [k_{AA} * k_{AE} / (k_{AA} * \sin^2 \emptyset + k_{AE} * \cos^2 \emptyset)] * A * \beta \quad (\text{pounds/inch})$$

$$K_z = [k_{EE} * k_{EA} / (k_{EE} * \sin^2 \emptyset + k_{EA} * \cos^2 \emptyset)] * A * \beta \quad (\text{pounds/inch})$$

$$k_x = [k_{AA} * k_{AE} / (k_{AA} * \sin^2 \emptyset + k_{AE} * \cos^2 \emptyset)] \quad (\text{pounds/inch})$$

$$k_z = [k_{EE} * k_{EA} / (k_{EE} * \sin^2 \emptyset + k_{EA} * \cos^2 \emptyset)] \quad (\text{pounds/inch})$$

$$K_{yy} = \beta * (k_x * I_x + k_z * I_z) \quad (\text{pound.inch/radian})$$

where

K_x, K_z = Translational nlink stiffnesses for a plate-wood contact area along the horizontal (x-axis) and the vertical (z-axis) directions, respectively.

K_{yy} = Rotational nlink stiffness for a plate-wood contact area

\emptyset = The angle between the grain orientation and the major axis of the plate. For the heel joint, \emptyset = the slope of the truss. For the bottom-chord- tension-splice joint, $\emptyset = 0^\circ$.

β = Tooth density of the metal plate. (In this study, all of the plates for the truss plate manufacturer's truss models are assumed to have the same tooth density, β_2 , and the plates for other truss models are assumed to have the same tooth density, β_1 .)

A = Plate-wood contact area. (in^2)

I_x, I_z = Moments of inertia of plate-wood contact area about the x- and z-axes, respectively. (in^4)

k_x, k_z = The initial stiffness of a single tooth along the horizontal (x-axis) and vertical (z-axis) directions from Foschi (1977b).

Examples of calculations for the nlink elements and the lengths of rigid links are shown in the following:

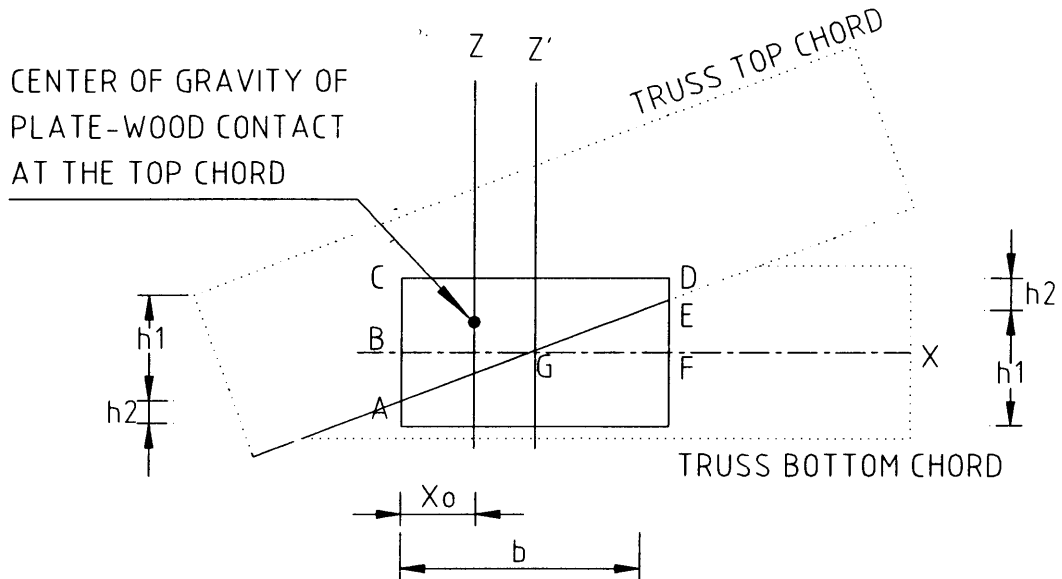
EXAMPLE I.

Figure B.1 Plate-Wood Contact Area for Heel Joint at Top Chord

HEEL JOINT ALONG TRUSS TOP CHORD

For Truss Types A, A1, and A2: $(\beta_2 = 8 \text{ teeth/in}^2)$

$\theta = \text{the slope of the truss} = \tan^{-1}\left(\frac{100.3}{16 \cdot 12}\right) = 27.57^\circ \text{ for the top chord}$

$b = 5''$; $h_1 = 2.805''$; $h_2 = 0.1947''$

$A = (h_1 + h_2) \cdot b / 2 = (2.805 + 0.1947) \cdot 5 / 2 = 7.5 \text{ (in.}^2\text{)}$

I_x = Moment of inertia of plate-wood contact area at the top chord (area ACDE) about x- axis

= Moment of inertia of rectangular area BCDF about x- axis (Triangular areas ABG and EFG have the same areas and the same moments of inertia about the x- axis, because point G is the center of gravity of the entire metal connector plate.)

$$= b \cdot (h_1 + h_2)^3 / 24$$

$$= 5 \cdot (2.805 + 0.1947)^3 / 24 = 5.625 \text{ (in}^4\text{.)}$$

I_z = Moment of inertia of plate-wood contact area at the top chord (area ACDE) about z- axis

$$= \frac{b^3 (h_1^2 + 4 \cdot h_1 \cdot h_2 + h_2^2)}{36 \cdot (h_1 + h_2)} = \frac{5^3 (2.805^2 + 4 \cdot 2.805 \cdot 0.1947 + 0.1947^2)}{36 \cdot (2.805 + 0.1947)}$$

$$= 11.68 \text{ (in}^4\text{.)}$$

$K_x = [k_{AA} \cdot k_{AE} / (k_{AA} \cdot \sin^2 \theta + k_{AE} \cdot \cos^2 \theta)] \cdot A \cdot \beta_2 \cdot 2$ (a factor of “2” for two metal- plate areas, one on either side of the MPC joint)

$$= \left[\frac{26630 \cdot 3533}{26630 \cdot \sin^2 (27.57^\circ) + 3533 \cdot \cos^2 (27.57^\circ)} \right] \cdot 7.5 \cdot 2 \cdot 8$$

$$= 1331000 \text{ pounds/inch}$$

$K_z = [k_{EE} \cdot k_{EA} / (k_{EE} \cdot \sin^2 \theta + k_{EA} \cdot \cos^2 \theta)] \cdot A \cdot \beta_2 \cdot 2$

$$= \left[\frac{4517 \cdot 11000}{4517 \cdot \sin^2 (27.57^\circ) + 11000 \cdot \cos^2 (27.57^\circ)} \right] \cdot 7.5 \cdot 2 \cdot 8$$

$$= 620400 \text{ pounds/inch}$$

$$k_x = [k_{AA} \cdot k_{AE} / (k_{AA} \cdot \sin^2 \theta + k_{AE} \cdot \cos^2 \theta)] = 11090 \text{ pounds/inch}$$

$$k_z = [k_{EE} * k_{EA} / (k_{EE} * \sin^2 \emptyset + k_{EA} * \cos^2 \emptyset)] = 5170 \text{ pounds/inch}$$

$$K_{yy} = 2 * \beta_2 * (k_x * I_x + k_z * I_z)$$

$$= 2 * 8 * (11090 * 5.625 + 5170 * 11.68) = 1965000 \text{ pound. inch/radian}$$

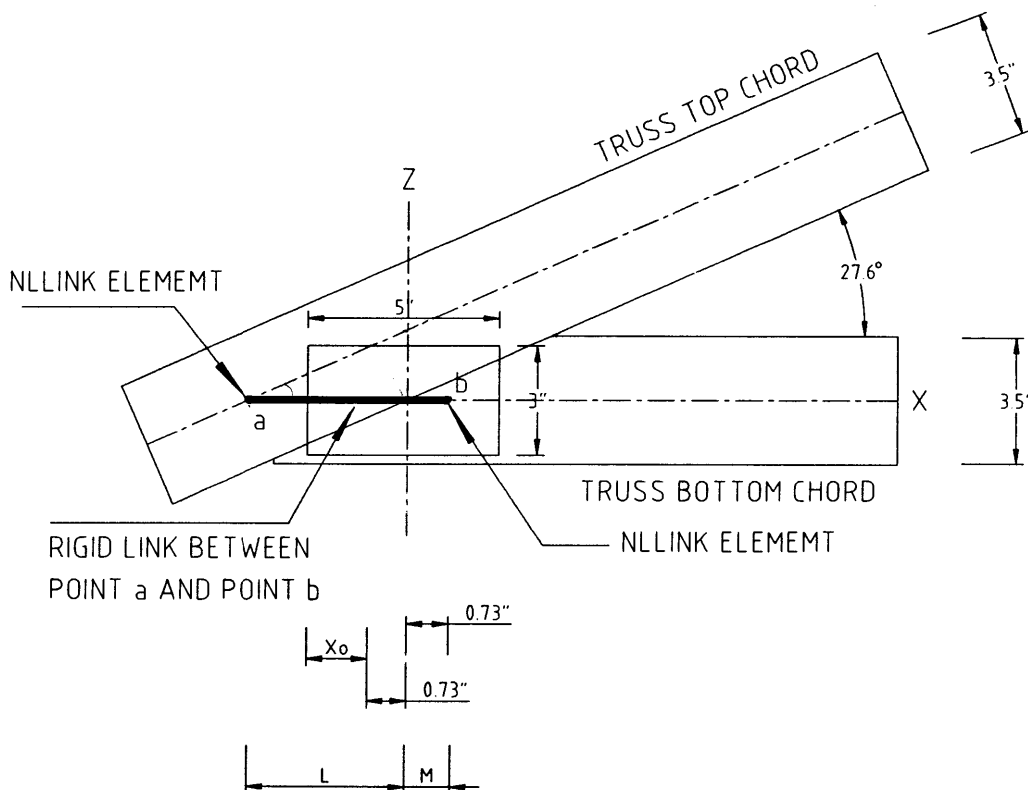


Figure B.2 Heel Joint Detail in the Truss Types A, A1, and A2

$$\emptyset = \text{the slope of the truss} = \tan^{-1}\left(\frac{100.3}{16 * 12}\right) = 27.57^\circ$$

$$X_o = \frac{b(2h_2 + h_1)}{3(h_1 + h_2)} = \frac{5(2 * 0.1947 + 2.805)}{3(2.805 + 0.1947)} = 1.775''$$

The distance from point a to the center line (Z-axis) of the metal-plate is L.

$$L = \frac{3.5/2}{\sin 27.57^\circ} = 3.781''$$

The distance from point b to the center line (Z-axis) of the metal-plate is M.

M = half of the width of the metal-plate – X_o

$$= 5''/2 - 1.775'' = 0.7252''$$

So, the length of the rigid link is equal to (L+M).

$$L+M = 3.781'' + 0.7252'' = 4.506''$$

EXAMPLE II.

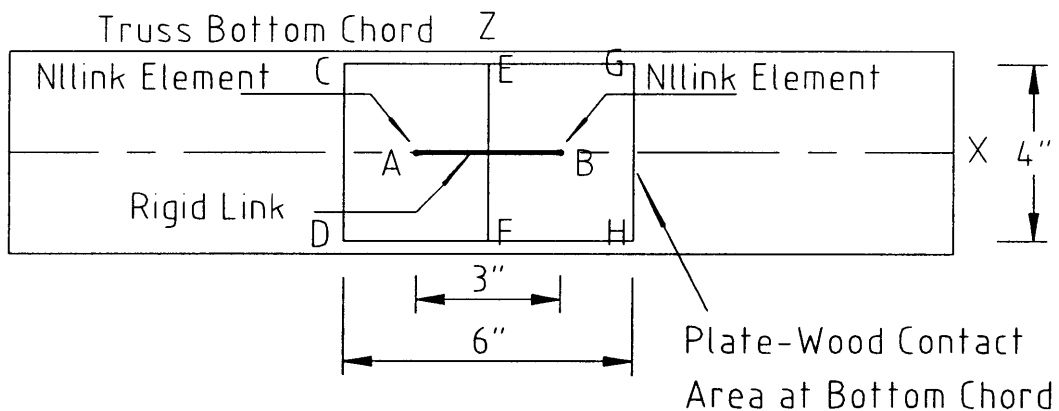


Figure B.3 Bottom-Chord-Tension-Splice Joint Detail for the Truss Type ASGR

TENSION SPLICE JOINT AT TRUSS BOTTOM CHORD

For truss type ASGR: $(\beta_2 = 8 \text{ teeth/in}^2)$

$$\theta = 0^\circ$$

$$A = 4*6/2=12 \text{ (in.}^2\text{)}$$

I_x = Moment of inertia of plate-wood contact area (area CDEF) at the
bottom chord about x- axis

$$= 3*(4)^3/12 = 16 \text{ (in}^4\text{.)}$$

I_z = Moment of inertia of plate-wood contact area (area ACDE) at the
bottom chord about z- axis

$$= 4*(3)^3/12 = 9 \text{ (in}^4\text{.)}$$

$K_x = [k_{AA}*k_{AE}/(k_{AA}*\sin^2 \emptyset + k_{AE}*\cos^2 \emptyset)]*A* \beta_2*2$ (a factor of “2” for two
metal- plate areas, one on either side of the MPC joint)

$$= [k_{AA}]*12*2*8$$

$$= 26630*12*16$$

$$= 5114000 \text{ pounds/inch}$$

$$K_z = [k_{EE}*k_{EA}/(k_{EE}*\sin^2 \emptyset + k_{EA}*\cos^2 \emptyset)]*A* \beta_2*2$$

$$= [k_{EE}]*12*2*8$$

$$= 4517*12*16$$

$$= 867300 \text{ pounds/inch}$$

$$k_x = k_{AA} = 26630 \text{ pounds/inch}$$

$$k_z = k_{EE} = 4517 \text{ pounds/inch}$$

$$K_{yy} = 2* \beta_2*(k_x*I_x + k_z*I_z)$$

$$= 2*8*(26630*16 + 4517*9) = 7468000 \text{ pound. inch/radian}$$

The distance from point A to point B is half of the length of the metal-plate, 3”.

EXAMPLE III

HEEL JOINT ALONG TRUSS BOTTOM CHORD

For truss types A, A1, and A2: $(\beta_2=8 \text{ teeth/in}^2)$

Recall that: $I_x = 5.625 \text{ (in}^4\text{.)}$; $I_z=11.68 \text{ (in}^4\text{.)}$

$\emptyset = 0^\circ$ for the bottom chord

$$\text{So, } K_x = k_{AA} * A * \beta_2 * 2$$

$$= 26630 * 7.5 * 8 * 2$$

$$= 3196000 \text{ pounds/inch}$$

$$K_z = k_{EE} * A * \beta_2 * 2$$

$$= 4517 * 7.5 * 8 * 2$$

$$= 542000 \text{ pounds/inch}$$

$$K_{yy} = 2 * \beta_2 * (k_x * I_x + k_z * I_z)$$

$$= 2 * 8 * (26630 * 5.625 + 4517 * 11.68)$$

$$= 3241000 \text{ pounds inch/radian}$$

Joint stiffness values for the truss models using LS joint models and TPM's joint models are listed in Table B.1. The plate stiffness values of the truss models using LS joint models were verified using Li's (1997) results and they are identically the same numbers. For plates with the same tooth density and similar locations in Table B.1, the plate stiffness is proportional to the plate area, so larger plate areas will also have larger stiffness. In Table B.1, the stiffness values for heel

joints have the same trend, $K_{yy} > K_x > K_z$. For the bottom-chord-tension-splice joint, the formulas can be simplified as follows because of the angle $\emptyset = 0^\circ$.

$$K_x = k_{AA} * A * \beta = 26630 * A * \beta \quad (\text{pounds/inch})$$

$$K_z = k_{EE} * A * \beta = 4517 * A * \beta \quad (\text{pounds/inch})$$

$$k_x = k_{AA} = 26630 \quad (\text{pounds/inch})$$

$$k_z = k_{EE} = 4517 \quad (\text{pounds/inch})$$

$$K_{yy} = \beta * (k_{AA} * I_x + k_{EE} * I_z) = \beta * (26630 * I_x + 4517 * I_z) \quad (\text{pound.inch/radian})$$

In this case, they show the trend, $K_x > K_z$.

Nlink Location	Heel Joint Along Truss Top Chord			Heel Joint Along Truss Bottom Chord			Bottom-Chord-Tension-Splice Joint		
	K _x	K _z	K _{yy}	K _x	K _z	K _{yy}	K _x	K _z	K _{yy}
Using LS Joint Model 3:12 Slope	2.60	0.64	5.99	3.60	0.61	6.60	2.52	0.43	2.32
Using LS Joint Model 6:12 Slope	1.25	0.55	3.01	2.88	0.49	5.02	1.80	0.30	1.51
Using TPM's Joint Model: A, A1, and A2	1.33	0.62	1.97	3.20	0.54	3.24	3.84	0.65	3.36
Using TPM's Joint Model: AS1, AS2, and AS3	1.78	0.84	3.82	4.27	0.73	6.97	3.84	0.65	3.36
Using TPM's Joint Model: ASGR	2.04	1.00	5.07	5.12	0.87	8.84	5.12	0.87	7.47
Using TPM's Joint Model: B and J	1.03	0.50	1.32	2.56	0.43	2.40	-----	-----	-----
Using TPM's Joint Model: BGR	3.08	1.51	6.17	3.84	0.66	4.02	-----	-----	-----
Using TPM's Joint Model: J1	1.00	0.50	1.30	2.56	0.43	2.38	-----	-----	-----
Using TPM's Joint Model: J2	0.96	0.52	1.26	2.56	0.43	2.38	-----	-----	-----
Using TPM's Joint Model: J3	0.82	0.50	1.10	2.56	0.43	2.35	-----	-----	-----
Using TPM's Joint Model: JGR	2.76	0.94	6.19	5.12	0.87	9.12	-----	-----	-----

K_x, K_z: 10⁶ pounds/in. K_{yy}: 10⁶ pounds.inch/radian

Where: J, J1, J2, J3, and JGR do not have bottom-chord-tension- splice joints, so there are no stiffness values for these trusses.

Table B.1 Joint Stiffness Values for Truss Models

APPENDIX C Conversion Factors for Strength

TS, CS, BS are wood tensile, compressive, and bending strengths and they are calculated from Gerhards' (1983) results (for Southern Pine):

$$\text{Tension Strength (TS)} = -717 + 0.002823 * \text{MOE (pounds/in.}^2\text{)}$$

$$\text{Compressive Strength (CS)} = 1245 + 0.001949 * \text{MOE (pounds/in.}^2\text{)}$$

$$\text{Bending Strength (BS)} = 90 + 0.004276 * \text{MOE (pounds/in.}^2\text{)}$$

In portions of this study, random material property values are used in the CSI calculations. Random MOE values were generated according to a lognormal distribution and the CS, TS, and BS, were obtained from Gerhards' (1983) formulae, based on the random MOE values. From these formulae, CS, TS, and BS are the values for the ultimate strengths, not the design strengths, so they have to be converted to design values.

There are two different grades used, Southern Pine No.2 and Spruce-Pine-Fir No.1/No.2. There are two steps to convert ultimate strengths to design values. First, we determine all of the design values, CS, TS, BS, and MOE from the NDS (1991) and then substitute the MOE design value into the above formulae to determine the ultimate strengths CS, TS, and BS. Second, by comparing the ultimate strengths with the design values, the conversion factors can be calculated. The following examples show the procedure to calculate the conversion factors and how to use them to change the ultimate strengths to design values. The 1991 edition

of the NDS was used here to provide design values rather than the current NDS (1997), because the TPM used the 1991 values in its calculations. In this study, the differences between the current NDS (1997) and the 1991 edition of the NDS involve only the tabulated design values for Spruce-Pine-Fir.

EXAMPLE I.

Southern Pine No.2

MOE=1600000 psi, $F_b=1500$ psi, $F_t=825$ psi, $F_c=1650$ psi. (from 1991 NDS)

From the formulae of Gerhards' (1983), the ultimate strengths are as follows:

$$F_{bu}=90 + 0.004276*1600000=6932 \text{ psi}$$

$$F_{cu}=1245 + 0.001949*1600000=4363 \text{ psi}$$

$$F_{tu}=-717 + 0.002823*1600000=3800 \text{ psi}$$

The conversion factors are calculated by the following method:

$$\text{Conversion factor for bending strength}=F_b/F_{bu}=1500 / 6932=0.216$$

$$\text{Conversion factor for compressive strength}=F_c/F_{cu}=1650 / 4363=0.378$$

$$\text{Conversion factor for tension strength}=F_t/F_{tu}=825 / 3800=0.217$$

Using the same method for Spruce-Pine-Fir No.1/No.2, the MOE is equal to 1400000 psi, and the conversion factors are the following:

$$\text{Conversion factor for bending strength}=0.216$$

$$\text{Conversion factor for compressive strength}=0.378$$

$$\text{Conversion factor for tension strength}= 0.217$$

EXAMPLE II.

One of the random MOE values from the lognormal distribution for Spruce-Pine-Fir No.1/No.2 is 1532567 psi.

From the formulae of Gerhards' (1983), the ultimate strengths are the following:

$$F_{bu}=90 + 0.004276*1532567=6643 \text{ psi}$$

$$F_{cu}=1245 + 0.001949*1532567=4232 \text{ psi}$$

$$F_{tu}=-717 + 0.002823*1532567=3609 \text{ psi}$$

Applying the following conversion factors:

$$\text{Conversion factor for bending strength}=0.216$$

$$\text{Conversion factor for compressive strength}=0.378$$

$$\text{Conversion factor for tension strength}= 0.217$$

Design values of BS, CS, and TS:

$$F_{bD}=6643*0.216=1435 \text{ psi}$$

$$F_{cD}=4232*0.378=1600 \text{ psi}$$

$$F_{tD}=3609*0.217=783 \text{ psi}$$

APPENDIX D CSI Values Calculation

In this appendix, an example is shown of how to calculate the CSI value for a truss member. This is for truss member 1 from truss type A1 and output results are from Appendix B. The MOE for this member is 1600000 psi. ($F_b=1500$ psi, $F_c=1650$ psi, and $F_t=825$ psi.) The nominal lumber dimensions are 2"x4", so the cross-section area is 5.25 in^2 and the section modulus about the main axis is 3.063 in^3 .

EXAMPLE

SEGMENT	AXL.	MOM.
0.0	-2235	-1024
4.0	-2227	-345
8.0	-2219	270
12.1	-2211	820
16.1	-2203	1305
20.1	-2194	1726
24.1	-2186	2081
28.2	-2178	2372
32.2	-2170	2597
36.2	-2162	2758
40.2	-2154	2854
44.2	-2146	2885
48.3	-2138	2852
52.3	-2130	2753
56.3	-2122	2590
60.3	-2114	2362
64.4	-2106	2068
68.4	-2098	1710
72.4	-2090	1288
76.4	-2082	800
80.4	-2074	248
84.5	-2065	-370
88.5	-2057	-1052
92.5	-2049	-1799
96.5	-2041	-2611
100.6	-2033	-3488
104.6	-2025	-4429

Member: top chord Length=104.6"

Where:

SEGMENT ≈ 4 (in.)

AXL. =AXIAL FORCE, (lb)

MOM.=BENDING MOMENT, (lb.in)

Step1.

Finding the inflection points from bending

moments: (moment=0)

By using the intercept function:

$$\frac{X1 - 4.0}{8.0 - 4.0} = \frac{0 - (-345)}{270 - (-345)} \quad X1=6.2$$

$$\frac{X2 - 80.4}{84.5 - 80.4} = \frac{0 - (248)}{(-370) - (248)} \quad X2=82.1$$

These two inflection points can separate the member into three parts, each part's length is as follows: $Le_1=6.2''$, $Le_2=75.9''$, $Le_3=22.5''$; $d_1=3.5''$, $d_2=1.5''$

Step 2.

Using the adjustment factors in the 1991 edition of the NDS, the following adjusted design values can be calculated:

$$F'_b = F_b * C_r * C_D = 1500 * 1.15 * 1.15 = 1984 \text{ psi} \quad (C_D = 1.15 \text{ for snow load})$$

C_r = Repetitive Member Factor, for truss chords or similar members with spacing not more than 24" on centers and not less than three in number and are jointed by floor, roof or other load distributing elements adequate to support the design load. (C_r was used for both assemblies and individual trusses in this study.)

$$F'_t = F_t * C_D = 825 * 1.15 = 949 \text{ psi}$$

$$F'_c = F_c * C_D = 1650 * 1.15 = 1898 \text{ psi}$$

$$C_{T1} = 1 + 2300 Le_1 / (0.59 * MOE) = 1 + 2300 * 6.2 / (0.59 * 1600000) = 1.02$$

$$C_{T2} = 1 + 2300 Le_2 / (0.59 * MOE) = 1 + 2300 * 75.9 / (0.59 * 1600000) = 1.19$$

$$C_{T3} = 1 + 2300 Le_3 / (0.59 * MOE) = 1 + 2300 * 22.5 / (0.59 * 1600000) = 1.06$$

$$F_{cEx1} = \frac{0.3 \times MOE \times C_{T1}}{\left(Le_1 / d_1\right)^2} = \frac{0.3 \times 1600000 \times 1.02}{(6.2 / 3.5)^2} = 152849 \text{ (psi)}$$

$$F_{cEx2} = \frac{0.3 \times MOE \times C_{T2}}{\left(Le_2 / d_1\right)^2} = \frac{0.3 \times 1600000 \times 1.19}{(75.9 / 3.5)^2} = 1212 \text{ (psi)}$$

$$F_{cEx3} = \frac{0.3 \times MOE \times C_{T3}}{\left(Le_3 / d_1\right)^2} = \frac{0.3 \times 1600000 \times 1.06}{(22.5 / 3.5)^2} = 12233 \text{ (psi)}$$

Using NDS 3.7.1 for column stability factor, C_p :

$$C_{p1} = (1 + F_{cEx1}/F'_c)/1.6 - \sqrt{\left(\frac{1 + F_{cEx1}/F'_c}{1.6}\right)^2 - \frac{F_{cEx1}/F'_c}{0.8}}$$

$$= (1 + 152849/1898)/1.6 - \sqrt{\left(\frac{1 + 152849/1898}{1.6}\right)^2 - \frac{152849/1898}{0.8}} = 0.997$$

$$C_{p2} = (1 + F_{cEx2}/F'_c)/1.6 - \sqrt{\left(\frac{1 + F_{cEx2}/F'_c}{1.6}\right)^2 - \frac{F_{cEx2}/F'_c}{0.8}}$$

$$= (1 + 1212/1898)/1.6 - \sqrt{\left(\frac{1 + 1212/1898}{1.6}\right)^2 - \frac{1212/1898}{0.8}} = 0.5237$$

$$C_{p3} = (1 + F_{cEx3}/F'_c)/1.6 - \sqrt{\left(\frac{1 + F_{cEx3}/F'_c}{1.6}\right)^2 - \frac{F_{cEx3}/F'_c}{0.8}}$$

$$= (1 + 12233/1898)/1.6 - \sqrt{\left(\frac{1 + 12233/1898}{1.6}\right)^2 - \frac{12233/1898}{0.8}} = 0.9660$$

$$F'_{c1} = F_c * C_{p1} * 1.15 = 1650 * 0.997 * 1.15 = 1892 \text{ psi}$$

$$F'_{c2} = F_c * C_{p2} * 1.15 = 1650 * 0.5237 * 1.15 = 994 \text{ psi}$$

$$F'_{c3} = F_c * C_{p3} * 1.15 = 1650 * 0.966 * 1.15 = 1833 \text{ psi}$$

Step3.

Finding f_c and f_b by the following formula: (ABS: absolute value)

$$f_c = \text{Axial Compression Force} / \text{Cross-section area} = AXL. / 5.25 \text{ (psi)}$$

$$f_b = \text{Bending Moment} / \text{Section modulus about the main axis} = MOM. / 3.063 \text{ (psi)}$$

SEGMENT	ABS(f_c)	ABS(f_b)
0.0	425.7	334
4.0	424.1	112
8.0	422.6	88
12.1	421.1	268
16.1	419.5	426
20.1	418.0	563
24.1	416.5	679
28.2	414.9	774
32.2	413.4	848
36.2	411.9	900
40.2	410.3	932
44.2	408.8	942
48.3	407.2	931
52.3	405.7	899
56.3	404.2	845
60.3	402.6	771
64.4	401.1	675
68.4	399.6	558
72.4	398.0	420
76.4	396.5	261
80.4	395.0	81
84.5	393.4	121
88.5	391.9	343
92.5	390.4	587
96.5	388.8	852
100.6	387.3	1139
104.6	385.7	1446

$$CSI = \left(\frac{f_c}{F'_c} \right)^2 + \left(\frac{f_{bx}}{F'_b \left(1 - \frac{f_c}{F_{cEx}} \right)} \right)$$

Step 4.

The inflection points separate the length into three sections. In each section, the CSI value can be calculated by substituting the three parameters, F_{cEx} , F'_c , and F'_b , in the formula:

	Section I (0 ~6.2")	Section II (6.2"~ 82.1")	Section III (82.1"~ 104.6")
F_{cEx}	152849	1212	12233
F'_c	1892	994	1833
F'_b	1984	1984	1984

Unit: psi

SEGMENT	ABS(f_c)	ABS(f_b)	CSI
0.0	425.7	334	0.22
4.0	424.1	112	0.11
8.0	422.6	88	0.25
12.1	421.1	268	0.39
16.1	419.5	426	0.51
20.1	418.0	563	0.61
24.1	416.5	679	0.70
28.2	414.9	774	0.77
32.2	413.4	848	0.82
36.2	411.9	900	0.86
40.2	410.3	932	0.88
44.2	408.8	942	0.89
48.3	407.2	931	0.87
52.3	405.7	899	0.85
56.3	404.2	845	0.80
60.3	402.6	771	0.75
64.4	401.1	675	0.67
68.4	399.6	558	0.58
72.4	398.0	420	0.48
76.4	396.5	261	0.35
80.4	395.0	81	0.22
84.5	393.4	121	0.11
88.5	391.9	343	0.22
92.5	390.4	587	0.35
96.5	388.8	852	0.49
100.6	387.3	1139	0.64
104.6	385.7	1446	0.80

Step 5.

Find the maximum CSI value over the entire length.

The maximum CSI value for this truss member is 0.89.

APPENDIX E Truss Design Drawings from the TPM

In this appendix, the truss design drawings from the TPM are shown in Figures E1~E15. Dimensions of wood members, sizes of metal connector plates and truss member number are indicated in each figure.

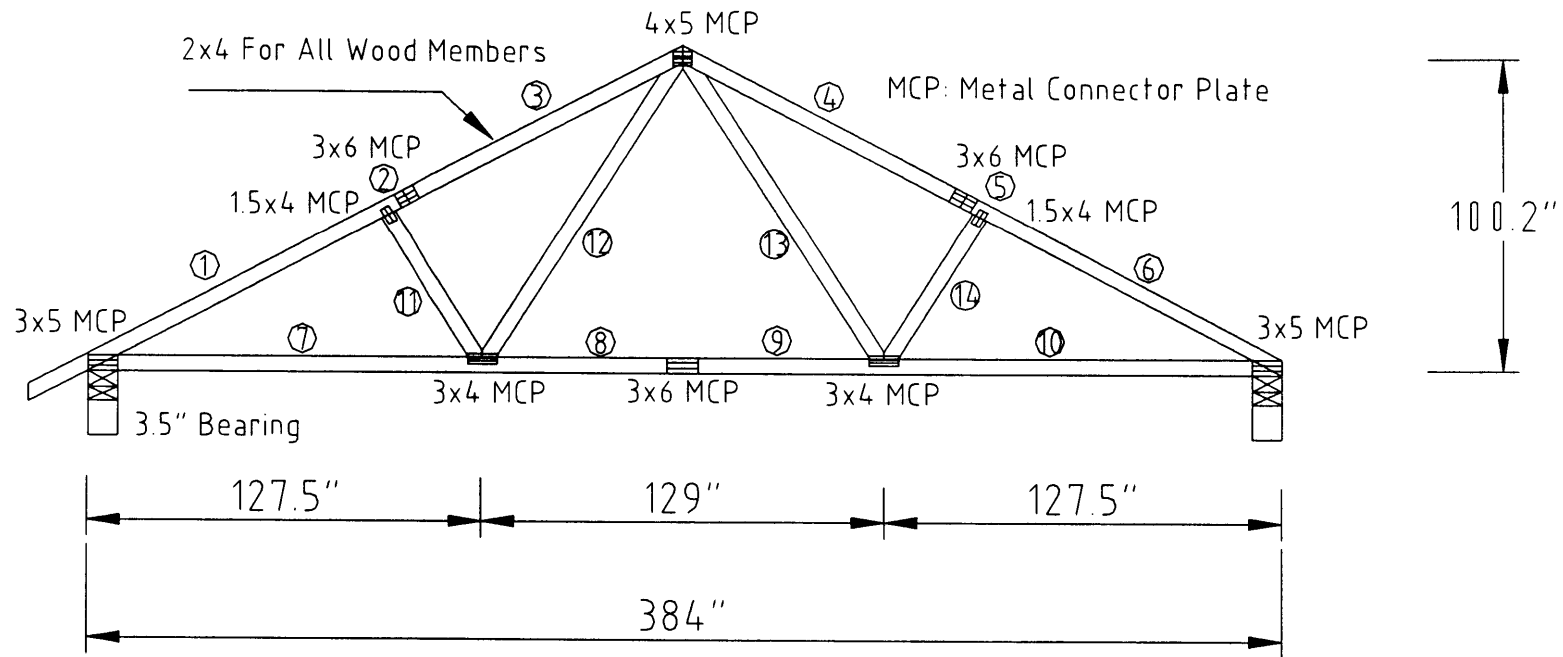


Figure E.1 MPC Truss Type A1 from a Truss Plate Manufacturer
(The difference between A and A1 is the overhang on the right side.)

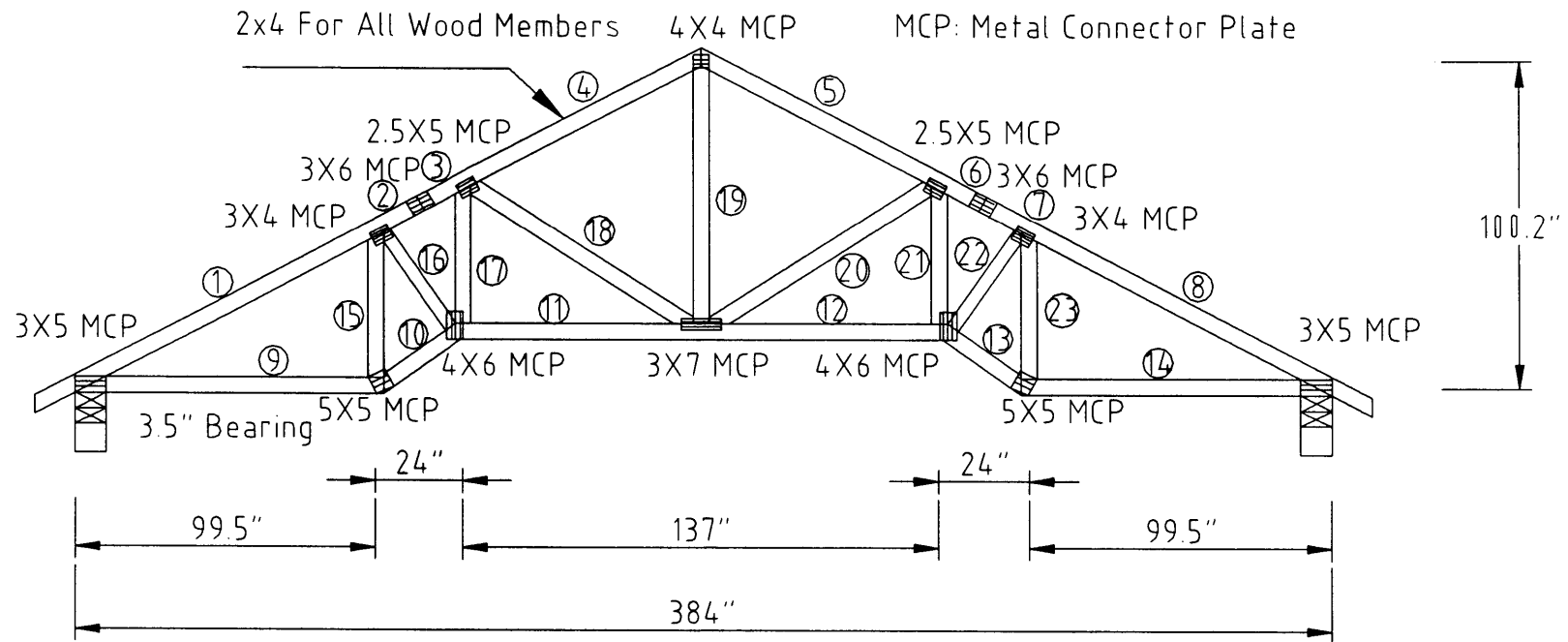


Figure E.2 MPC Truss Type A2 from a Truss Plate Manufacturer

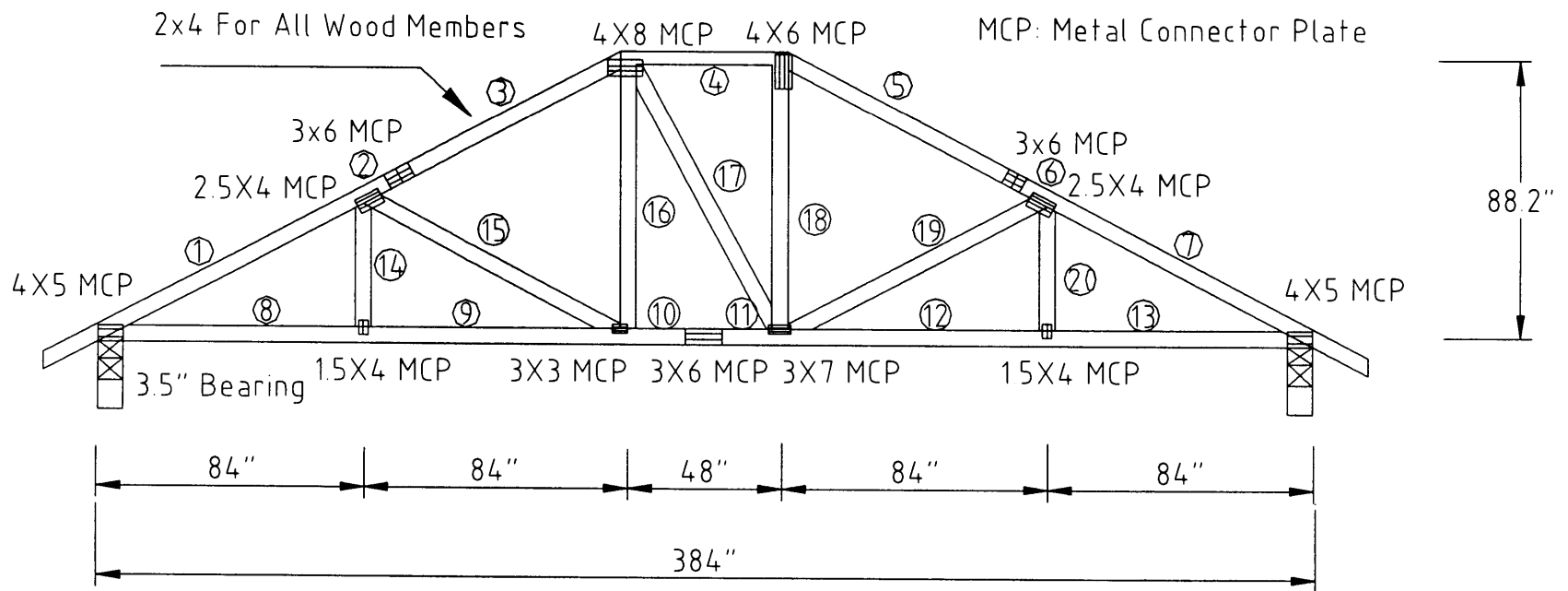


Figure E.3 MPC Truss Type AS1 from a Truss Plate Manufacturer

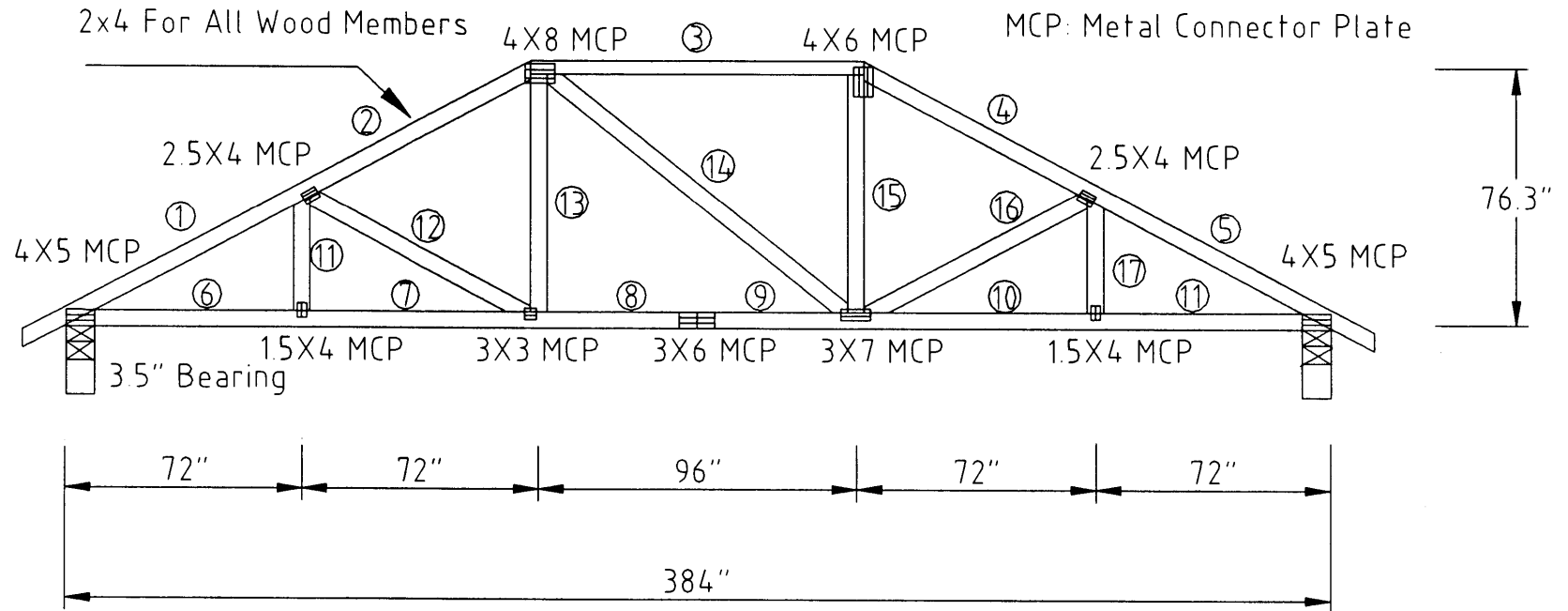


Figure E.4 MPC Truss Type AS2 from a Truss Plate Manufacturer

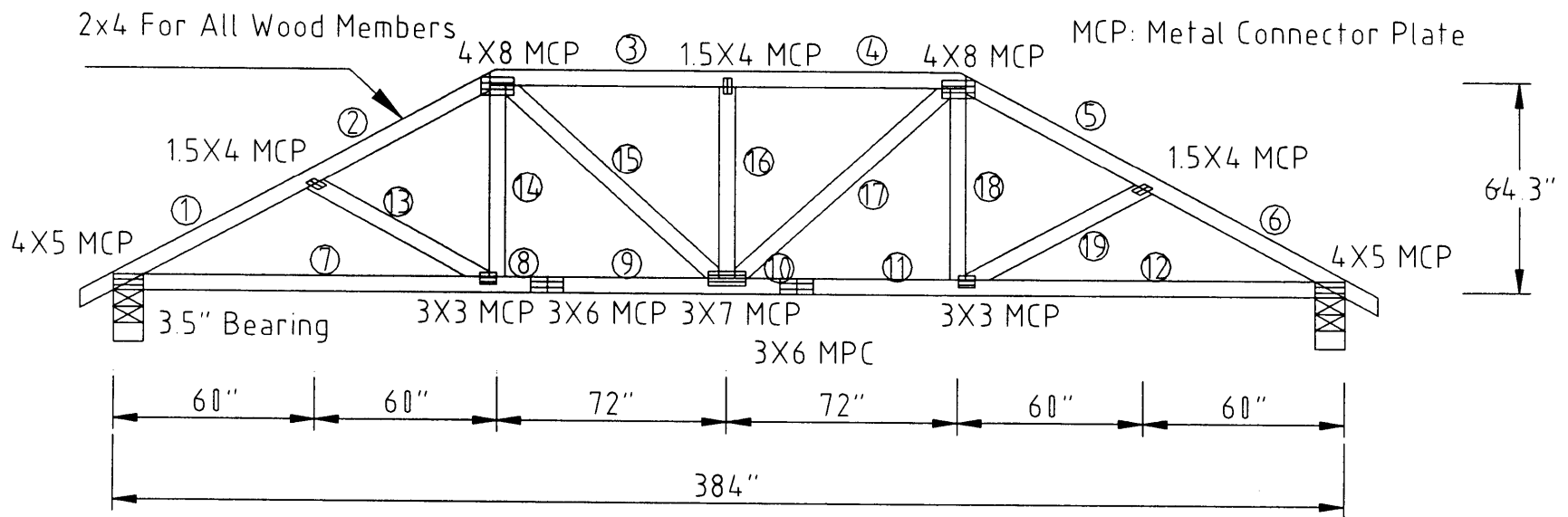


Figure E.5 MPC Truss Type AS3 from a Truss Plate Manufacturer

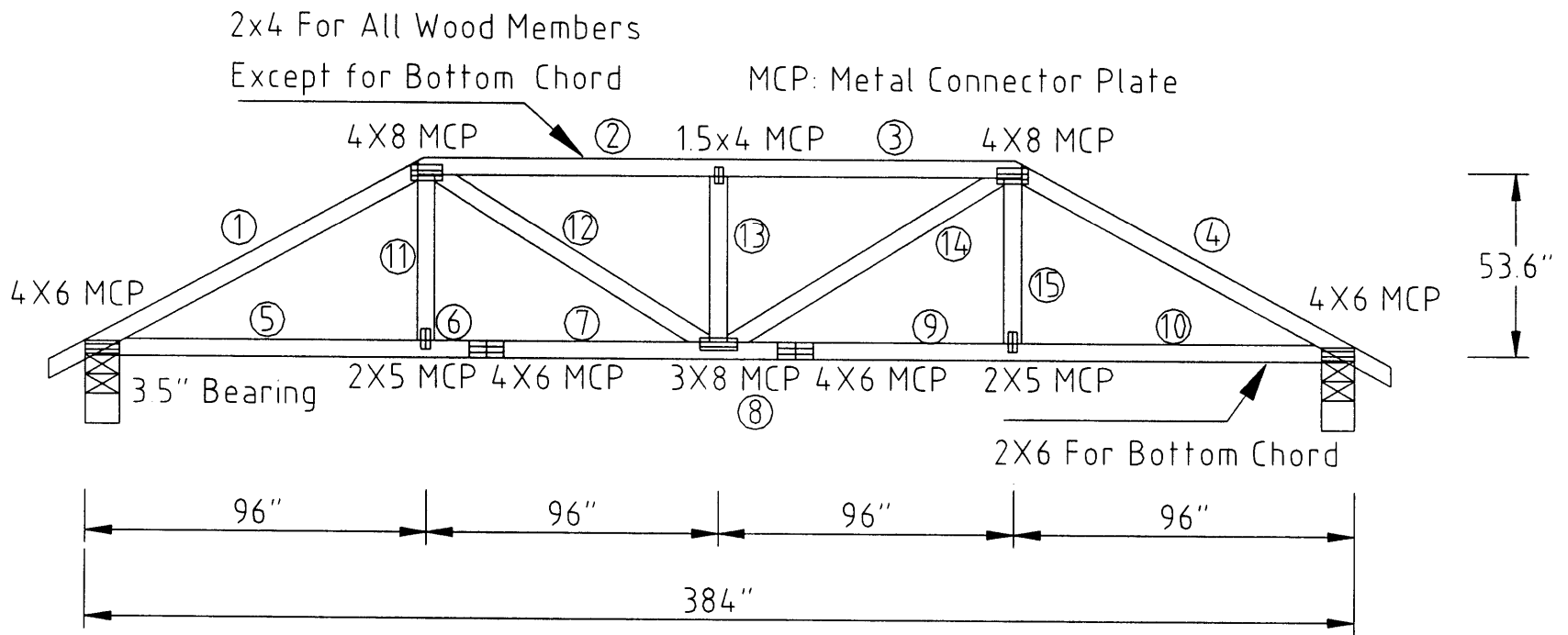


Figure E.6 MPC Truss Type ASGR from a Truss Plate Manufacturer

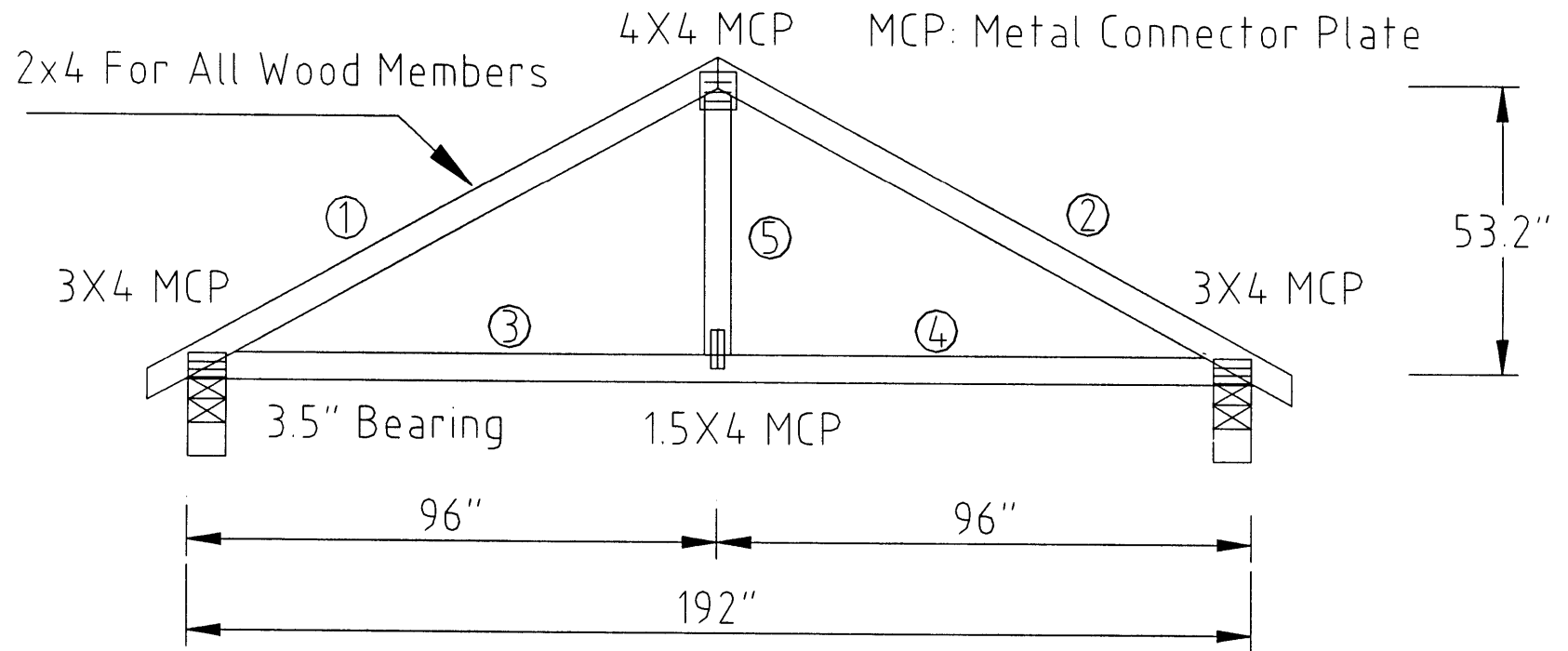


Figure E.7 MPC Truss Type B from a Truss Plate Manufacturer

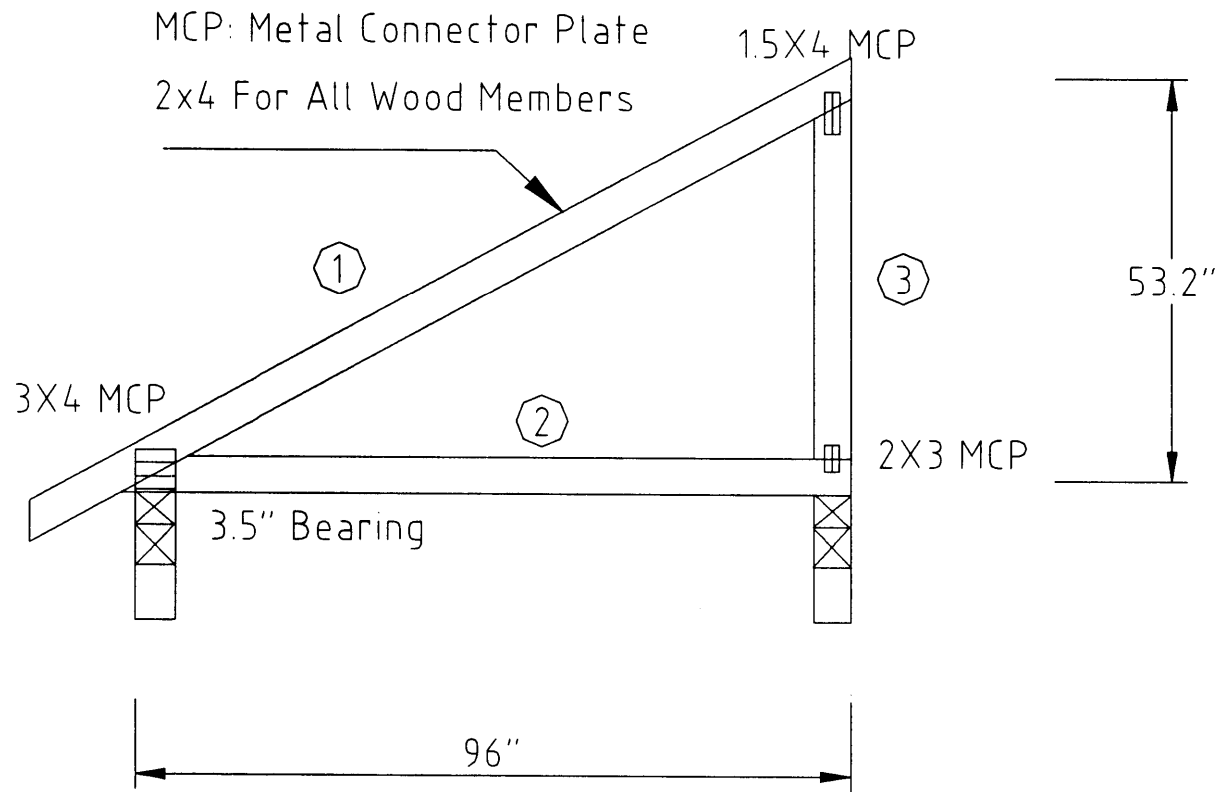


Figure E.9 MPC Truss Type J from a Truss Plate Manufacturer

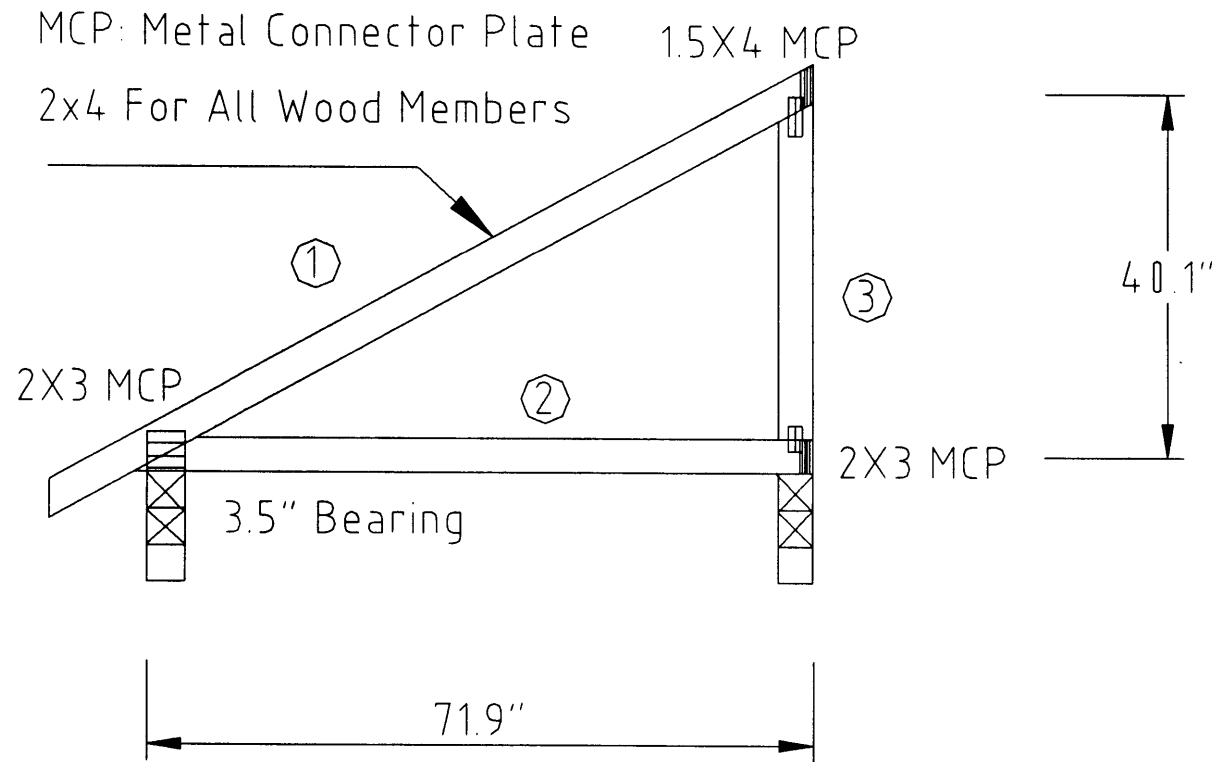


Figure E.10 MPC Truss Type J1 from a Truss Plate Manufacturer

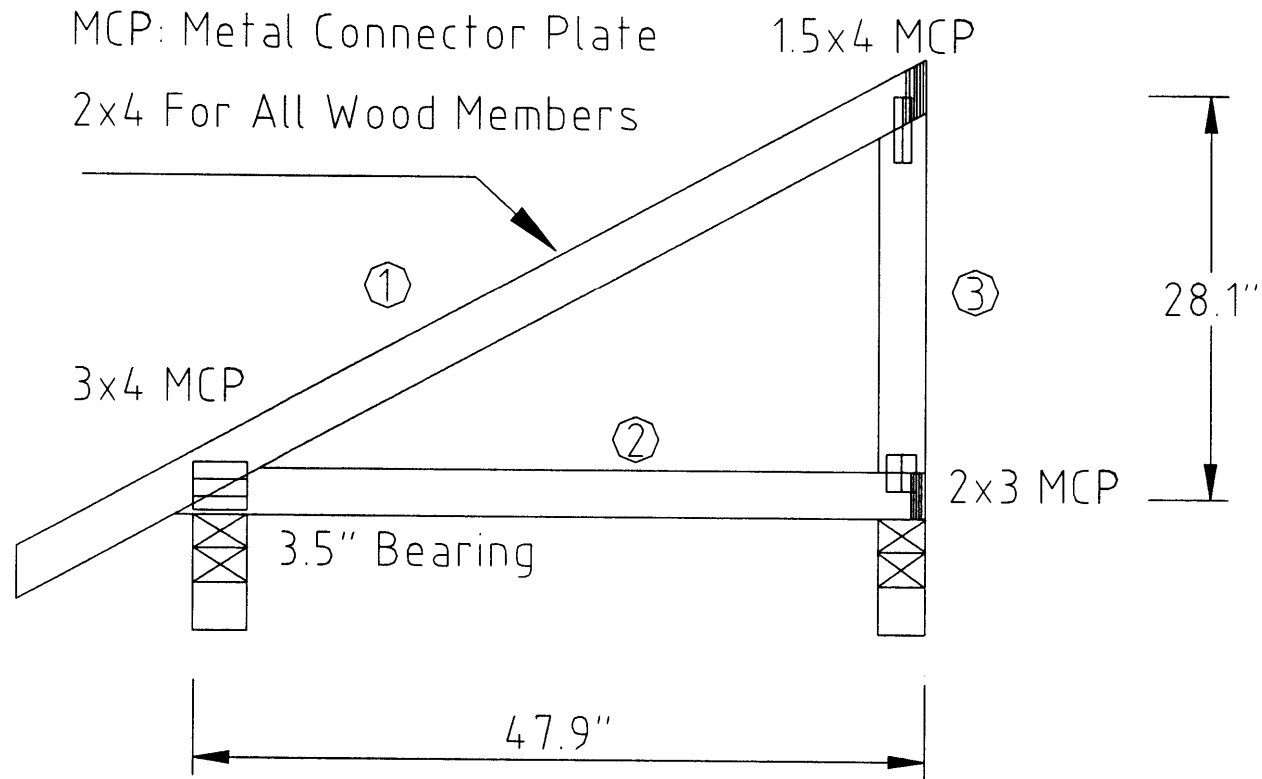


Figure E.11 MPC Truss Type J2 from a Truss Plate Manufacturer

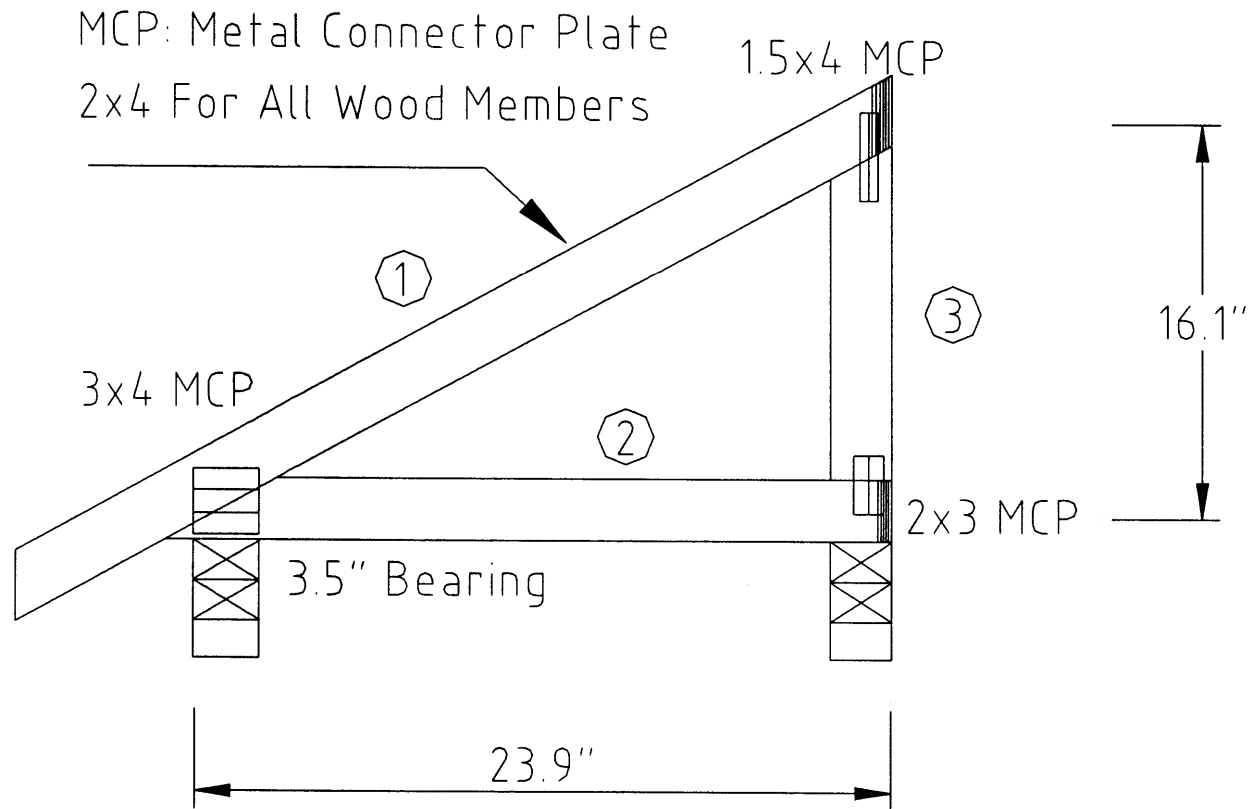


Figure E.12 MPC Truss Type J3 from a Truss Plate Manufacturer

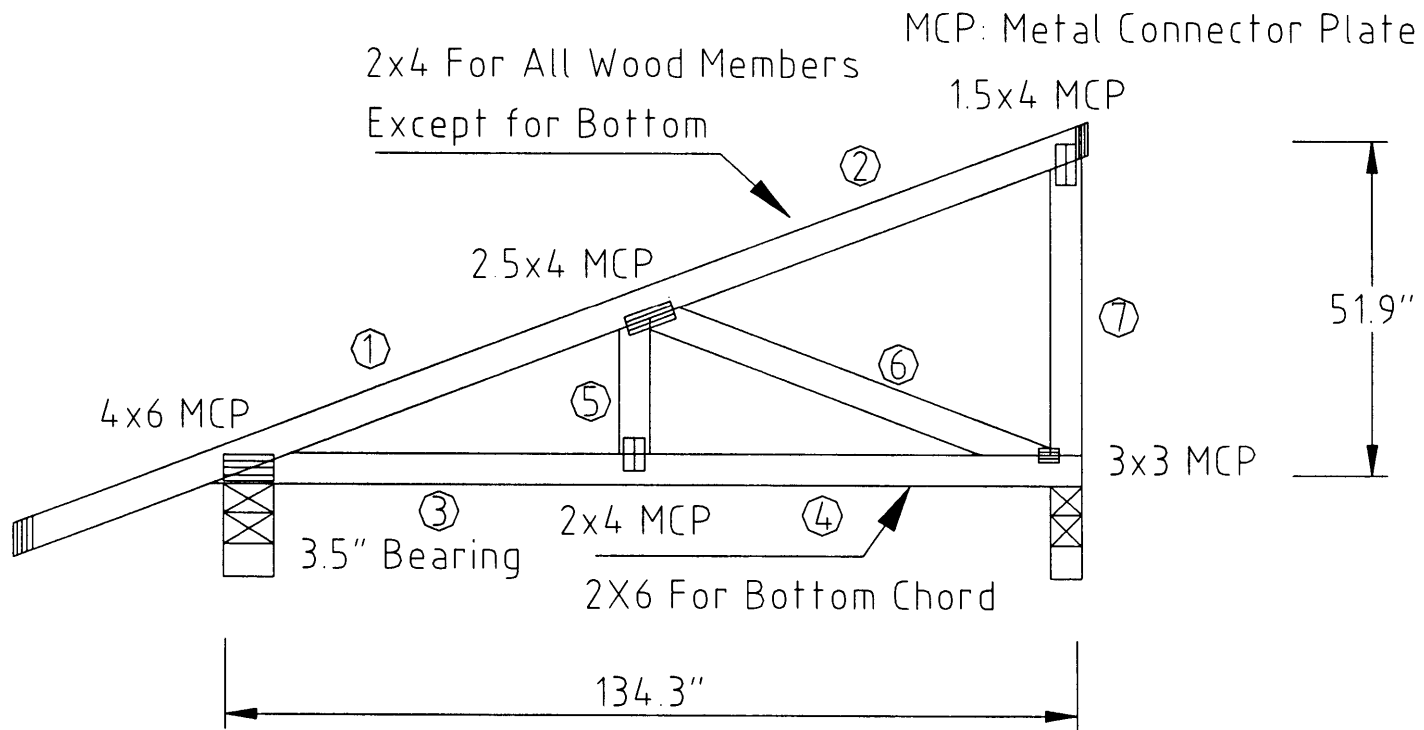


Figure E.13 MPC Truss Type JGR from a Truss Plate Manufacturer

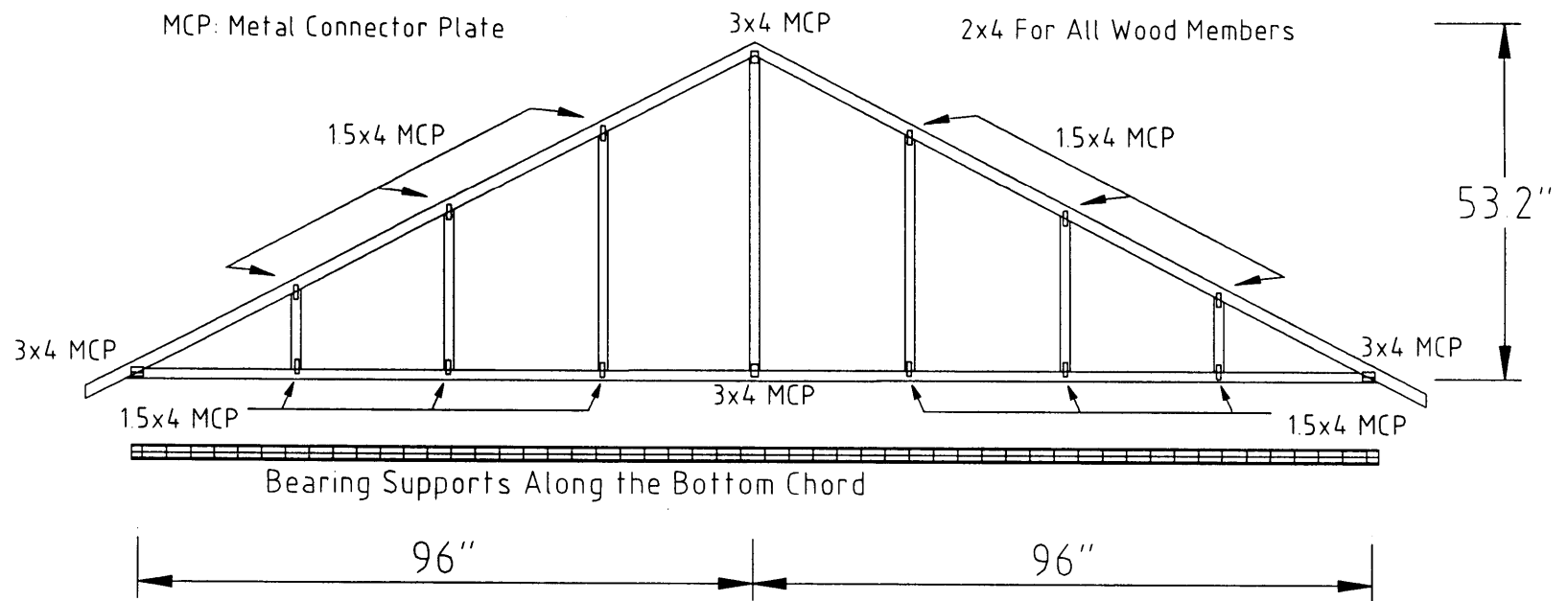


Figure E.14 MPC Truss Type BGB from a Truss Plate Manufacturer

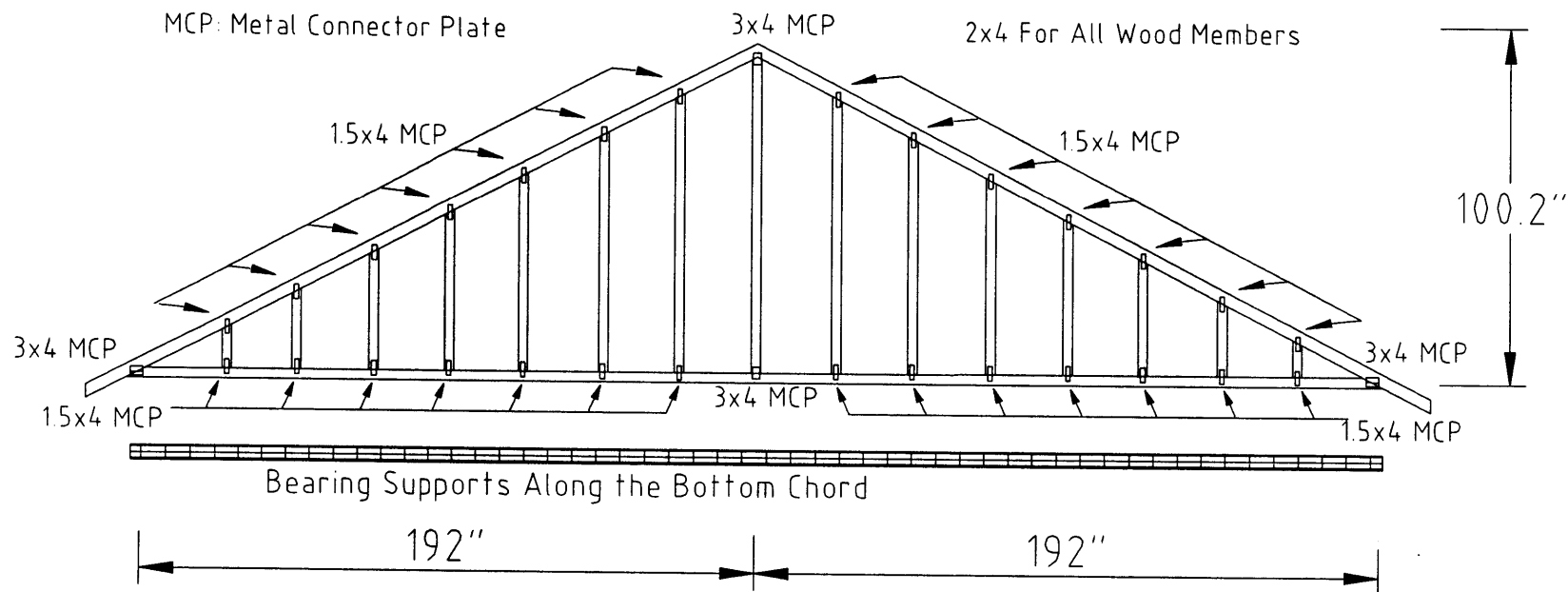


Figure E.15 MPC Truss Type AGB from a Truss Plate Manufacturer

APPENDIX F The TPM's Models (Analog) for Individual Trusses with Semi- Rigid Joints

This appendix shows the truss models (analog) with the TPM's joint models in Figures F1~F15. These truss models correspond to the truss designs from the previous appendix.

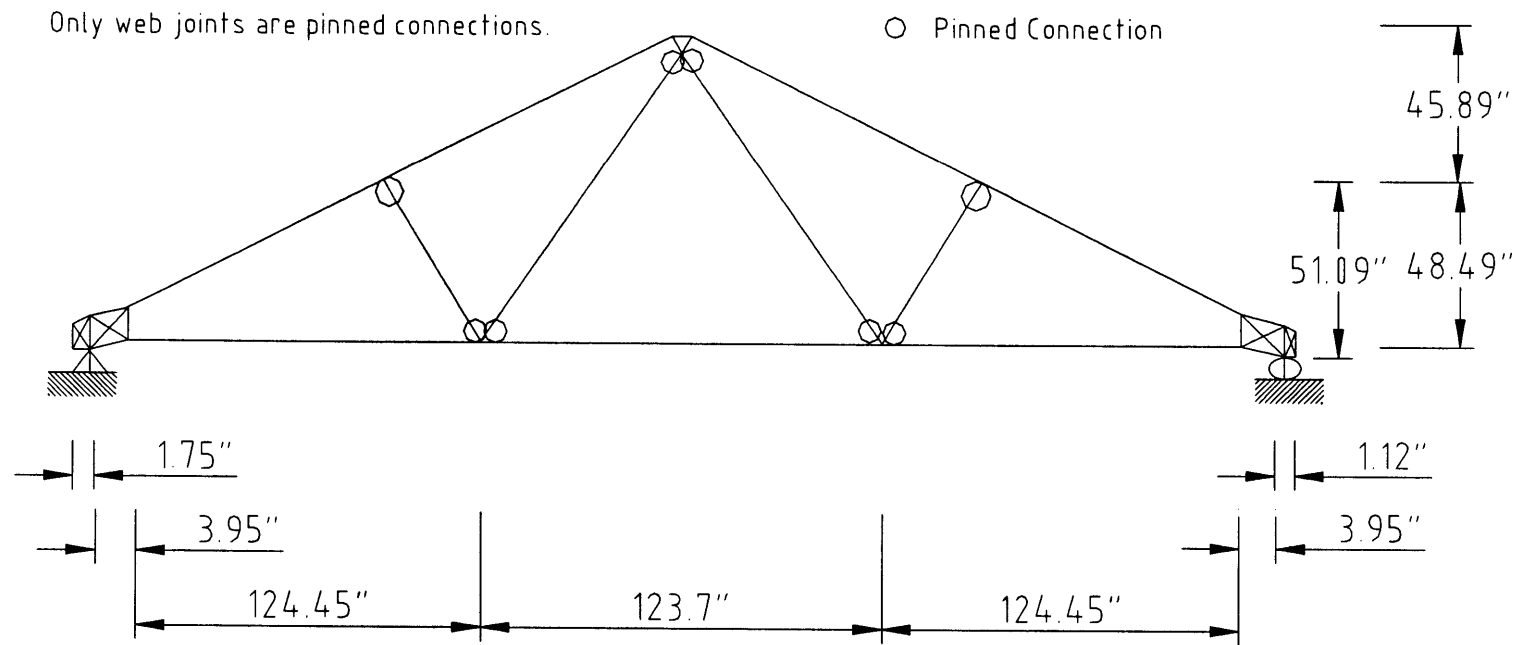


Figure F.1 The TPM's Model for Truss Type A1 with Semi-Rigid Joints Using SAP2000

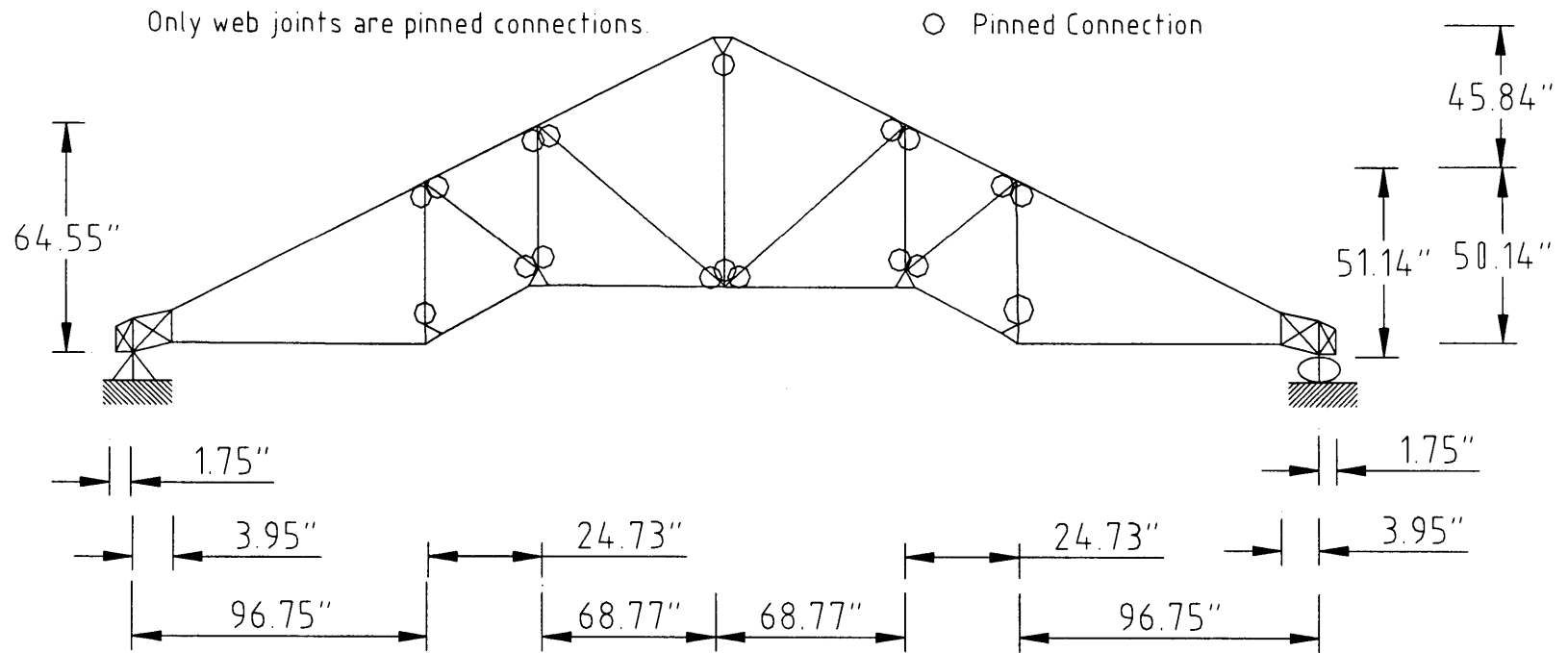


Figure F.2 The TPM's Model for Truss Type A2 with Semi-Rigid Joints Using SAP2000

Only web joints are pinned connections.

○ Pinned Connection

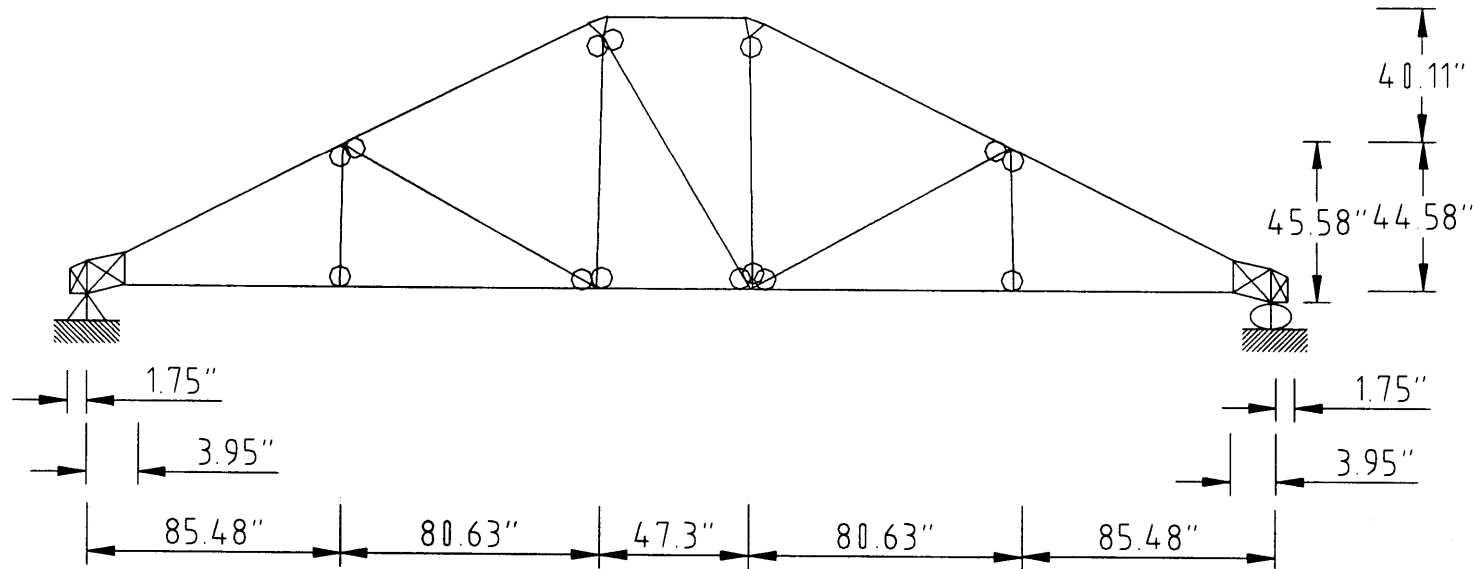


Figure F.3 The TPM's Model for Truss Type AS1 with Semi-Rigid Joints Using SAP2000

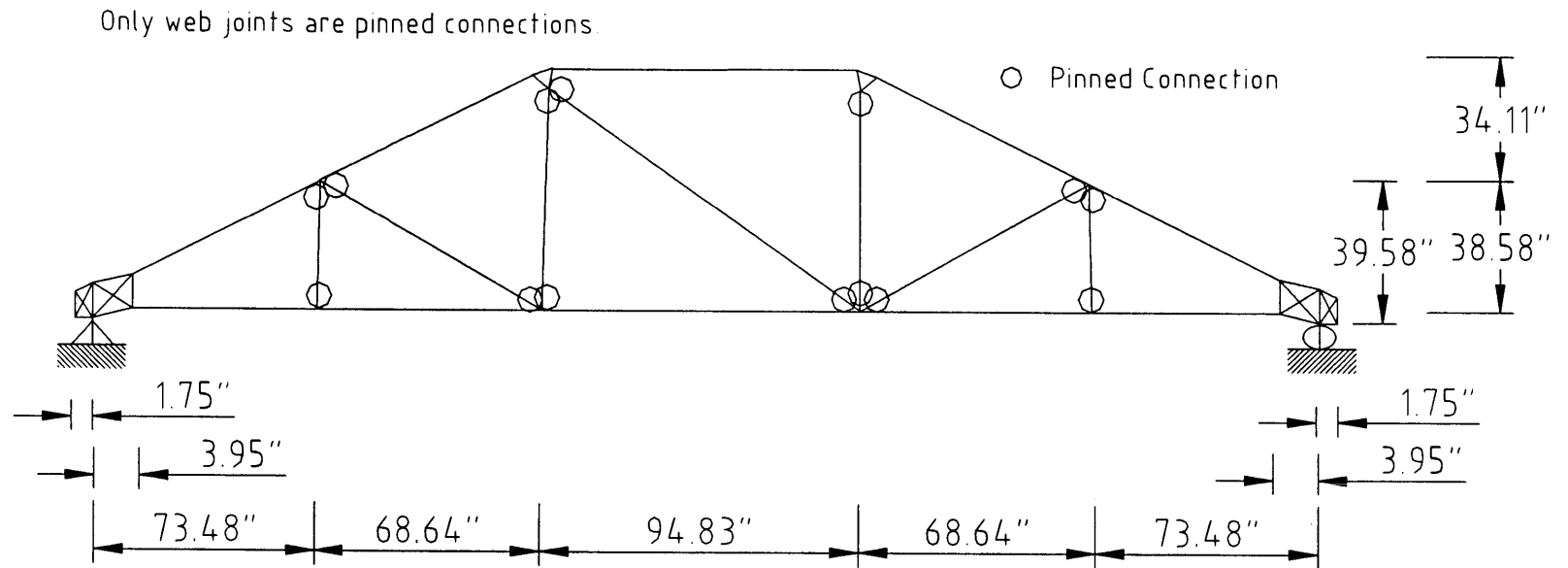


Figure F.4 The TPM's Model for Truss Type AS2 with Semi-Rigid Joints Using SAP2000

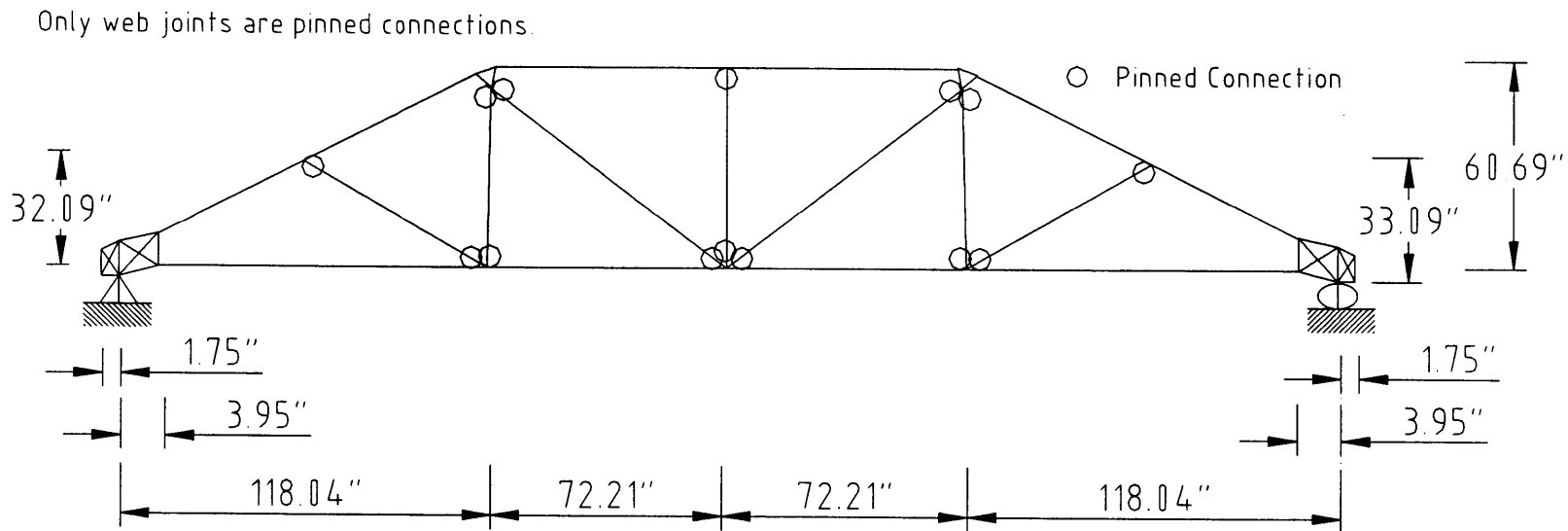


Figure F.5 The TPM's Model for Truss Type AS3 with Semi-Rigid Joints Using SAP2000

Only web joints are pinned connections.

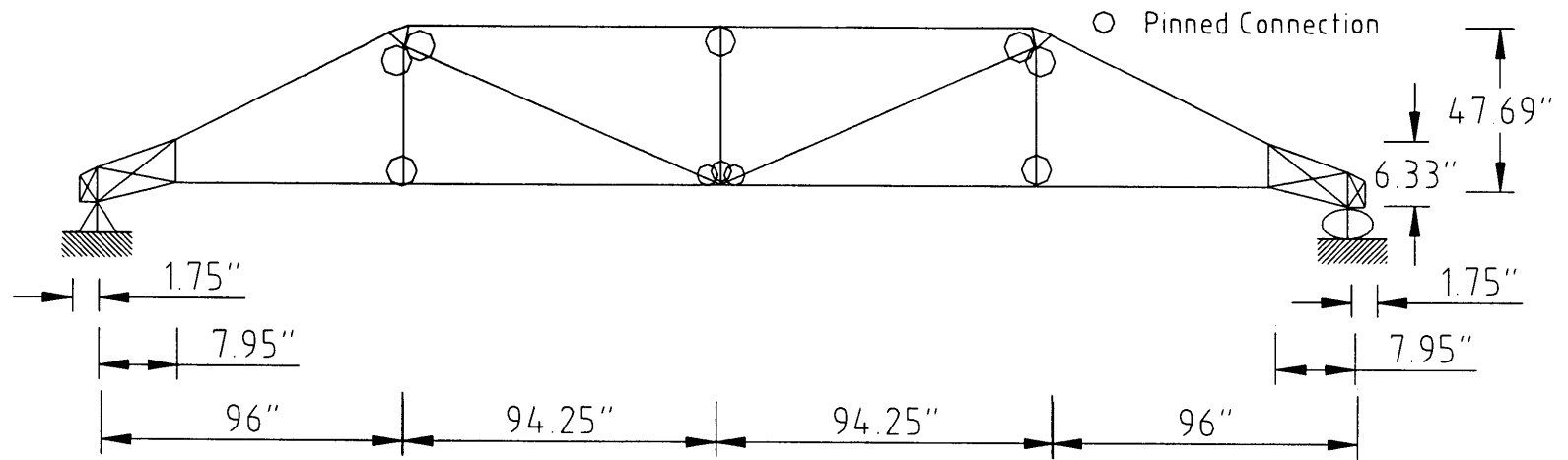


Figure F.6 The TPM's Model for Truss Type ASGR with Semi-Rigid Joints Using SAP2000

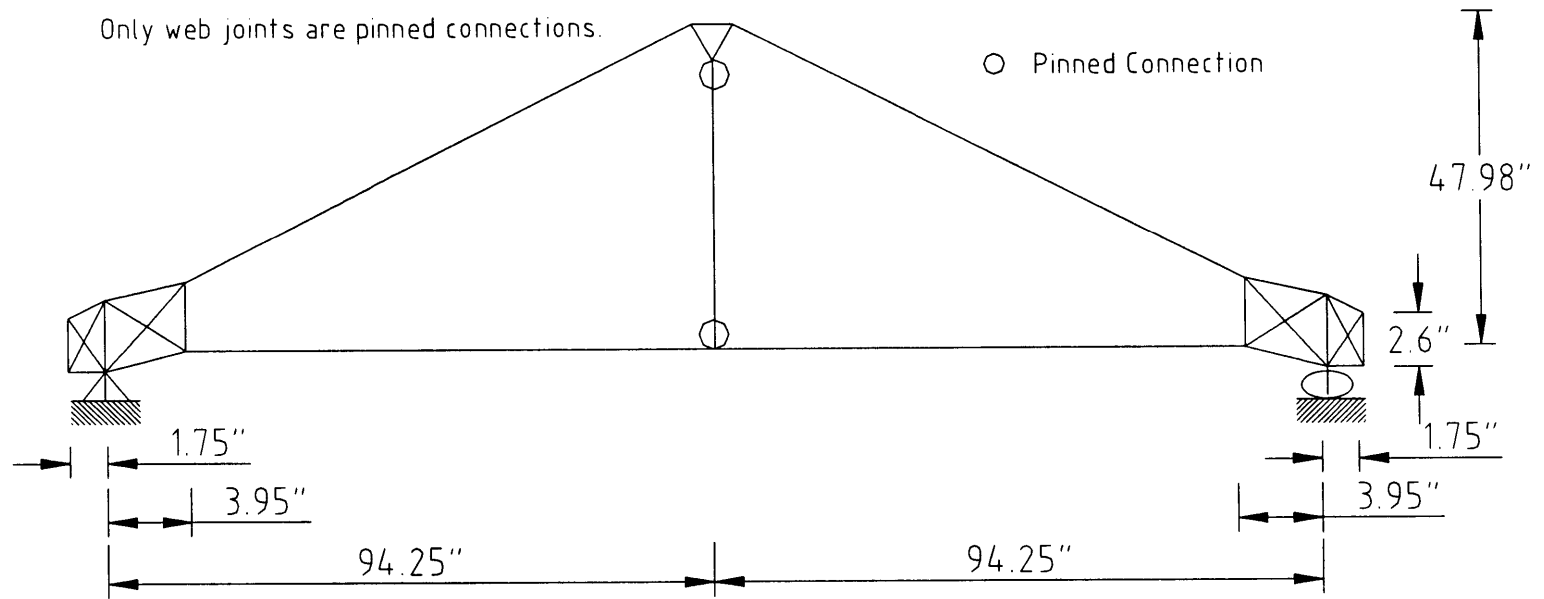


Figure F.7 The TPM's Model for Truss Type B with Semi-Rigid Joints Using SAP2000

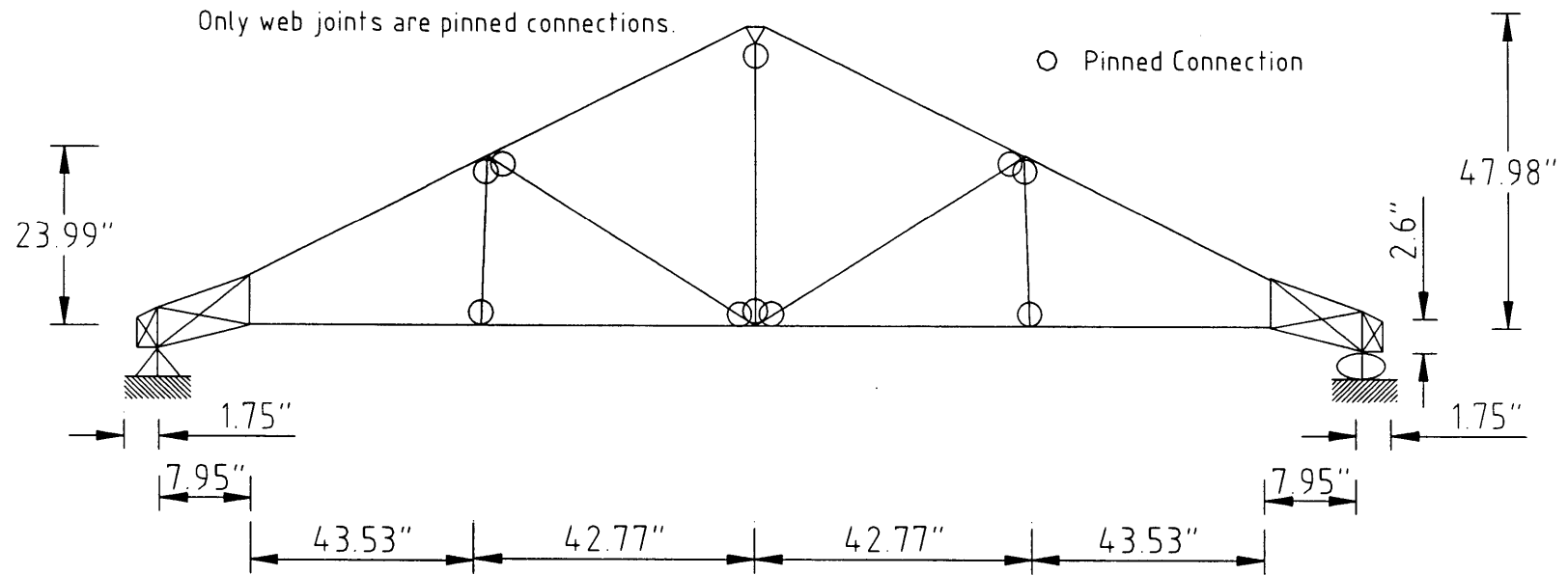


Figure F.8 The TPM's Model for Truss Type BGR with Semi-Rigid Joints Using SAP2000

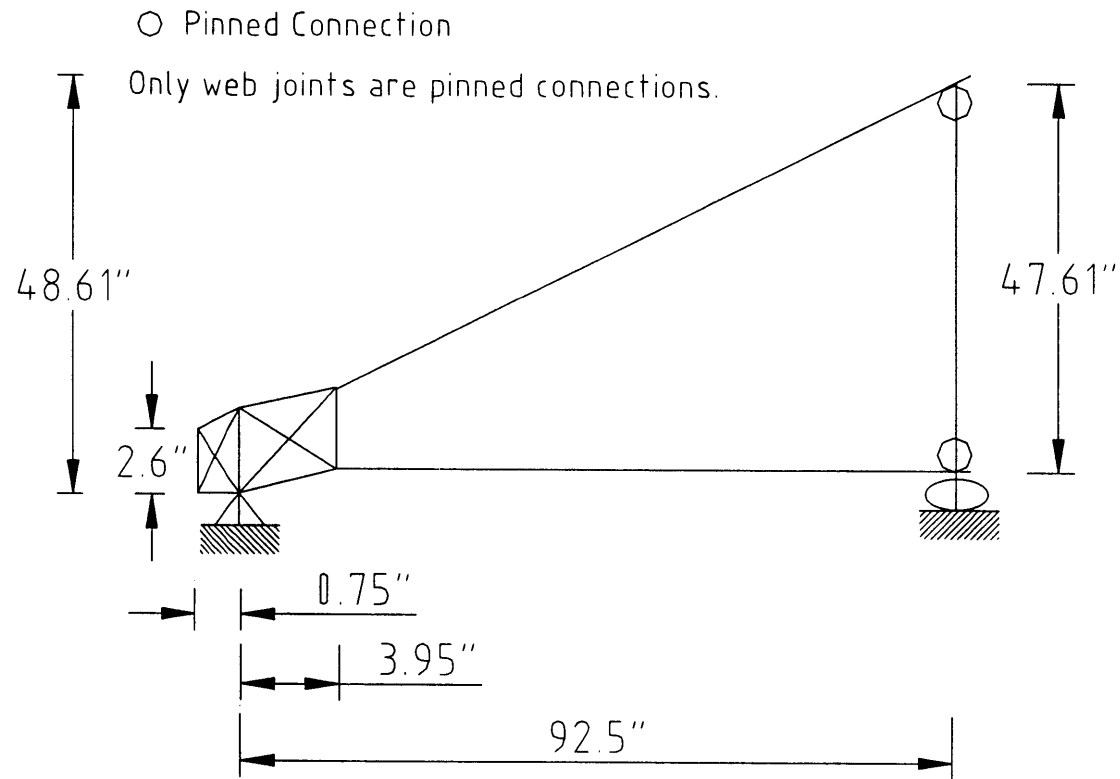


Figure F.9 The TPM's Model for Truss Type J with Semi-Rigid Joints Using SAP2000

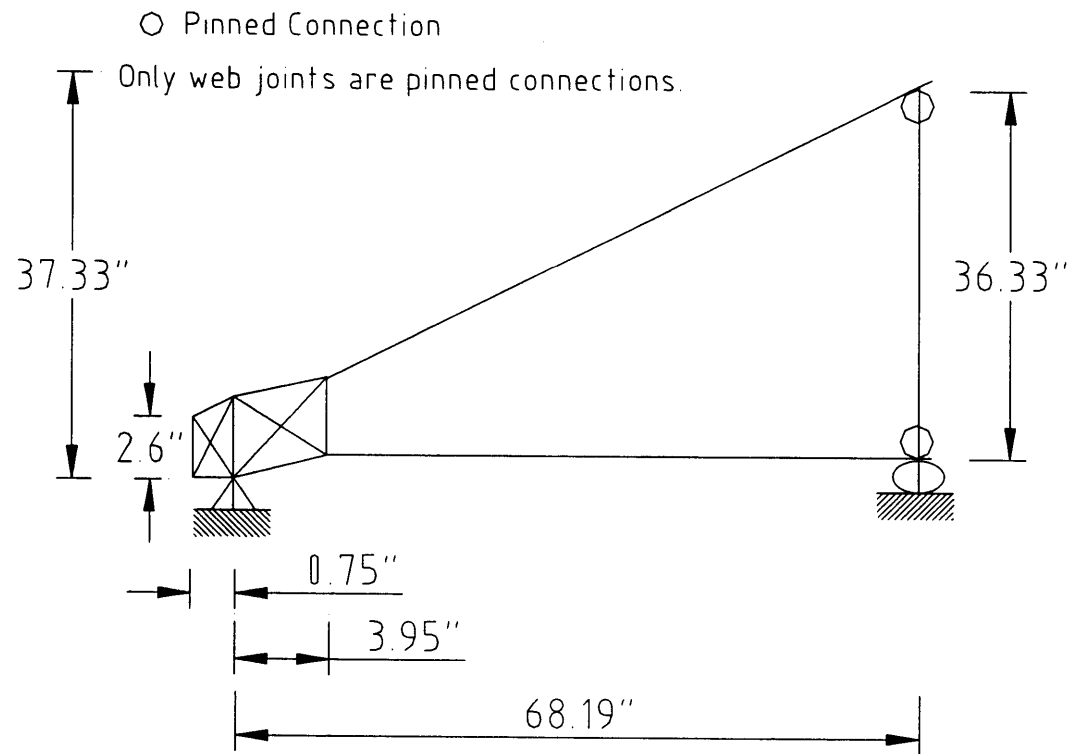


Figure F.10 The TPM's Model for Truss Type J1 with Semi-Rigid Joints Using SAP2000

○ Pinned Connection

Only web joints are pinned connections.

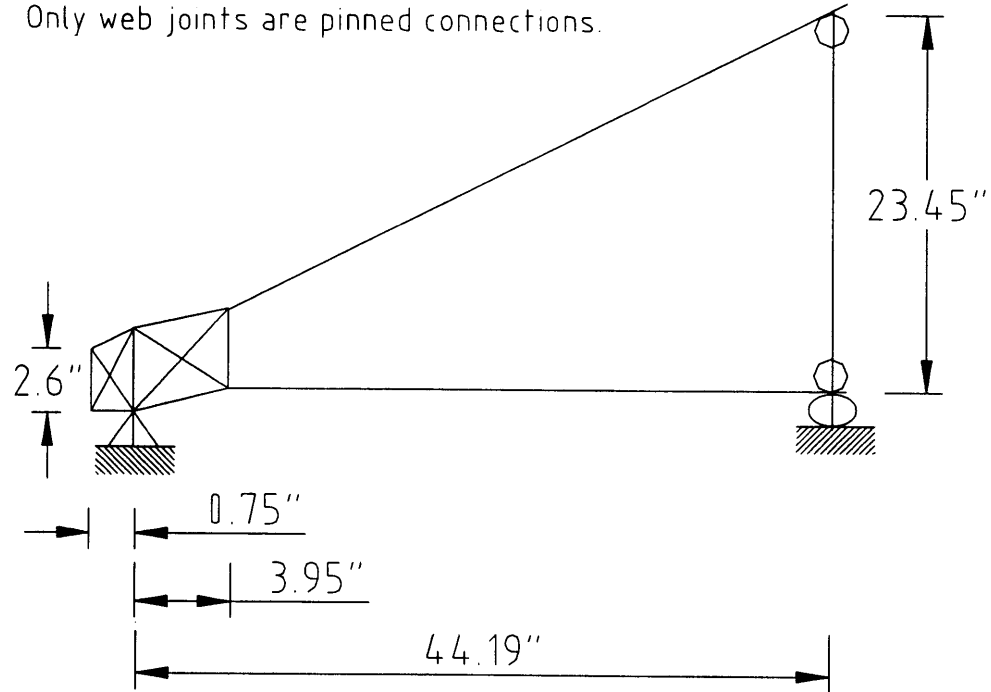


Figure F.11 The TPM's Model for Truss Type J2 with Semi-Rigid Joints Using SAP2000

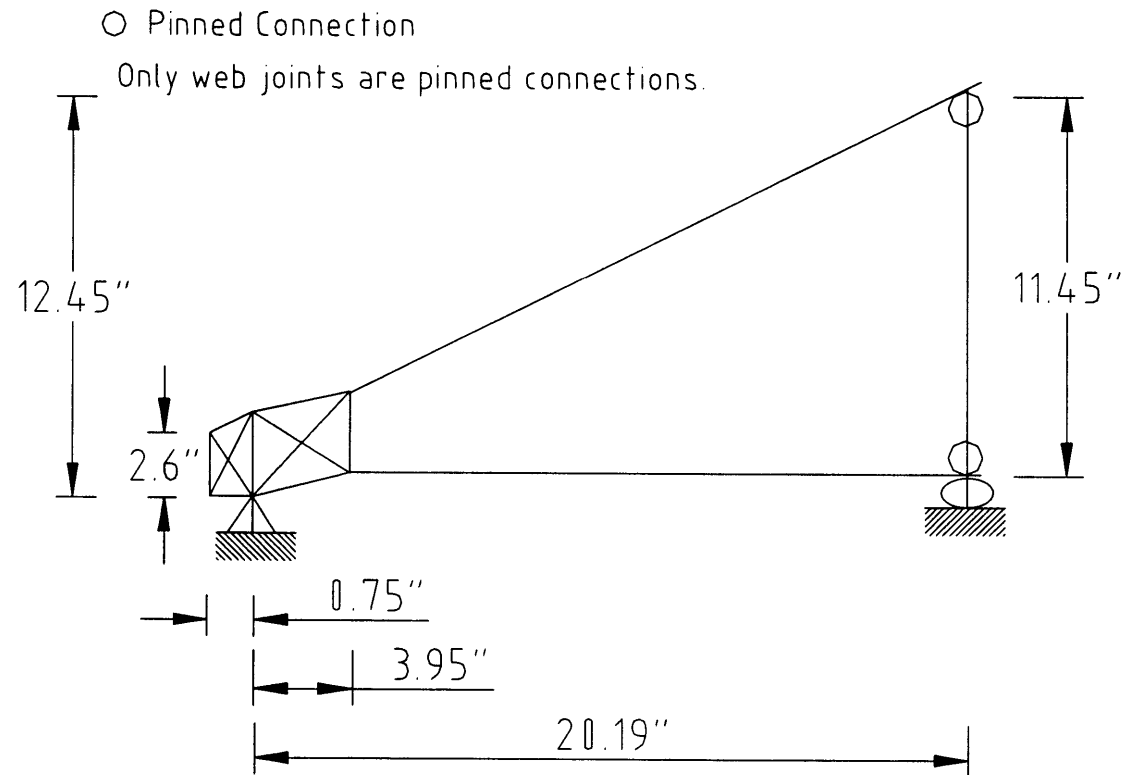


Figure F.12 The TPM's Model for Truss Type J3 with Semi-Rigid Joints Using SAP2000

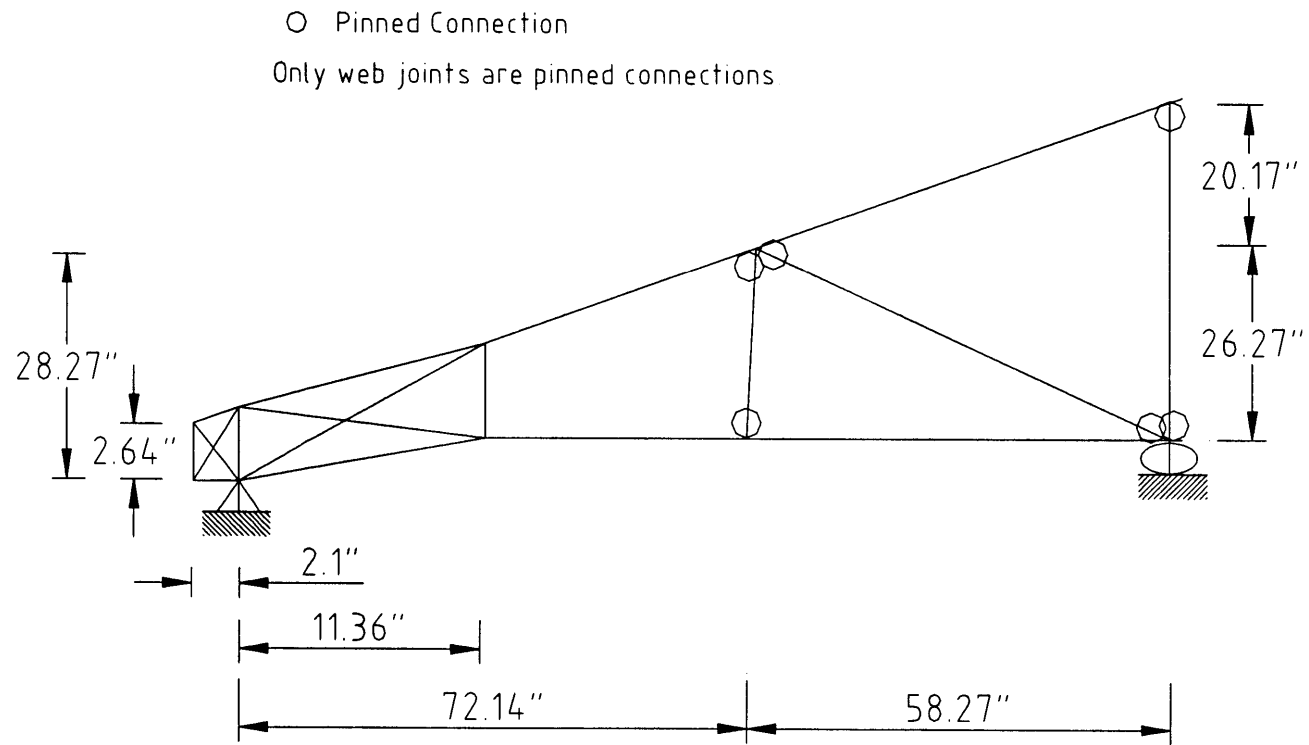


Figure F.13 The TPM's Model for Truss Type JGR with Semi-Rigid Joints Using SAP2000

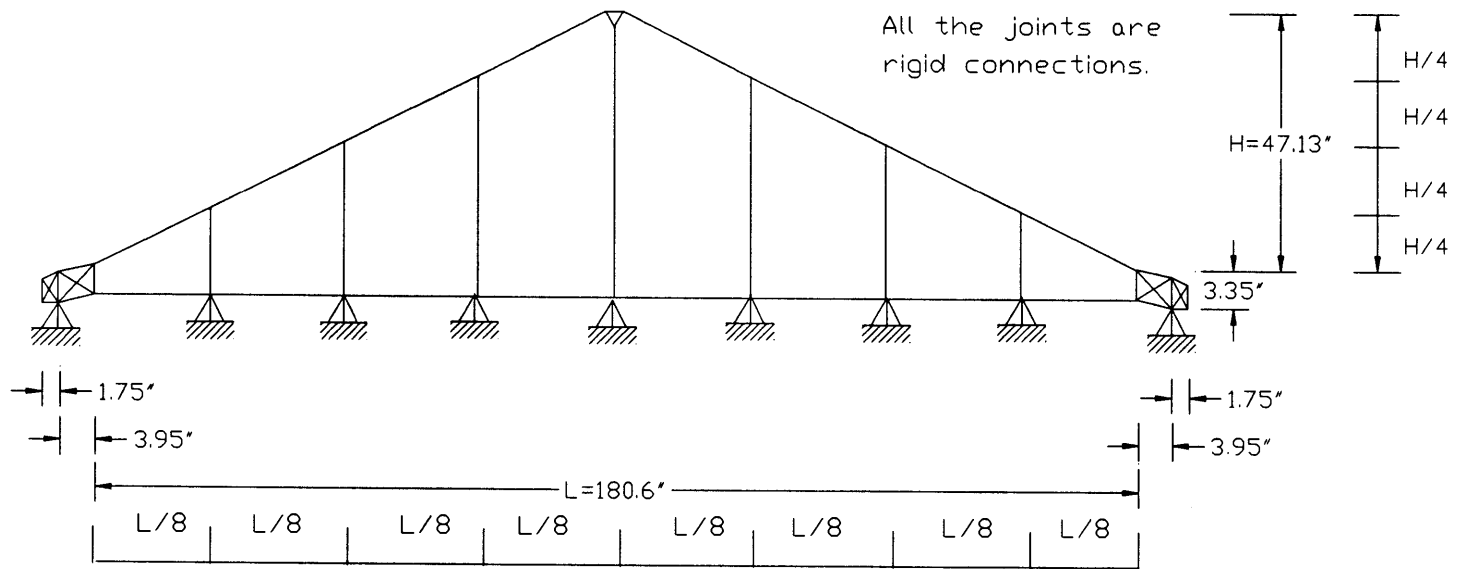


Figure F.14 The TPM's Model for Gable Truss BGB with Semi-Rigid Joints Using SAP2000

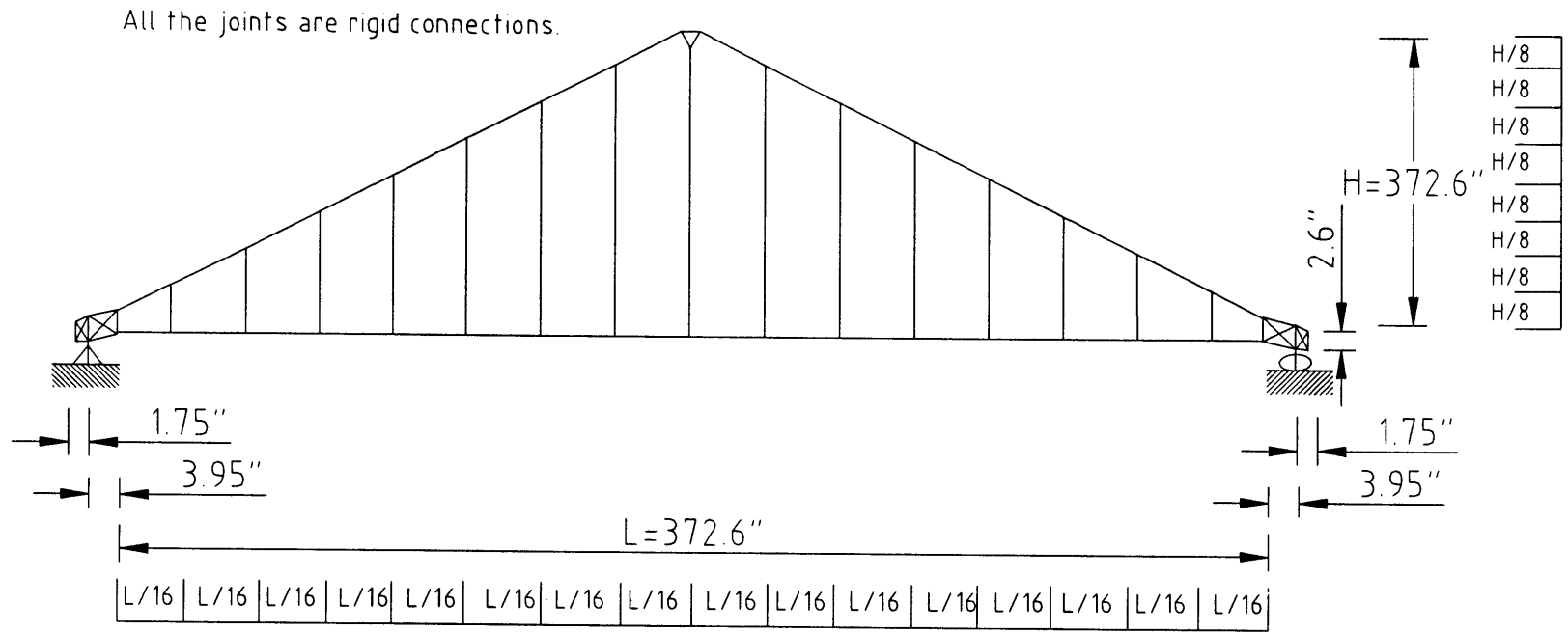


Figure F.15 The TPM's Model for Gable Truss AGB with Semi-Rigid Joints Using SAP2000

APPENDIX G SAP2000 Input and Output Files

Figure G.1 shows the geometry for truss type A1 and Figure G.2 shows the corresponding TPM's truss model (analog). The complete SAP2000 input and output files for the analysis of individual truss type A1 follow. Live load and dead load for the top chords are 20 psf and 10 psf, respectively. Dead load for the bottom chord is 10 psf. The truss design loads are applied on the horizontal projection and truss spacing is 2' from center to center.

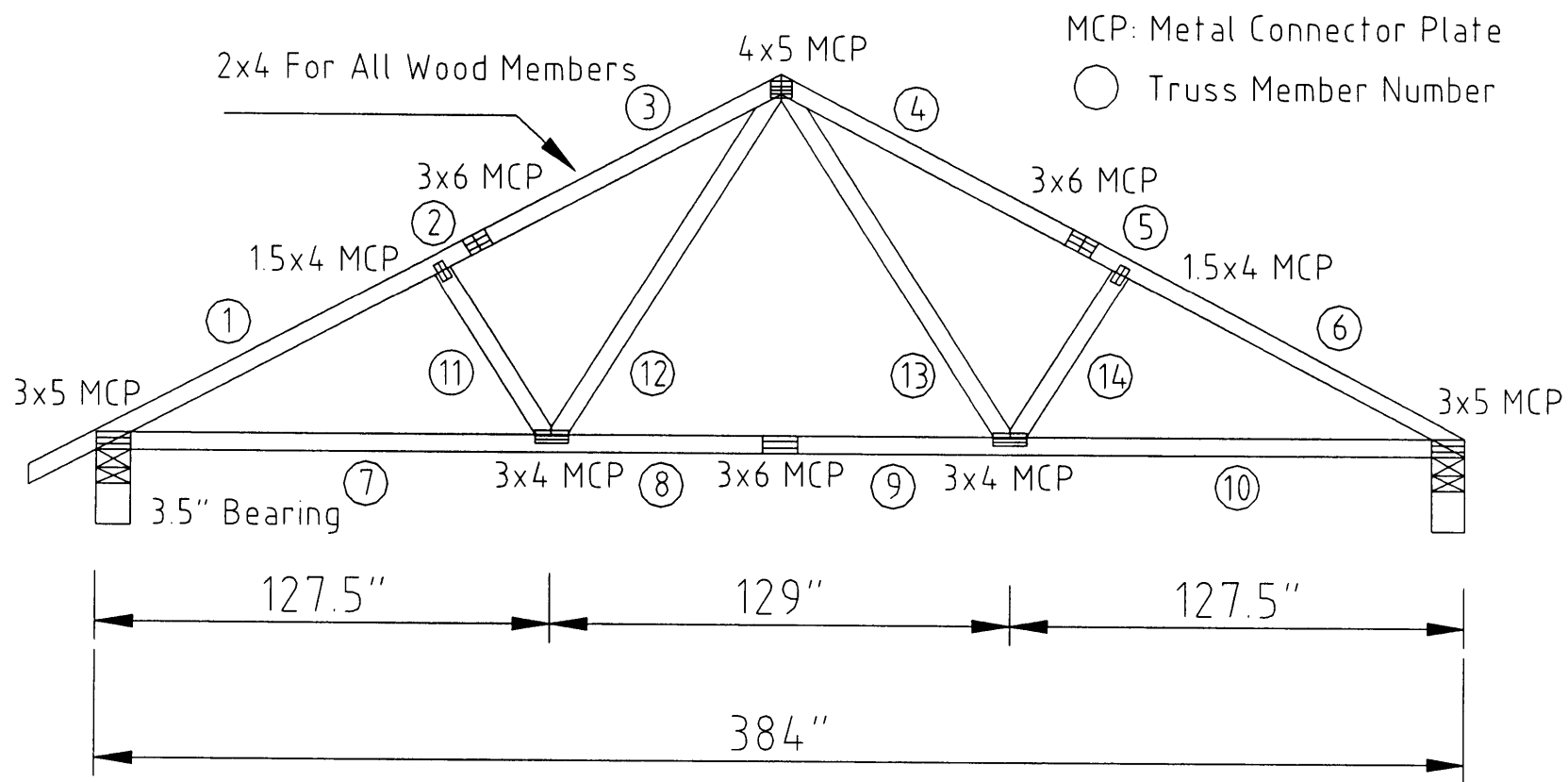


Figure G.1 MPC Truss Type A1

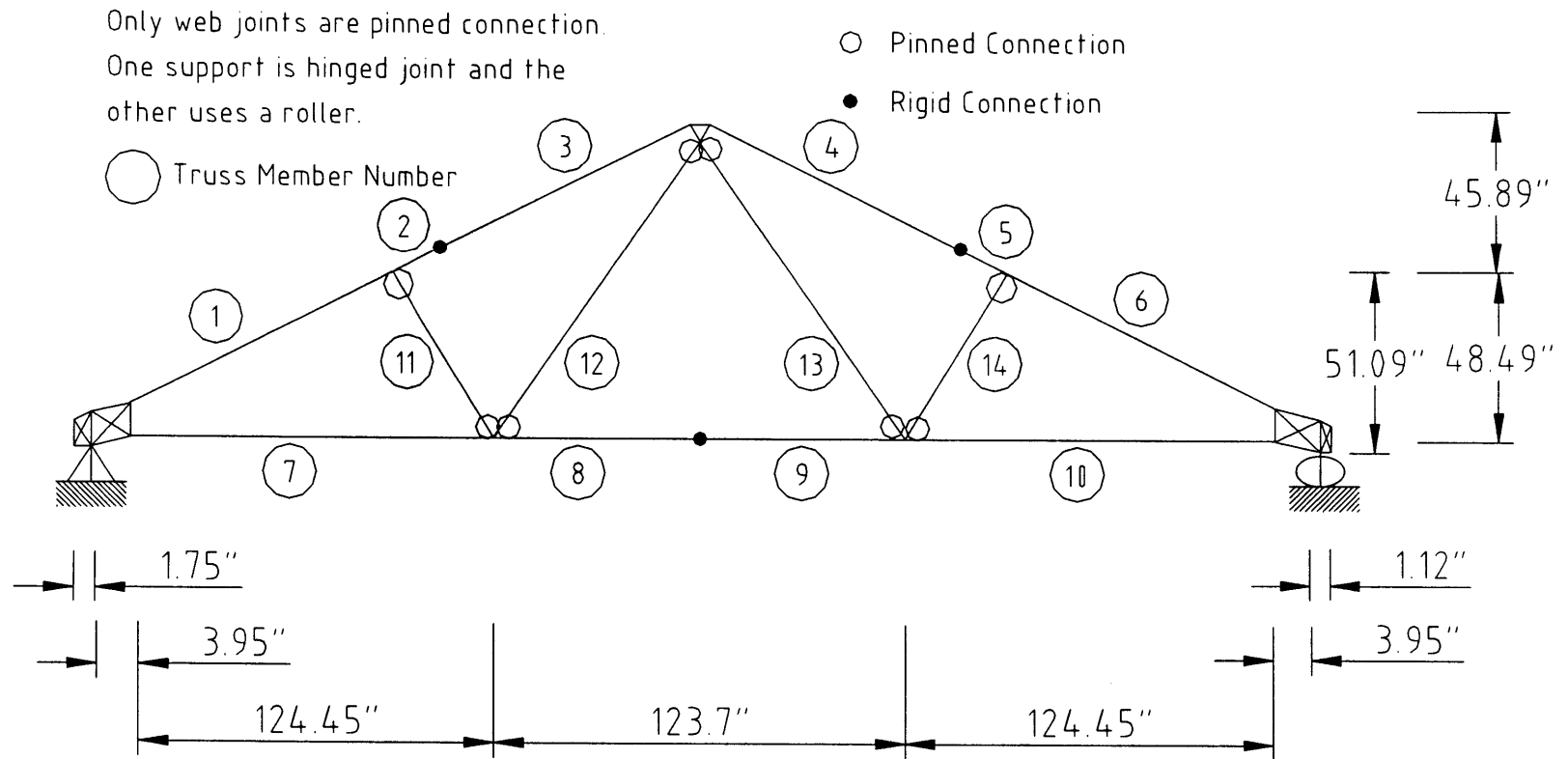


Figure G.2 TPM's Joint Model for Truss Type A1 Using SAP2000

SAP2000 Input File

SYSTEM DOF=UX,UZ,RY LENGTH=IN FORCE=LB PAGE=SECTIONS

JOINT

1 X=0 Y=0 Z=3.35
 2 X=0 Y=0 Z=.75
 3 X=1.75 Y=0 Z=4.22
 4 X=1.75 Y=0 Z=.75
 5 X=5.7 Y=0 Z=5.08
 6 X=5.7 Y=0 Z=1.75
 7 X=99.23 Y=0 Z=51.84
 8 X=109.96 Y=0 Z=57.21
 9 X=130.15 Y=0 Z=1.75
 10 X=191 Y=0 Z=97.73
 11 X=192 Y=0 Z=96
 12 X=193 Y=0 Z=97.73
 13 X=192 Y=0 Z=1.75
 14 X=253.85 Y=0 Z=1.75
 15 X=274.04 Y=0 Z=57.21
 16 X=284.77 Y=0 Z=51.84
 17 X=378.3 Y=0 Z=5.08
 18 X=378.3 Y=0 Z=1.75
 19 X=382.88 Y=0 Z=3.91
 20 X=382.88 Y=0 Z=.75
 21 X=384 Y=0 Z=3.35
 22 X=384 Y=0 Z=.75

RESTRAINT

ADD=4 DOF=U1,U3
 ADD=20 DOF=U3

PATTERN

NAME=DEFAULT

MATERIAL

NAME=STEEL IDES=S
 T=0 E=2.9E+07 U=.3 A=0 FY=36000
 NAME=CONC IDES=C M=2.246377E-04 W=8.679999E-02
 T=0 E=3600000 U=.2 A=.0000055
 NAME=OTHER IDES=N M=2.246377E-04 W=8.679999E-02
 T=0 E=3600000 U=.2 A=.0000055

NAME=SP IDES=N
 T=0 E=1600000 U=.2 A=0
 NAME=SPF12 IDES=N
 T=0 E=1400000 U=.2 A=0
 NAME=SP3 IDES=N
 T=0 E=1200000 U=.2 A=0
 NAME=W1 IDES=N
 T=0 E=1500000 U=.2 A=0
 NAME=WS IDES=N
 T=0 E=3500000 U=.25 A=0

FRAME SECTION

NAME=FSEC1 MAT=STEEL SH=R T=18,10 A=180 J=3916.671 I=4860,1500
 AS=150,150
 NAME=TC1 MAT=SP SH=R T=3.5,1.5 A=5.25 J=0 I=5.359375,.984375
 AS=4.375,4.375
 NAME=TC2 MAT=SPF12 SH=R T=3.5,1.5 A=5.25 J=0 I=5.359375,.984375
 AS=4.375,4.375
 NAME=BC1 MAT=SPF12 SH=R T=3.5,1.5 A=5.25 J=0 I=5.359375,.984375
 AS=4.375,4.375
 NAME=W1 MAT=SP3 SH=R T=3.5,1.5 A=5.25 J=0 I=5.359375,.984375
 AS=4.375,4.375
 NAME=RL MAT=W1 SH=R T=1.5,1.5 A=2.25 J=.7129688 I=.421875,.421875
 AS=1.875,1.875
 NAME=RL1 MAT=WS SH=R T=3,1 A=3 J=.7902161 I=2.25,.25 AS=2.5,2.5
 NAME=RL2 MAT=STEEL SH=R T=1,.12 A=.12 J=5.324552E-04 I=.01,.000144
 AS=.1,.1

NLPROP

NAME=NLPR1 TYPE=Damper
 DOF=U1 KE=0 CE=0
 NAME=N1 TYPE=Damper
 DOF=U1 KE=748836 CE=0
 DOF=U2 KE=348956 CE=0
 DOF=R3 KE=1105112 CE=0
 NAME=N2 TYPE=Damper
 DOF=U1 KE=1797728 CE=0
 DOF=U2 KE=304898 CE=0
 DOF=R3 KE=1823163 CE=0
 NAME=N3 TYPE=Damper
 DOF=U1 KE=2157273 CE=0
 DOF=U2 KE=365877 CE=0
 DOF=R3 KE=1892363 CE=0

FRAME

```

1 J=5,7 SEC=TC1 NSEG=26 ANG=0
2 J=7,8 SEC=TC1 NSEG=2 ANG=0
3 J=8,10 SEC=TC2 NSEG=2 ANG=0
4 J=12,15 SEC=TC2 NSEG=2 ANG=0
5 J=15,16 SEC=TC1 NSEG=2 ANG=0
6 J=16,17 SEC=TC1 NSEG=2 ANG=0
7 J=6,9 SEC=BC1 NSEG=2 ANG=0
8 J=9,13 SEC=BC1 NSEG=2 ANG=0
9 J=13,14 SEC=BC1 NSEG=2 ANG=0
10 J=14,18 SEC=BC1 NSEG=2 ANG=0
11 J=7,9 SEC=W1 NSEG=2 ANG=0 IREL=R3 JREL=R3
12 J=9,11 SEC=W1 NSEG=2 ANG=0 IREL=R3 JREL=R3
13 J=11,14 SEC=W1 NSEG=2 ANG=0 IREL=R3 JREL=R3
14 J=14,16 SEC=W1 NSEG=2 ANG=0 IREL=R3 JREL=R3
15 J=2,1 SEC=RL NSEG=2 ANG=0
16 J=1,3 SEC=RL NSEG=2 ANG=0
17 J=2,4 SEC=RL NSEG=2 ANG=0
18 J=1,4 SEC=RL NSEG=2 ANG=0
19 J=2,3 SEC=RL NSEG=2 ANG=0
20 J=4,3 SEC=RL NSEG=2 ANG=0
21 J=6,5 SEC=RL NSEG=2 ANG=0
22 J=3,5 SEC=RL NSEG=2 ANG=0
23 J=4,6 SEC=RL NSEG=2 ANG=0
24 J=3,6 SEC=RL1 NSEG=2 ANG=0
25 J=4,5 SEC=RL1 NSEG=2 ANG=0
26 J=10,12 SEC=RL2 NSEG=2 ANG=0
27 J=10,11 SEC=RL2 NSEG=2 ANG=0
28 J=11,12 SEC=RL2 NSEG=2 ANG=0
29 J=18,17 SEC=RL NSEG=2 ANG=0
30 J=20,19 SEC=RL NSEG=2 ANG=0
31 J=17,19 SEC=RL NSEG=2 ANG=0
32 J=18,20 SEC=RL NSEG=2 ANG=0
33 J=17,20 SEC=RL1 NSEG=2 ANG=0
34 J=18,19 SEC=RL1 NSEG=2 ANG=0
35 J=19,21 SEC=RL NSEG=2 ANG=0
36 J=20,22 SEC=RL NSEG=2 ANG=0
37 J=22,21 SEC=RL NSEG=2 ANG=0
38 J=19,22 SEC=RL NSEG=2 ANG=0
39 J=20,21 SEC=RL NSEG=2 ANG=0

```

LOAD

```

NAME=LOAD1 SW=1
TYPE=FORCE

```

ADD=3 UZ=-60
TYPE=DISTRIBUTED SPAN
ADD=1 RD=0,1 UZ=-4.482452,-4.482452
ADD=2 RD=0,1 UZ=-4.482452,-4.482452
ADD=3 RD=0,1 UZ=-4.482452,-4.482452
ADD=16 RD=0,1 UZ=-4.482452,-4.482452
ADD=22 RD=0,1 UZ=-4.482452,-4.482452
ADD=26 RD=0,1 UZ=-4.482452,-4.482452
ADD=4 RD=0,1 UZ=-4.482818,-4.482818
ADD=5 RD=0,1 UZ=-4.482818,-4.482818
ADD=6 RD=0,1 UZ=-4.482818,-4.482818
ADD=31 RD=0,1 UZ=-4.482818,-4.482818
ADD=35 RD=0,1 UZ=-4.482818,-4.482818
ADD=9 RD=0,1 UZ=-1.665731,-1.665731
ADD=10 RD=0,1 UZ=-1.665731,-1.665731
ADD=32 RD=0,1 UZ=-1.665731,-1.665731
ADD=36 RD=0,1 UZ=-1.665731,-1.665731
ADD=7 RD=0,1 UZ=-1.665586,-1.665586
ADD=8 RD=0,1 UZ=-1.665586,-1.665586
ADD=17 RD=0,1 UZ=-1.665586,-1.665586
ADD=23 RD=0,1 UZ=-1.665586,-1.665586

SAP2000 Output File

JOINT DISPLACEMENTS

JOINT LOAD	UX	UY	UZ	RX	RY	RZ
1 LOAD1	0.0269	0.0000	0.0179	0.0000	0.0104	0.0000
2 LOAD1	-7.820E-06	0.0000	0.0179	0.0000	0.0103	0.0000
3 LOAD1	0.0361	0.0000	-4.425E-04	0.0000	0.0103	0.0000
4 LOAD1	0.0000	0.0000	0.0000	0.0000	0.0103	0.0000
5 LOAD1	0.0440	0.0000	-0.0410	0.0000	0.0104	0.0000
6 LOAD1	0.0113	0.0000	-0.0409	0.0000	0.0102	0.0000
7 LOAD1	0.0803	0.0000	-0.1730	0.0000	-8.941E-04	0.0000
8 LOAD1	0.0868	0.0000	-0.1922	0.0000	3.545E-03	0.0000
9 LOAD1	0.0438	0.0000	-0.1903	0.0000	-2.365E-03	0.0000
10 LOAD1	0.0560	0.0000	-0.1821	0.0000	-3.422E-03	0.0000
11 LOAD1	0.0560	0.0000	-0.1823	0.0000	-1.539E-04	0.0000
12 LOAD1	0.0554	0.0000	-0.1818	0.0000	3.141E-03	0.0000
13 LOAD1	0.0545	0.0000	-0.2493	0.0000	-6.295E-05	0.0000
14 LOAD1	0.0651	0.0000	-0.1925	0.0000	2.726E-03	0.0000
15 LOAD1	0.0255	0.0000	-0.1900	0.0000	-3.150E-03	0.0000
16 LOAD1	0.0295	0.0000	-0.1757	0.0000	1.430E-03	0.0000
17 LOAD1	0.0604	0.0000	-0.0543	0.0000	-0.0118	0.0000

18 LOAD1	0.0978	0.0000	-0.0541	0.0000	-0.0116	0.0000
19 LOAD1	0.0730	0.0000	-3.256E-04	0.0000	-0.0118	0.0000
20 LOAD1	0.1107	0.0000	0.0000	0.0000	-0.0118	0.0000
21 LOAD1	0.0797	0.0000	0.0132	0.0000	-0.0119	0.0000
22 LOAD1	0.1107	0.0000	0.0132	0.0000	-0.0119	0.0000

JOINT REACTIONS

JOINT LOAD	F1	F2	F3	M1	M2	M3
4 LOAD1	0.0000	0.0000	1342.1429	0.0000	0.0000	0.0000
20 LOAD1	0.0000	0.0000	1277.8569	0.0000	0.0000	0.0000

FRAME ELEMENT FORCES

(FRAME number is equal to the truss member number.)

FRAME LOAD	LOC	P	V2	V3	T	M2	M3
1 LOAD1							
0.00	-2234.77	-177.06	0.00	0.00	0.00	-1024.23	
4.02	-2226.71	-160.93	0.00	0.00	0.00	-344.56	
8.04	-2218.65	-144.81	0.00	0.00	0.00	270.27	
12.07	-2210.59	-128.68	0.00	0.00	0.00	820.24	
16.09	-2202.52	-112.56	0.00	0.00	0.00	1305.36	
20.11	-2194.46	-96.43	0.00	0.00	0.00	1725.62	
24.13	-2186.40	-80.31	0.00	0.00	0.00	2081.04	
28.15	-2178.34	-64.18	0.00	0.00	0.00	2371.61	
32.17	-2170.28	-48.06	0.00	0.00	0.00	2597.32	
36.20	-2162.22	-31.94	0.00	0.00	0.00	2758.19	
40.22	-2154.16	-15.81	0.00	0.00	0.00	2854.20	
44.24	-2146.09	3.141E-01	0.00	0.00	0.00	2885.36	
48.26	-2138.03	16.44	0.00	0.00	0.00	2851.67	
52.28	-2129.97	32.56	0.00	0.00	0.00	2753.14	

56.31	-2121.91	48.69	0.00	0.00	0.00	2589.74
60.33	-2113.85	64.81	0.00	0.00	0.00	2361.50
64.35	-2105.79	80.94	0.00	0.00	0.00	2068.41
68.37	-2097.72	97.06	0.00	0.00	0.00	1710.47
72.39	-2089.66	113.19	0.00	0.00	0.00	1287.67
76.41	-2081.60	129.31	0.00	0.00	0.00	800.03
80.44	-2073.54	145.44	0.00	0.00	0.00	247.53
84.46	-2065.48	161.56	0.00	0.00	0.00	-369.82
88.48	-2057.42	177.69	0.00	0.00	0.00	-1052.02
92.50	-2049.36	193.81	0.00	0.00	0.00	-1799.06
96.52	-2041.29	209.94	0.00	0.00	0.00	-2610.96
100.55	-2033.23	226.06	0.00	0.00	0.00	-3487.72
104.57	-2025.17	242.19	0.00	0.00	0.00	-4429.32

2 LOAD1

0.00	-1983.25	-225.58	0.00	0.00	0.00	-4429.32
6.00	-1971.21	-201.53	0.00	0.00	0.00	-3148.11
12.00	-1959.18	-177.48	0.00	0.00	0.00	-2011.18

3 LOAD1

0.00	-1959.11	-178.21	0.00	0.00	0.00	-2011.18
45.30	-1868.29	3.41	0.00	0.00	0.00	1948.27
90.61	-1777.48	185.04	0.00	0.00	0.00	-2320.57

4 LOAD1

0.00	-1785.72	-184.18	0.00	0.00	0.00	-2337.11
45.30	-1876.54	-2.54	0.00	0.00	0.00	1892.47
90.61	-1967.36	179.10	0.00	0.00	0.00	-2106.92

5 LOAD1

0.00	-1967.43	178.37	0.00	0.00	0.00	-2106.92
6.00	-1979.47	202.42	0.00	0.00	0.00	-3249.17
12.00	-1991.50	226.47	0.00	0.00	0.00	-4535.71

6 LOAD1

0.00	-2033.96	-247.24	0.00	0.00	0.00	-4535.71
52.28	-2138.77	-37.60	0.00	0.00	0.00	2910.68
104.57	-2243.58	172.04	0.00	0.00	0.00	-603.64

7 LOAD1

0.00	1919.71	-87.86	0.00	0.00	0.00	-409.45
62.22	1919.71	15.78	0.00	0.00	0.00	1832.96

124.45	1919.71	119.42	0.00	0.00	0.00	-2373.70
--------	---------	--------	------	------	------	----------

8 LOAD1

0.00	1264.52	-102.06	0.00	0.00	0.00	-2373.70
30.93	1264.52	-50.56	0.00	0.00	0.00	-13.83
61.85	1264.52	9.528E-01	0.00	0.00	0.00	753.15

9 LOAD1

0.00	1264.52	9.528E-01	0.00	0.00	0.00	753.15
30.93	1264.52	52.47	0.00	0.00	0.00	-72.83
61.85	1264.52	103.98	0.00	0.00	0.00	-2491.84

10 LOAD1

0.00	1929.83	-123.07	0.00	0.00	0.00	-2491.84
62.22	1929.83	-19.42	0.00	0.00	0.00	1941.42
124.45	1929.83	84.23	0.00	0.00	0.00	-74.96

11 LOAD1

0.00	-470.47	0.00	0.00	0.00	0.00	0.00
29.43	-470.47	0.00	0.00	0.00	0.00	0.00
58.86	-470.47	0.00	0.00	0.00	0.00	0.00

12 LOAD1

0.00	743.76	0.00	0.00	0.00	0.00	0.00
56.37	743.76	0.00	0.00	0.00	0.00	0.00
112.73	743.76	0.00	0.00	0.00	0.00	0.00

13 LOAD1

0.00	756.50	0.00	0.00	0.00	0.00	0.00
56.37	756.50	0.00	0.00	0.00	0.00	0.00
112.73	756.50	0.00	0.00	0.00	0.00	0.00

14 LOAD1

0.00	-476.44	0.00	0.00	0.00	0.00	0.00
29.43	-476.44	0.00	0.00	0.00	0.00	0.00
58.86	-476.44	0.00	0.00	0.00	0.00	0.00

APPENDIX H CSI Values for Individual Trusses Using SAP2000 Truss Model and TPM Model

In this appendix, a CSI value comparison for individual trusses using both the SAP2000 truss model and the TPM model is performed. The SAP2000 truss model and the TPM model use the same truss analog and semi-rigid joint model (TPM's joint model) provided from the TPM, but different analysis software is used. This comparison is provided for verification of the single truss SAP2000 model using the TPM's joint model. The comparisons are shown in Figures H1 ~ H13.

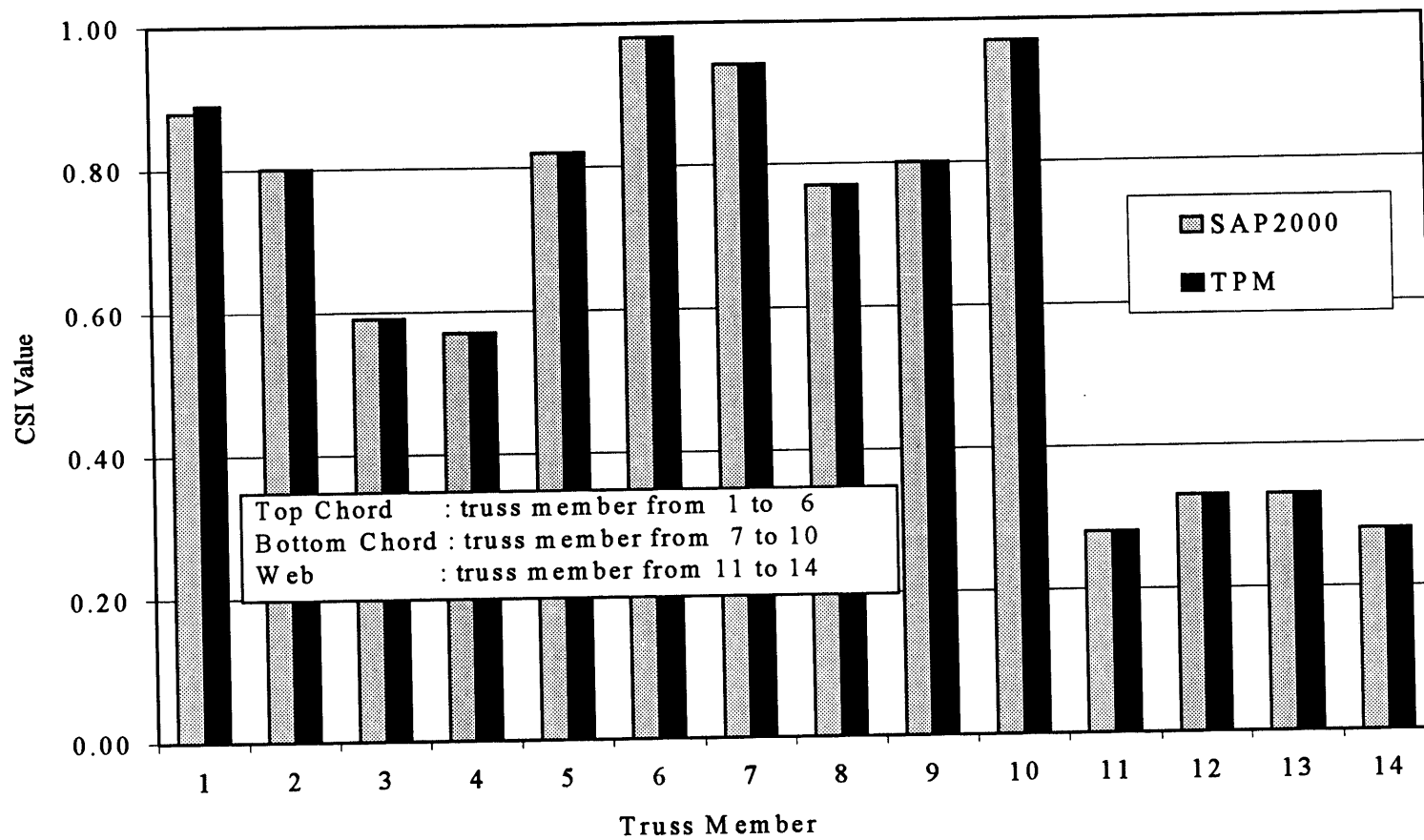


Figure H.1 CSI Values for Truss Type A1 Using SAP2000 Model and TPM's Output
 (Percent Difference: 0%~-1%)

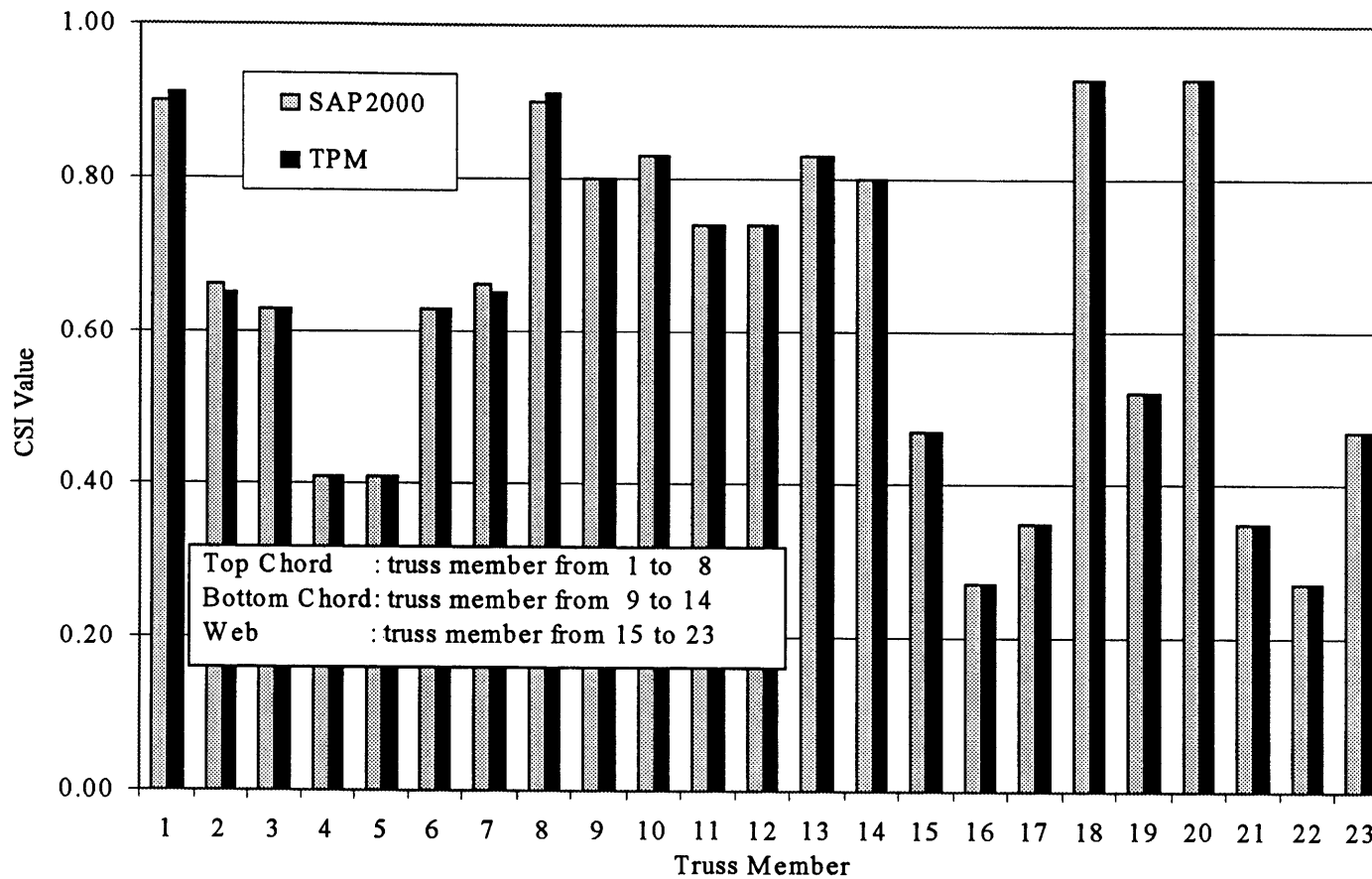


Figure H.2 CSI Values for Truss Type A2 Using SAP2000 Model and TPM's Output
(Percent Difference: 0 %~-2 %)

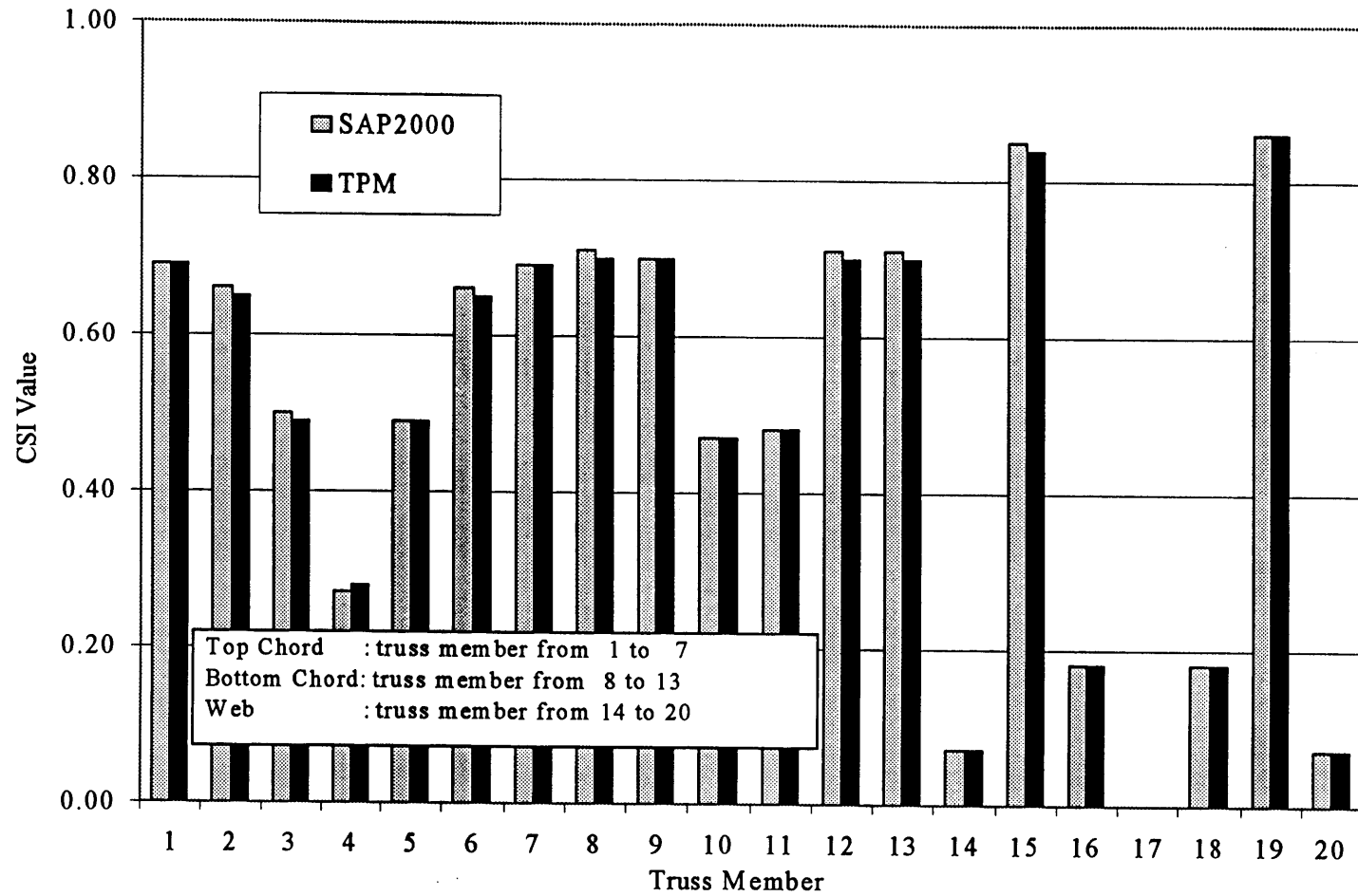


Figure H.3 CSI Values for Truss Type AS1 Using SAP2000 Model and TPM's Output
(Percent Difference: 0%~4%)

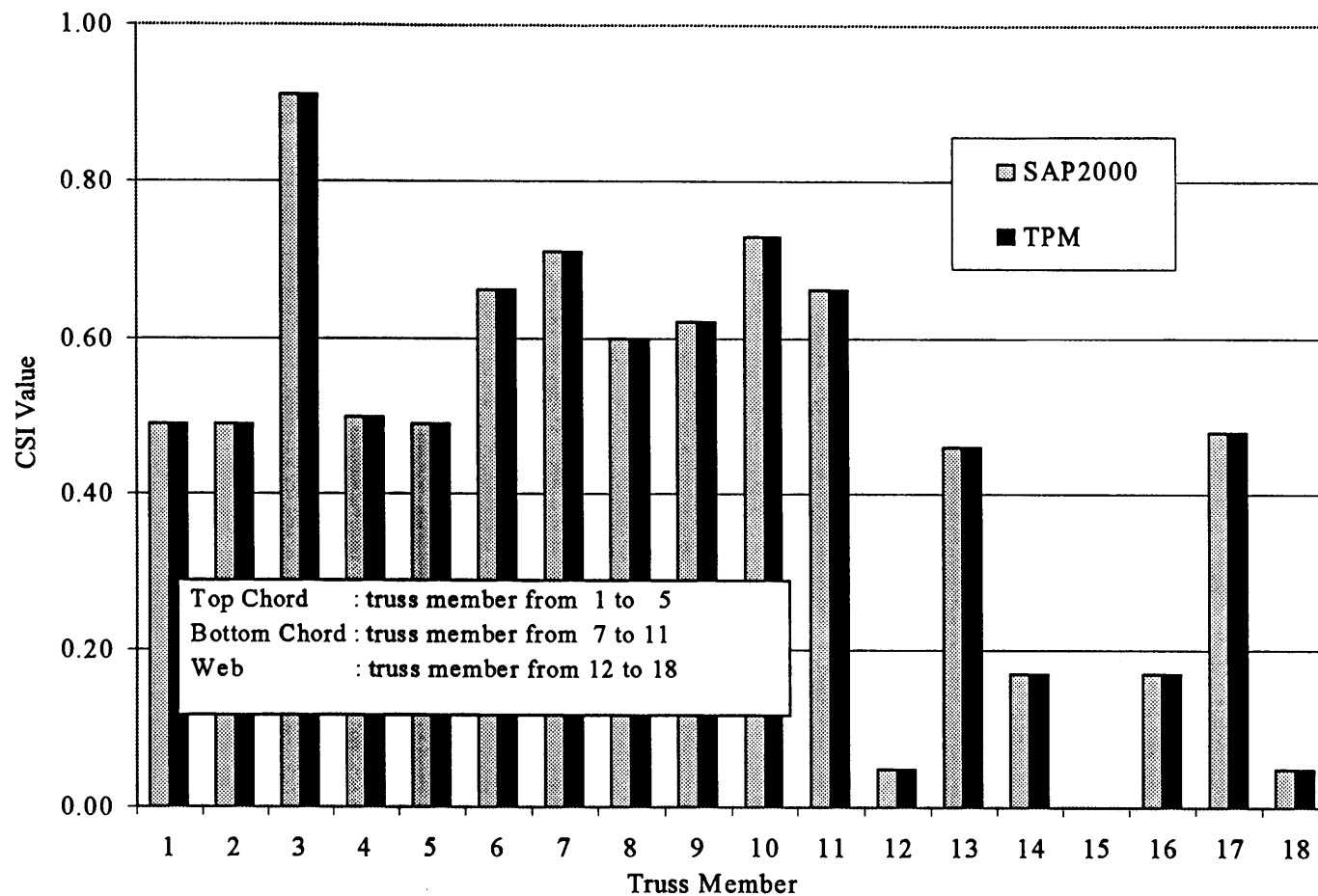


Figure H.4 CSI Values for Truss Type AS2 Using SAP2000 Model and TPM's Output
(Percent Difference: 0%)

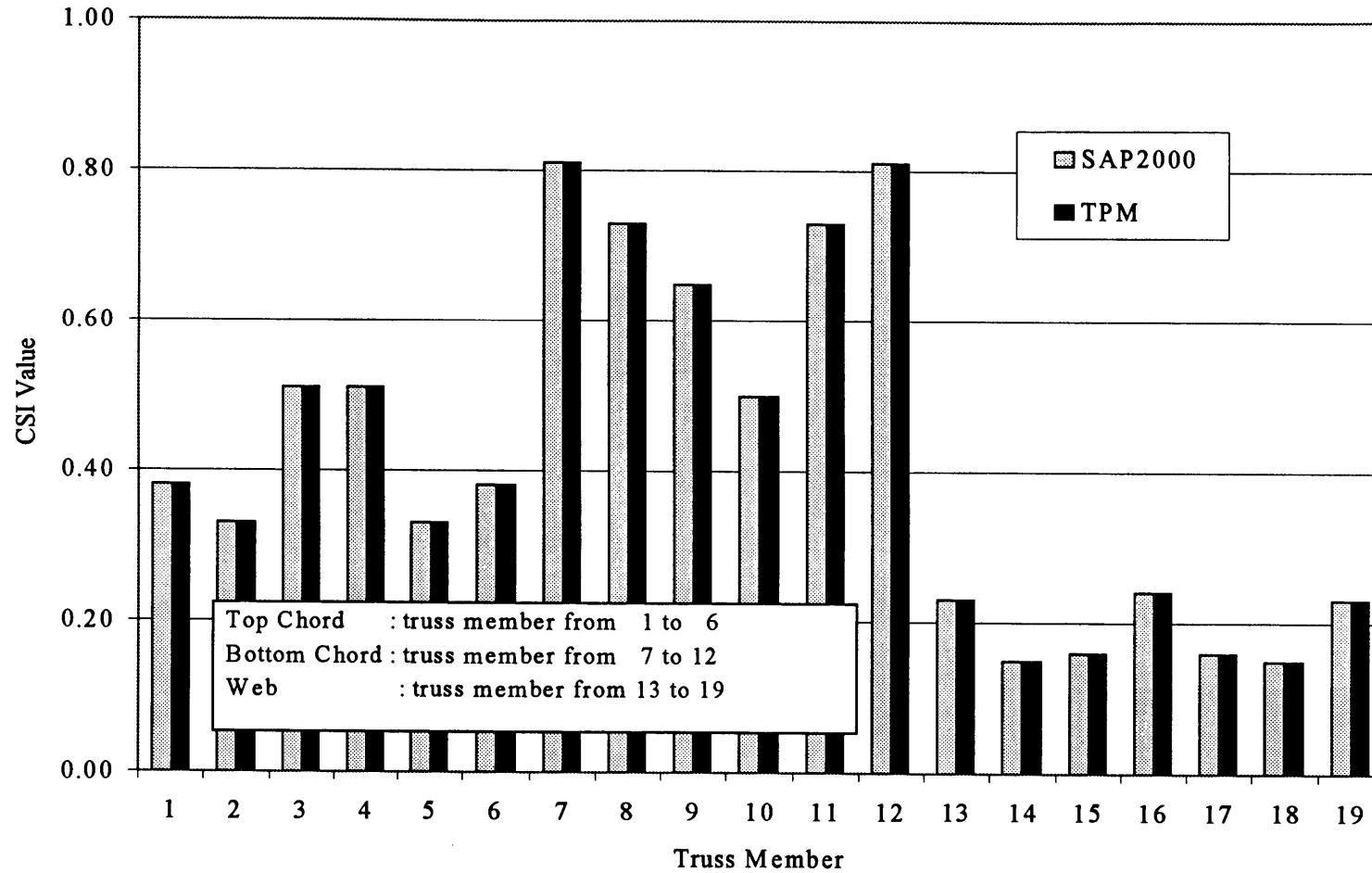


Figure H.5 CSI Values for Truss Type AS3 Using SAP2000 Model and TPM's Output
 (Percent Difference: 0%)

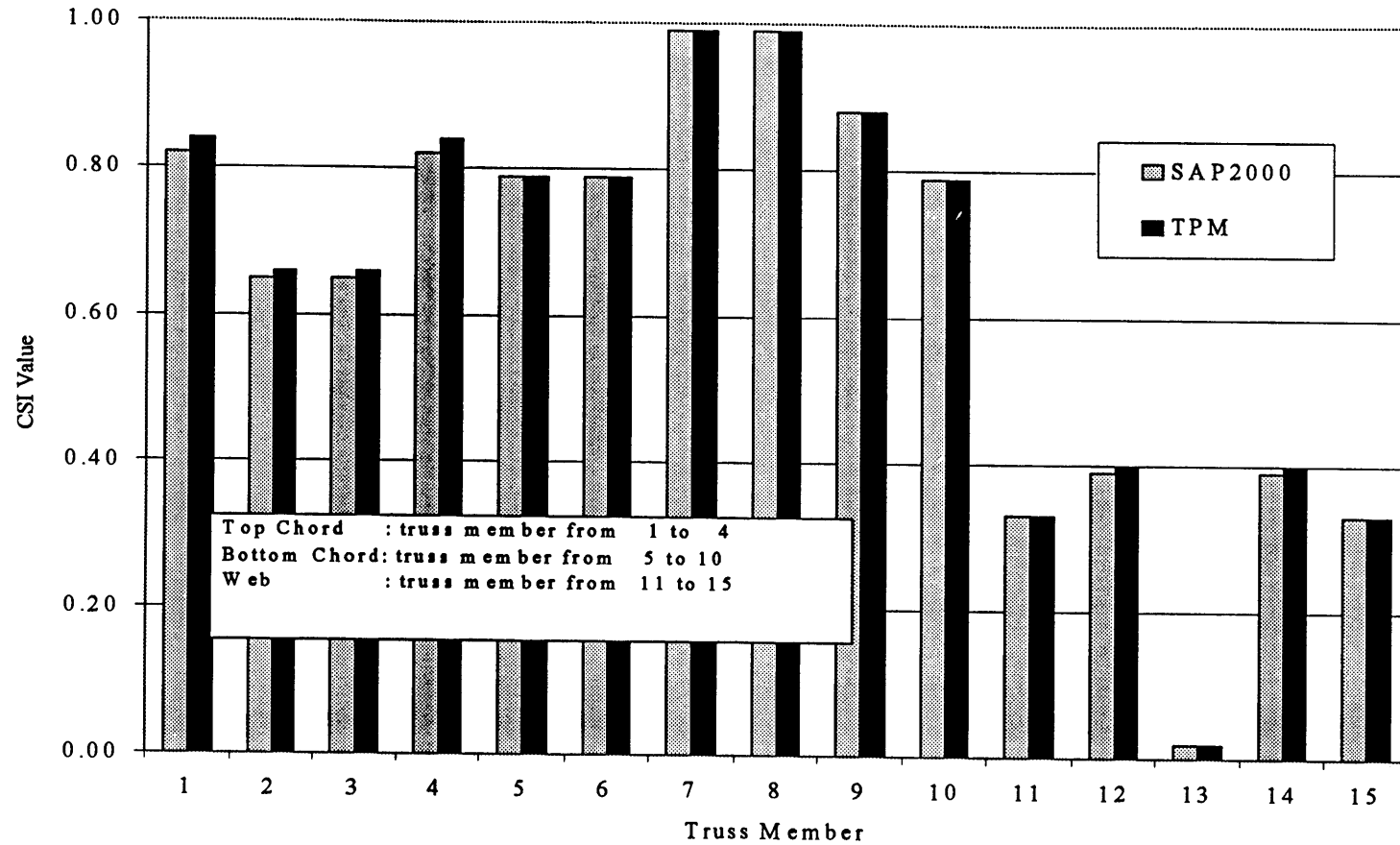


Figure H.6 CSI Values for Truss Type ASGR Using SAP2000 Model and TPM's Output
 (Percent Difference: 0%~~2%)

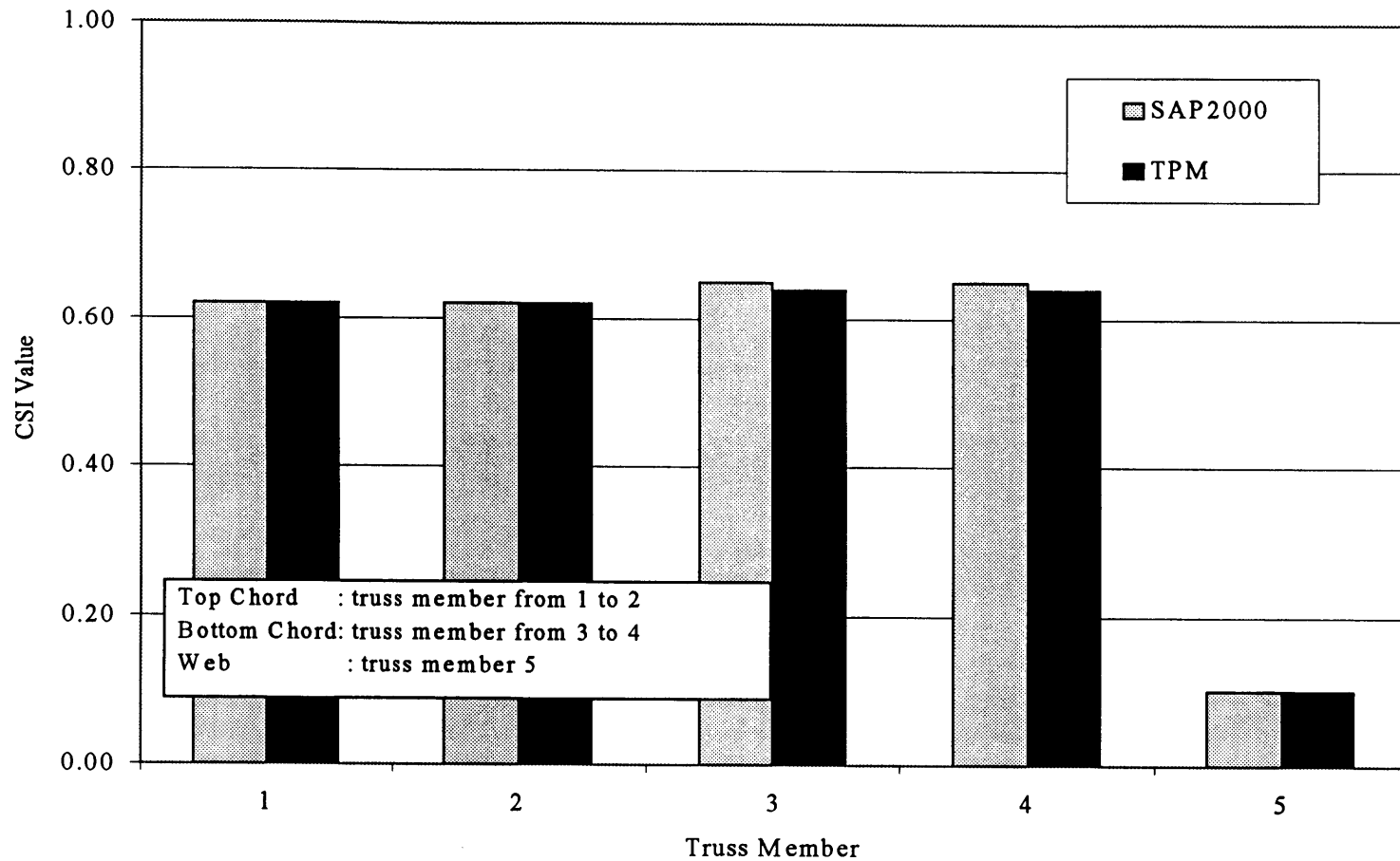


Figure H.7 CSI Values for Truss Type B Using SAP2000 Model and TPM's Output
(Percent Difference: 0%~2%)

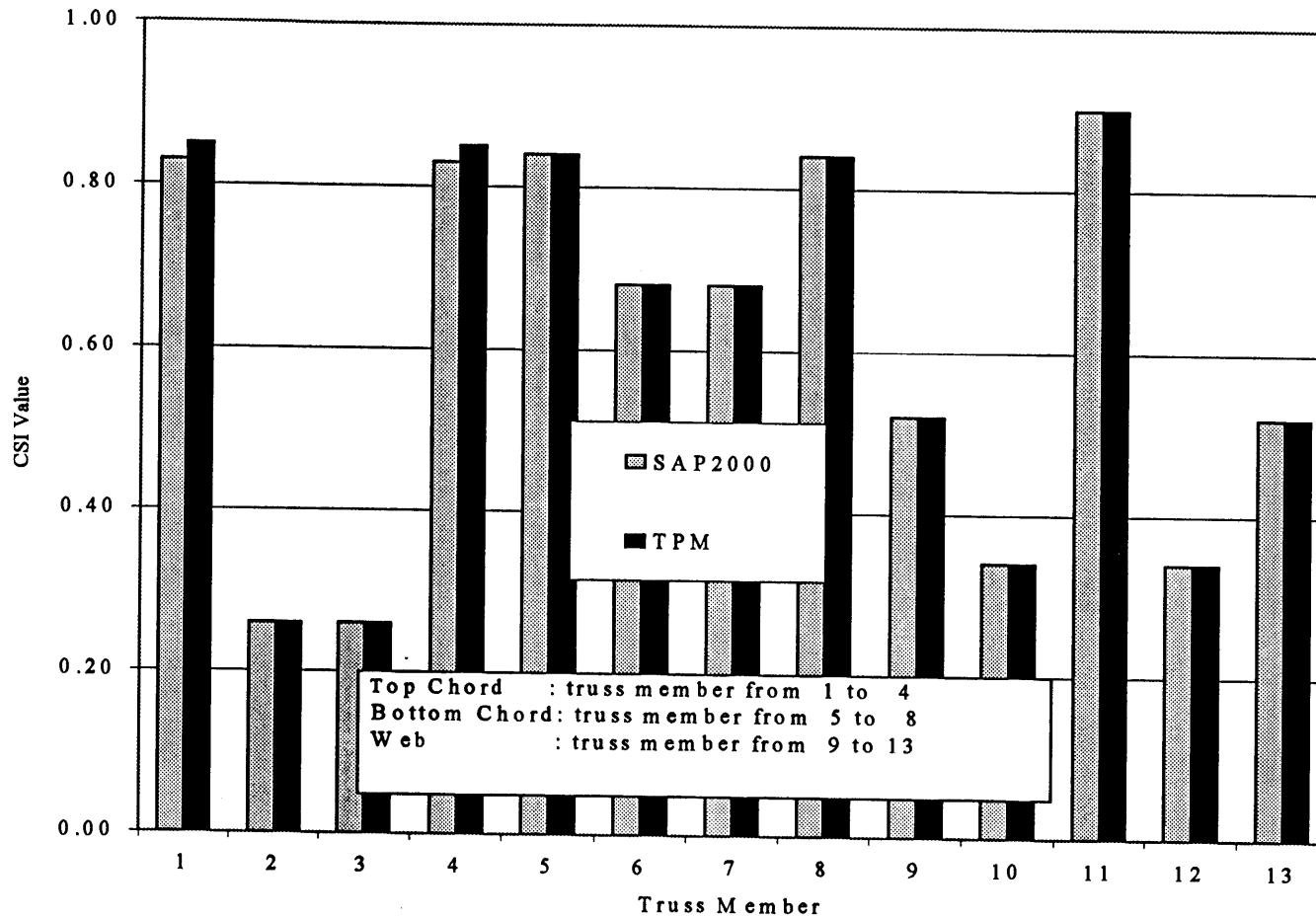


Figure H.8 CSI Values for Truss Type BGR Using SAP2000 Model and TPM's Output
 (Percent Difference: 0%~2%)

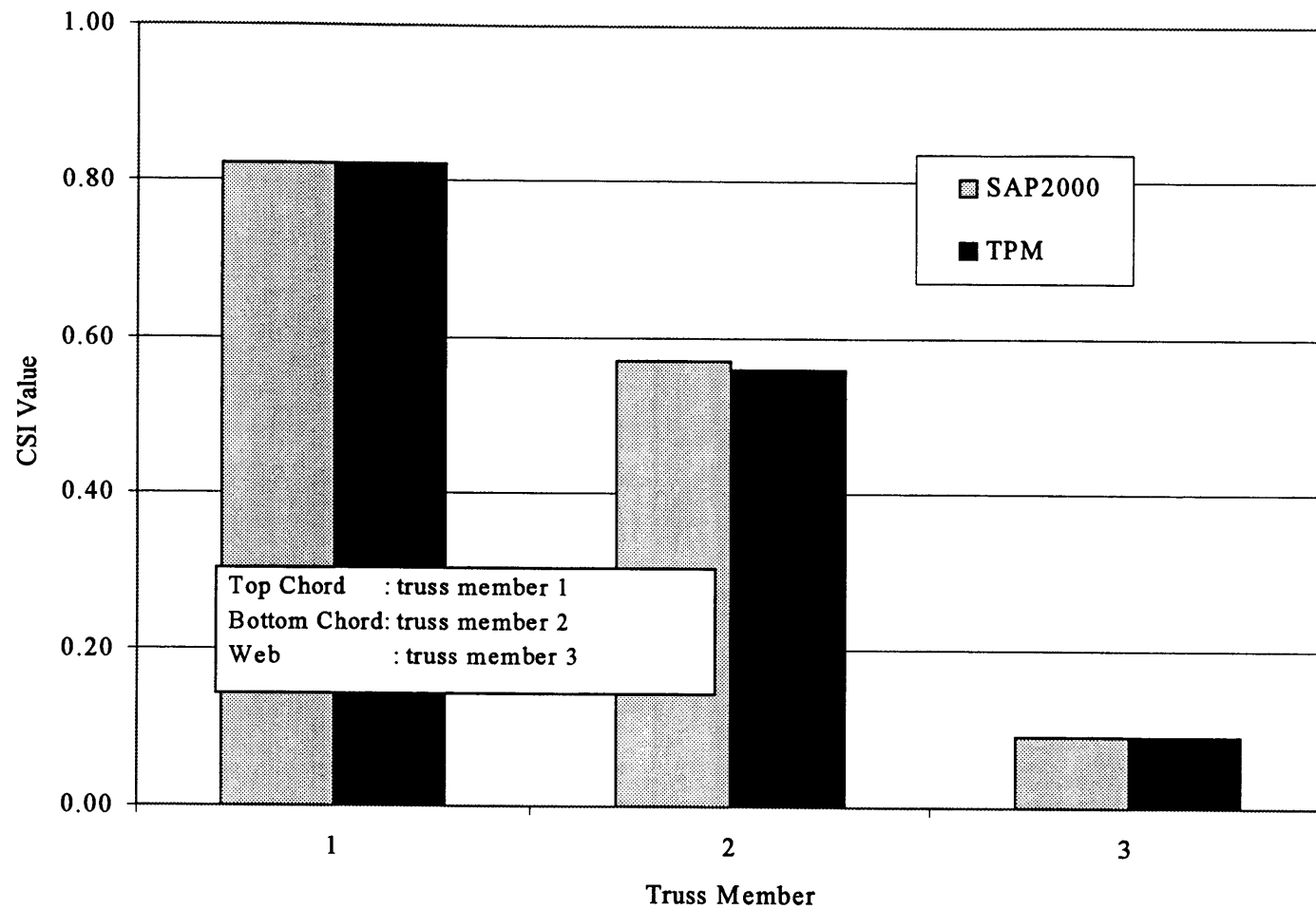


Figure H.9 CSI Values for Truss Type J Using SAP2000 Model and TPM's Output
 (Percent Difference: 0%~2%)

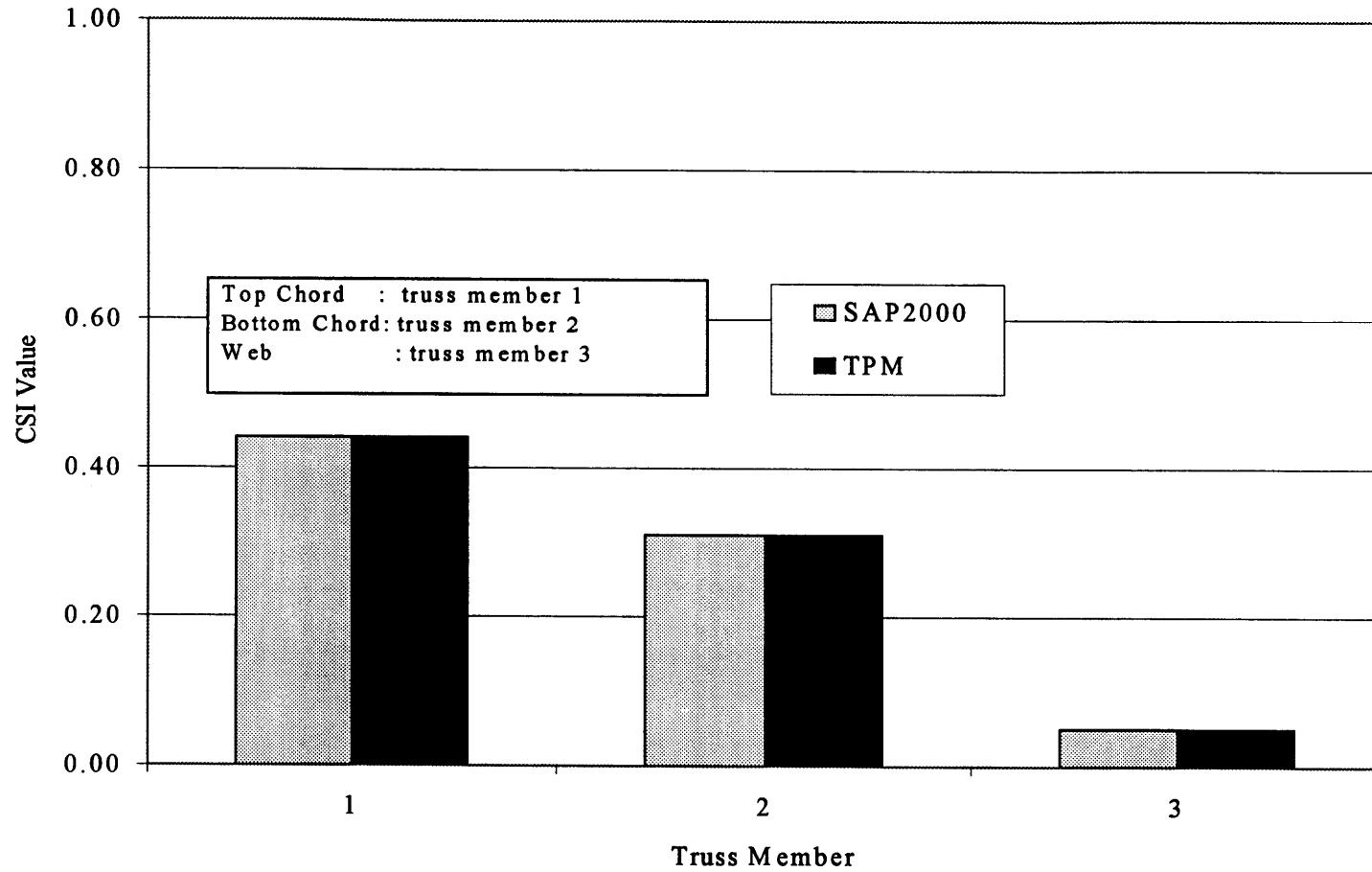


Figure H.10 CSI Values for Truss Type J1 Using SAP2000 Model and TPM's Output
(Percent Difference: 0%)

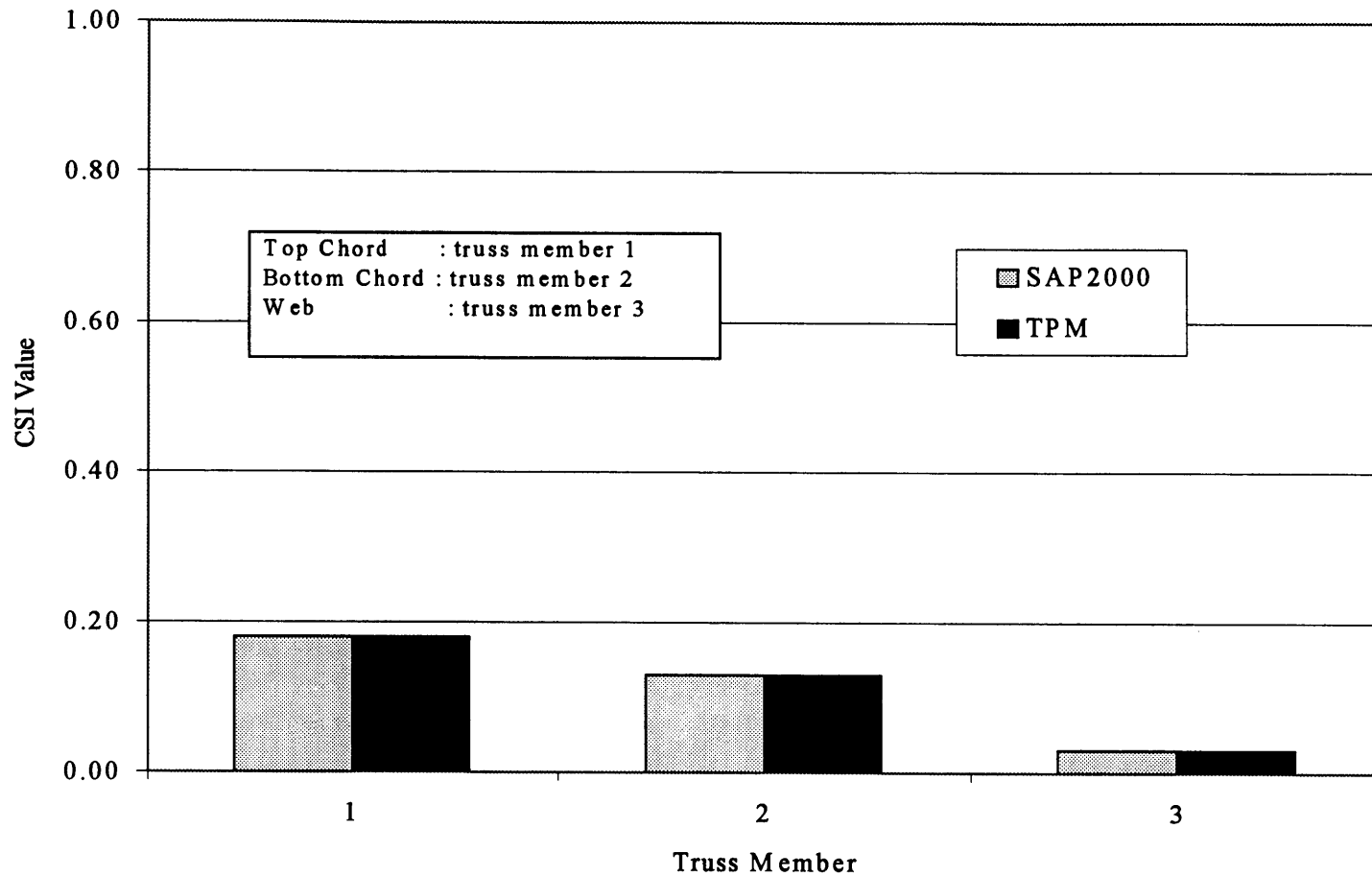


Figure H.11 CSI Values for Truss Type J2 Using SAP2000 Model and TPM's Output
(Percent Difference: 0%)

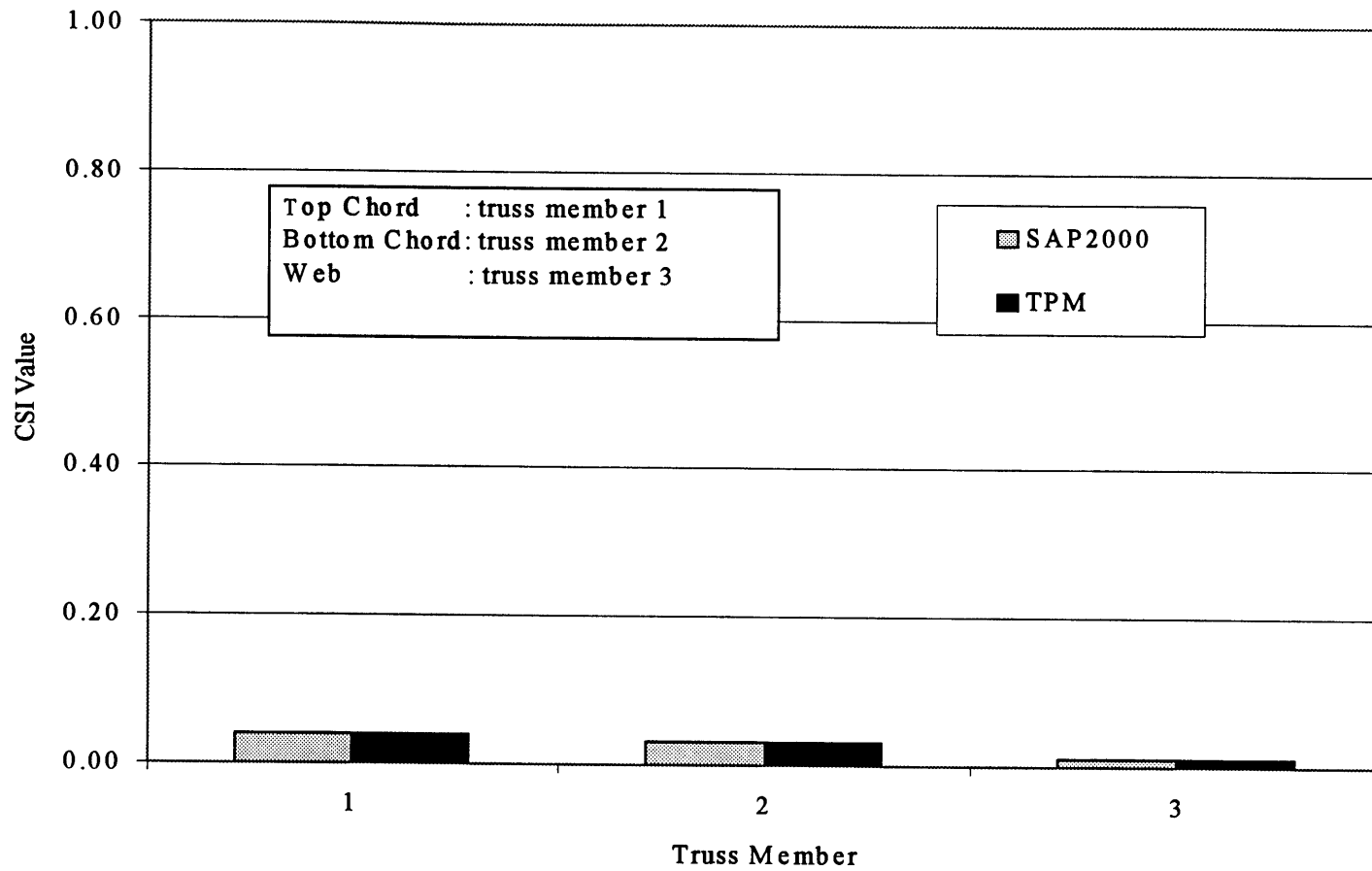


Figure H.12 CSI Values for Truss Type J3 Using SAP2000 Model and TPM's Output
(Percent Difference: 0%)

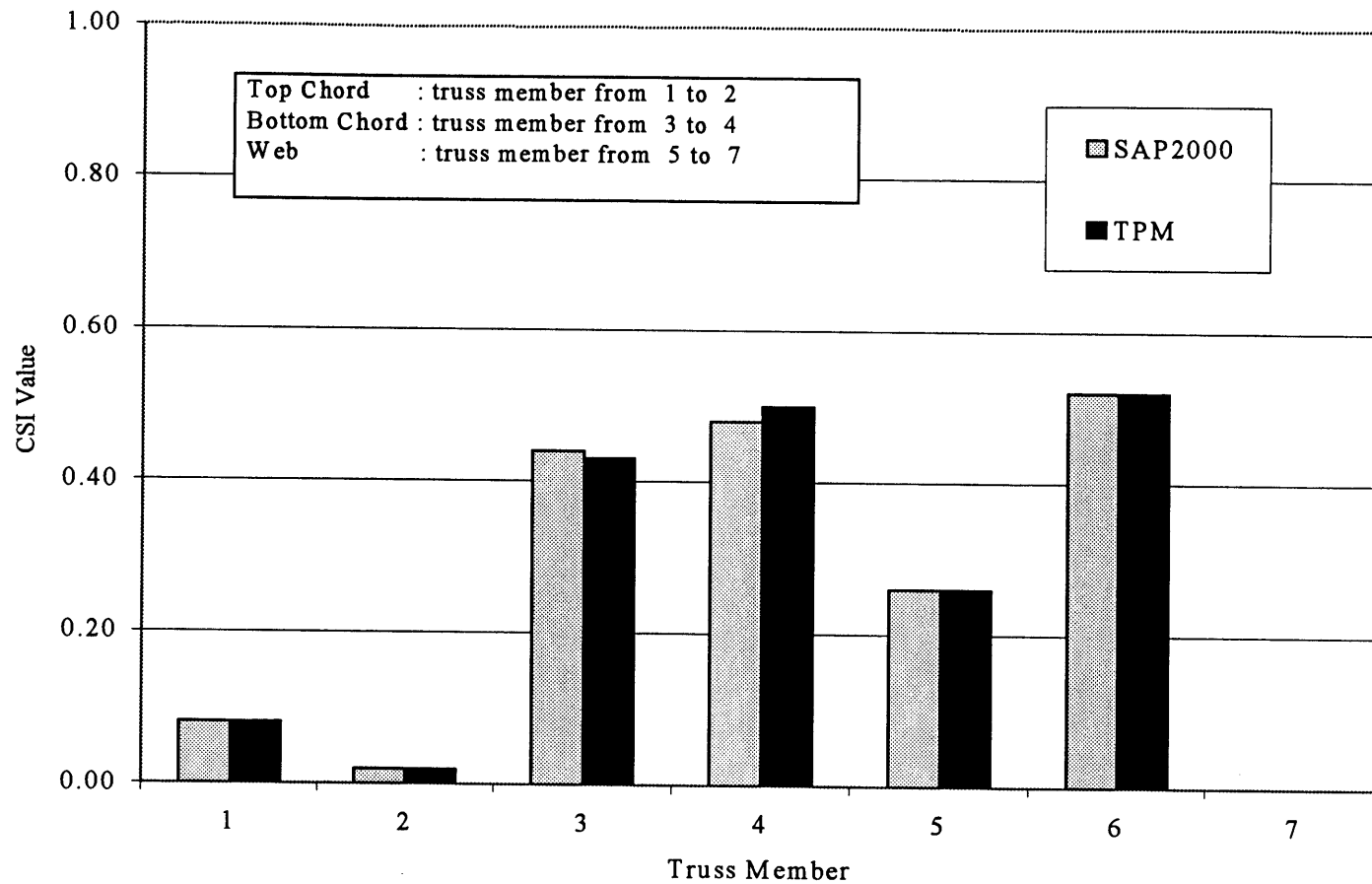


Figure H.13 CSI Values for Truss Type JGR Using SAP2000 Model and TPM's Output
 (Percent Difference: 4%~-2%)

APPENDIX I Comparison for Two Types of Semi-Rigid Joints

In this comparison, all the trusses were according to design from a TPM, but two types of semi-rigid joints, the TPM's joint model and a linear spring (LS) joint model, were used in the truss modeling. CSI values for all truss members in all trusses are shown in Figures I.1~I.14. In the figures, the truss member numbers are shown in Appendix E. As shown in these figures, the CSI values for webs were close in both models, because webs had pinned connections at their ends. The CSI values for top chords show more difference between the two types because of the locations of the semi-rigid joints for each type. In the LS joint model, only the heel joints and bottom-chord-tension-splice joints were modeled as semi-rigid and other joints were pinned or rigid connections. In the TPM's joint model, the peak joints, heel joints, and bottom-chord-panel joints were all modeled as semi-rigid. The main difference between the two models was in the peak joint. One model used a pinned connection and the other used a semi-rigid connection for the peak joint. In Figure I.1, one end of truss member 4 (on top chord) is connected to the peak joint, and the CSI value of truss member 4 for the LS joint model is higher than that from the TPM's joint model. Figure I.15 shows the moment diagrams of truss member 4 of truss type A with different peak joint models. Because the pinned connection at the one end of the truss member can not resist a moment (Case 2 in Figure I.15), the other end will resist a larger moment according to moment distribution theory.

The increased moment will cause the CSI to increase for this member in the truss model with an LS joint model.

The actual roof truss assembly used the TPM's semi-rigid joint model for the following reasons: 1) the modeling is simpler than the LS joint model, because the TPM's semi-rigid joint model only uses Frame elements, while both Nlink and Frame elements are used for LS joint modeling; 2) truss models with the TPM's semi-rigid joint model have already been applied in practice; 3) the joint modeling considers the semi-rigid behavior for the peak joints; and 4) the model building can be done in less time than the LS joint model, because the LS joint model can not be duplicated in SAP2000. The LS joint model has no physical dimensions, and when the same truss type is duplicated in the assembly, we need to take time to model it again.

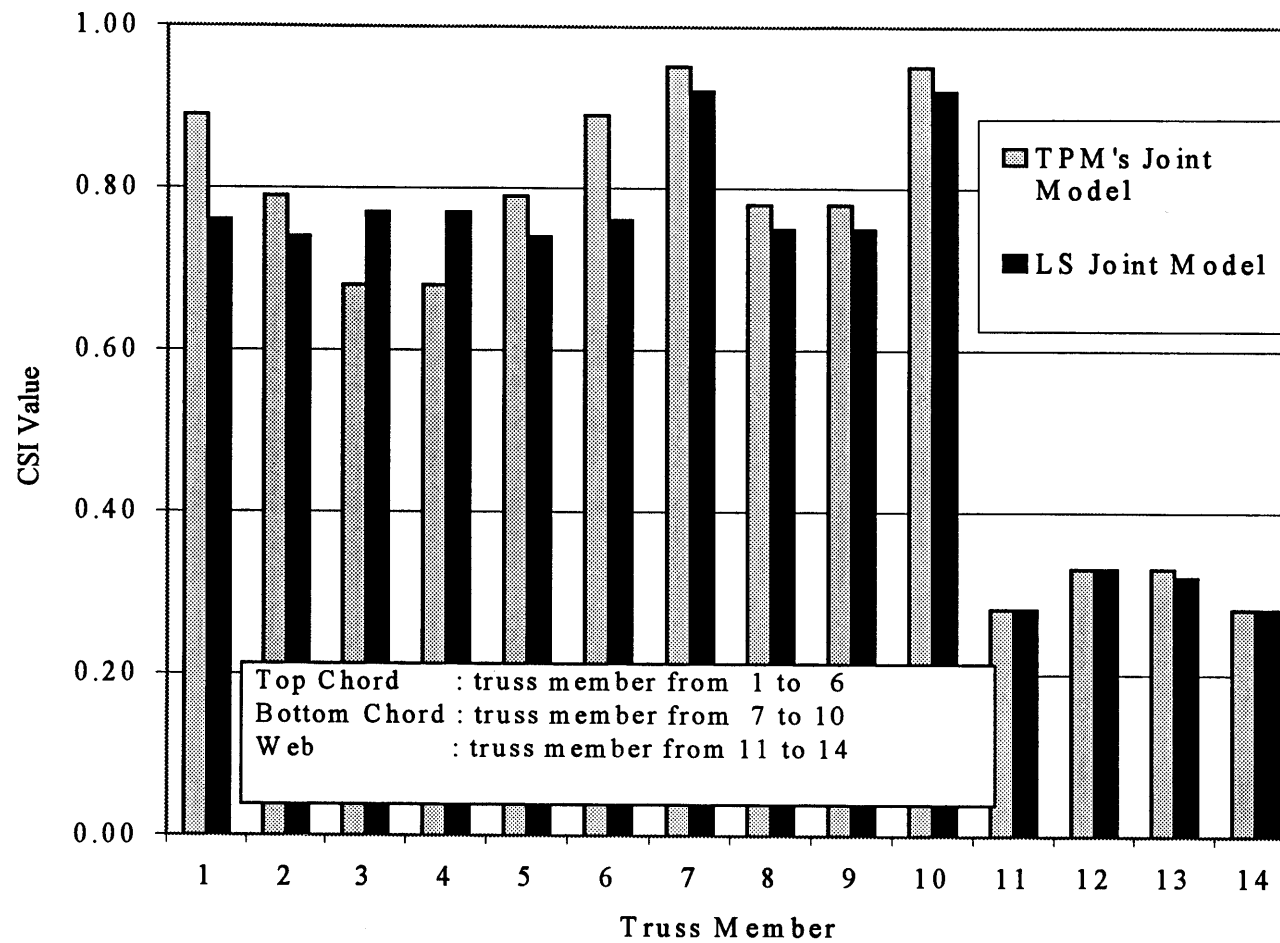


Figure I.1 CSI Values for Two Types of Semi-Rigid Joint Models for Truss Type A

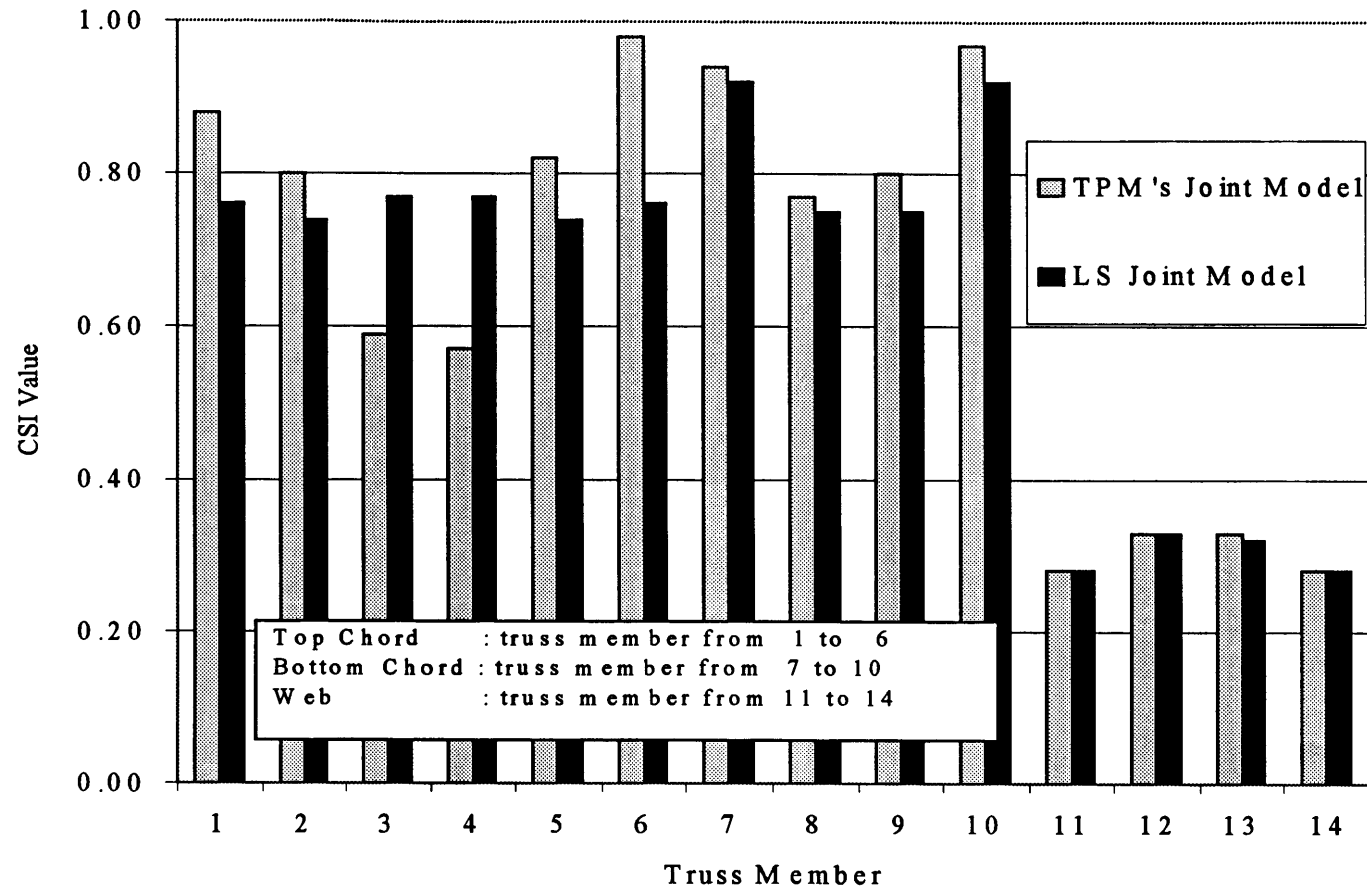


Figure I.2 CSI Value for Two Types of Semi-Rigid Joint Models for Truss Type A1

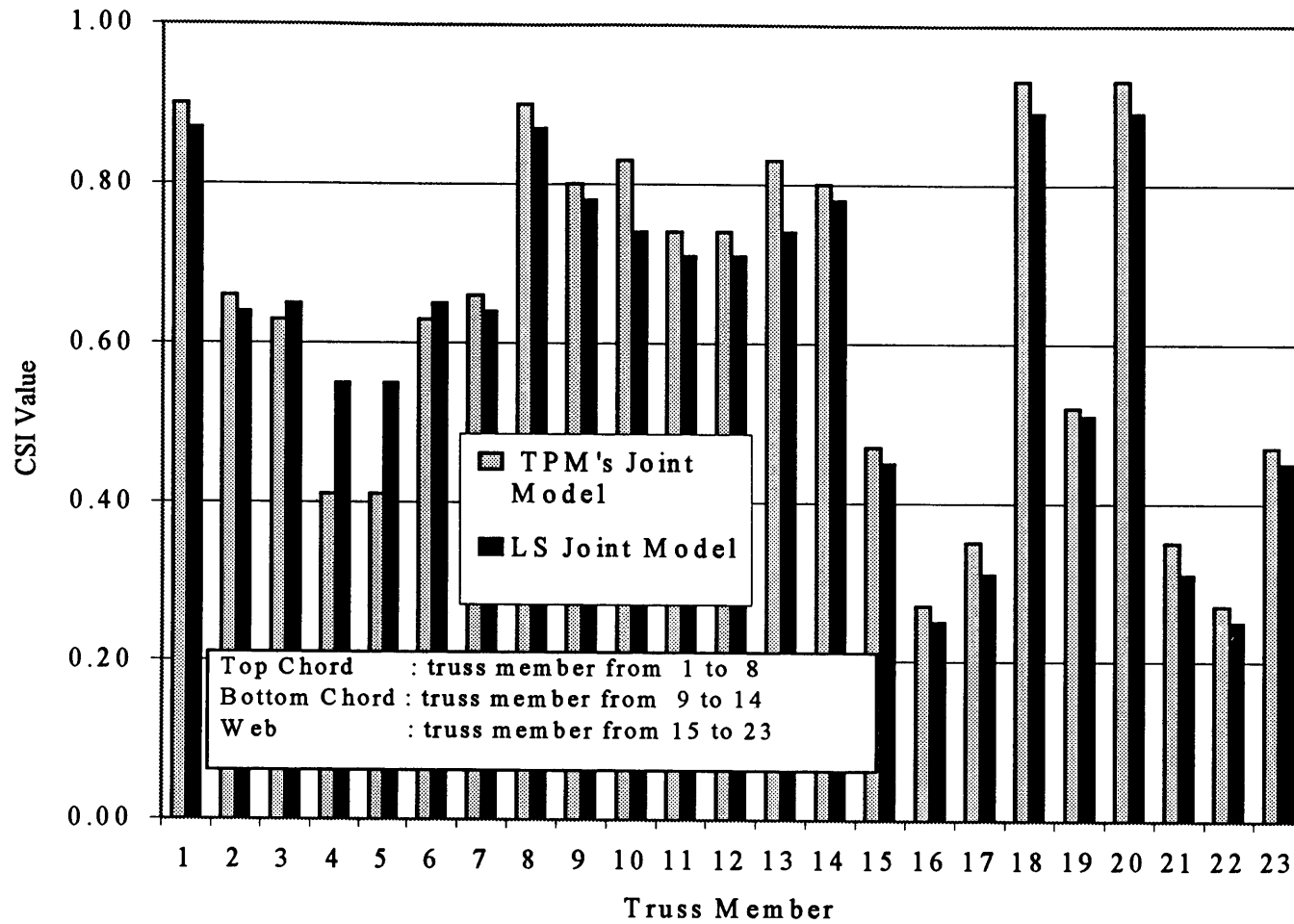


Figure I.3 CSI Value for Two Types of Semi-Rigid Joint Models for Truss Type A2

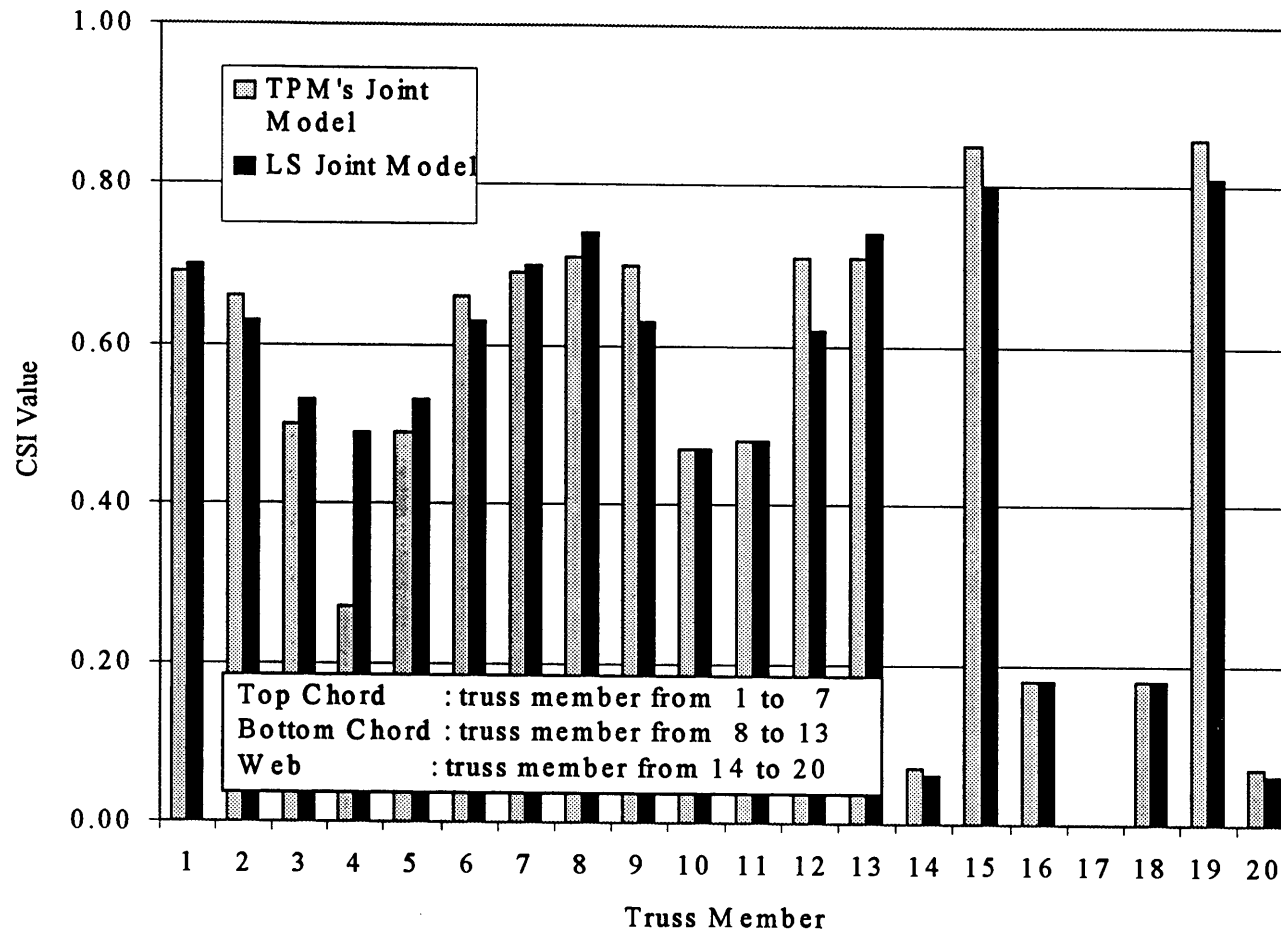


Figure I.4 CSI Value for Two Types of Semi-Rigid Joint Models for Truss Type AS1

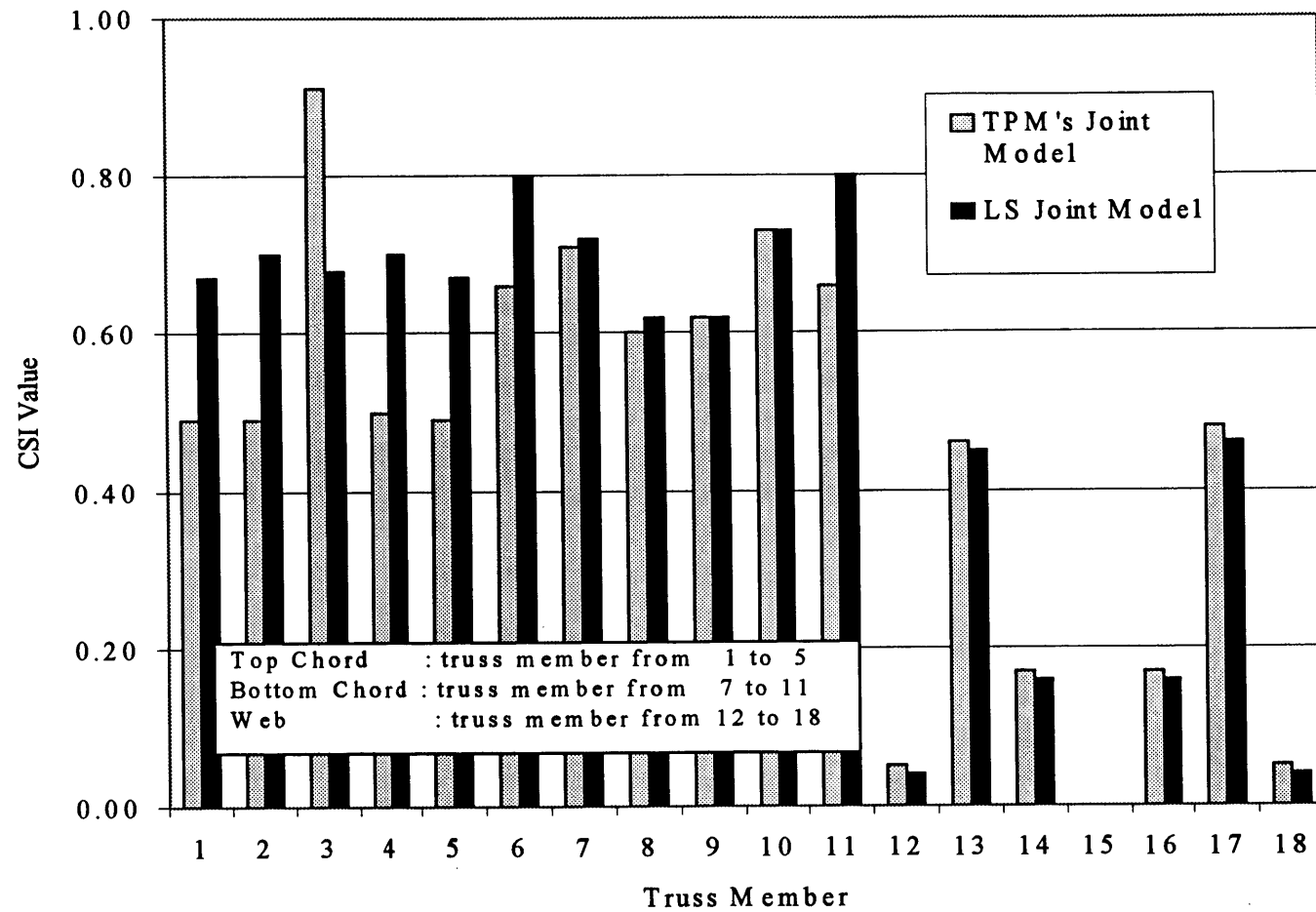


Figure I.5 CSI Value for Two Types of Semi-Rigid Joint Models for Truss Type AS2

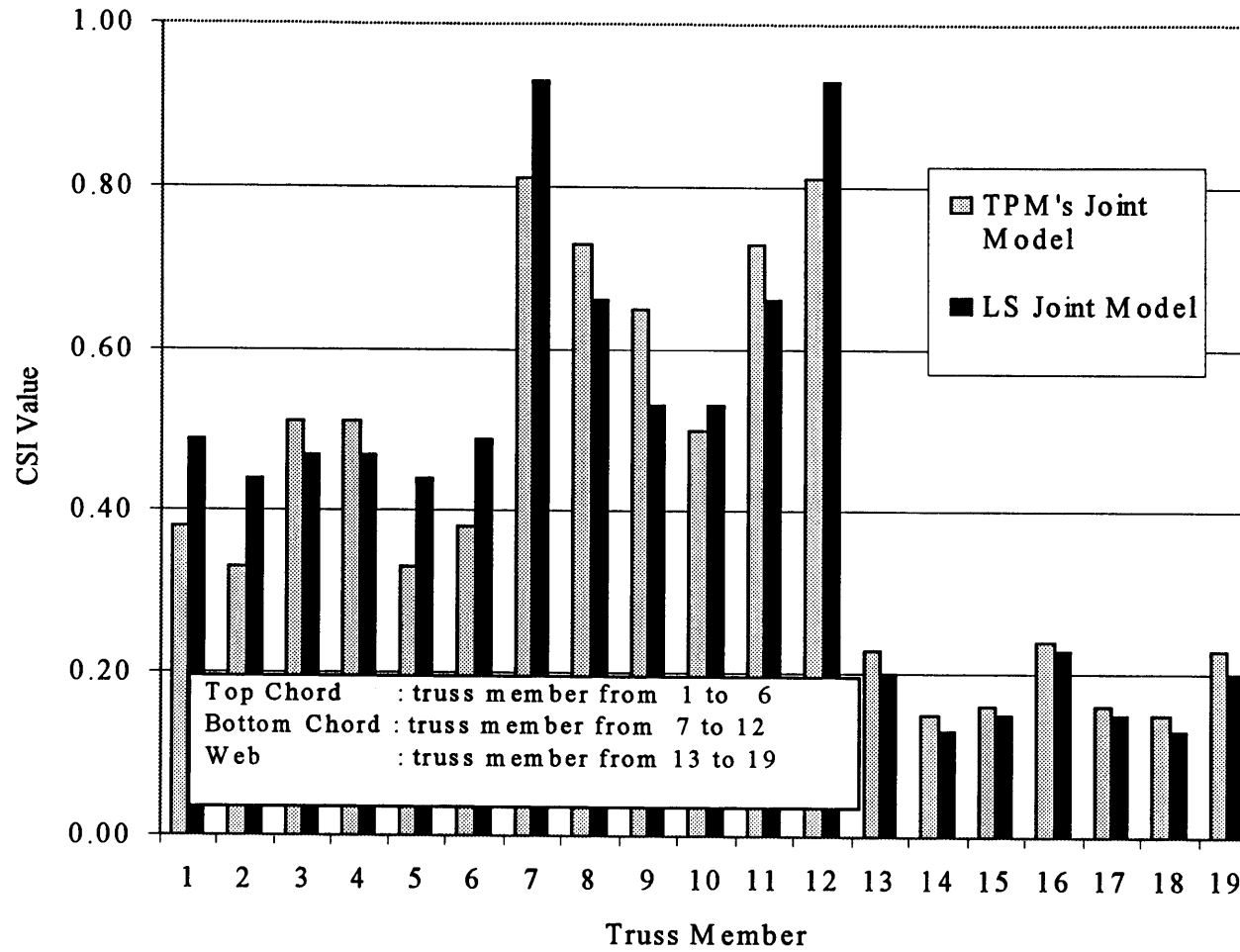


Figure I.6 CSI Value for Two Types of Semi-Rigid Joint Models for Truss Type AS3

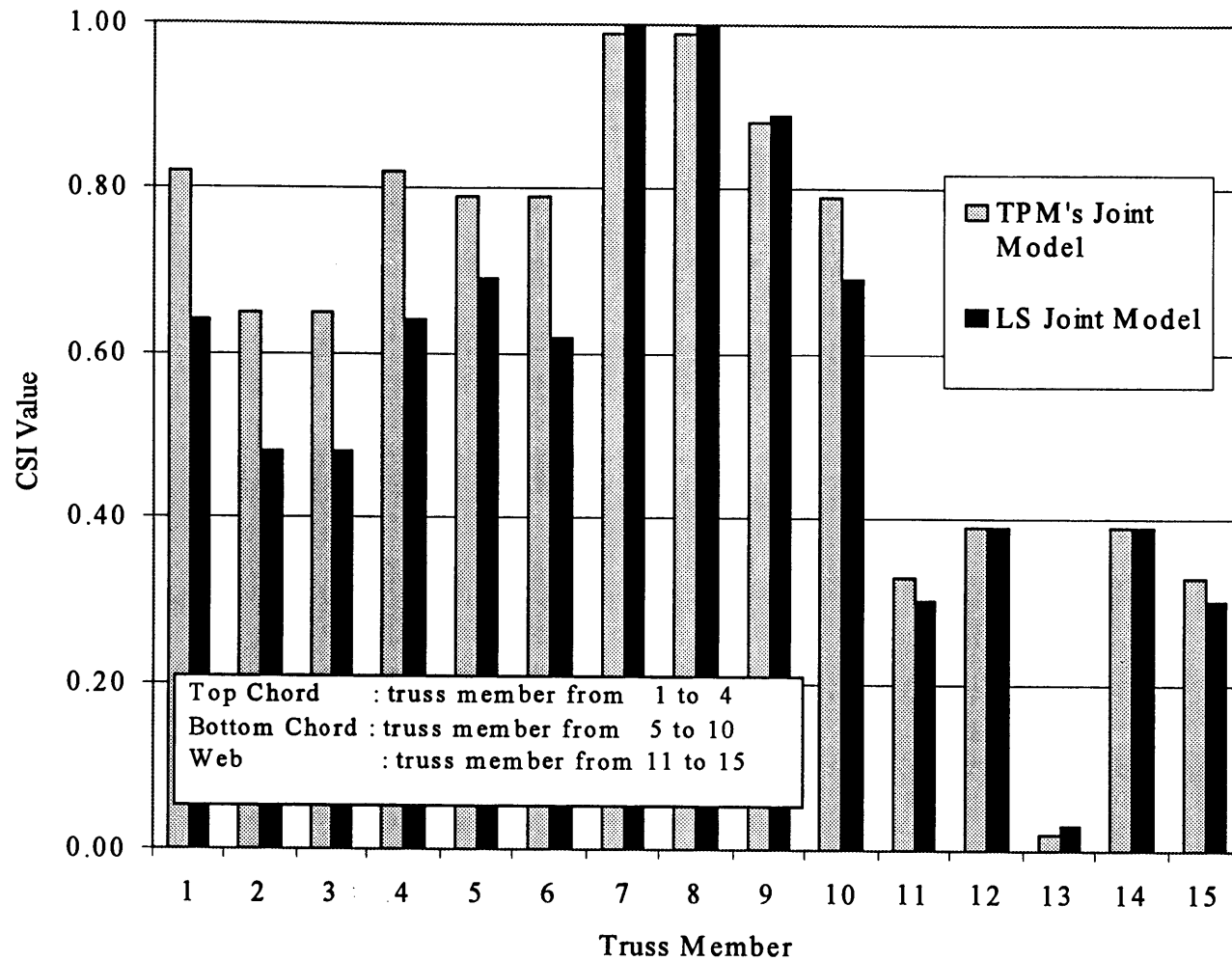


Figure I.7 CSI Value for Two Types of Semi-Rigid Joint Models for Truss Type ASGR

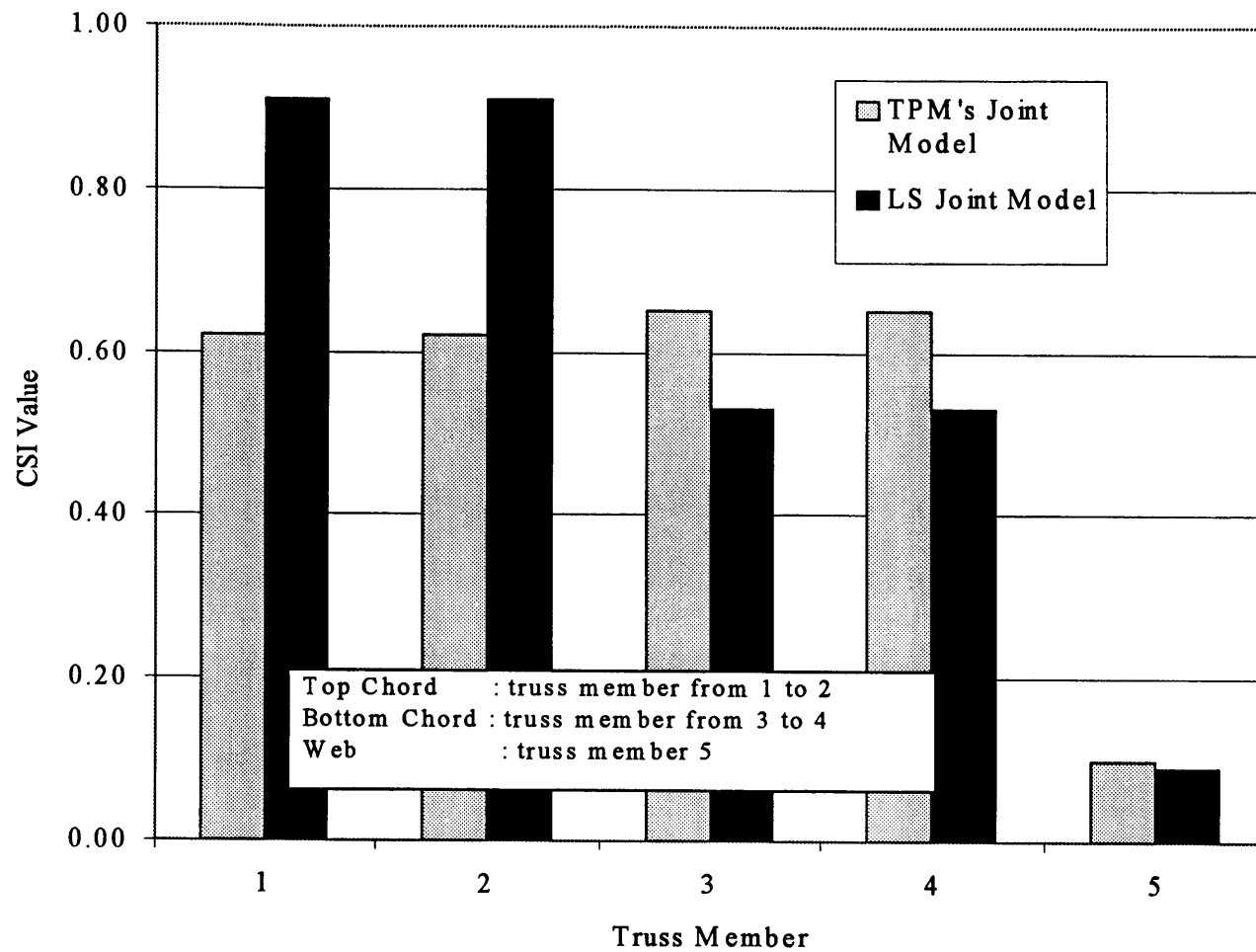


Figure I.8 CSI Value for Two Types of Semi-Rigid Joint Models for Truss Type B

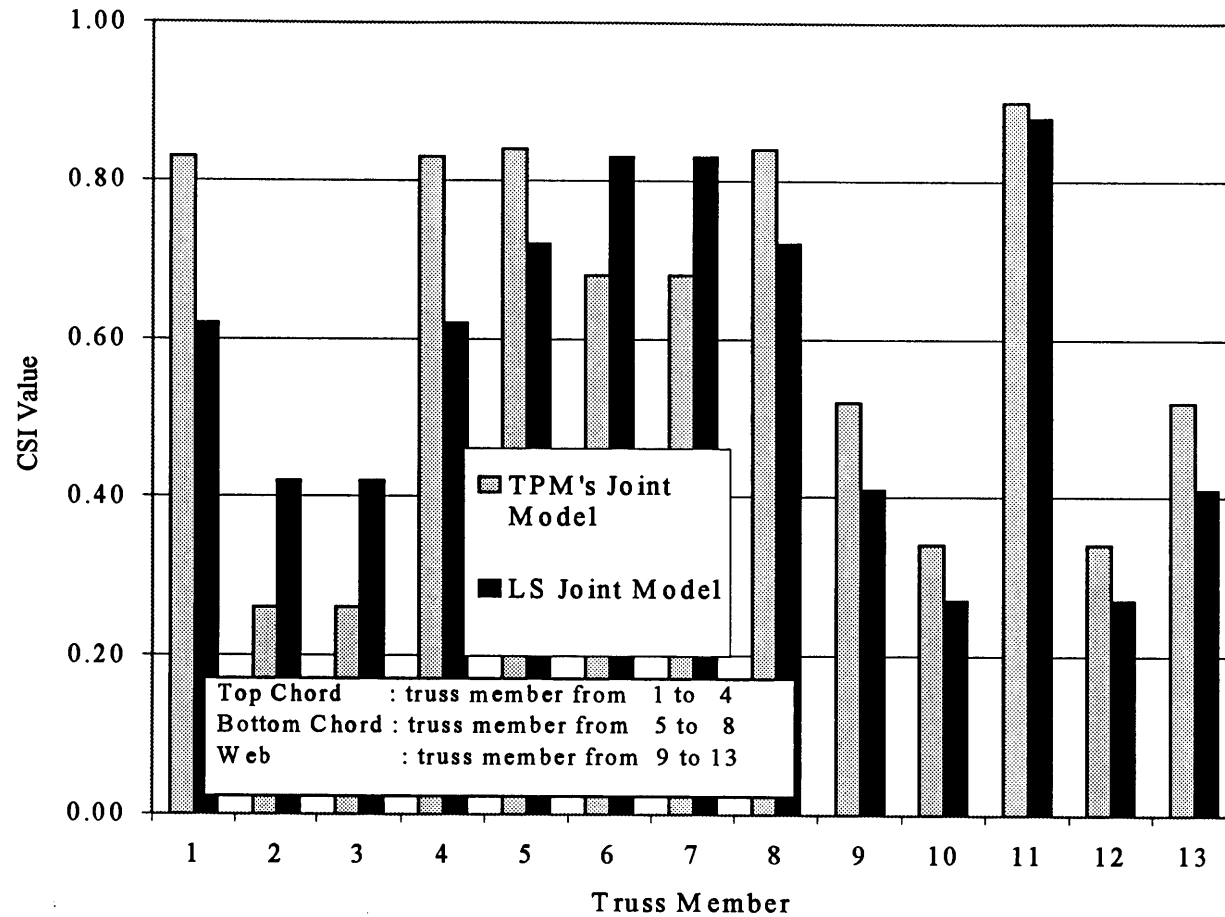


Figure I.9 CSI Value for Two Types of Semi-Rigid Joint Models for Truss Type BGR

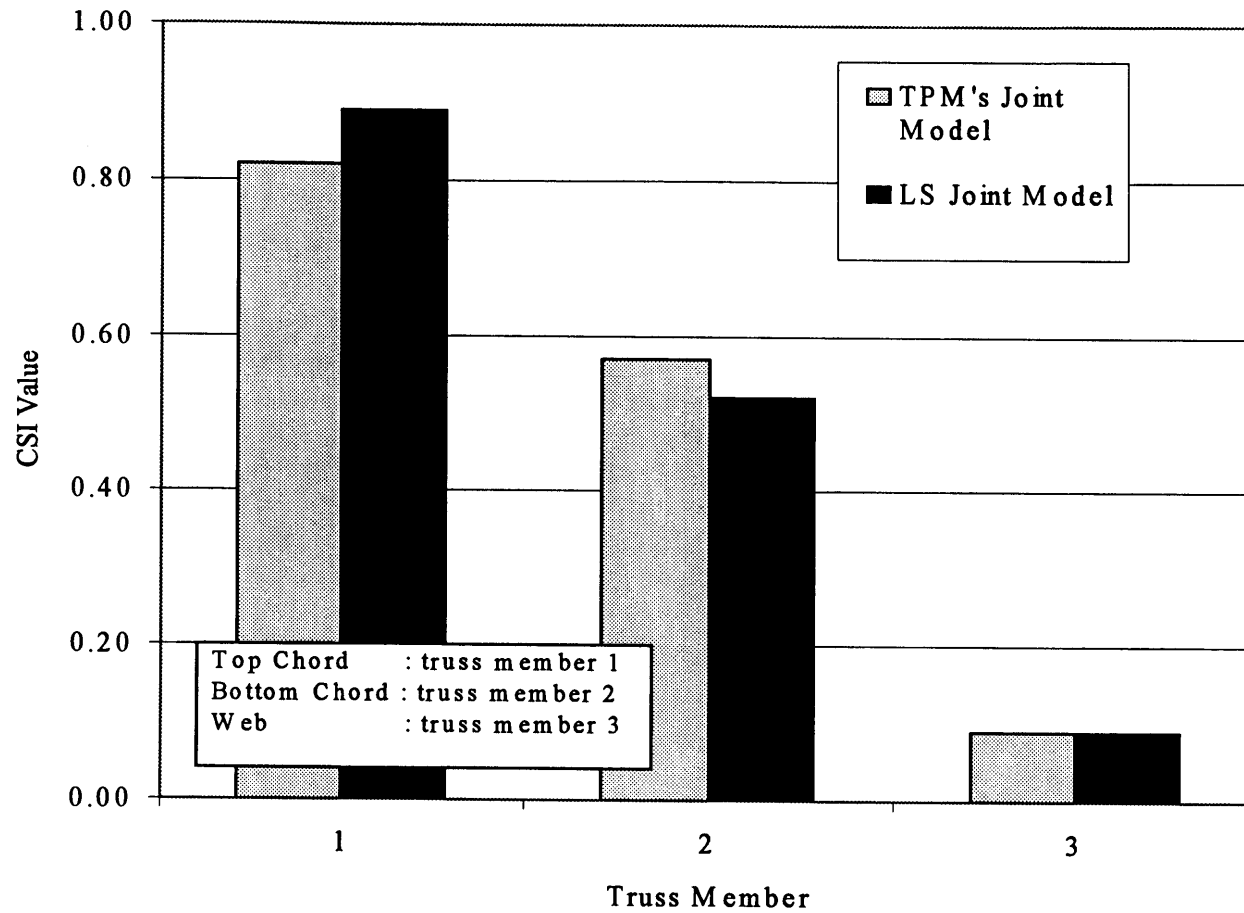


Figure I.10 CSI Value for Two Types of Semi-Rigid Joint Models for Truss Type J

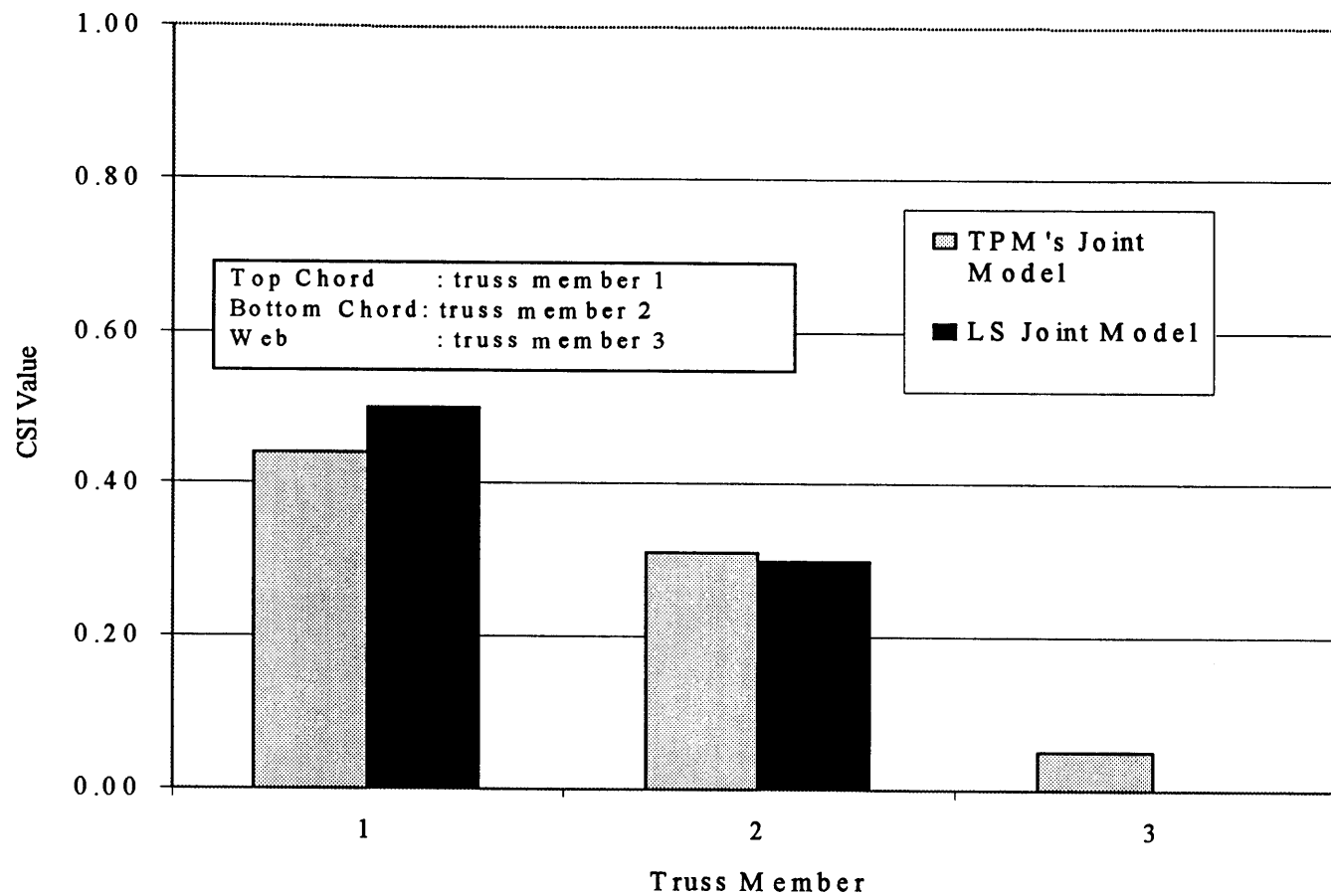


Figure I.11 CSI Value for Two Types of Semi-Rigid Joint Models for Truss Type J1

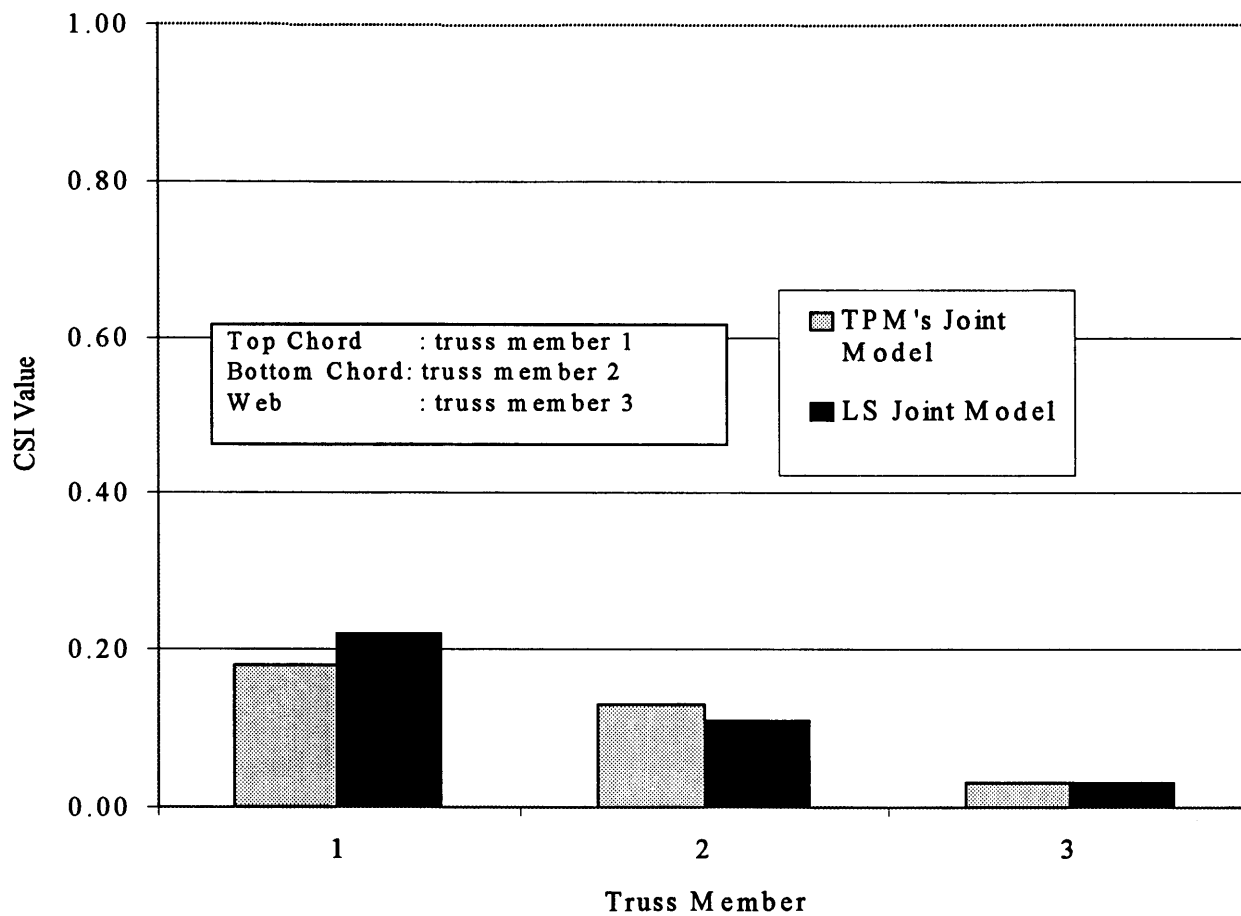


Figure I.12 CSI Value for Two Types of Semi-Rigid Joint Models for Truss Type J2

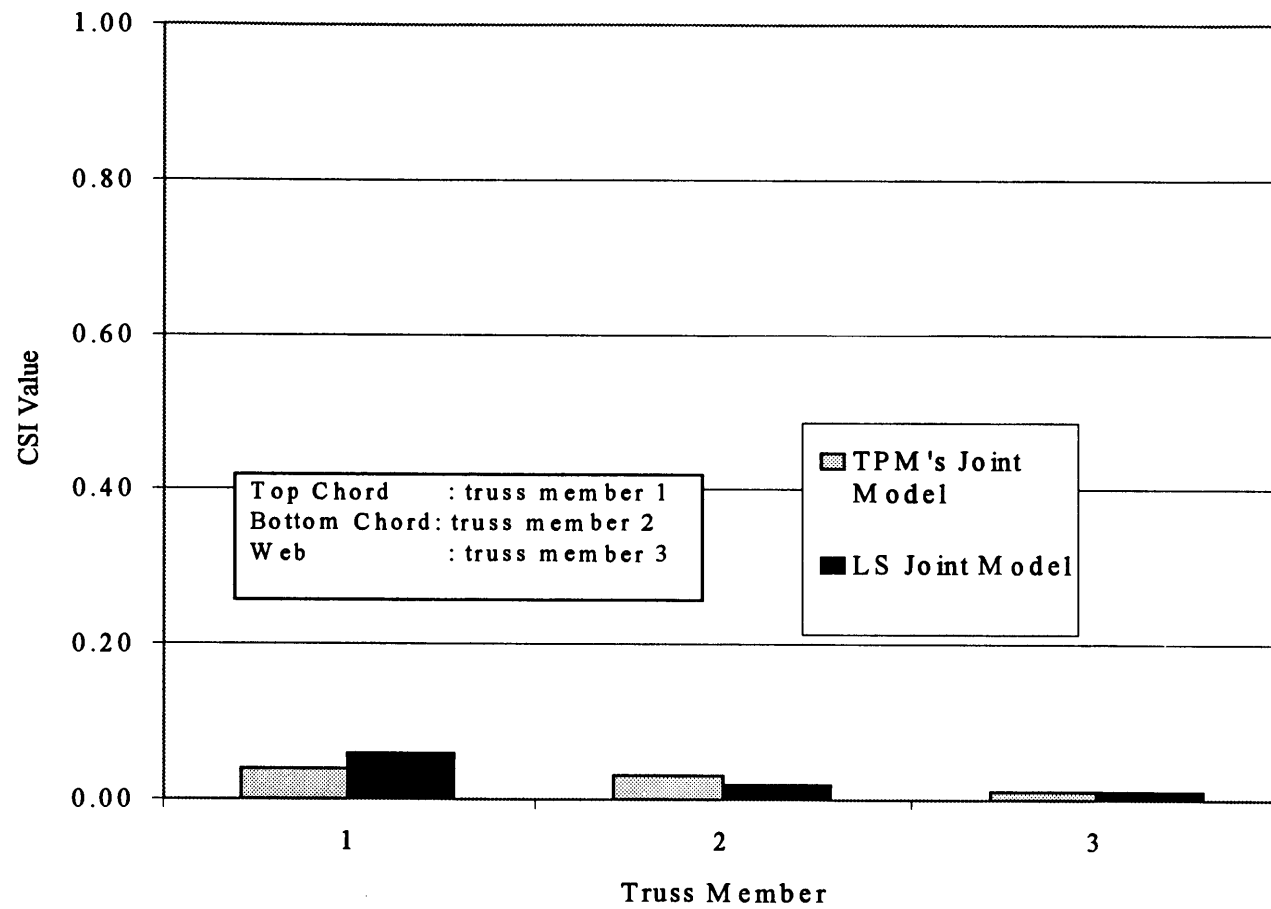


Figure I.13 CSI Value for Two Types of Semi-Rigid Joint Models for Truss Type J3

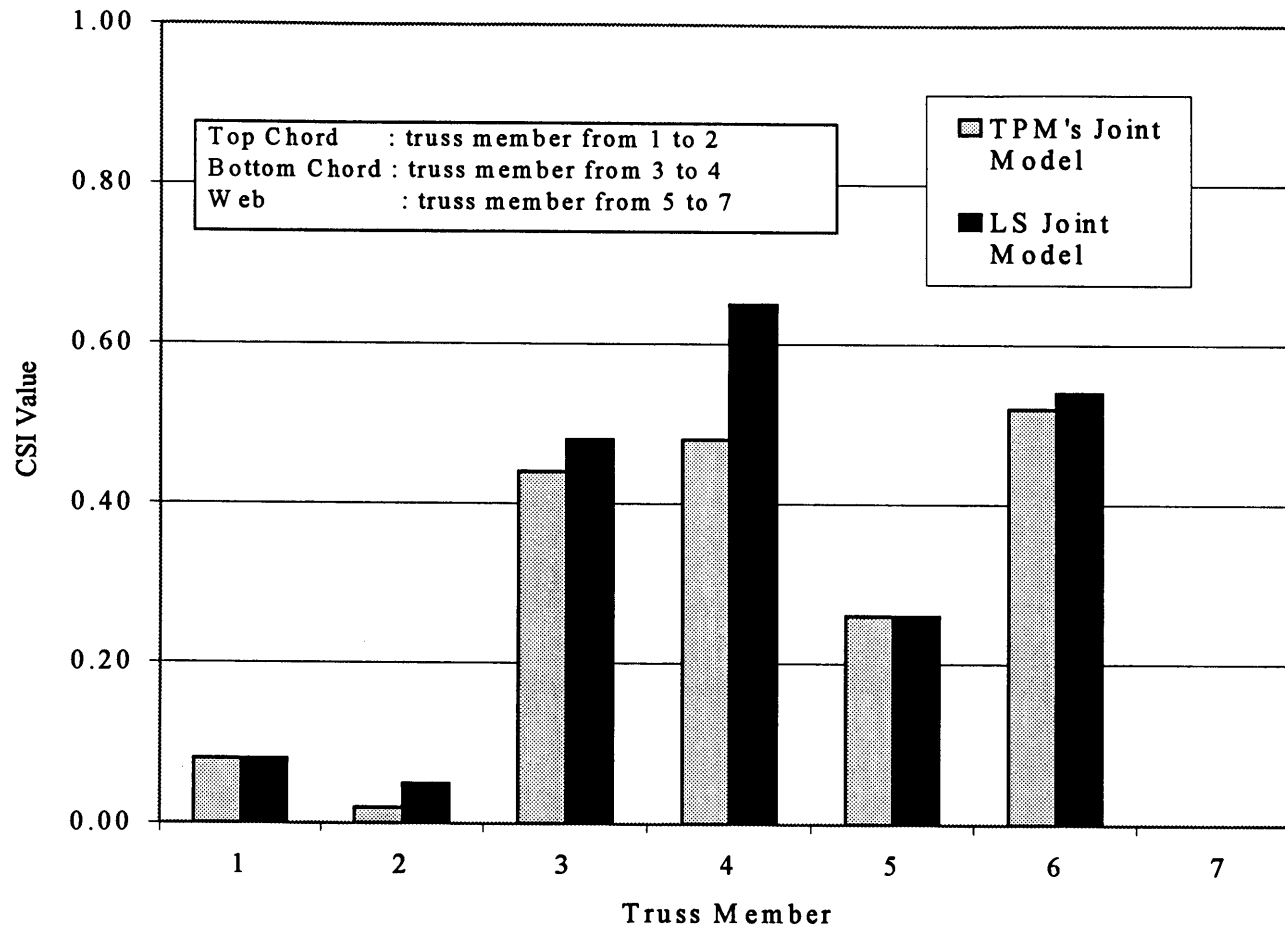


Figure I.14 CSI Value for Two Types of Semi-Rigid Joint Models for Truss Type JGR

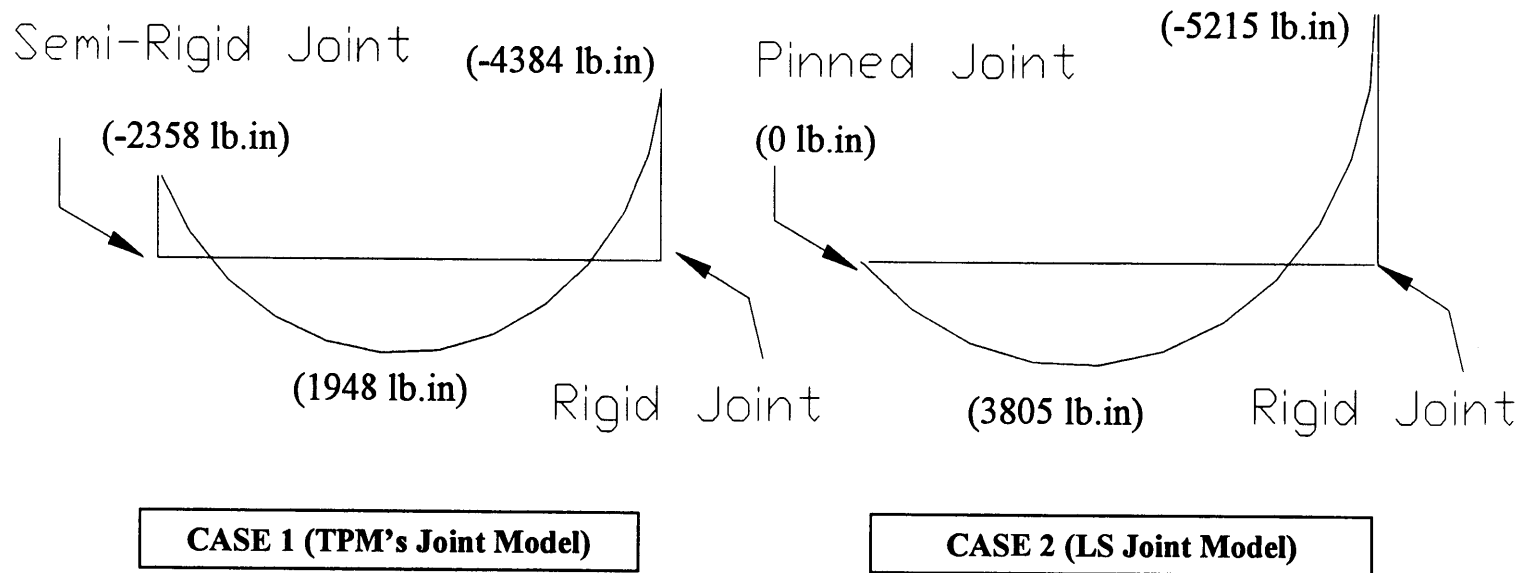


Figure I.15 Moment Diagrams of Truss Member 4 of Truss Type A with Different Peak Joints

APPENDIX J Joint Reactions for Truss Type A1 Series in The Assembly

Figure J.1 shows the location of joint A in truss type A1-4. In this appendix, an example is shown of how to calculate the reaction for a joint (Joint A) connected to the bottom chord of truss type BGR-1.

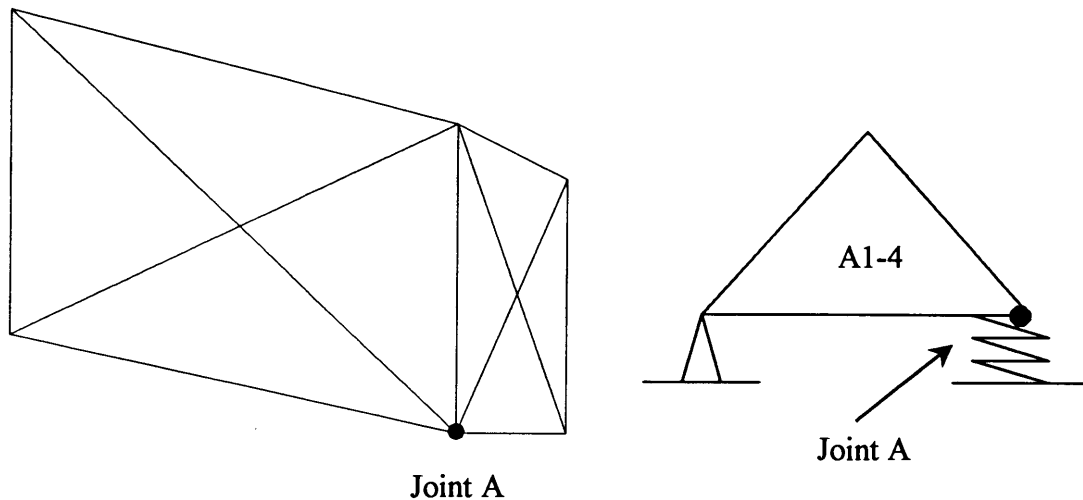


Figure J.1 Joint A in Truss Type A1-4

Figure J.2 shows the free body diagram for Joint A for the reaction calculations. Joint A connects five members and the reaction at Joint A can be calculated by the joint equilibrium for the five members. Table J.1 shows the axial forces and shear forces for the five members.

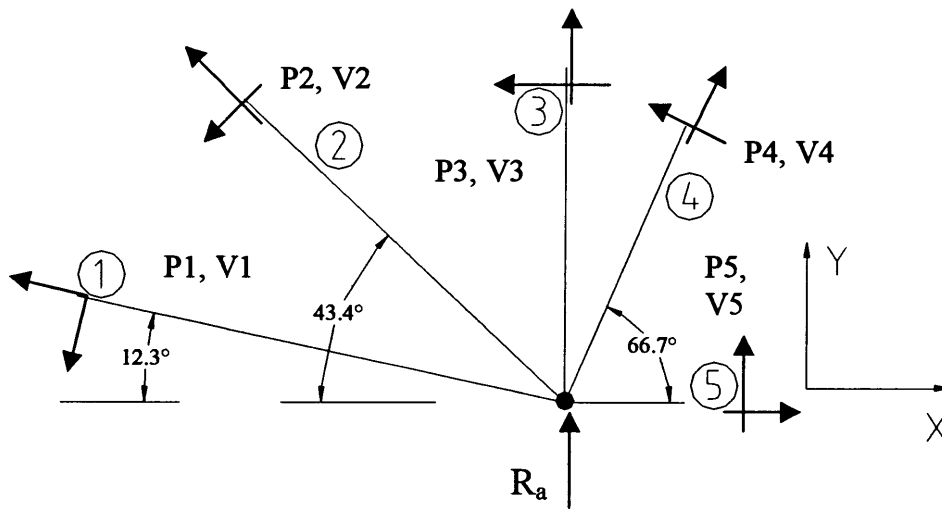


Figure J.2 The Free Body Diagram of Joint A

Member Number	(P) Axial Force (lb)	(V) Shear Force (lb)
1	305 (T)	50
2	-677 (C)	44
3	-203 (C)	-66
4	-115 (C)	41
5	-22 (C)	15

Table J.1 Axial Forces and Shear Forces for Five Members

$$\Sigma F_Y = 0$$

Reaction Force at Joint A = R_a

$$R_a + 305 \sin(12.3^\circ) - 677 \sin(43.4^\circ) - 203 - 115 \sin(66.7^\circ) - 50 \cos(12.3^\circ) -$$

$$44 \cos(43.4^\circ) + 41 \cos(66.7^\circ) + 15 = 0 \quad R_a = 758 \text{ (lb) (shown in Figure J.2)}$$

Check:

In Figure J.1, the reaction at joint A can not be calculated using SAP2000, because joint A is not connected to a support. To check the calculation, the same truss A1-4 with different boundary condition is shown in Figure J.2 and used for verification. In Figure J.3, the reaction at joint A is 1277 lb, provided by SAP2000.

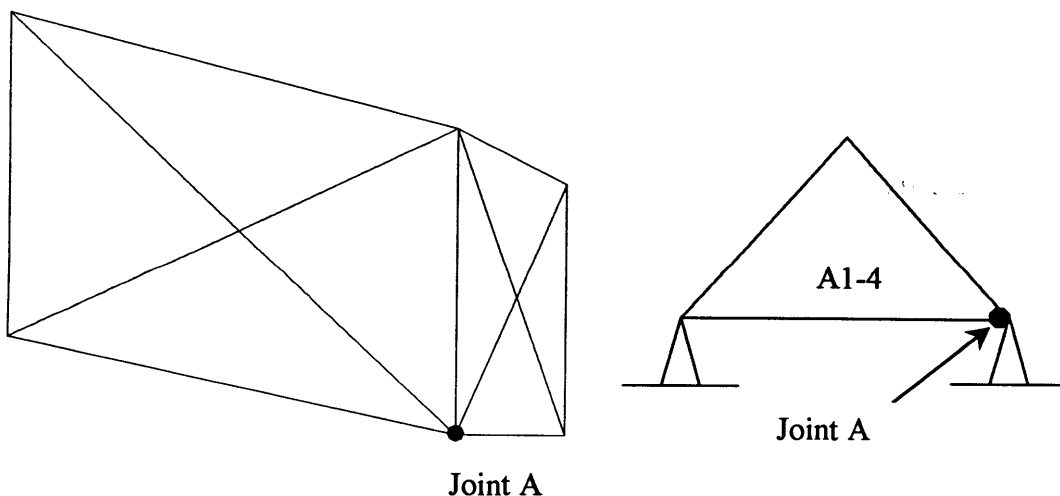


Figure J.3 Joint A in Truss Type A1-4 with Different Boundary Condition

Member Number	(P) Axial Force (lb)	(V) Shear Force (lb)
1	772 (T)	42
2	-1217 (C)	-63
3	-348 (C)	-65
4	-191 (C)	10
5	-15 (C)	-89

Table J.2 Axial Forces and Shear Forces for Five Members (check)

$$\Sigma F_y = 0$$

Reaction Force at Joint A = R_a $R_a = 1277$ lb (known reaction for check)

$$R_a + 772 \sin(12.3^\circ) - 1217 \sin(43.4^\circ) - 348 - 191 \sin(66.7^\circ) - 42 \cos(12.3^\circ) +$$

$$63 \cos(43.4^\circ) + 10 \cos(66.7^\circ) - 89 = 0 \quad R_a = 1275 \text{ (lb)} \approx 1277 \text{ (lb)}, \underline{OK}$$

APPENDIX K CSI Comparison for Individual Trusses with Different Boundary Conditions

Comparison of the individual trusses with different boundary conditions, hinge-roller and hinge-hinge, is shown in Figures K.1~K.14. From these comparison figures, we can see that the CSI values from the fourteen trusses with the “HINGE- HINGE” boundary condition are generally lower than those with the “HINGE-ROLLER” boundary condition. The main differences in CSI values for the two different boundary conditions are seen for the bottom chords. In the “HINGE-ROLLER” boundary condition, the bottom chord always carries tension force. Nevertheless, in the “HINGE-HINGE” boundary condition, the bottom chord can carry tension or compression because of the joint modeling method from the TPM (slight arching of bottom chord in some cases), which reduces or eliminates the tension force in the bottom chords. Figure K.15 shows a simplified truss model from the TPM. In Figure K.15, due to the geometry of the semi-rigid joint modeling for the heel joint (arching shown in figure), the bottom chord may carry compression for the “Hinge-Hinge” boundary condition. Some trusses have compression force in the bottom chords and some trusses have both compression and tension forces in different segments of the bottom chords. For this reason, the CSI values are generally lower for the “HINGE-HINGE” boundary condition.

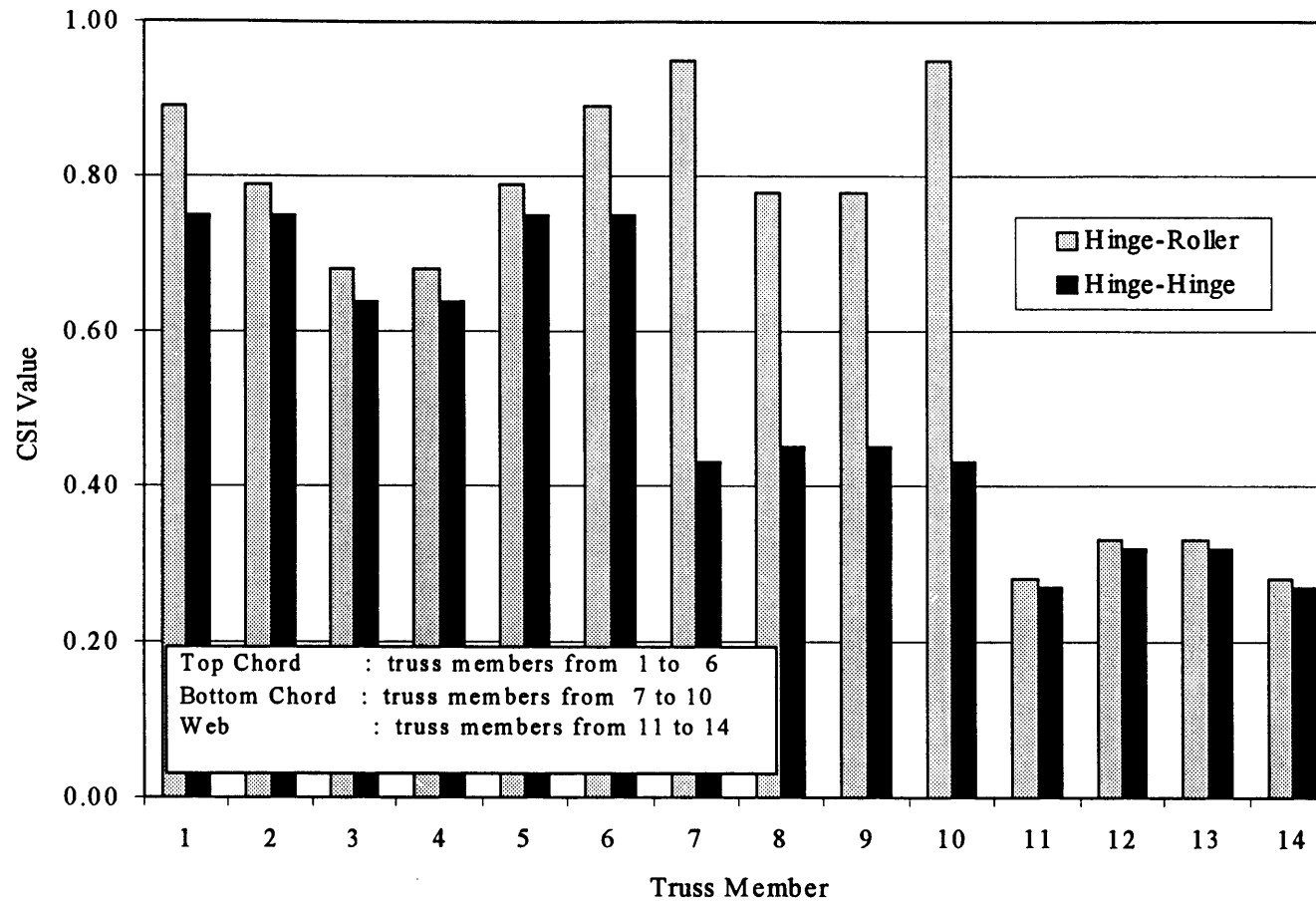


Figure K.1 CSI Comparison for The Truss Type A with Different Boundary Conditions, Hinge-Roller and Hinge-Hinge

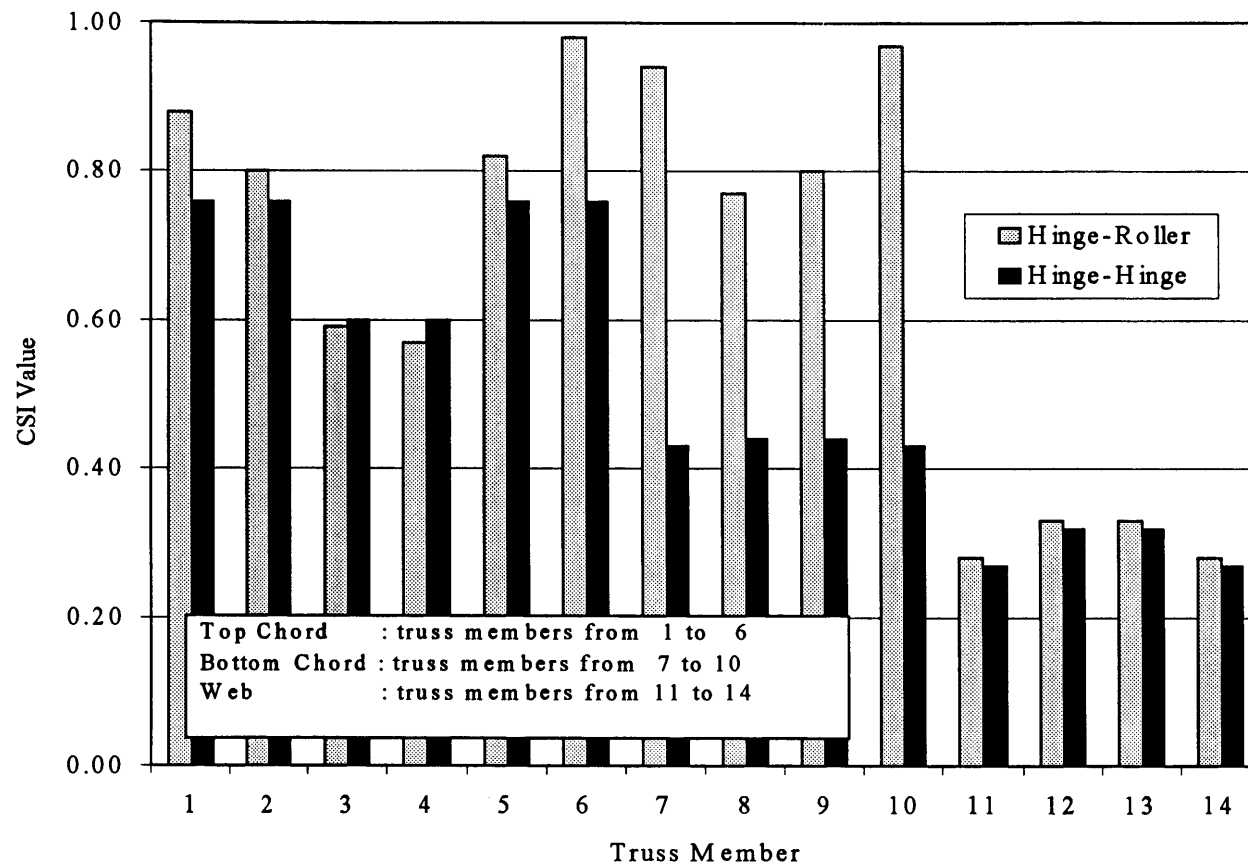


Figure K.2 CSI Comparison for The Truss Type A1 with Different Boundary Conditions, Hinge-Roller and Hinge-Hinge

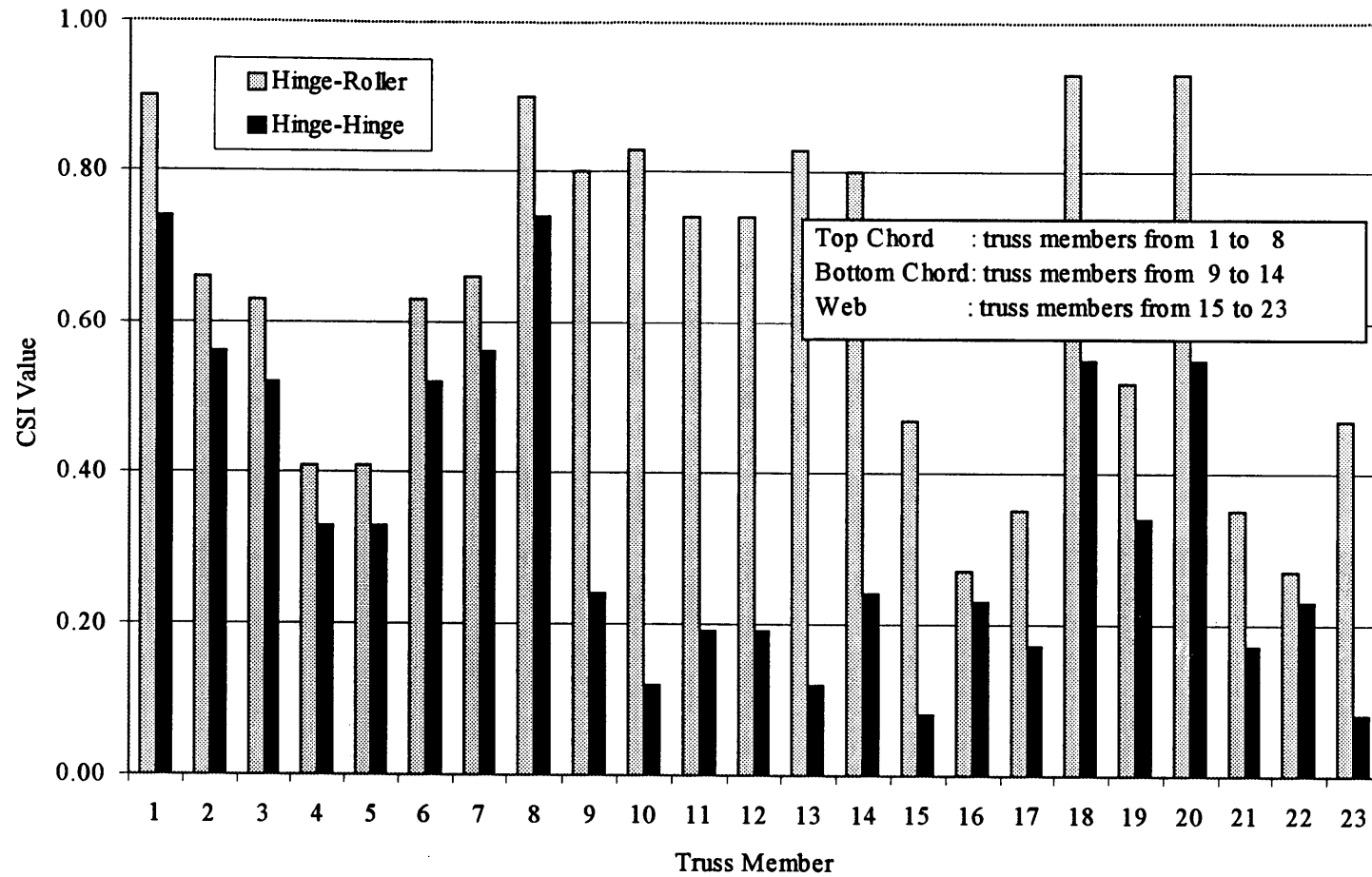


Figure K.3 CSI Comparison for The Truss Type A2 with Different Boundary Conditions, Hinge-Roller and Hinge-Hinge

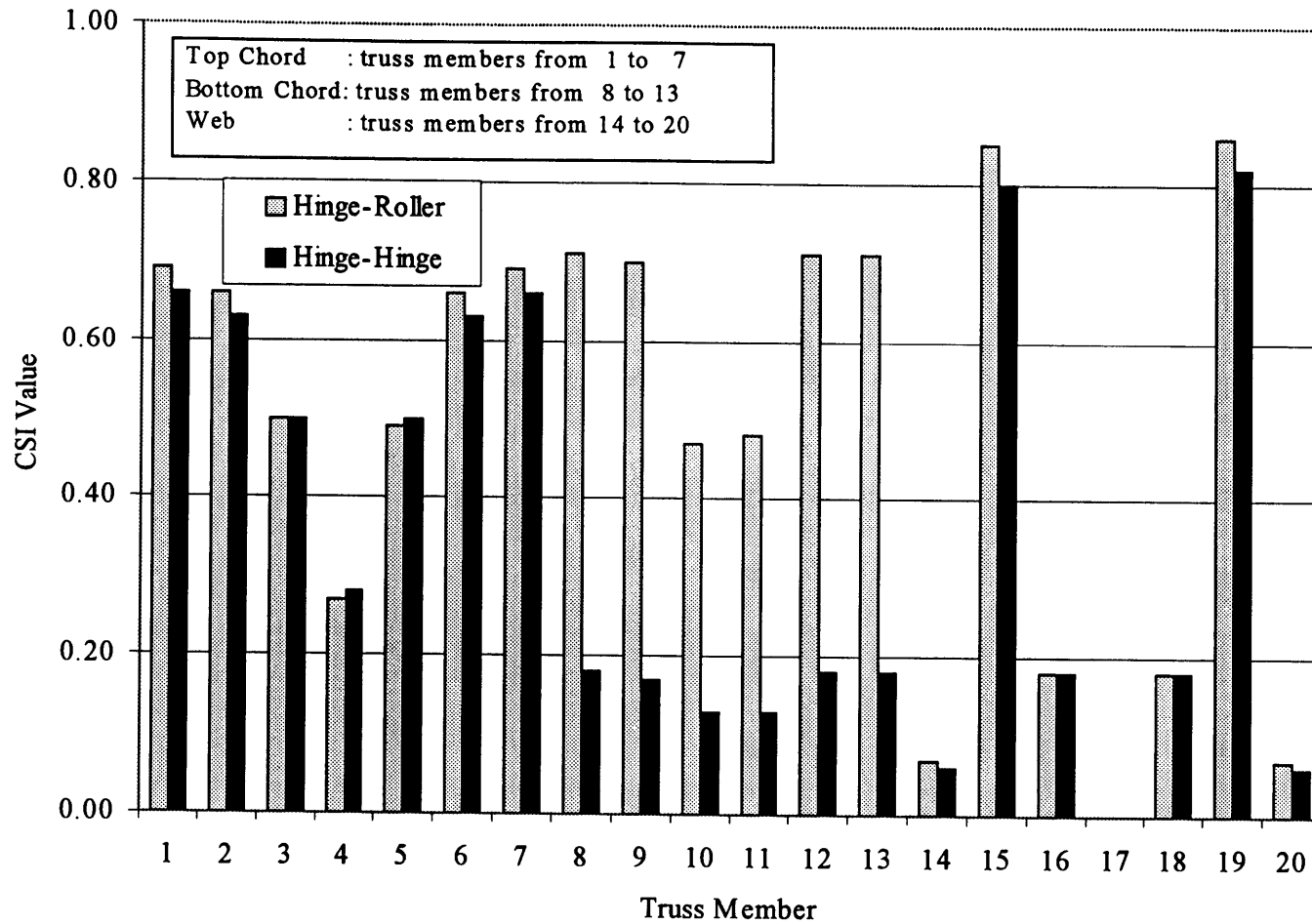


Figure K.4 CSI Comparison for The Truss Type AS1 with Different Boundary Conditions, Hinge-Roller and Hinge-Hinge

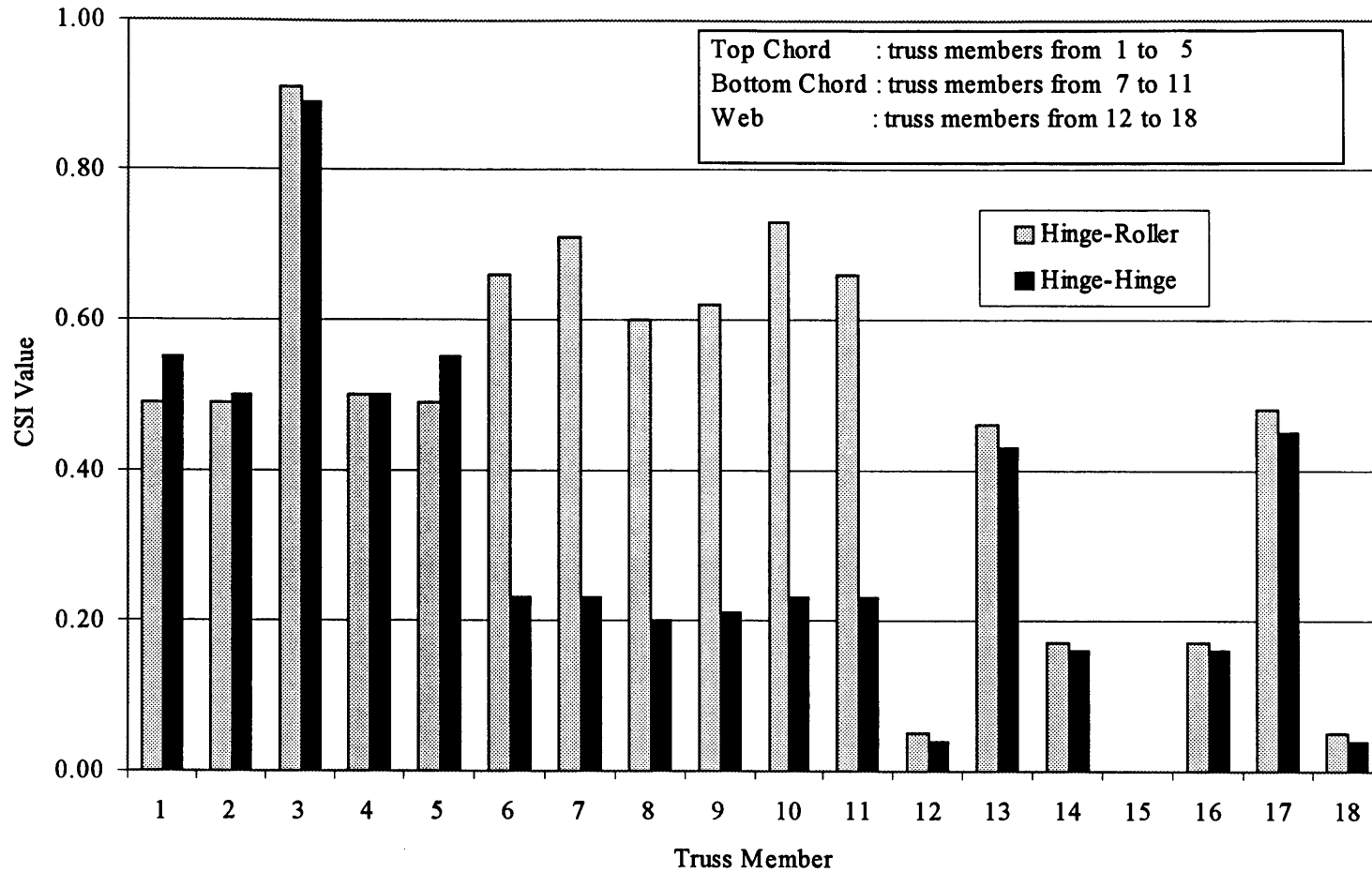


Figure K.5 CSI Comparison for The Truss Type AS2 with Different Boundary Conditions, Hinge-Roller and Hinge-Hinge

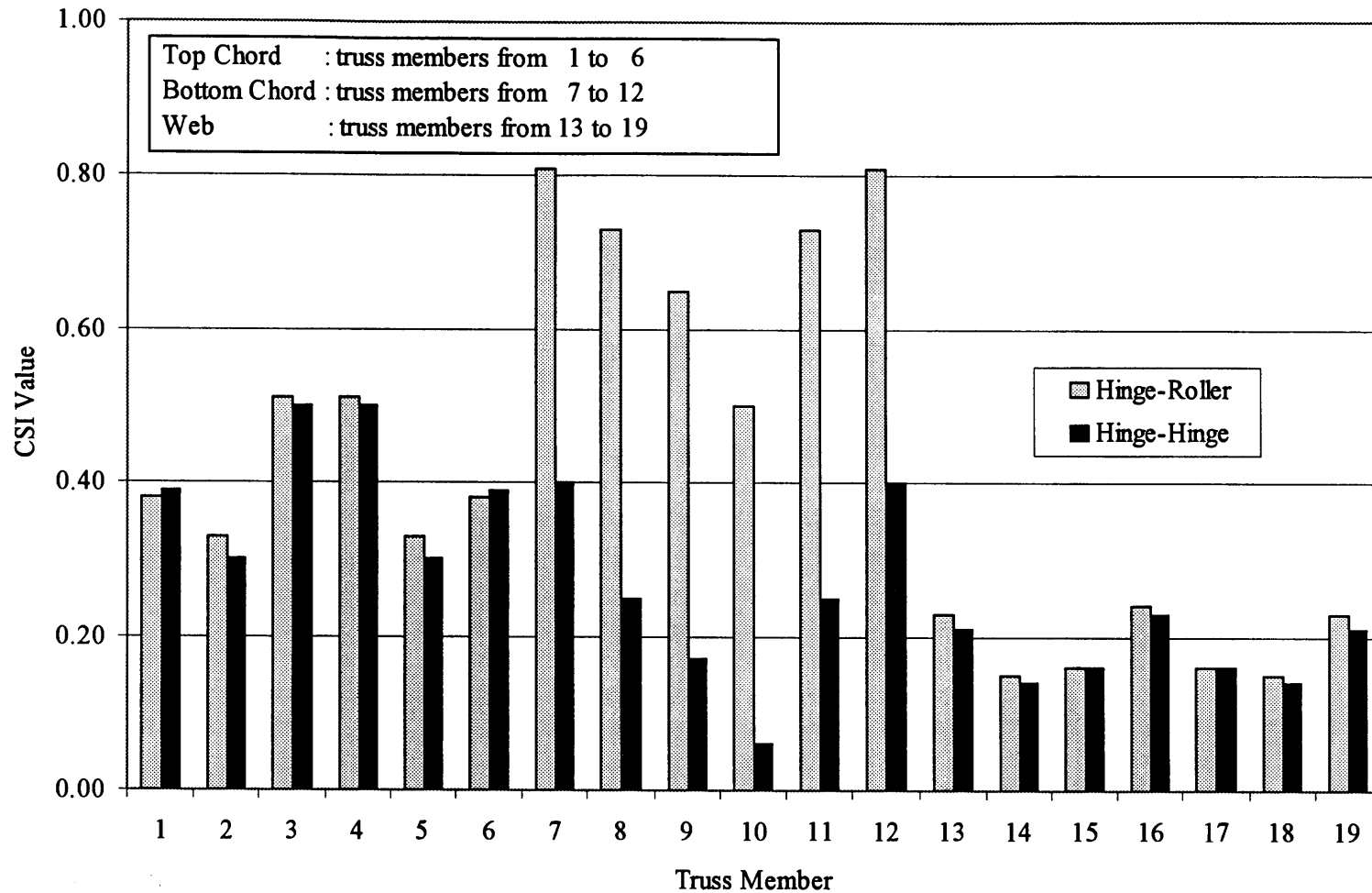


Figure K.6 CSI Comparison for The Truss Type AS3 with Different Boundary Conditions, Hinge-Roller and Hinge-Hinge

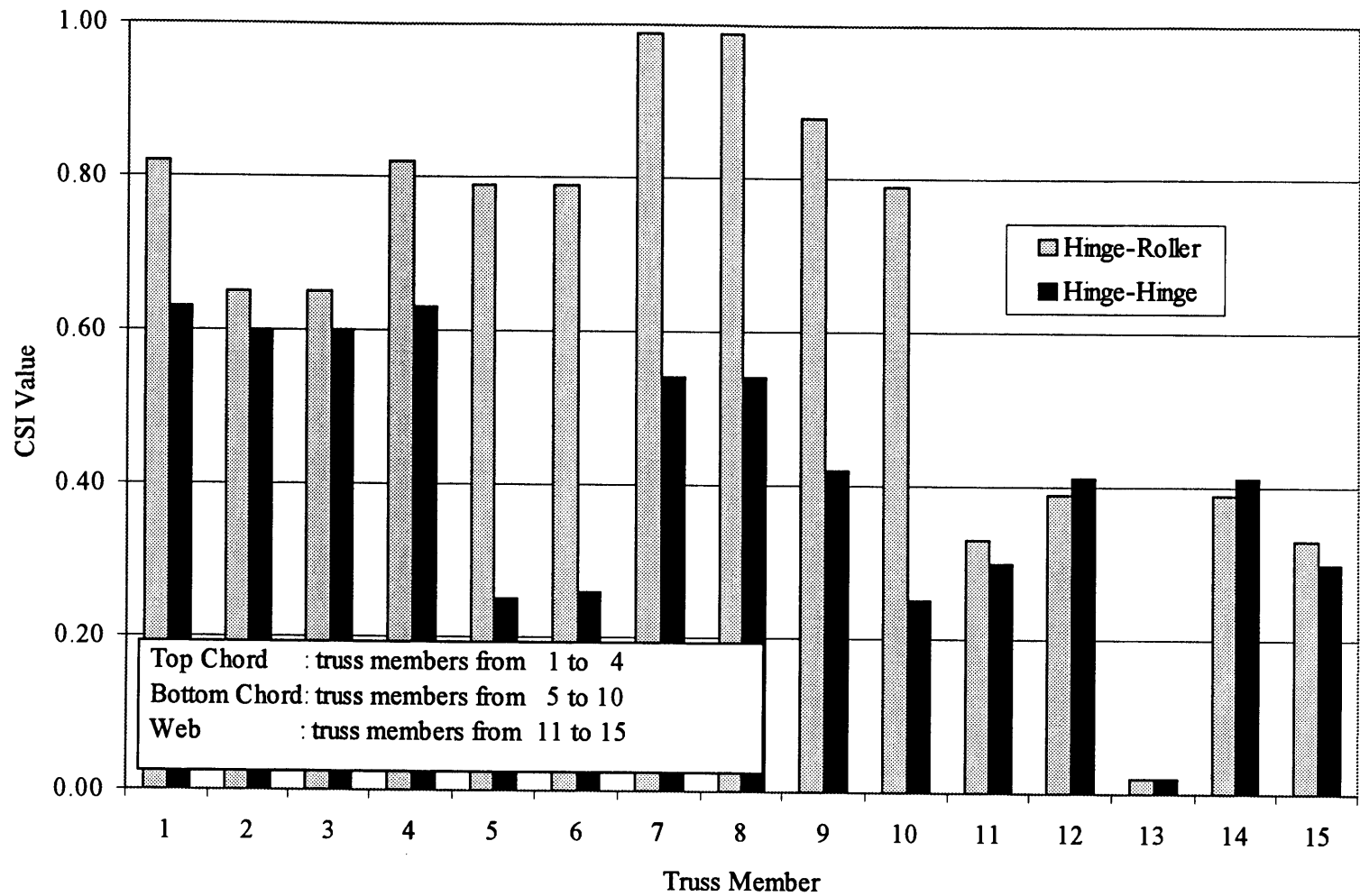


Figure K.7 CSI Comparison for The Truss Type ASGR with Different Boundary Conditions, Hinge-Roller and Hinge-Hinge

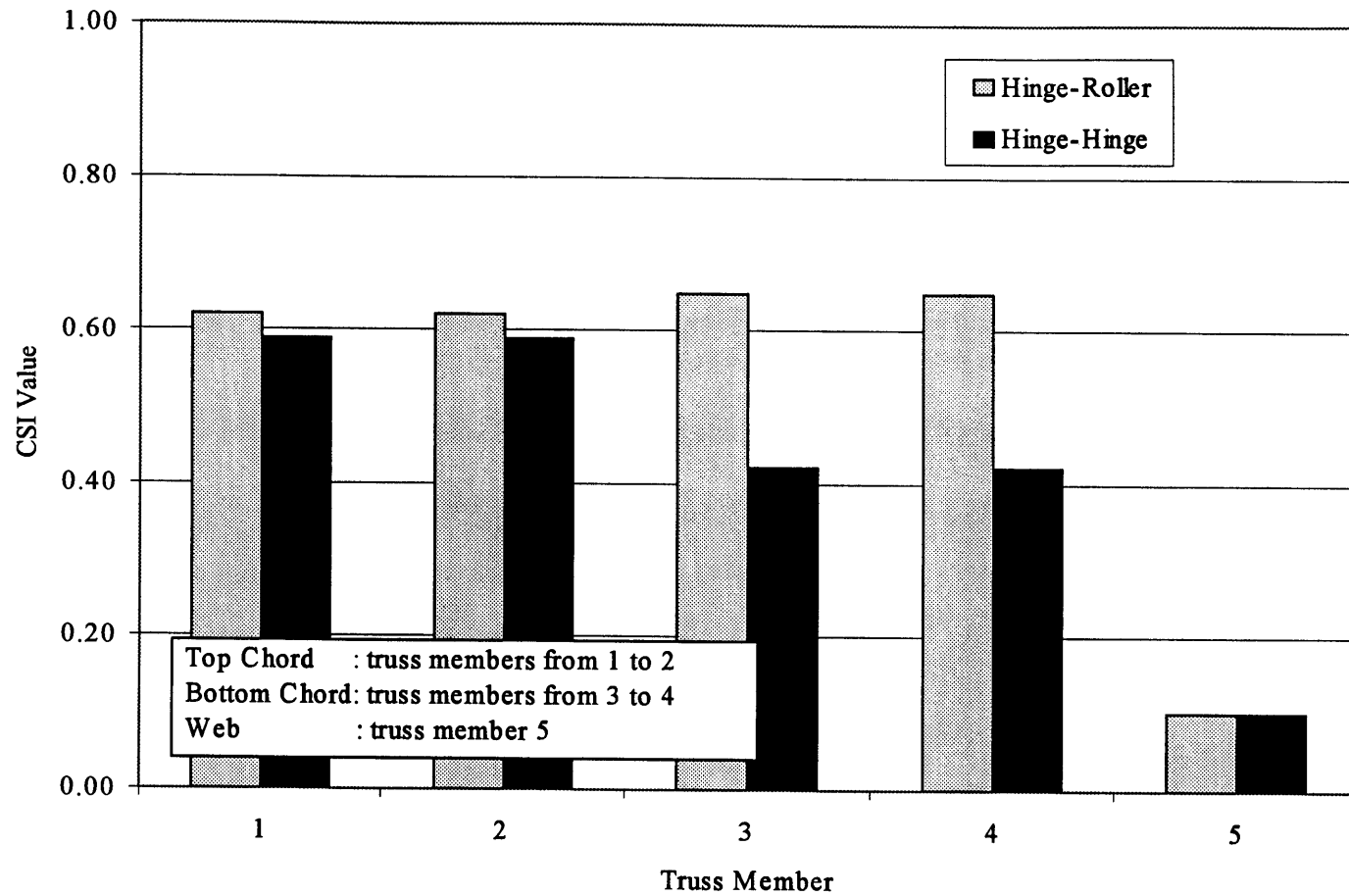


Figure K.8 CSI Comparison for The Truss Type B with Different Boundary Conditions, Hinge-Roller and Hinge-Hinge

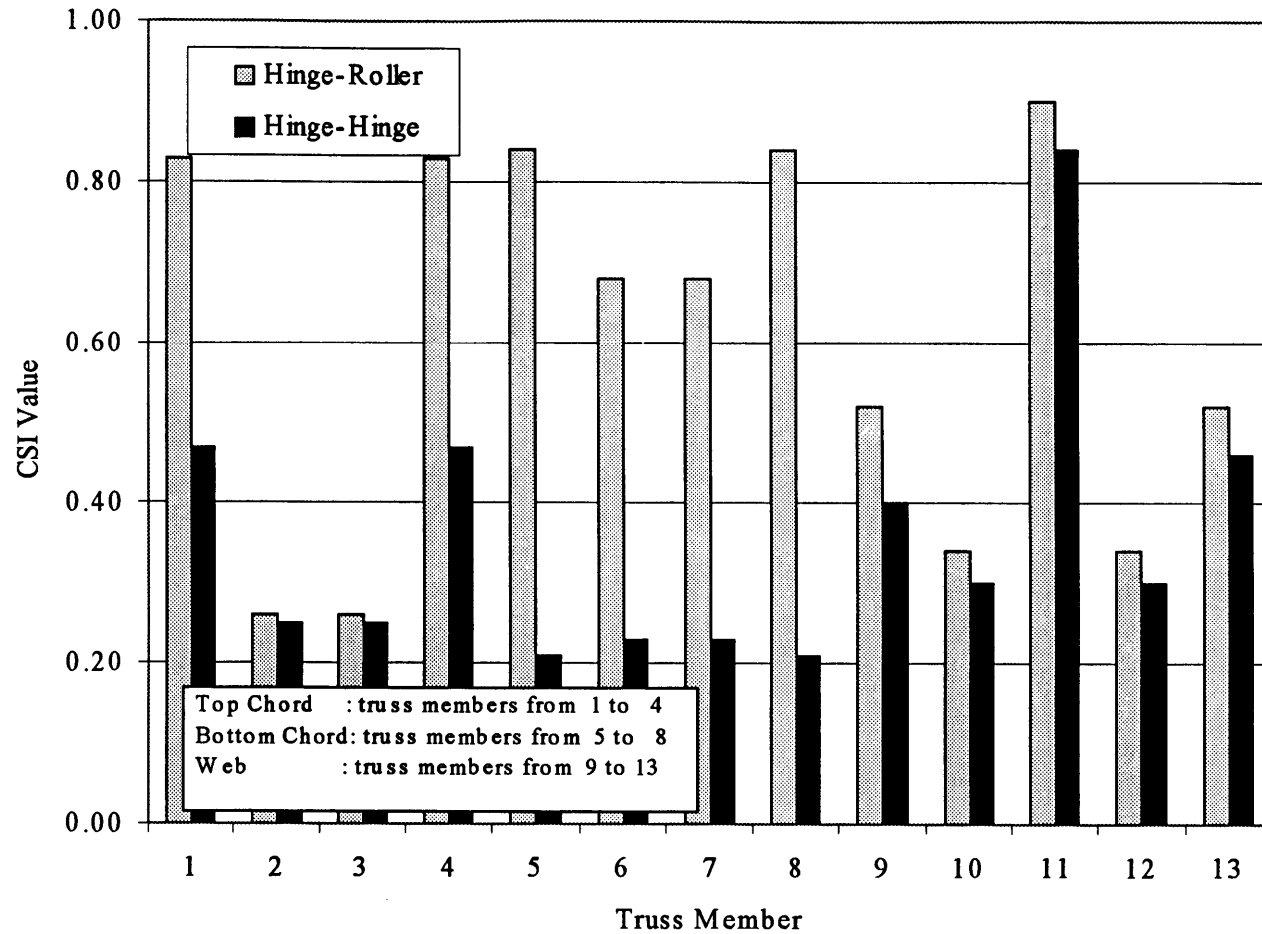


Figure K.9 CSI Comparison for The Truss Type BGR with Different Boundary Conditions, Hinge-Roller and Hinge-Hinge

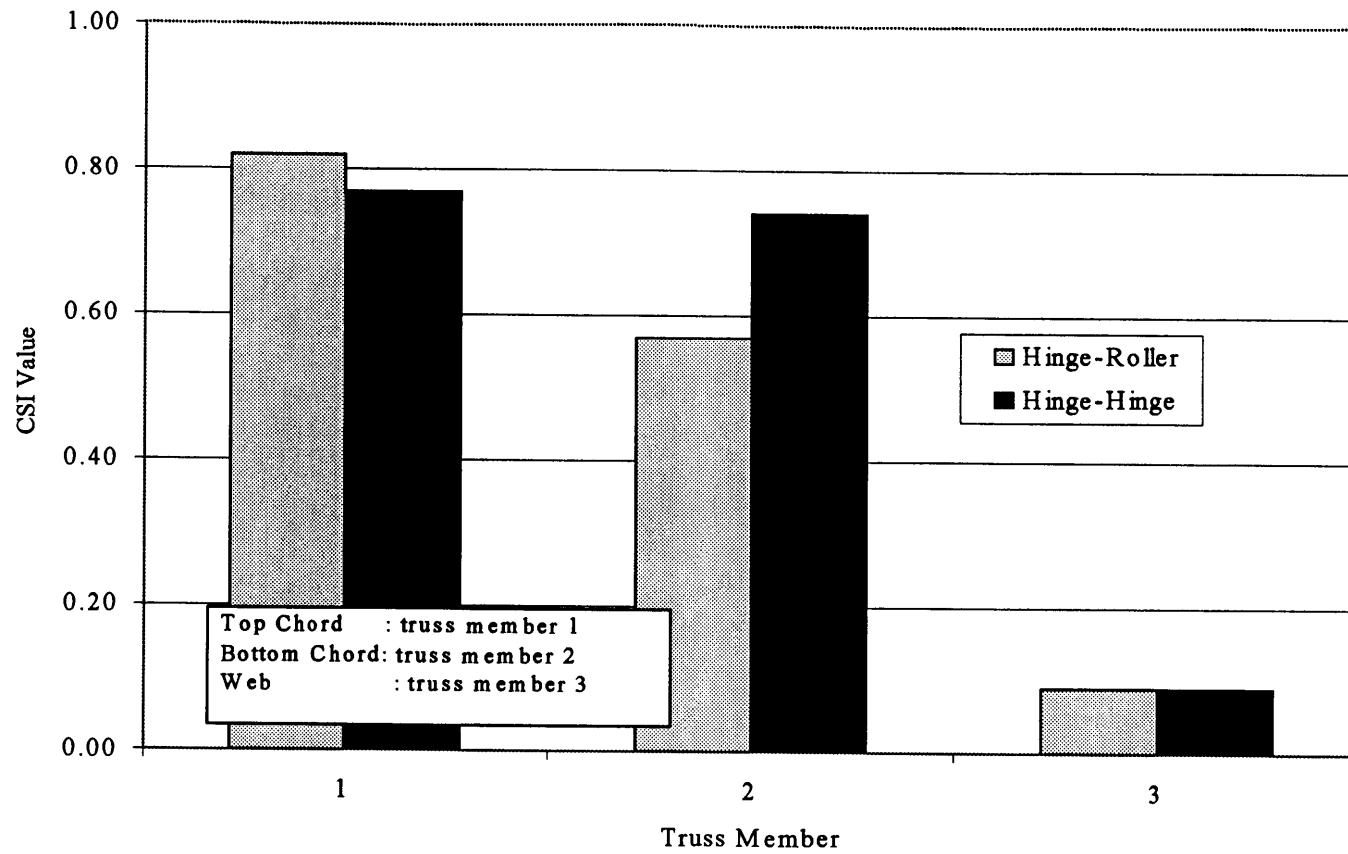


Figure K.10 CSI Comparison for The Truss Type J with Different Boundary Conditions, Hinge-Roller and Hinge-Hinge

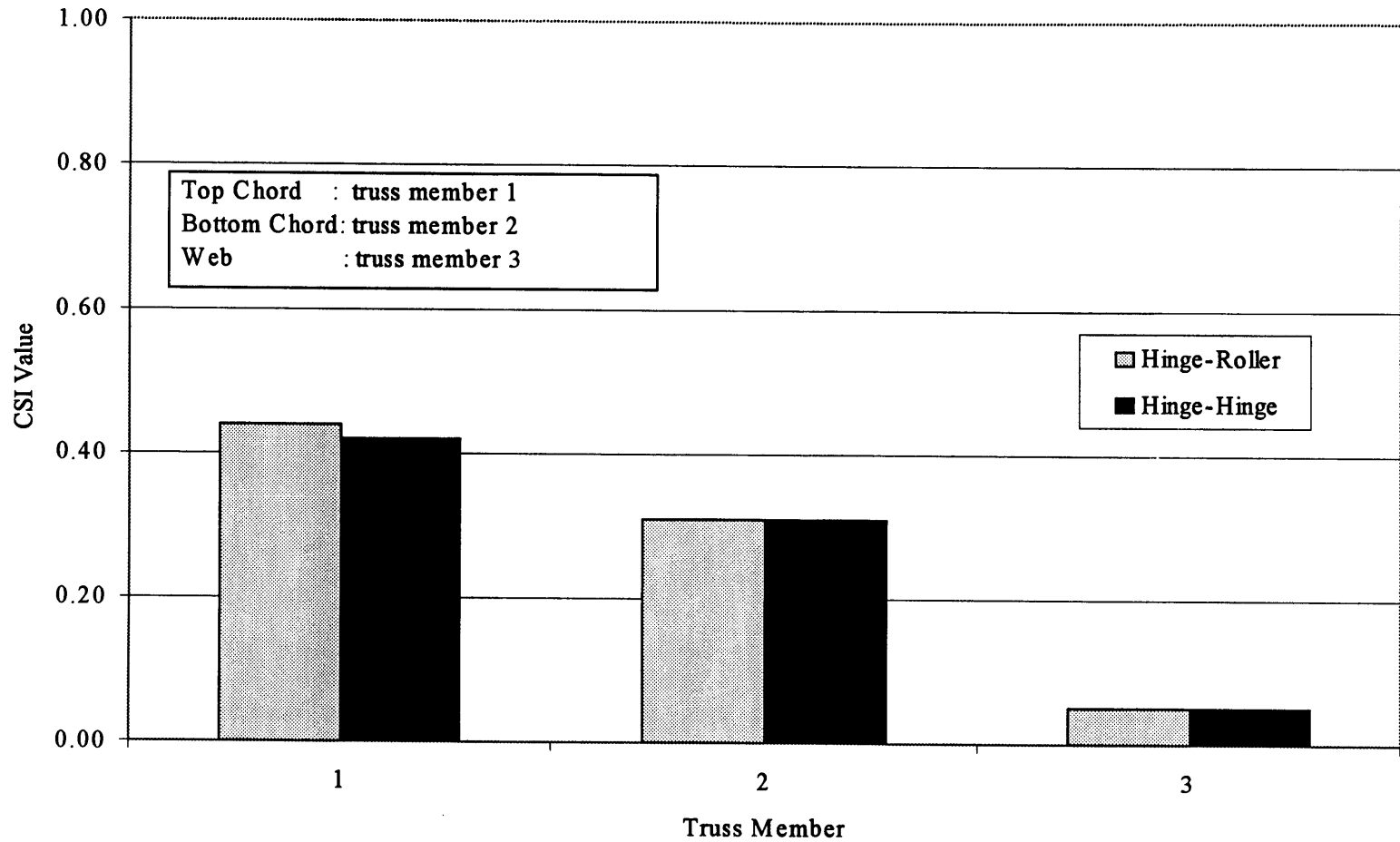


Figure K.11 CSI Comparison for The Truss Type J1 with Different Boundary Conditions, Hinge-Roller and Hinge-Hinge

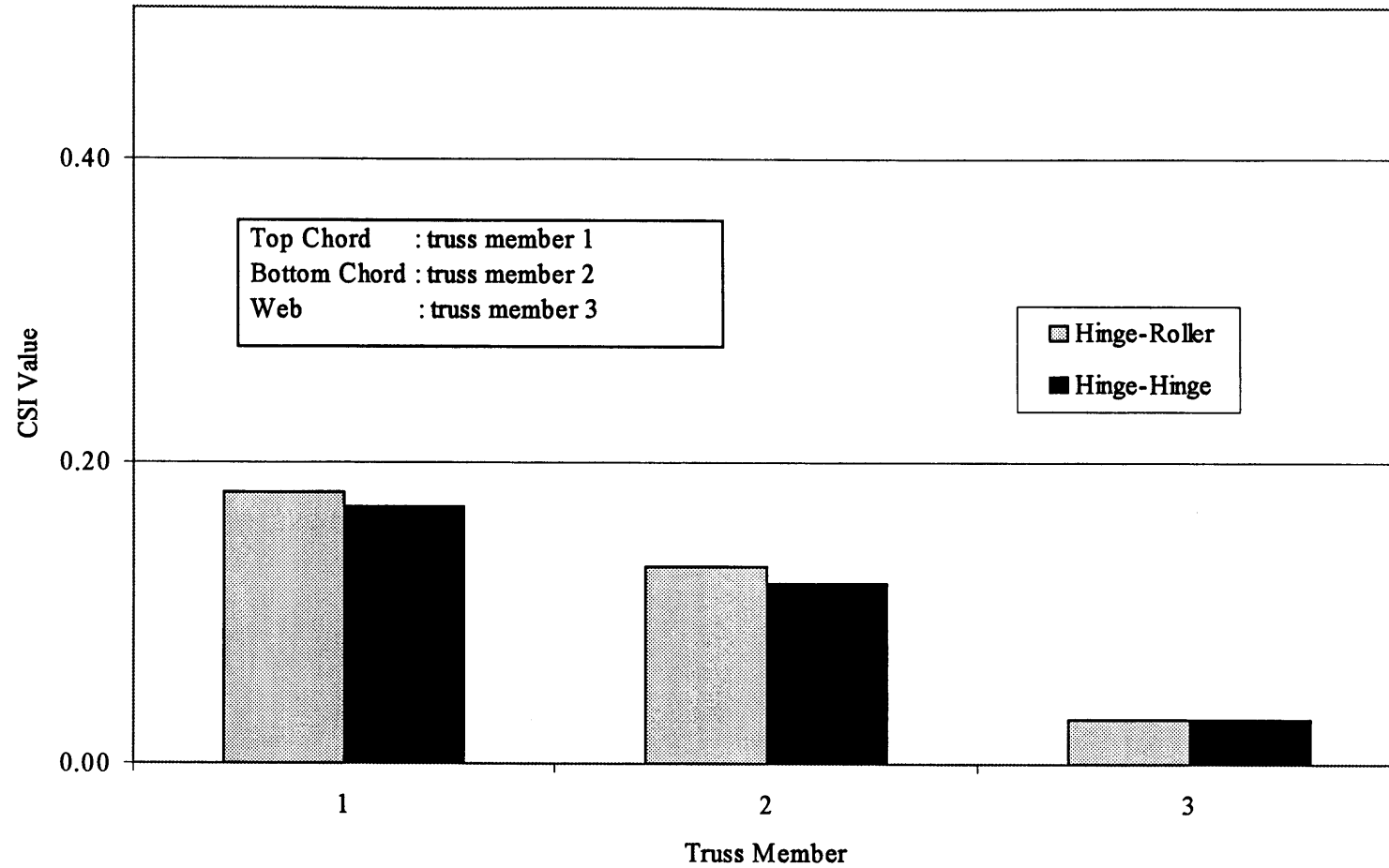


Figure K.12 CSI Comparison for The Truss Type J2 with Different Boundary Conditions, Hinge-Roller and Hinge-Hinge

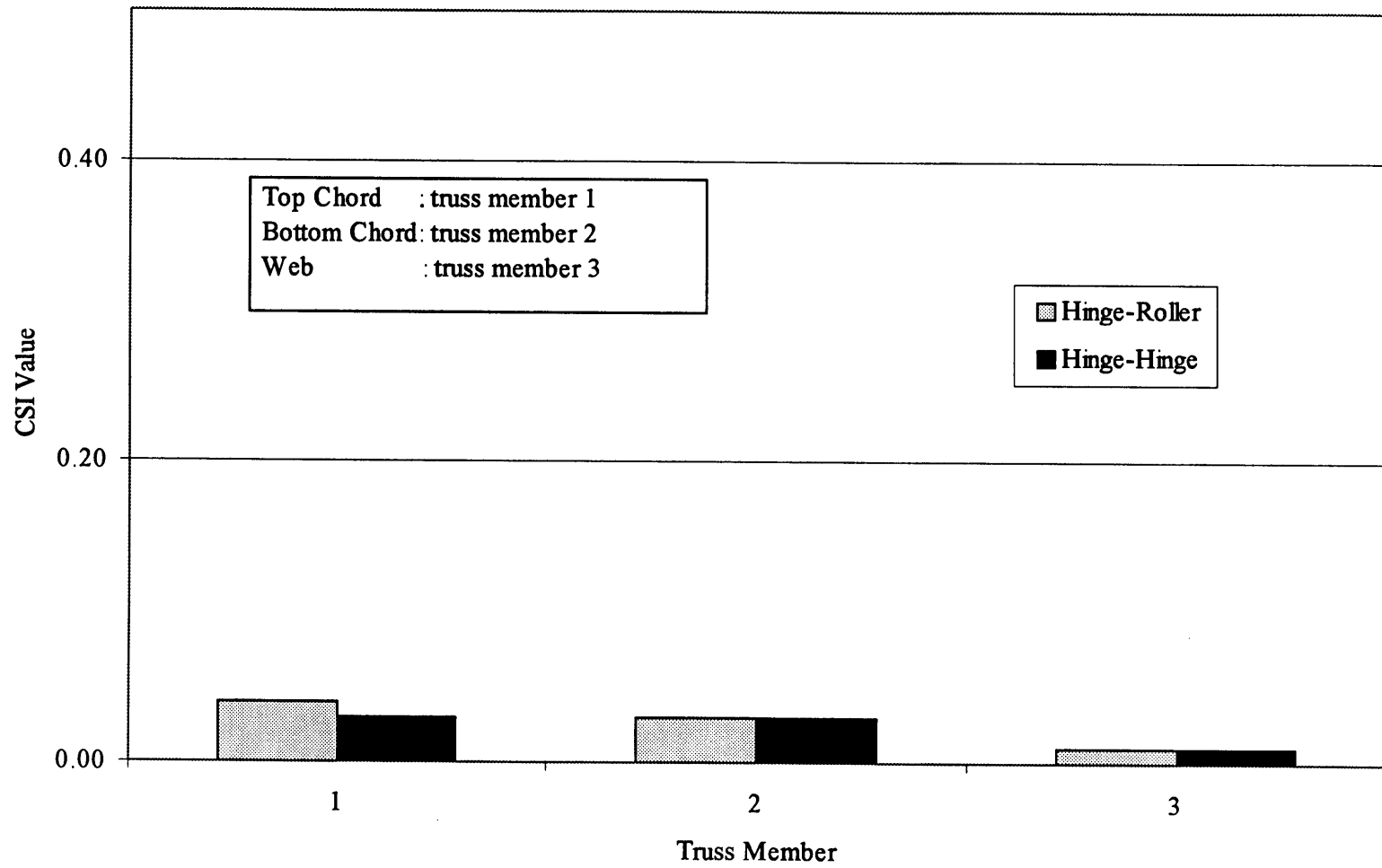


Figure K.13 CSI Comparison for The Truss Type J3 with Different Boundary Conditions, Hinge-Roller and Hinge-Hinge

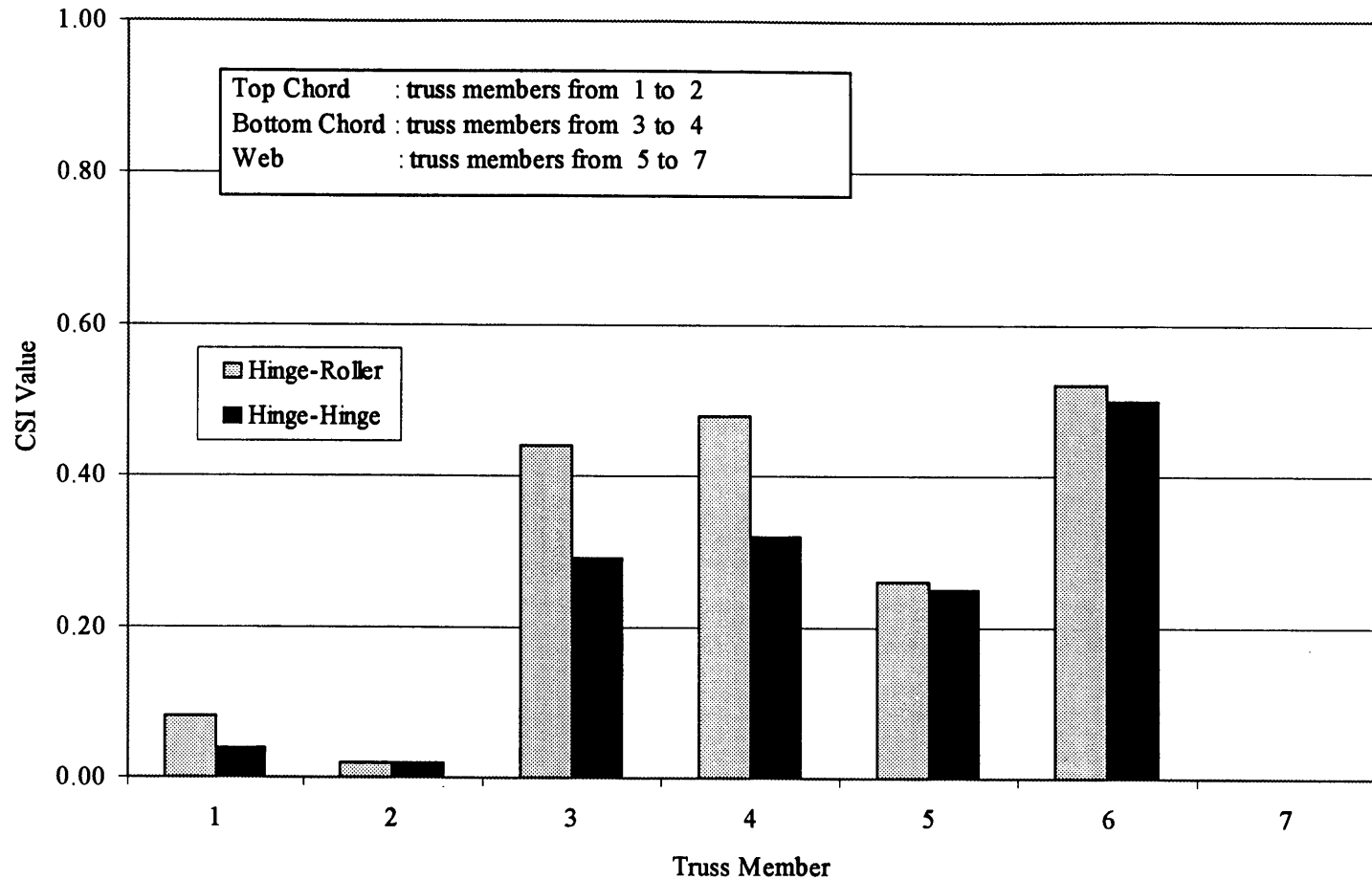


Figure K.14 CSI Comparison for The Truss Type JGR with Different Boundary Conditions, Hinge-Roller and Hinge-Hinge

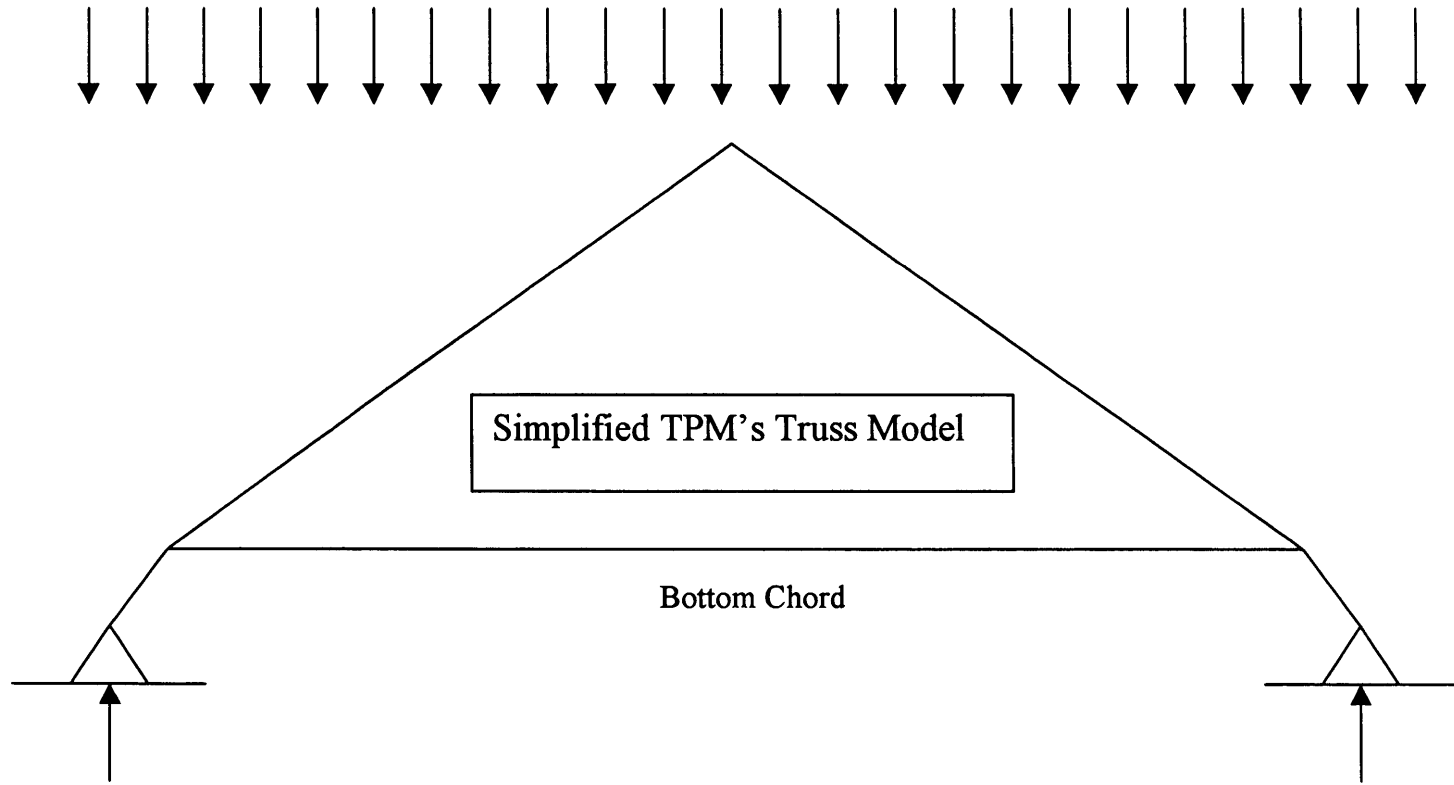


Figure K.15 Simplified TPM's Truss Model